Studies Towards the Synthesis of 1,4-Thiazines, 1,4-Thiomorpholines and Imidazolidines

A Thesis Submitted

in Partial Fulfilment of the Requirements

for the Degree of

DOCTOR OF PHILOSOPHY

by

Vijay M

Roll No. 126122010

Department of Chemistry
Indian Institute of Technology Guwahati
Guwahati- 781039
December 2019

Dedicated to
my family members

INDIAN INSTITUTE OF TECHNOLOGY GUWAHATI

Department of Chemistry

STATEMENT

I hereby declare that the matter embodied in this thesis is the result of investigations carried out by me in the Department of Chemistry, Indian Institute of Technology Guwahati, Guwahati, India under the supervision of Prof. Tharmalingam Punniyamurthy.

In keeping with the general practice of reporting scientific observations, due acknowledgement has been made wherever the work described is based on the findings of other investigators.

Guwahati Vijay M

December 2019

INDIAN INSTITUTE OF TECHNOLOGY GUWAHATI

Department of Chemistry

CERTIFICATE

This is to certify that Mr. Vijay M has been working under my supervision since July 2012. I am forwarding his thesis entitled "*Studies Towards the Synthesis of 1,4-Thiazines, 1,4-Thiomorpholines and Imidazolidines*" being submitted for the Ph.D. degree of this institute. I certify that he has fulfilled all the requirements according to the rules of this institute and regarding the investigations embodied in his thesis and this work has not been submitted elsewhere for a degree.

Guwahati

December 2019

Prof. Tharmalingam Punniyamurthy

Supervisor

ACKNOWLEDGEMENT

First and foremost, I express my heartfelt gratitude to my research supervisor **Prof. Tharmalingam Punniyamurthy** for his invaluable guidance, constant encouragement, unflinching support and profound understanding towards the completion of my research work. His continuous support towards research had given me enough freedom to think, plan and execute my ideas towards my work, which has provided a good basis for the present thesis. I would like to thank him for spending his precious time for discussion by which I have gained immense skills of knowledge in terms of research. I am also indebted to Prof. Tharmalingam Punniyamurthy for instilling in me a craving for perfection. I believe it will always remain with me in my future life.

Besides my supervisor, I would like to thank my doctoral committee members, **Prof. G. Krishnamoorthy, Dr. Lal Mohan Kundu,** Department of Chemistry, and **Prof. Arun Goyal,** Department of Biosciences and Bioengineering, for their valuable suggestions and comments during all assessments in the entire period of my doctoral studies.

I feel pleased to extend my gratitude to thanks to my lab mates Dr. M. Kannan, Dr. G. Murugavel, Dr. M. Sengoden, Dr. G. Bharathiraja, Dr. Pradeep Sadhu, Dr. Dinabandhu Sar, Dr. D. Mahesh, Dr. Vanaparthi Satheesh, Dr. Raghunath Bag, Mr. Pinaki Bhusan De, Mr. Sourav Pradhan, Mr. Tanumai Sarkar, Mr. Bijay Ketan Das, Mr. Kangkan Talukdar, Mr. Manmath Mishra, Ms. Sonbidya Baneerji, Mr. Pallab Karjee, Mr. Shubhajit Basak, Mr. Prabhat Kumar Maharana, Mr. Bijoy Debnath, Ms. Tripti Paul, Ms. Subhradeep Kar, Dr. Subhasis Roy and Dr. G. Sathish Kannan (RA) for their moral support and invaluable encouragement whenever I approached them and friendly relationship.

I take this opportunity to thank all the faculty members, Department of Chemistry, staff of Central Instruments Facility and the non-teaching staff of Department of Chemistry for their help during my Ph.D. tenure.

I would like to thank IIT Guwahati, India for financial support and Central Instrument Facility for providing the Instrument facility and DST for providing the XRD facility in the Department of Chemistry.

I express my profound gratefulness to all friends from IITG for their help and encouragement. Special thanks to Dr. Babulal Das, Dr. Krapa Shankar Kashyap and Mr. Munendra Pal Singh for helping me during XRD data collection and Dr. Sidick Basha, Dr. Johny Mertens, Dr. Balasubramani, Dr. Vignesh Babu, Dr. Radha Krishna Gattu, Dr. R. Unnava, Mr. Narendaren, Mr. Suresh Rajamanickam, Mr. Vigneshwaran, Mr. Rahul

Narasimhan, Mr. Subas Chandra Sahoo and Ms. Rupa from IIT Guwahati for their valuable help and support. And also my sincere thanks to தமிழ் சங்கம் (Tamizh Sangam) at IITG for their support and joyful moments spend with them.

I was fortunate enough to get excellent and close friends Mr. Abdul Kathar Jaillani, Mr. Nishanth Kumar, Mr. Siva Kumar, Mr. Justice, Mr. Suresh, Mr. Sathish, Mr. Siva Sakthi Mr. Logesh, Mr. Manikandan, and Dr. Vinoth Kumar, for their support during my tough periods.

I am grateful to my teachers Ms. Anita, Mr. John, Dr. N. Xavier, Dr. S. Raja, Dr. S. R. Bheeter and Mr. C. Rajaratnam for their great teachings, motivation and support.

I am indebted to my family, whose value to me only grows with age. Without their love and support, none of this would have been possible.

Vijay M

Though fate-divine should make your labour vain;
Effort its labour's sure reward will gain.

-Thirukural couplet 619

LIST OF ABBREVIATIONS

Ac	Acetyl
Bn	Benzyl
Boc	*tert*-butoxycarbonyl
BQ	Benzoquinone
Bu	Butyl
Bu_4NI	Tetrabutylammonium iodide
Bz	Benzoyl
DBU	1,8-diazabicyclo[5.4.0]undec-7-ene
DCE	1,2-dichloroethane
DCM	Dichloromethane
DFT	Density functional theory
DMAP	4-Dimethylaminopyridine
DME	Dimethoxyethane
DMEA	Dimethylethanolamine
DMSO	Dimethylsulfoxide
dr	Diastereomeric ratio
EDG	Electron donating group
ee	Enantiomeric excess
equiv	Equivalent
ESI	Electrospray ionization
Et	Ethyl
EWG	Electron withdrawing group
FT-IR	Fourier transform infrared spectroscopy
HPLC	High-performance liquid chromatography
HRMS	High-resolution mass spectrometry
Me	Methyl
MHz	Megahertz
Mp	Melting point
Ms	Methanesulfonyl
MS	Molecular sieves
m/z	Mass to charge ratio
NEt_3	Triethylamine

NMR	Nuclear magnetic resonance
Ns	*p*-nitrophenylsulfonyl
O.P	Optical rotation
Ph	Phenyl
PPh_3	Triphenyphosphine
Pr	Propyl
rt	Room temperature
R_f	Retention factor
TBABF	Tetrabutylammonium bifluoride
TD-DFT	Time dependent - density functional theory
THF	Tetrahydrofuran
TLC	Thin-layer chromatography
TMS	Tetramethylsilane
Ts	*p*-toluenesulfonyl
V	Volt
W	Watt

ABSTRACT

The thesis contains five chapters. First chapter describes the general introduction on the importance of aziridines. Second chapter deals with the regiospecific Bi-catalyzed domino *C–N* and *C–S* bonds formation for the synthesis of 1,4-thiazines and 1,4-thiomorpholines. Third chapter focuses on the synthesis, photophysical and electrochemical studies of indazoloquinolines. Fourth chapter demonstrates the construction of fused imidazolidines from aziridines and cyclic secondary amines using indazoloquinolines photoredox catalysis. Chapter five covers summary and important points.

Chapter I. The Importance of Aziridines and Their Reactions

Heterocycles play a significant architectural role in the realm of organic chemistry. Aziridines are important building blocks and widely applied in medicinal chemistry. This chapter focuses on aziridines, which contains a brief introduction and literature review of heterocyclic molecules using aziridines. The literature gaps are highlighted along with the objectives of the thesis.

Chapter II. Bi-Catalyzed Domino C–N/C–S Bonds Formation: Synthesis of 1,4-Thiazines/1,4-Thiomorpholines

N,S-Heterocycles are privileged structural scaffolds due to their interesting medicinal and agrochemical properties. Aziridines serve as the synthetic intermediates and several excellent examples are available for the selective nucleophilic ring-opening. This chapter demonstrates the Bi-catalyzed domino ring expansion of aziridines with 1,4-dithiane-2,5-diol for the synthesis of 3,4-dihydro-2*H*-1,4-thiazines.

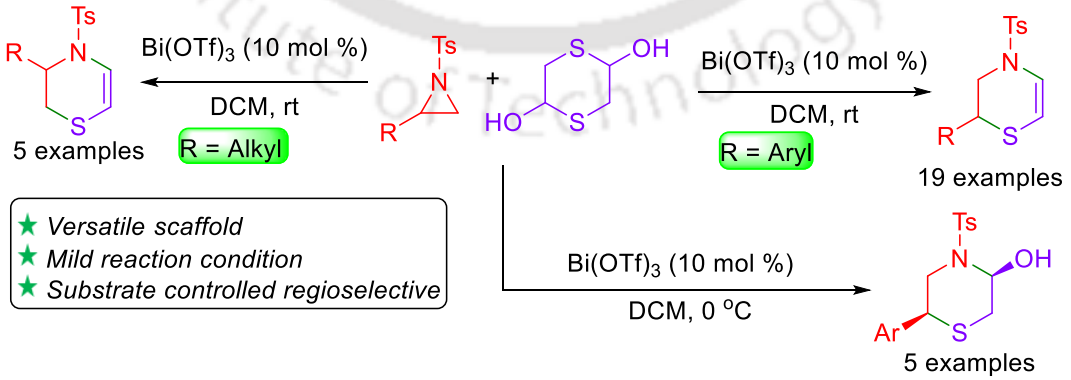

Scheme 1. Bi-catalyzed synthesis of 3,4-dihydro-2*H*-1,4-thiazine and thiomorpholines.

Chapter III. Synthesis, Photophysical and Electrochemical Studies of Indazoloquinolines

Visible-light photoredox catalysis affords a powerful synthetic tool for the generation of carbon–carbon and carbon–heteroatom bonds. Rh-catalyzed C-H activation and C-C bond formations of 2*H*-indazoles with alkynes produces indazolo[2,3-*a*]quinolines whose photophysical and electrochemical properties are studied for photoredox catalysis of the reaction of aziridines with cyclic secondary amines.

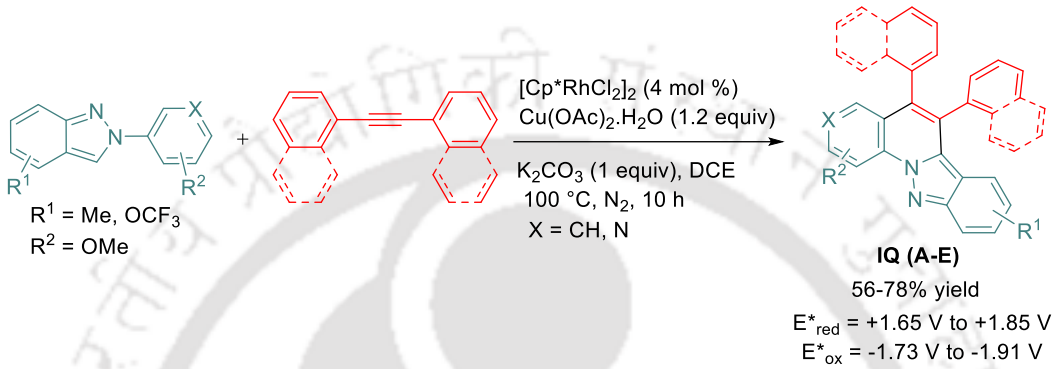

Scheme 2. Rh-catalyzed synthesis of indazolo[2,3-*a*]quinolones.

Chapter IV. Tandem Ring Opening/Oxidative Amination of Aziridines with Cyclic Secondary Amines Using Indazoloquinolines

Sustainable assembly of imidazolidines is important in synthetic chemistry. This chapter focuses a sequential stereospecific ring-opening and C–H amination of aziridines with secondary cyclic amines under visible-light mediated indazoloquinoline photoredox catalysis. Optically active aziridines can be stereospecifically coupled with high enantiomeric purities (99% ee).

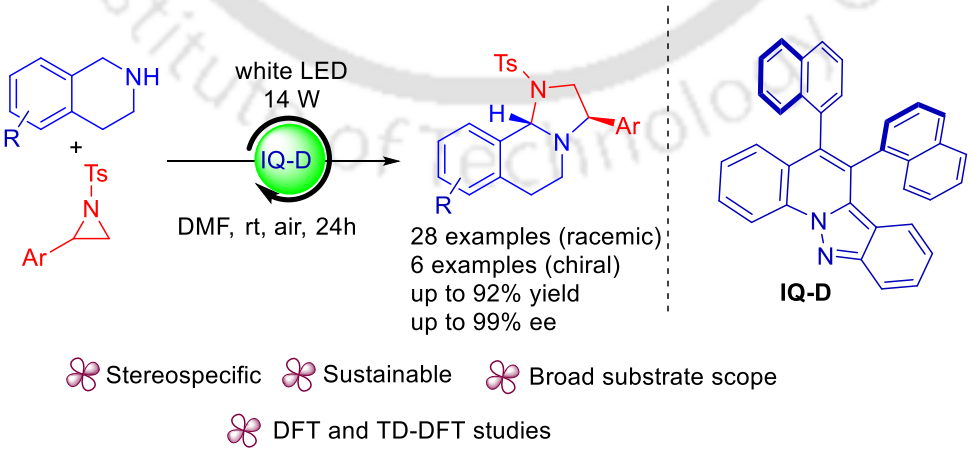

Scheme 3. Organo-photoredox catalyzed synthesis of fused imidazolidines.

Chapter V. Conclusions

This chapter covers the summary and outlook.

Contents

The Importance of Aziridines and Their Reactions

Heterocycles are an essential class of structural scaffolds in organic and medicinal sciences. In particular, aziridine is abundant in synthetic products with wide applications in drug discovery and medicinal chemistry including antimalarial,[1a,b] antimicrobial,[1c] antibiotic,[1d] anticancer,[1e] anti-inflammatory,[1f,g] antidepressant,[1h] anti-HIV,[1i,j] antifungal,[1k] antibacterial,[1l] antiviral,[1m] herbicidal[1n] and antidiabetic[1o] agents (Figure 1). Considerable efforts are thus made on the development of synthetic routes for the use of aziridine for the construction of diverse scaffolds.

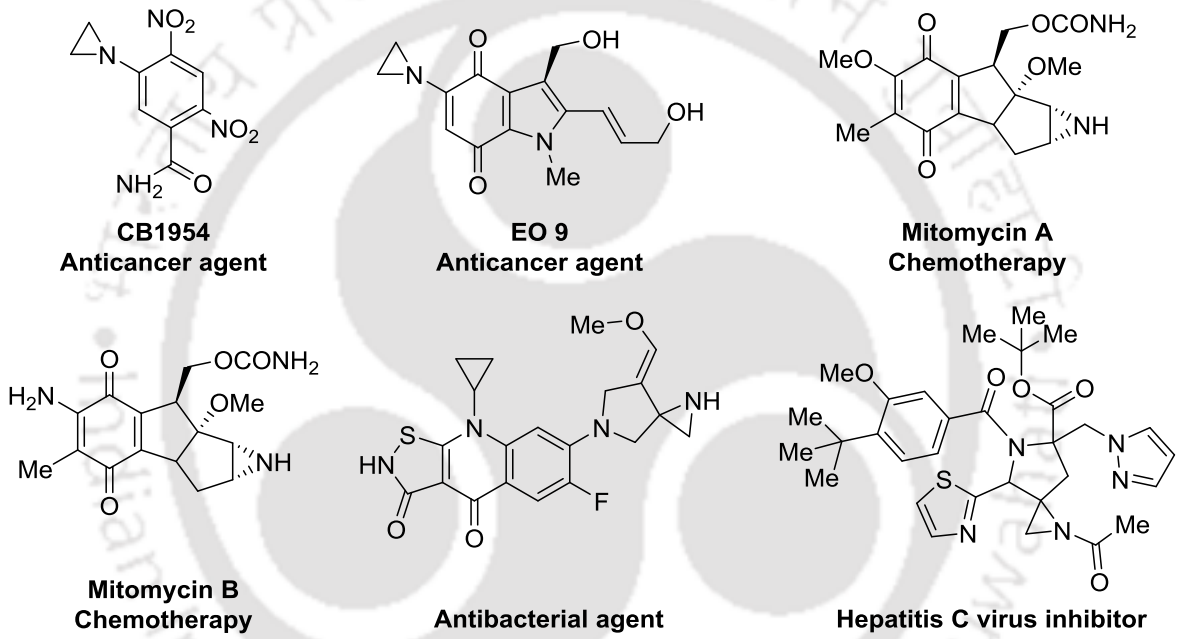

Figure 1. Some examples of biologically compounds having aziridine motif.

1.1 Classification

Based on the substitution on nitrogen, aziridine can be classified into two types: (i) activated and (ii) unactivated aziridines (Figure 2), which can undergo cycloaddition as well as tandem reaction.

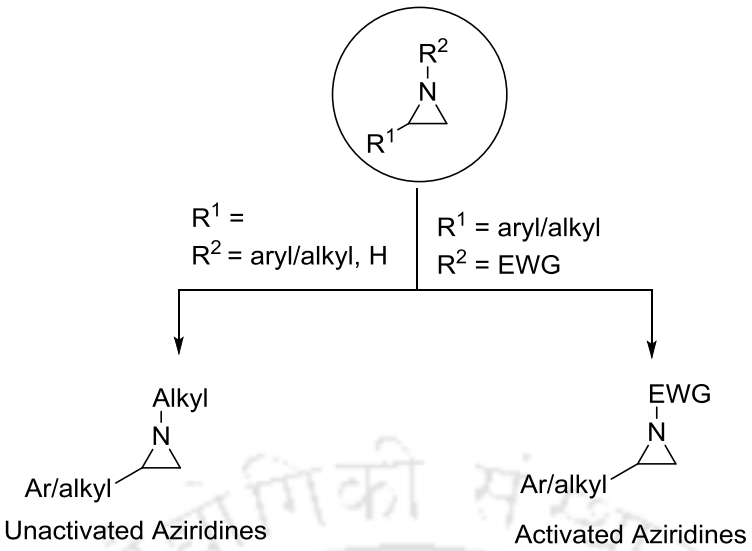

Figure 2. Classification of aziridines.

1.2 Cycloaddition

In general, the nucleophile reacts with unactivated aziridine, which requires metal or Lewis acid catalyst for selective ring open. On the other hand, activated aziridine does not require them for activation. Such opening of the ring is possible through C–N and C–C bond cleavages. In presence of Lewis acid, activated aziridine undergoes selective C–N bond cleavage to give a 1,3- zwitterionic dipole, which is electron-deficient and can react with dipolarophile to give [3+2]-cycloadduct, whereas unactivated aziridine reacts through C–C bond cleavage to provide azomethine ylide, which can react with dipolarophile to afford [3+2]-cycloadduct (Figure 3).

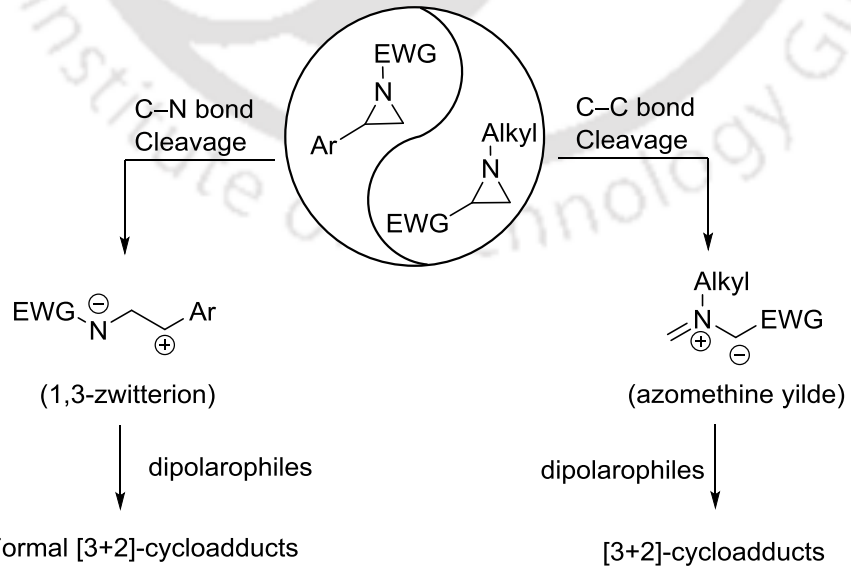

Figure 3. Reactivities of aziridines towards dipolarophiles.

1.3 Synthesis of Heterocyles

1.3.1 Compounds with One Heteroatom

Mann and co-workers developed cycloaddition of aziridines with alkenes in presence of $BF_3.OEt_2$ to afford spiro-pyrrolidines at low temperature (Scheme 1).[3] The reaction is general and the coupling of a series of substrates is covered.

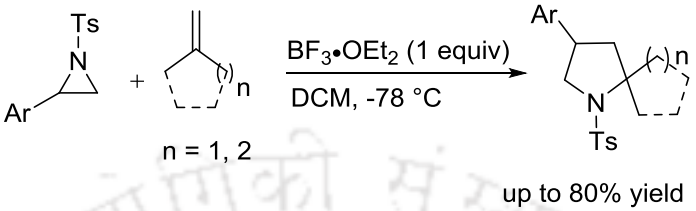

Scheme 1. $BF_3.OEt_2$-mediated synthesis of spiro-fused pyrrolidines.

Strand group reported a silver catalyzed [3+2]-cycloaddition of aziridines with internal or electron-rich alkynes at room temperature. This reaction proceeds through 1,3-diploes generated from aziridines that were reacted with alkynes to give dihydropyrroles (Scheme 2).[4]

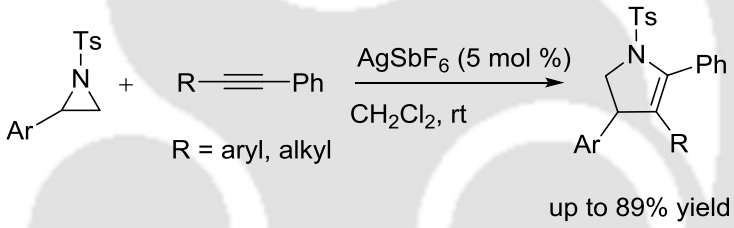

Scheme 2. Ag-catalyzed synthesis of 2,3-dihydropyrroles.

The synthesis of functionalized benzoindolines achieved using a Ag catalyzed coupling of 2-phenyl-*N*-sulfonylaziridines with 2-naphthols (Scheme 3).[5] In this reaction, S_N1 ring-opening of aziridine happens to avail 1,3-dipoles that react with 2-naphthols to give [3+2] cycloaddition products.

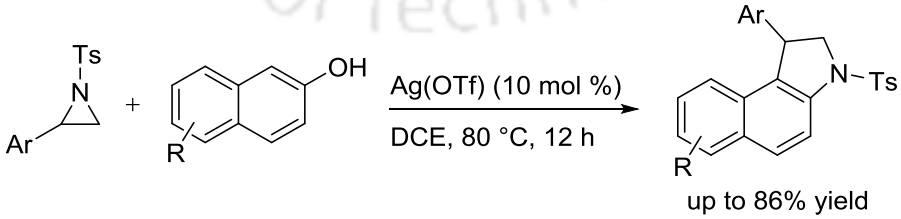

Scheme 3. Ag-catalyzed synthesis of benzoindolines.

1.3.2 Compounds Containing Two Heteroatoms

Sc-catalyzed cycloaddition of electron-rich alkenes with aziridines afforded fused bicyclic heterocycles (Scheme 4).[6] Subsequently, the reaction of aziridines with nitrile has been accomplished to furnish dihydroimidazoles (Scheme 5).[7] This reaction is performed as neat at room temperature

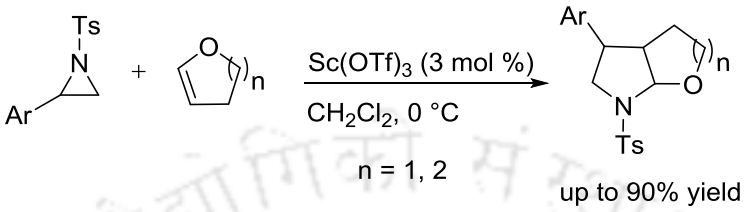

Scheme 4. Sc-catalyzed synthesis of fused pyrrolidines.

.

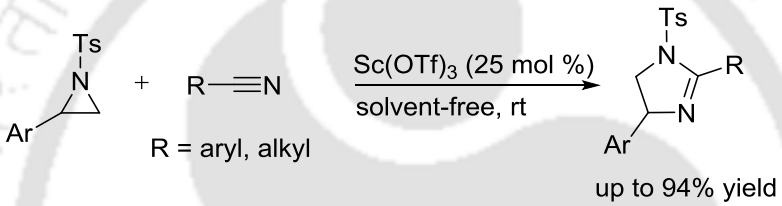

Scheme 5. Sc-promoted synthesis of dihydroimidazoles.

Our group showed a Fe-catalyzed [3+2]-cycloaddition of *N*-alkylaziridines with heterocumulenes to afford iminothiazolidines (Scheme 6).[8] This reaction uses water as a solvent.

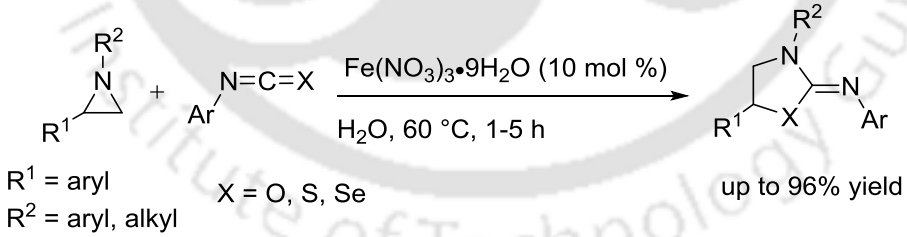

Scheme 6. Fe-catalyzed synthesis of iminothiazolidines.

Gua and co-workers developed cycloaddition of tropone with aziridines using a Ni-catalysis to afford 2,3,4,4a-tetrahydrocyclohepta-[1,4]-oxazines (Scheme 7).[9] The reaction of electron-withdrawing and donating substrates has been demonstrated.

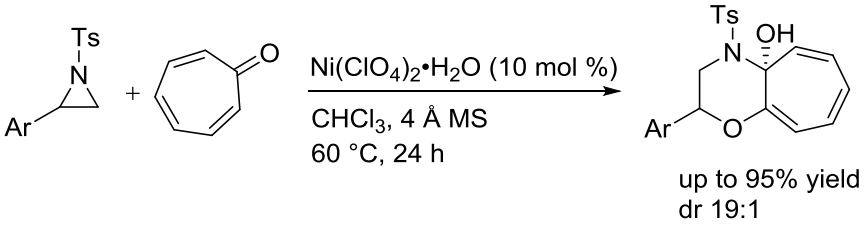

Scheme 7. Ni-catalyzed synthesis of tetrahydrocyclohepta[*b*][1,4]-oxazines.

Our group reported an Al-salen catalyzed coupling of chiral *N*-alkylaziridines with isothiocyanates at room temperature (Scheme 8).[10] High enantiomeric purity and substrate scope are the important practical features.

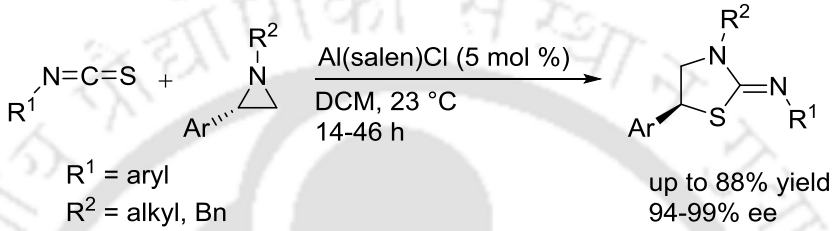

Scheme 8. Al-catalyzed synthesis of iminothiazolidines.

Zhou group demonstrated the synthesis of highly substituted morpholines using 2-alkyl-*N*-sulfonylaziridines with propargyl alcohol (Scheme 9).[11] The reaction involves the tandem nucleophilic ring-opening and cyclization of aziridines through less substituted carbon.

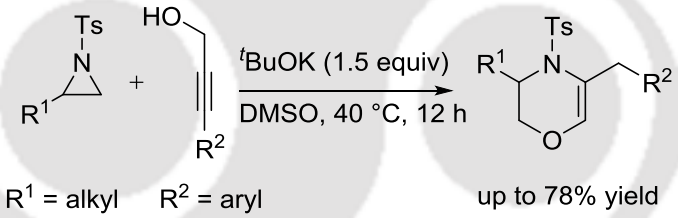

Scheme 9. Base-promoted synthesis of substituted morpholines.

Our group presented the coupling of *N*-sulfonylaziridines with propargyl amines to give piperazines (Scheme 10).[12] Optically active aziridines can be coupled with high enantiomeric purity (>98%).

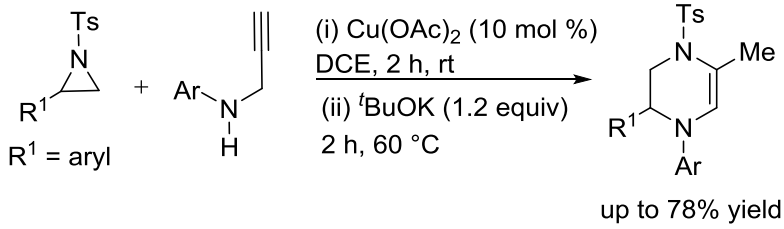

Scheme 10. Cu-catalyzed synthesis of piperazines.

Our group developed a Cu-catalyzed coupling of aziridines with benzimidazole to afford dihydroimidazobenzimidazoles (Scheme 11)[13]. The reaction involves stereospecific ring-opening of aziridine and their subsequent intramolecular dehydrogenative cross-coupling. The reaction of both activated and unactivated aziridines has been covered.

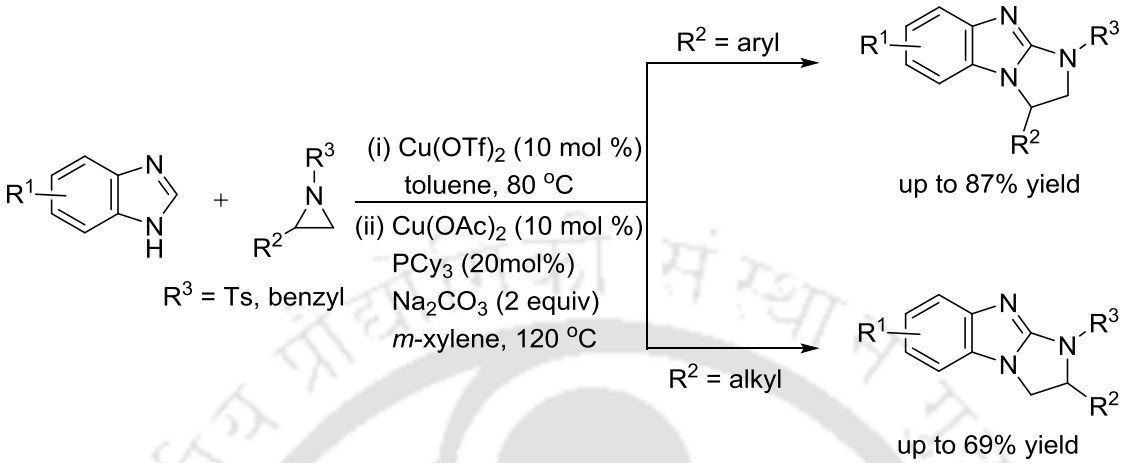

Scheme 11. Cu-catalyzed synthesis of imidazobenzimidazoles.

1.3.3 Compounds Containing Three Heteroatoms

Selander and co-workers reported the reaction of aziridines with nitrones in presence Al-catalysis (Scheme 12).[14] The substrate scope and mild reaction conditions are the important features.

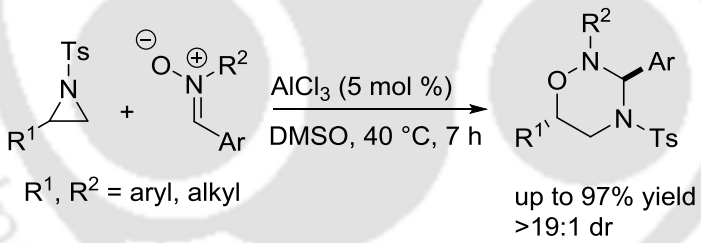

Scheme 12. Al-catalyzed synthesis of 1,2,4-oxadiazinanes.

1.4 Tandem Reactions

Tandem reaction affords an efficient synthetic tool to construct complex molecules from simple substrates. This strategy allows to form one or more bonds in one-pot without isolation of the intermediates that enhances the synthetic efficiency. Wan group reported a Cu-catalyzed synthesis of tetrahydrotriazines from aziridines and *N*-alkyl hydrazones (Scheme 13).[15] This reaction involves a tandem ring-opening of aziridine with hydrazone followed by direct oxidative amidation.

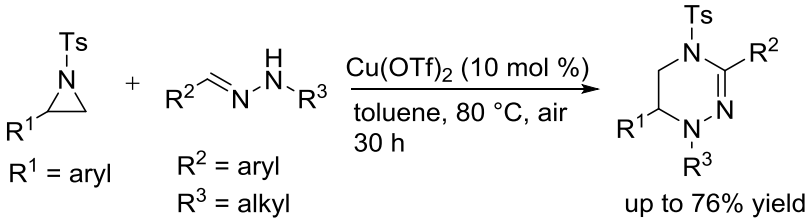

Scheme 13. Cu-catalyzed synthesis of triazines.

1.5 Literature Gaps and Objectives

The following literature gaps and objectives of the thesis are identified from the above-discussed work:

- As mentioned above, the studies regarding the construction of nitrogen heterocycles using aziridines are limited to [3+2]-cycloaddition,[3-8] [8+3]-cycloaddition[9] and tandem approach.[15] There is a wide scope to construct 1,4-thiomorpholines and 1,4-thiazine backbones *via* domino approach. Such thiomorpholines and thiazine motif synthesis can be achieved using mercaptoacetaldehyde
- The studies regarding the assembly of functionalized imidazolidines have been explored using conventional methods. Development of an alternative approach via C-H functionalization would thus be valuable. Such a study can be validated using Density Functional Theory (DFT) approach.
- The synthetic application of photoredox catalysis is still fairly limited to a few catalyst choices. To achieve imidazolidines *via* oxidative C–H functionalization, the use of photoredox catalysts with a broad range of oxidation and reduction potentials would be valuable.

1.6 References

1. (a) Kesten, S. J.; Johnson, J.; Werbel, L. M.; *J. Med. Chem*. **1987**, *30*, 906. (b) White, N. J. *Br. Med. Bull*. **1998**, *54*, 703. (c) Uno, T.; Kondo, H.; Inoue, Y.; Kawahata, Y.; Sotomura, M.; Iuchi, K.; Tsukamoto, G. *J. Med. Chem*. **1990**, *33*, 2929. (d) Fleming, A. *B. influenza. Br. J. Exp. Pathol*. **1929**, *10*, 226. (e) Sosnovsky, G.; Paul, B. D. *J. Med. Chem*. **1984**, *27*, 782. (f) Amir, M.; Kumar, S. *Indian J. Chem*. **2005**, *44B*, 2532. (g) Dunwell, D. W.; Evans, D. *J. Med. Chem*. **1975**, *18*, 158. (h) Hu, B.; Song, Q.; Xu, Y. *Org. Process Res. Dev*. **2012**, *16*, 155. (i) Solyev, P. N.; Shipitsin, A. V.; Karpenko, I. L.; Nosik, D. N.; Kalnina, L. B.; Kochetkov, S. N.; Kukhanova, M. K.; Jasko, M. V. *Chem. Biol. Drug Des*. **2012**, *80*, 947. (j) Mandala, D.; Thompson, W. A.; Watts, P.

Tetrahedron **2016**, *72*, 3389. (k) Andriole, V. T. *Int J Antimicrob Ag*. **2000**, *16*, 317. (l) Goueffon, Y.; Montay, G.; Roquet, F.; Pesson, M. C. R. *Hebd. Seances Acad. Sci*. **1981**, *292*, 37. (m) Van Hoof, L.; Vanden Berghe, D. A.; Hatfield, G. M.; Vlietinck, A. J. *Planta Med*, **1984**, *50*, 513. (n) Ikeguchi, M.; Sawaki, M.; Nakayama, H.; Kikugawa, H.; Yoshii, H. *Pest Manag Sci*. **2004**, *60*, 981. (o) Cossy, J.; Menciu, C.; Rakotoarisoa, H.; Kahna, P. H.; Desmurs, J.-R. *Bioorg. Med. Chem. Lett.* **1999**, *9*, 3439.

2. For aziridine reviews, see: (a) Watson, I. D. G.; Yu, L.; Yudin, A. K. *Acc. Chem. Res*. **2006**, *39*, 194. (b) Sweeney, J. B. *Chem. Soc. Rev.* **2002**, *31*, 247. (c) Degennaro, L.; Trinchera, P.; Luisi, R. *Chem. Rev.* **2014**, *114*, 7881.
3. Ungureanu, I.; Klotz, P.; Mann, A. *Angew. Chem., Int. Ed*. **2000**, *39*, 24.
4. Wender, P. A.; Strand, D. *J. Am. Chem. Soc.* **2009**, *131*, 7528.
5. Kaicharla, T.; Jacob, A.; Gonnade, R. G.; Biju, A. T. *Chem. Commun*. **2017**, *53*, 8219.
6. Yadav, J. S.; Reddy, B. V. S.; Pandey, S. K.; Srihari, P.; Prathap, I. *Tetrahedron Lett.* **2001**, *42*, 9089.
7. Wu, J.; Sun, X.; Xia, H.-G.; *Tetrahedron Lett*. **2006**, *47*, 1509.
8. Sengoden, M.; Punniyamurthy, T. *Angew. Chem., Int. Ed*. **2013**, *52*, 572.
9. Liu, H.; Jia, H.; Shi, W.; Wang, C.; Zhang, C.; Guo, H. *Org. Lett.* **2018**, *20*, 3570.
10. Sengoden, M.; Irie, R.; Punniyamurthy, T. *J. Org. Chem.* **2016**, *81*, 11508.
11. Wang, L.; Liu, Q. B.; Wang, D-S.; Li, X.; Han, X-W.; Xiao, W-J.; Zhou, Y-G. *Org. Lett.* **2009**, *11*, 1119.
12. Das, B. K.; Pradhan, S.; Punniyamurthy, T. *Org. Lett.* **2018**, *20*, 4444.
13. De, P. B.; Pradhan, S.; Punniyamurthy, T. *J. Org. Chem.* **2017**, *82*, 3183.
14. Pathipati, S. R.; Singh, V.; Eriksson, L.; Selander, N. *Org. Lett.* **2015**, *17*, 4506.
15. Hong, D.; Lin, X.; Zhu, Y.; Lei, M.; Wang, Y. *Org. Lett.* **2009**, *11*, 5678.

Chapter II

Bi-Catalyzed Domino C–N/C–S Bonds Formation: Synthesis of 1,4-Thiazines/1,4-Thiomorpholines

N,S-Containing heterocycles are privileged structural scaffolds due to their interesting medicinal properties.[1] Among them, the structural frameworks with 1,4-thiazine motifs have been studied broadly because of their antibacterial,[2] antibiotics,[3] 5-lipoxygenase (5-LO) inhibitor[4] properties and use in flavor (Figure 1).[5] In addition, the compounds having 1,4-thiomorpholine structural units possess a wide range of biological activities such as antiinflammatory,[6] antimycobacterial,[7] hypolipidemic[8] and DPP-IV inhibitor properties.[9] Development of synthetic routes for the construction of 1,4-thiazine backbone *via* domino approach is thus desirable.

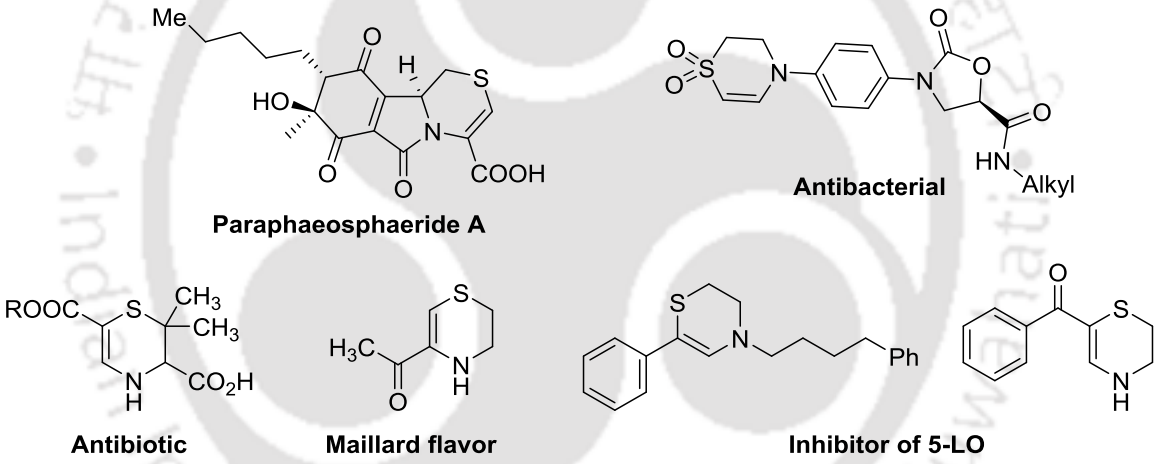

Figure 1. Representative examples of biologically active thiazine motifs.

2.1 Classical Method

The synthesis of thiomorpholine core motif involves the base promoted nucleophilic substitution of 2-bromoacetophenone with *β*-aminoethanethiol followed by condensation to provide imine, which is further reduced by $NaBH_4$ to deliver thiomorpholines (Scheme 1).[10] However, this approach has limitation due to the unavailability of the suitably substituted substrates precursors.

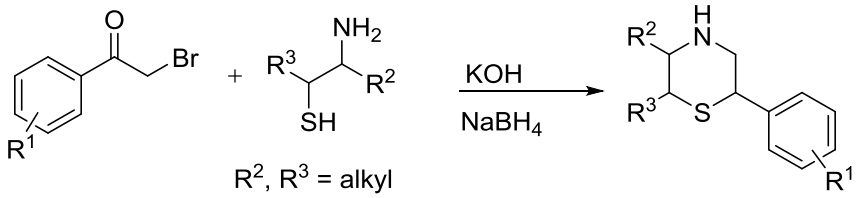

Scheme 1. Base-promoted cyclization of 2-bromoacetophenone with *β*-aminoethanethiol.

2.2 Modern Methods

2.2.1 Copper Catalysis

Sekar and co-workers constructed bicyclic-phenothiazines using the domino ring-opening of *meso*-aziridines with 2-halothiolphenol in presence of Cu-catalysis (Scheme 2).[11] This method has been successfully utilized for the synthesis of anti-histamine agent.

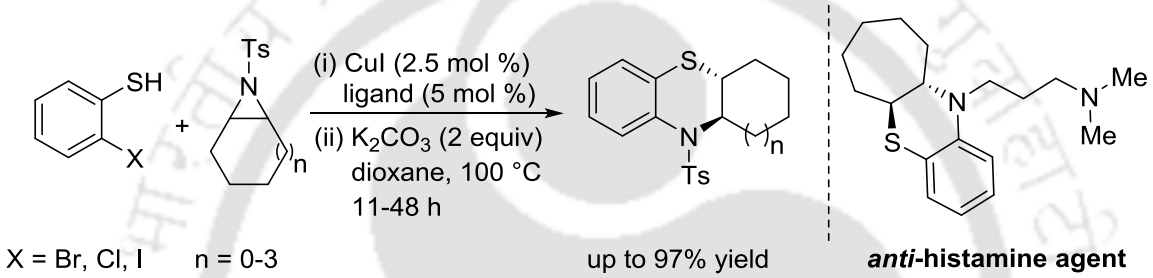

Scheme 2. Cu-catalyzed synthesis of phenothiazines.

Similar approach has been applied to the coupling of 2-phenyl-*N*-sulfonylaziridines with 2-halothiopenol under a Cu-mediated conditions. Substrates with electron-withdrawing and donating groups can be readily reacted (Scheme 3).[12]

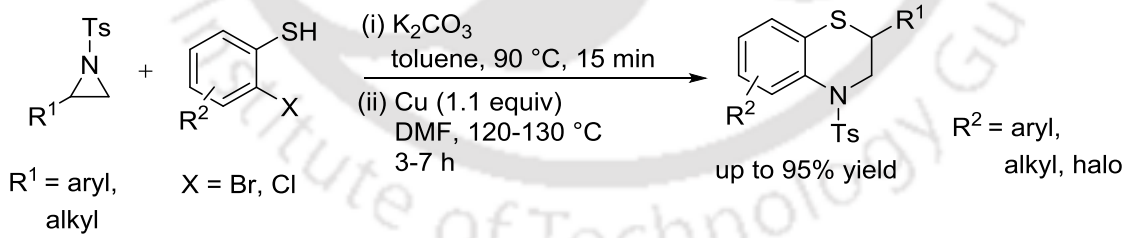

Scheme 3. Cu-mediated synthesis of benzothiazines.

Oretans and co-workers reported the synthesis of benzothiazines and 1,4-thiazines from *N*-tosyl-1,5,2,6-dithiadiazocane with lithiated nucleophile in presence of CuI in good yield (Scheme 4).[13]

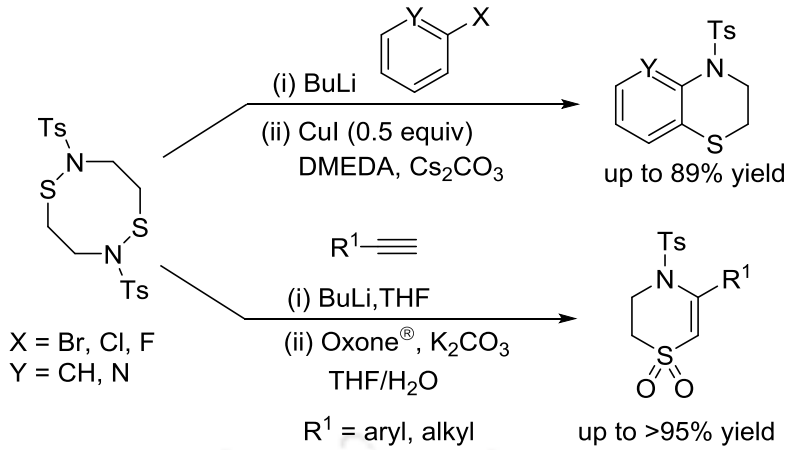

Scheme 4. Cu-mediated synthesis of 1,4-thiazines.

Wan and co-workers reported the synthesis of 3,4-dihydro-1,4-thiazines from *N*,*N*-dimethylenaminones and *β*-aminoethanethiol in presence of CuI at moderate temperature (Scheme 5).[14] The reaction occurs *via* transamination and thiolation of C(sp^2)−H bond.

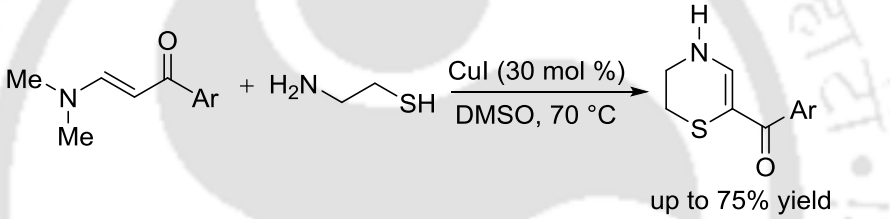

Scheme 5. Cu-catalyzed synthesis of 1,4-thiazines.

2.2.2 Iron Catalysis

Jeong and co-workers reported the synthesis of benzothiazine-4-carbonitrile from 2-aminobenzothiazole and terminal alkynes in presence of iron-catalysis under microwave irradiation (Scheme 6).[15a] The reaction involves ring expansion of 2-aminobenzothiazole, and the substrates with electron-withdrawing and donating group can be readily reacted.

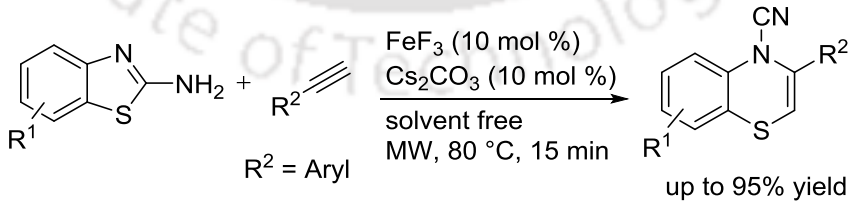

Scheme 6. Fe-catalyzed ring expansion of 2-aminobenzothiazole with terminal alkynes.

Cossy and co-workers developed a one-pot protocol to access thiomorpholines with *α*,*β*–unsaturated amino alcohols using iron-catalysis. The catalyst co-ordinates with hydroxyl group, which triggers the intramolecular cyclization by elimination of hydroxide group (Scheme 7).[15b]

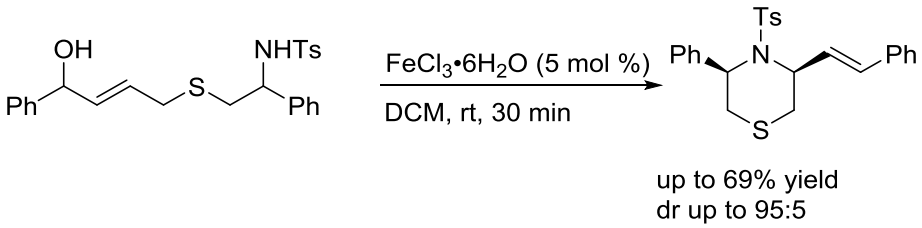

Scheme 7. Fe-catalyzed synthesis of functionalized thiomorpholines.

2.2.3 Rhodium Catalysis

Direct synthesis of *N*-sulfonyl-dihydro-1,4-thiazines is accomplished by the coupling of *N*-sulfonyl triazole through regioselective ring-opening of thiiranes. The system consists 2 mol % of $Rh_2(esp)_2$ and acetic acid as an additive in toluene (Scheme 8).[16] This reaction involves a formal [3+3]-cycloaddition followed by 1,3-azavinyl carbene insertion into the thiirane C–S bond.

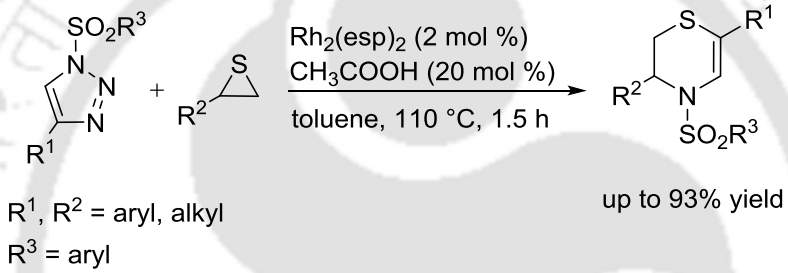

Scheme 8. Rh-catalyzed reaction of thiiranes with *N*-sulfonyl-1,2,3-triazoles.

2.3 Cycloaddition of Dithiane-2,5-diol

Commercially available 1,4-dithiane-2,5-diol is a masked dimer of mercaptoacetaldehyde. Such reagent has proved to be an attractive synthon for the construction of S-heterocycles through annulation, cycloaddition, and domino strategy. Wang and coworkers developed a DABCO-catalyzed [3+3]-cycloaddition of 1,4-dithiane-2,5-diol with azomethine imine. Several bicyclic-fused thiomorpholines have been prepared (Scheme 9).[17]

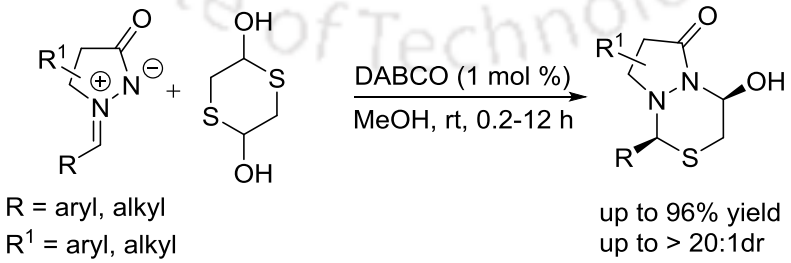

Scheme 9. DABCO-catalyzed [3+3] cycloaddition of dithianediol with azomethine imines.

Mantellini group reported the coupling of 1,4-dithiane-2,5-diol with 1,2-diaza-1,3-dienes (Scheme 10).[18] The reaction of a series of substrates has been presented to produce hydroxy-3,4-dihydro-2*H*-1,4-thiazines.

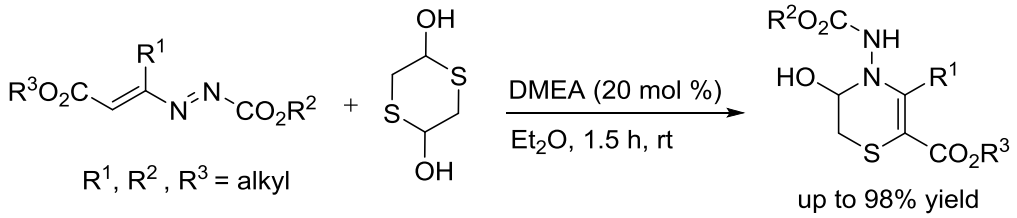

Scheme 10. Base-catalyzed cascade synthesis of 1,4-thiazines.

[3+2]-Cycloaddition of 2-mercaptocarbaldehyde with *N*-substituted maleimide reported to produce biheterocyclic in the presence of DABCO (Scheme 11).[19]

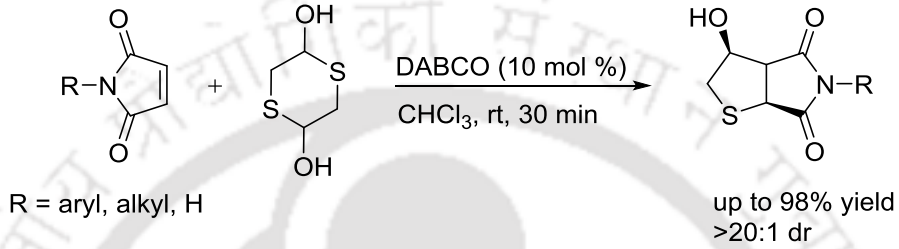

Scheme 11. [3+2]-cycloaddition of 1,4-dithiane-2,5-diol with maleimides.

2.4 Present Study

Herein synthesis of 1,4-thiazine core motifs is described through a Bi-catalyzed domino process of aziridines with 1,4-dithiane-2,5-diol. Table 1 summarizes the optimization of the conditions using 2-(*p*-toluyl)aziridine **1j** as a model substrate with 1,4-dithiane-2,5-diol **2** in presence of different Lewis acids. Gratifyingly, the reaction occurred to give 2-phenyl-4-tosyl-3,4-dihydro-2*H*-1,4-thiazine **3j** in 68% yield when the substrates were stirred employing 10 mol % $Bi(OTf)_3$ in CH_2Cl_2 at room temperature (entry 1). In a set of Lewis acids screened, $Bi(OTf)_3$, $Sc(OTf)_3$, $Yb(OTf)_3$, $Cu(OTf)_2$, $Zn(OTf)_2$ and Ag(OTf), the former furnished the best results (entries 1-6). CH_2Cl_2 was found to be the solvent of choice, whereas toluene, $(CH_2Cl)_2$, and THF produced **3j** in <62% yield (entries 7-9). At 0 °C, 1,4-thiomorpholin-3-ol **4j** was formed in 45% yield (entry 10), which led to dehydration to give **3j** at room temperature. Control experiment confirmed that **3j** was not formed in the absence of the Lewis acid.

Table 1. Optimization of the Reaction Conditions[a]

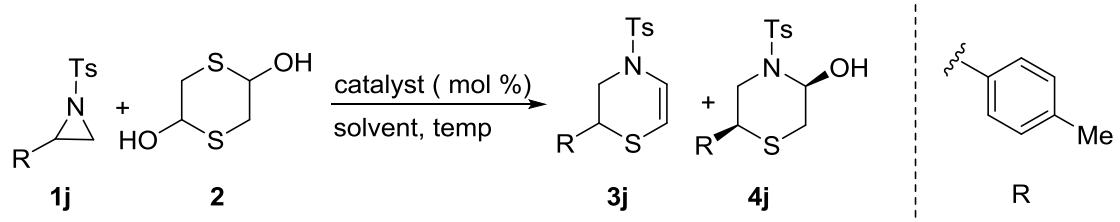

1j 2 3j 4j

Entry	Catalyst	Solvent	Time (h)	Yield (%)[b]	
				3j	**4j**
1	**$Bi(OTf)_3$**	**DCM**	**0.5**	**68**	**n.d**
2	$Sc(OTf)_3$	DCM	3	30	n.d
3	$Yb(OTf)_3$	DCM	3	n.d	n.d
4	$Cu(OTf)_2$	DCM	3	60	n.d
5	$Zn(OTf)_2$	DCM	3	10	trace
6	Ag(OTf)	DCM	3	n.d	n.d
7	$Bi(OTf)_3$	$PhCH_3$	3	20	n.d
8	$Bi(OTf)_3$	DCE	0.5	62	n.d
9	$Bi(OTf)_3$	THF	3	32	n.d
10[c]	$Bi(OTf)_3$	DCM	3	trace	45

[a]Reaction condition: Aziridine **1j** (0.5 mmol), 1,4-dithiane-2,5-diol **2** (0.3 mmol), catalyst (10 mol %), solvent (1 mL), rt. [b]Isolated yield. [c]Reaction temperature 0 °C. n.d = not detected.

Having the optimized conditions in hand, the substrate scope was studied (Table 2). 2-Phenylaziridine **1a** reacted to give 3,4-dihydro-1,4-thiazine **3a** in 62% yield. The reaction of aziridines bearing substitution at the 2-position of the aryl ring with chloro **1b** and fluoro **1c** groups gave **3b** and **3c** in 54 and 56% yields, respectively. Aziridines containing substitution at the 3-position of the aryl ring with bromo **1d**, methyl **1e** and nitro **1f** functional groups provided **3d-f** in 64-68% yields. The reaction of aziridines having substitution at the 4-position with bromo **1g**, chloro **1h**, fluoro **1i**, methyl **1j**, chloromethyl **1k** and acetate **1l** groups afforded thiazines **3g-l** in 56-68% yields. Similar results were observed with aziridine **1m** having 2,4,6-trimethyl group producing **3m** in 57% yield.

Table 2. Reaction of Various 2-Arylaziridines with 1,4-Dithane-2,5-diol[a]

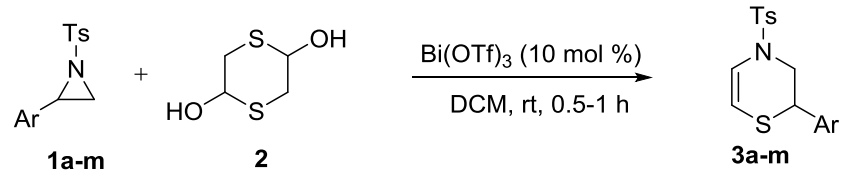

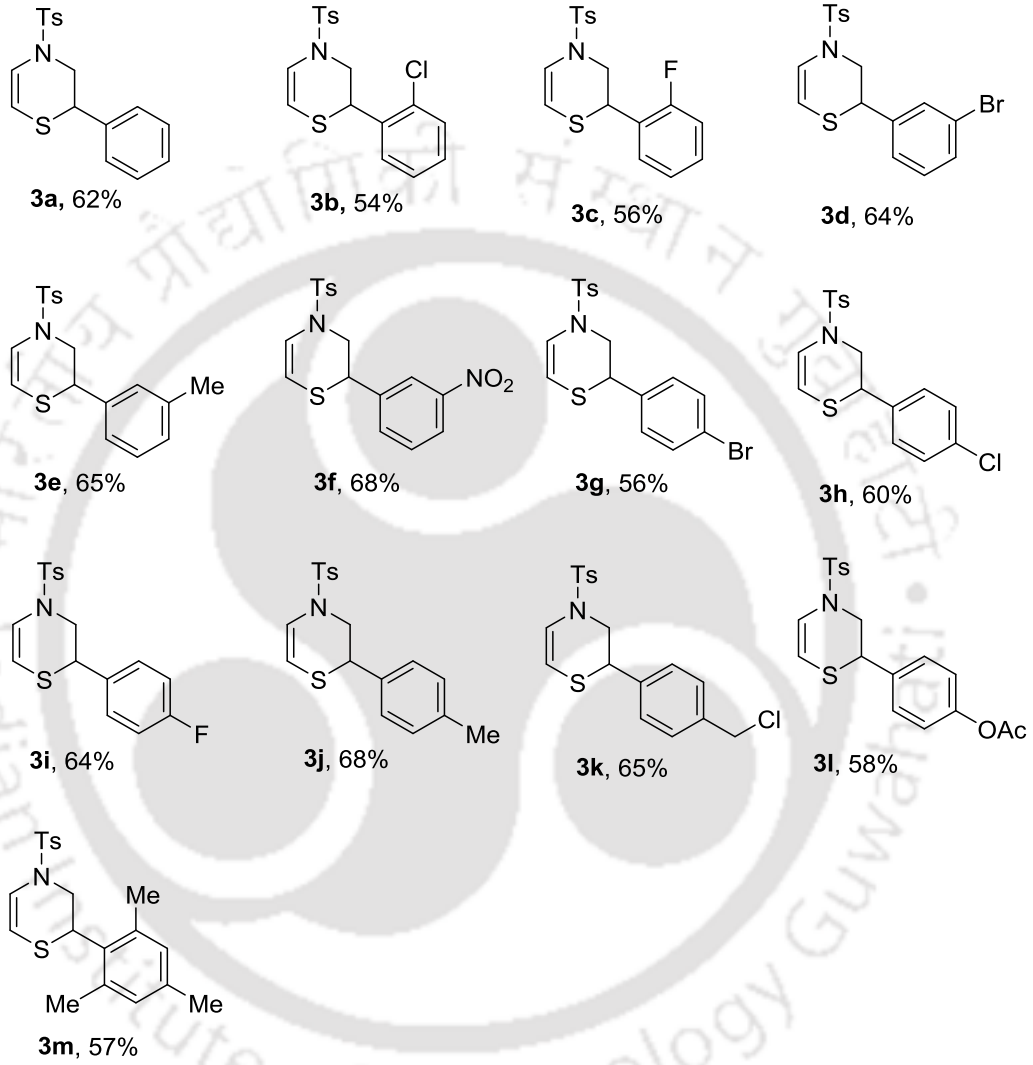

[a]Reaction conditions: Aziridine **1a-m** (0.5 mmol), **2** (0.3 mmol), $Bi(OTf)_3$ (10 mol %), CH_2Cl_2 (1 mL). [b]Isolated yield.

Table 3. Reaction of *N*-Substituted Aziridines with 1,4-dithiane-2,5-diol[a]

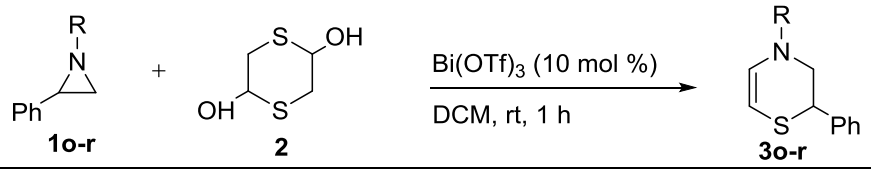

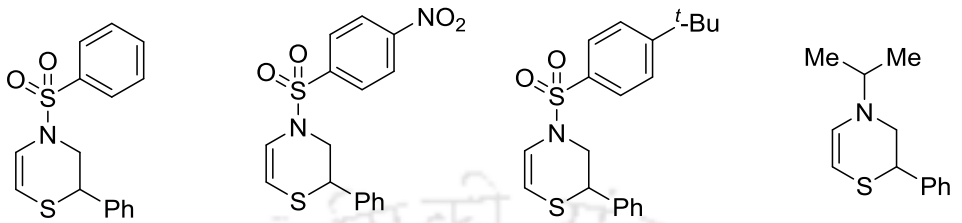

[a]Reaction conditions: Aziridine **1o-r** (0.5 mmol), **2** (0.3 mmol), $Bi(OTf)_3$ (10 mol %), CH_2Cl_2 (1 mL).
[b]Isolated yield.

Table 4. Reaction of 2-alkylaziridines with 1,4-dithiane-2,5-diol[a]

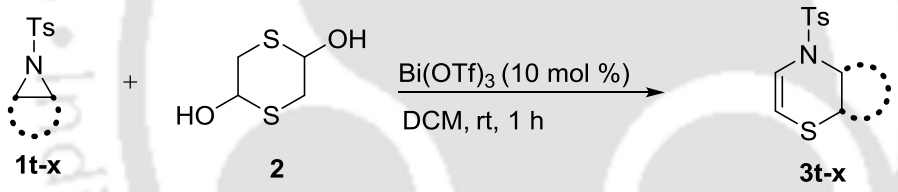

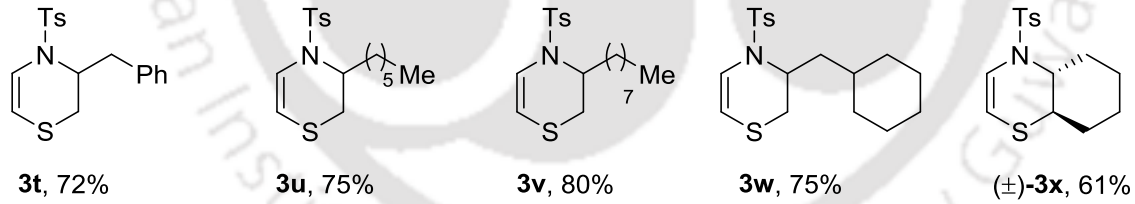

[a]Reaction conditions: Aziridine **1t-x** (0.5 mmol), **2** (0.3 mmol), $Bi(OTf)_3$ (10 mol %), CH_2Cl_2 (1 mL).
[b]Isolated yield.

The utility of the protocol was further extended to the coupling of various *N*-sulfonyl aziridines (Table 3). Aziridine **1o** having phenylsulfonyl group gave **3o** in 66% yield. Similar result observed with **1p** having 1-(4-nitrophenyl)sulfonyl group, affording **3p** in 58% yield. In addition, **1q** with 1-(4-*tert*-butylphenyl)sulfonyl group underwent reaction to afford **3q** in 64% yield. In contrast, 1-alkylaziridine **1r** was an unsuccessful substrate and the starting material was recovered intact.

Next, we explored the scope of the reaction with 2-alkylaziridines (Table 4). 2-Benzyl-1-tosylaziridine **1t** reacted to give 3-benzyl-4-tosyl-3,4-dihydro-2*H*-1,4-thiazine **3t** in 72%

yield. The reaction of **1u-v** bearing 2-hexyl and 2-octyl groups afforded 3-hexyl-4-tosyl-3,4-dihydro-*2H*-1,4-thiazine **3u** and 3-octyl-4-tosyl-3,4-dihydro-*2H*-1,4-thiazine **3v** in 75 and 80% yields, respectively. Similar results observed with 2-(cycloxhexylmethyl)-aziridine **1w** giving 3-(cyclohexylmethyl)-4-tosyl-3,4-dihydro-*2H*-1,4-thiazine **3w** in 75% yield. Furthermore, *meso*-cyclohexylaziridine **1x** reacted to afford 4-tosyl-4a,5,6,7,8,8a-hexahydro-*4H*-benzo[*b*][1,4]-thiazine **3x** in 61% yield.

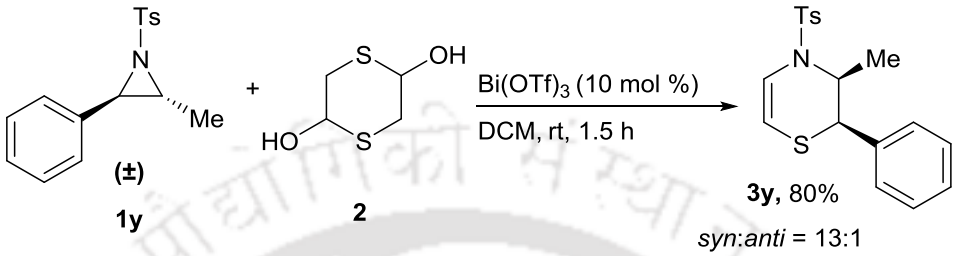

Scheme 12. Synthesis of 3-methyl-2-phenyl-4-tosyl-3,4-dihydro-*2H*-1,4-thiazine.

Table 5. Synthesis of Thiomorpholin-3-ol[a]

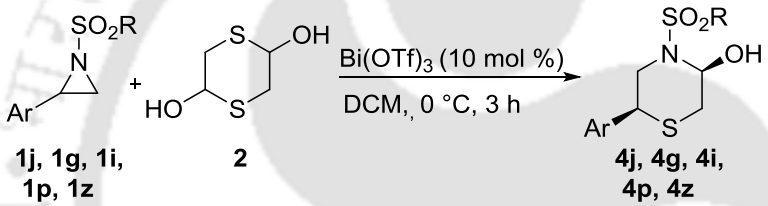

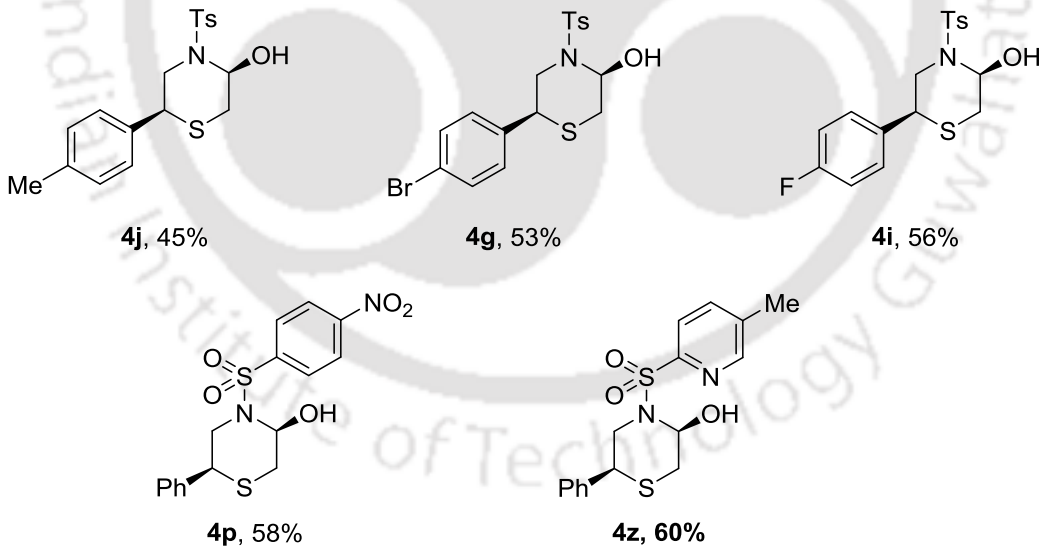

[a]Reaction conditions: Aziridine **1(j, g, i, p, z)** (0.5 mmol), **2** (0.3 mmol), $Bi(OTf)_3$ (10 mol %), CH_2Cl_2 (1 mL). [b]Isolated yield.

Finally, the reaction of 2-methyl-3-phenylaziridine **1y** was studied (Scheme 12). The reaction produced **3y** in 80% yield as a 13:1 (*syn*:*anti*) mixture of diastereomers. *Syn* isomer

was crystallized in a mixture of EtOAc and hexane and the structure was determined using a single crystal X-ray analysis (Figure 2).

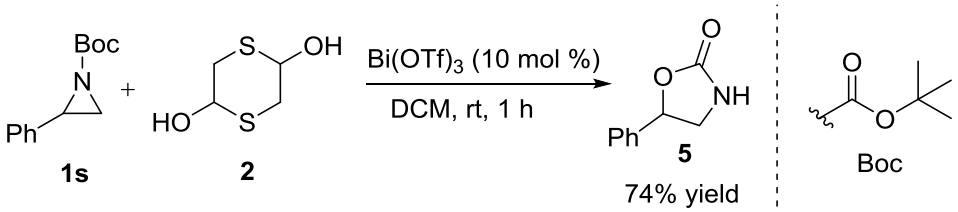

Scheme 13. Synthesis of 5-phenyloxazolidin-2-one from *N*-Boc aziridine.

The reaction was further studied with *N*-Boc aziridine **1s** and the cyclization occurred to produce the 5-phenyloxazolidin-2-one **5** in 74% yield (Scheme 13).[25] The reaction is temperature dependent. When the reaction was carried out at 0 °C, stopped at alcohol stage rather than 3,4-dihydro-1,4-thiazine (Table 5). For example, the reaction of 2-(4-bromophenyl)aziridine gave 6-(4-Bromophenyl)-4-tosylthiomorpholin-3-ol **4g** in 53% yield. Similar result observed with 2-(4-flurophenyl)aziridine to give thiomorpholin-3-ol **4i** in 56% yield. In addition, 2-phenylaziridine bearing arylsulfonyl with electron withdrawing 4-nitro group underwent reaction to give **4p** in 58% yield, whereas **1z** with *N*-(4-methylpyridinyl)-2-sulfonyl group furnished **4z** in 60% yield. Recrystallization of **4p** in $CDCl_3$ afforded crystals whose structure was determined using X-ray analysis.

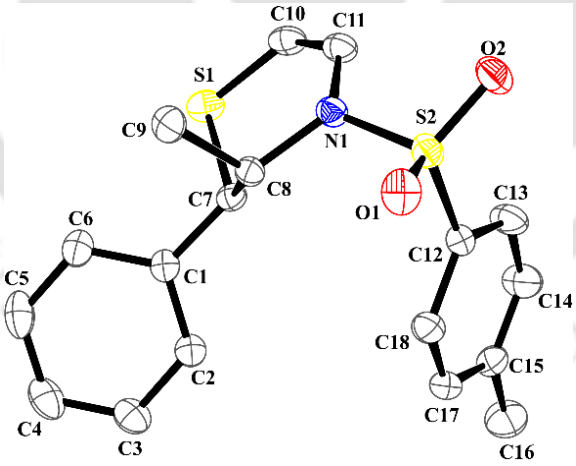

Figure 2. Crystal structure of compound **3y** (CCDC 1590250).

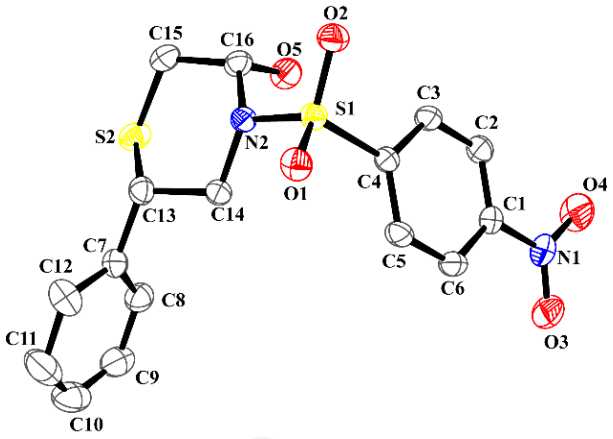

Figure 3. Crystal structure of compound **4p** (CCDC 1524781).

Regarding the reaction pathway, chelation of $Bi(OTf)_3$ with 2-arylaziridine can lead to ring opening to give carbocation **A**, which can react with masked aldehyde **2′** to yield **B**. Intramolecular cyclization of **B** can furnish **C** that can give 1,4-thiomorpholin-3-ol (0 ^{o}C). Alternatively, **C** can undergo dehydration at room temperature to furnish 3,4-dihydro-1,4-thiazines **3** to complete the catalytic cycle (Scheme 14).

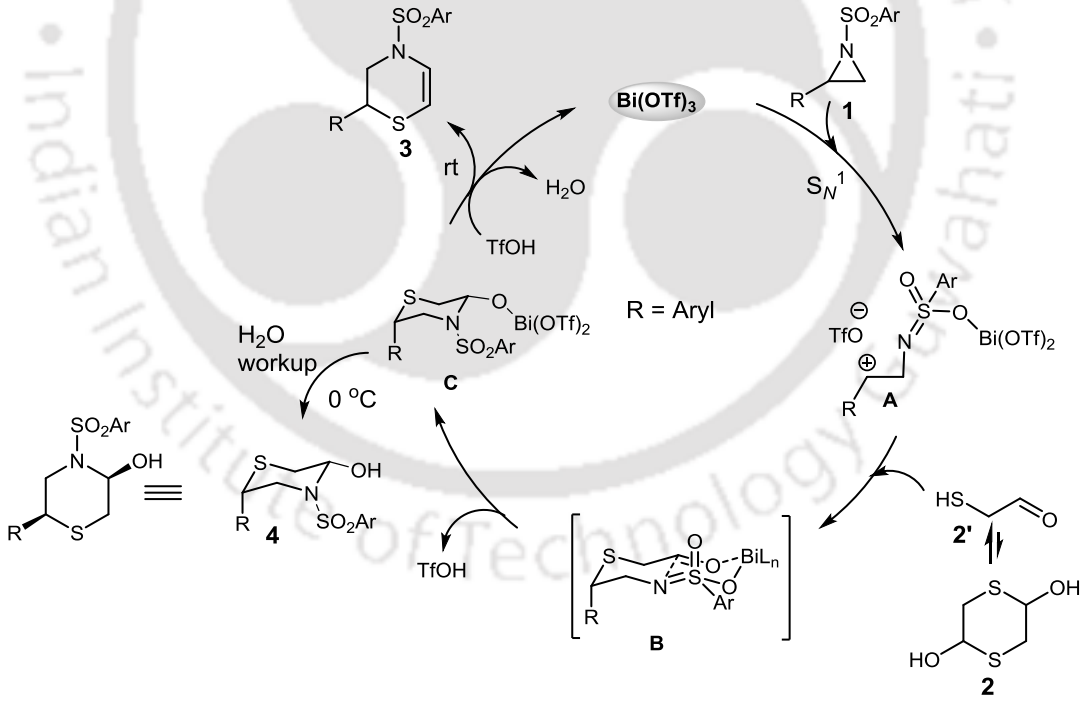

Scheme 14. Proposed catalytic cycle.

The formation of a single diastereoisomer of **4** suggests that a chair like transition state **B** is favoured, in which, the carbonyl and sulfonyl groups are *trans* to each other due to steric and electronic repulsion (please see the crystal structure of **4p**, Figure 3), whereas the transition state **B'** is disfavoured due to unfavourable interaction between the -C=O and -SO_2 groups (Figure 4).

Stereochemical Model

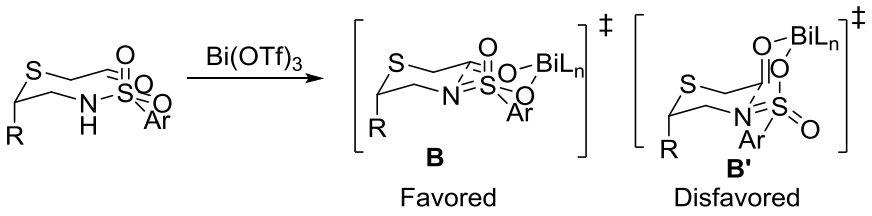

Figure 4. Proposed favoured transition state.

These results suggest that the ring opening takes place in 2-arylaziridines at the benzylic carbon due to an electronic effect, while steric effect favours in 2-alkylaziridines to occur the ring opening occurs at the less hindered methylene carbon.[26] The reaction of enantiomerically pure aziridine *(S)*-**1a** (99% ee) was studied (Scheme 15). The annulation occurred to give **3a** in 64% yield with 52:48 er, which suggests that the reaction involves a S_N1 pathway.

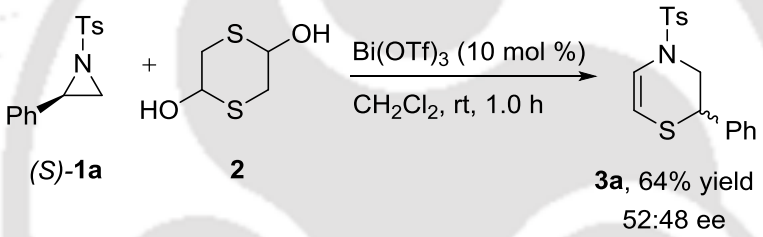

Scheme 15. Reaction of enantiomeric pure aziridine **1a** with **2.**

Table 6. Synthesis of 1,4-Thiazine 1,1-Dioxide[a]

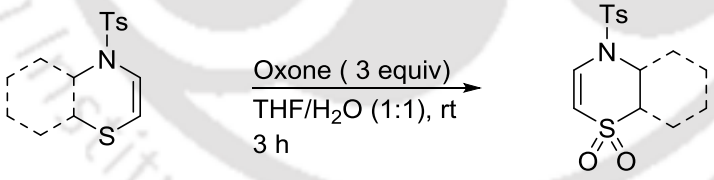

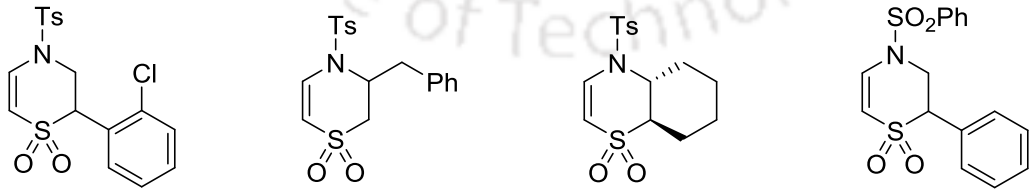

[a]Reaction conditions: **3** (0.2 mmol), Oxone (0.6 mmol), THF/H_2O (1:1) (1 mL). [b]Isolated yield.

The product can be oxidized using oxone® in THF-water (Table 6). For examples, the oxidation of **3b**, **3o, 3t** and **3x** performed as the representative examples. The reaction took place to produce **6b**, **6t** and **6x** in 92, 96 and 95% yields, respectively. Similar result

observed with 3,4-dihydro-1,4-thiazine bearing phenyl sulfonyl **3o** group giving **6o** in 90% yield.

In summary, the coupling of aziridines with 1,4-dithiane-2,5-diol is presented using a Bi-catalysis to produce 3,4-dihydro-1,4-thiazines and 1,4-thiomorpholines. The products can be oxidized to sulfones in quantitative yields. The regioselectivity and mild reaction condition are important practical aspects.

2.5 Experimental Section

General Information. Ag(OTf) (98%), $Zn(OTf)_2$ (98%), $Cu(OTf)_2$ (98%), $Bi(OTf)_3$, $Sc(OTf)_3$ (99%) and $Yb(OTf)_3$ (99.99%) were purchased from Aldrich. Aziridines were prepared as per the literature.[27] Solvents were purchased from Merck and distilled by the standard protocol prior to use. The reactions were monitored by analytical TLC on Merck silica gel G/GF 254 plates. The column chromatography was performed with SRL silica gel (100-200 mesh). NMR spectra were recorded on Bruker Avance III 600, 400 and DRX-400 Varian spectrometers using $CDCl_3$ and TMS as an internal standard. The data are accounted as follows: chemical shifts (δ ppm) (multiplicity, coupling constant (Hz), and integration). The abbreviations for multiplicity are as follows: s = singlet, d = doublet, t = triplet, q = quartet, m = multiplet and dd = doublet of doublet. Melting points were determined with a Büchi B-540 apparatus and are uncorrected. FT-IR spectra recorded on a Perkin Elmer spectrometer. HRMS were analyzed with Agilent Q-TOF 6500. HPLC analysis was carried out using Waters-2489 equipped with Chiralcel OJ-H.

General Procedure for the Synthesis of 3,4-Dihydro-1,4-Thiazines. Aziridine (0.5 mmol), 1,4-dithiane-2,5-diol (0.3 mmol) and $Bi(OTf)_3$ (10 mol %) were stirred in CH_2Cl_2 (1 mL) at room temperature. The progress of the reaction was monitored by TLC using ethyl acetate and hexane as an eluent. After completion, the solvent was evaporated and the residue was purified by silica gel column chromatography using ethyl acetate and hexane as solvent.

General Procedure for the Synthesis of Thiomorpholines. Aziridine (0.5 mmol), 1,4-dithiane-2,5-diol (0.3 mmol) and $Bi(OTf)_3$ (10 mol %) were stirred in CH_2Cl_2 (1 mL) at 0° C. The progress of the reaction was monitored by TLC using ethyl acetate and hexane. The reaction mixture was quenched with water and the aqueous layer was extracted using CH_2Cl_2 (3 x 10 mL). Drying (Na_2SO_4) and evaporation of the solvent gave a residue, which was purified on a silica gel column chromatography using ethyl acetate and hexane as eluent.

General Procedure for the Synthesis of 1,4-Thiazine 1,1-dioxide. To a stirred solution of 1,4-thiazines (0.2 mmol) in THF/H_2O (1 mL, 1:1) was added oxone® (0.6 mmol) and allowed the reaction mixture to stir at room temperature. The progress of the reaction was monitored by TLC using ethyl acetate and hexane. After completion, THF was evaporated and the aqueous solution was extracted using ethyl acetate (3 x 10 mL). The combined organic solution was washed with saturated NaCl (1 x 5 ml) and water (1 x 5 mL). Drying (Na_2SO_4) and evaporation of the solvent gave a residue that was purified on silica gel column chromatography using ethyl acetate and hexane.

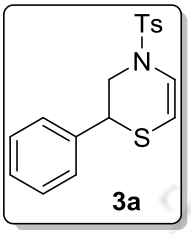

2-Phenyl-4-tosyl-3,4-dihydro-*2H*-1,4-thiazine 3a. Analytical TLC on silica gel, 1:9 ethyl acetate/hexane R_f = 0.42; yellow liquid; yield 62% (103 mg). ^{1}H NMR (600 MHz, $CDCl_3$) δ 7.67 (d, *J* = 8.4 Hz, 2H), 7.36 (d, *J* = 7.8 Hz, 2H), 7.34-7.30 (m, 3H), 7.14-7.12 (m, 2H), 6.96 (d, *J* = 8.4 Hz, 1H), 5.59 (d, *J* = 8.4 Hz, 1H), 4.28 (dd, *J* = 13.2, 2.4 Hz, 1H), 3.60 (dd, *J* = 10.2, 2.4 Hz, 1H), 3.30 (dd, *J* = 13.8, 10.2 Hz, 1H), 2.47 (s, 3H). ^{13}C NMR (150 MHz, $CDCl_3$) δ 144.5, 137.8, 135.1, 130.3, 129.2, 128.6, 128.0, 127.4, 120.3, 103.7, 50.4, 41.9, 21.9. FT-IR (neat) 3064, 3030, 2924, 2853, 1613, 1597, 1494, 1453, 1360, 1296, 1166, 1092, 945, 814 cm^{-1}. HRMS (ESI) m/z $[M+H]^+$ calcd for $C_{17}H_{17}NO_2S_2$ 332.0779, found 332.0768. HPLC: 52:48 ee [CHIRALCEL OJ-H, hexane/iPrOH = 70:30, flow rate: 1 mL /min, λ = 254 nm, t_R = 14.22 min (major), 21.31 min (minor)].

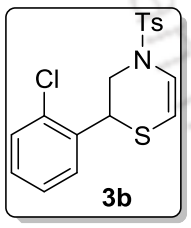

2-(2-Chlorophenyl)-4-tosyl-3,4-dihydro-*2H*-1,4-thiazine 3b. Analytical TLC on silica gel, 1:9 ethyl acetate/hexane R_f = 0.42; gummy liquid; yield 54% (99 mg). ^{1}H NMR (600 MHz, $CDCl_3$) δ 7.65 (d, *J* = 8.4 Hz, 2H), 7.33-7.729 (m, 4H), 7.24-7.20 (m, 2H), 7.01 (d, *J* = 8.4 Hz, 1H), 5.58 (d, *J* = 8.4 Hz, 1H), 4.24-4.18 (m, 2H), 3.44 (dd, *J* = 13.2, 9.0 Hz, 1H), 2.43 (s, 3H). ^{13}C NMR (150 MHz, $CDCl_3$) δ 144.3, 135.4, 135.2, 133.4 130.2, 129.9, 129.5, 129.4, 127.8, 127.3, 120.4, 102.5, 48.8, 37.8, 21.8. FT-IR (neat) 3067, 2956, 2924, 2854, 1726, 1611, 1597, 1468, 1447, 1342, 1092, 1055, 938, 813 cm^{-1}. HRMS (ESI) m/z $[M+H]^+$ calcd for $C_{17}H_{16}ClNO_2S_2$ 366.0389, found 366.0394.

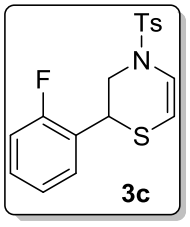

2-(2-Fluorophenyl)-4-tosyl-3,4-dihydro-*2H*-1,4-thiazine 3c. Analytical TLC on silica gel, 1:19 ethyl acetate/hexane R_f = 0.42; yellow solid; yield 56% (98 mg). Mp 86-87 ^{o}C. ^{1}H NMR (600 MHz, $CDCl_3$) δ 7.65 (d, *J* = 7.8 Hz, 2H), 7.33 (d, *J* = 7.8 Hz, 2H), 7.28-7.22 (m, 2H), 7.10 (t, *J* = 7.8 Hz, 1H), 7.02 (t, *J* = 9.0 Hz, 1H), 6.96 (d, *J* = 8.4 Hz, 1H), 5.58 (d, *J* = 8.4 Hz, 1H), 4.25

(dd, *J* = 13.2, 2.4 Hz, 1H), 4.0 (dd, *J* = 9.0, 2.4 Hz, 1H), 3.43 (dd, *J* = 13.8, 9.6 Hz, 1H), 2.44 (s, 3H). ^{13}C NMR (150 MHz, $CDCl_3$) δ 160.9 (d, *J* = 246.0 Hz), 144.4, 135.0, 130.2, 130.0, 129.9, 129.4 (d, *J* = 3.0 Hz), 127.2, 125.0, 124.9, 120.4, 115.9 (d, *J* = 21.0 Hz), 103.1, 49.2, 34.2 (d, *J* = 4.5 Hz), 21.8. FT-IR (KBr) 2964, 2925, 2853, 1641, 1492, 1456, 1361, 1166, 1097, 937, 791 cm^{-1}. HRMS (ESI) m/z $[M+H]^+$ calcd for $C_{17}H_{16}FNO_2S_2$ 350.0685, found 350.0686.

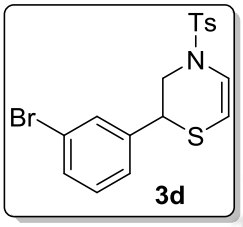

2-(3-Bromophenyl)-4-tosyl-3,4-dihydro-*2H*-1,4-thiazine 3d. Analytical TLC on silica gel, 1:9 ethyl acetate/hexane R_f = 0.42; gummy liquid; yield 64% (131 mg). ^{1}H NMR (600 MHz, $CDCl_3$) δ 7.65 (d, *J* = 8.4 Hz, 2H), 7.43-7.41 (m, 1H), 7.36 (d, *J* = 7.8 Hz, 2H), 7.264-7.261 (m, 1H), 7.19 (t, *J* = 7.8 Hz, 1H), 7.09 (d, *J* = 7.8 Hz, 1H), 6.97 (d, *J* = 9.0 Hz, 1H), 5.56 (d, *J* = 8.4 Hz, 1H), 4.23 (dd, *J* = 13.2, 2.4 Hz, 1H), 3.60 (dd, *J* = 9.0, 2.4 Hz, 1H), 3.31 (dd, *J* = 13.8, 9.6 Hz, 1H), 2.47 (s, 3H). ^{13}C NMR (150 MHz, $CDCl_3$) δ 144.6, 140.2, 134.9, 131.7, 131.1, 130.7, 130.3, 127.3, 126.7, 123.1, 120.5, 102.9, 50.1, 41.4, 21.8. FT-IR (neat) 3065, 2956, 2494, 2853, 1614, 1595, 1568, 1474, 1360, 1166, 1092 cm^{-1}. HRMS (ESI) m/z $[M+H]^+$ calcd for $C_{17}H_{16}BrNO_2S_2$ 409.9884, found 409.9883.

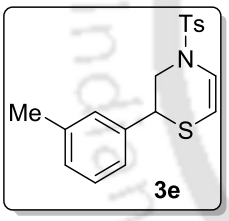

2-(*m*-Tolyl)-4-tosyl-3,4-dihydro-*2H*-1,4-thiazine 3e. Analytical TLC on silica gel, 1:9 ethyl acetate/hexane R_f = 0.43; gummy liquid; yield 65% (112 mg). ^{1}H NMR (600 MHz, $CDCl_3$) δ 7.67 (d, *J* = 8.4 Hz, 2H), 7.36 (d, *J* = 7.8 Hz, 2H), 7.22 (t, *J* = 7.8 Hz, 1H), 7.12 (d, *J* = 7.2 Hz, 1H), 6.95-6.92 (m, 3H), 5.58 (d, *J* = 8.4 Hz, 1H), 4.28 (dd, *J* = 13.8, 2.4 Hz, 1H), 3.58 (d, *J* = 9.6, 2.4 Hz, 1H), 3.28 (dd, *J* = 13.8, 10.2 Hz, 1H), 2.47 (s, 3H), 2.33 (s, 3H). ^{13}C NMR (150 MHz, $CDCl_3$) δ 144.4, 139.0, 137.7, 135.1, 130.2, 129.4, 129.1, 128.7, 127.4, 125.1, 120.3, 103.7, 50.4, 41.9, 21.8, 21.6. FT-IR (neat) 2955, 2924, 2853, 1638, 1463, 1377, 1163, 1091, 812 cm^{-1}. HRMS (ESI) m/z $[M+H]^+$ calcd for $C_{18}H_{19}NO_2S_2$ 346.0935, found 346.0939.

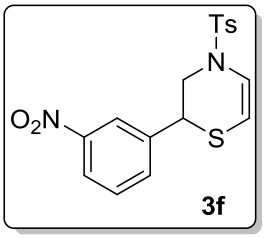

2-(3-Nitrophenyl)-4-tosyl-3,4-dihydro-*2H*-1,4-thiazine 3f. Analytical TLC on silica gel, 1:9 ethyl acetate/hexane R_f = 0.40; yellow liquid; yield 68% (128 mg). ^{1}H NMR (600 MHz, $CDCl_3$) δ 8.14-8.12 (m, 1H), 7.98-7.97 (m, 1H), 7.61 (d, *J* = 8.4 Hz, 2H), 7.53-7.48 (m, 2H),7.34 (d, *J* = 7.8 Hz, 2H), 7.01 (d, *J* = 8.4 Hz, 1H), 5.58 (d, *J* = 8.4 Hz, 1H), 4.18 (dd, *J* = 13.2, 2.4 Hz, 1H), 3.81 (dd, *J* = 9.0, 2.4 Hz, 1H), 3.49 (dd, *J* = 13.2, 8.4 Hz, 1H), 2.46 (s, 3H). ^{13}C NMR (150 MHz, $CDCl_3$) δ 148.6, 144.8, 140.3,

134.9, 134.1, 130.3, 130.1, 127.2, 123.5, 123.2, 120.9, 102.5, 49.8, 41.3, 21.8. FT-IR (neat) 3086, 2924, 2854, 1614, 1530, 1350, 1165, 1092, 948, 812 cm^{-1}. HRMS (ESI) m/z $[M+H]^+$ calcd for $C_{17}H_{16}N_2O_4S_2$ 377.0630, found 377.0639.

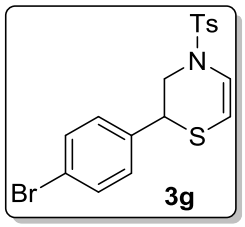

2-(4-Bromophenyl)-4-tosyl-3,4-dihydro-*2H*-1,4-thiazine 3g. Analytical TLC on silica gel, 1:9 ethyl acetate/hexane R_f = 0.42; gummy liquid; yield 56% (115 mg). ^{1}H NMR (600 MHz, $CDCl_3$) δ 7.62 (d, *J* = 7.8 Hz, 2H), 7.43 (d, *J* = 8.4 Hz, 2H), 7.35 (d, *J* = 7.8, 2H), 7.01 (d, *J* = 8.4 Hz, 2H), 6.96 (d, *J* = 8.4 Hz, 1H), 5.56 (d, *J* = 9.0 Hz, 1H), 4.20 (dd, *J* = 13.2, 2.4 Hz, 1H), 3.63 (dd, *J* = 9.6, 2.4 Hz, 1H), 3.33 (dd, *J* = 13.2, 9.0 Hz, 1H), 2.47 (s, 3H). ^{13}C NMR (150 MHz, $CDCl_3$) δ 144.5, 137.0, 135.1, 132.2, 130.3, 129.6, 127.3, 122.6, 120.5, 102.9, 50.1, 41.4, 21.9. FT-IR (neat) 3085, 2956, 2924, 2853, 1637, 1597, 1488, 1359, 1165, 1010, 814 cm^{-1}. HRMS (ESI) m/z $[M+H]^+$ calcd for $C_{17}H_{16}BrNO_2S_2$ 409.9884, found 409.9884.

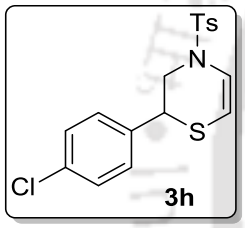

2-(4-Chlorophenyl)-4-tosyl-3,4-dihydro-*2H*-1,4-thiazine 3h. Analytical TLC on silica gel, 1:9 ethyl acetate/hexane R_f = 0.42; colorless solid; yield 60% (110 mg). Mp 103-104 ^{o}C. ^{1}H NMR (600 MHz, $CDCl_3$) δ 7.63 (d, *J* = 8.4 Hz, 2H), 7.35 (d, *J* = 8.4 Hz, 2H), 7.28-7.26 (m, 2H), 7.08 (d, *J* = 8.4 Hz, 2H), 6.97 (d, *J* = 8.4 Hz, 1H), 5.56 (d, *J* = 8.4 Hz, 1H), 4.20 (dd, *J* = 13.2, 1.8 Hz, 1H), 3.65 (dd, *J* = 9.6, 2.4 Hz, 1H), 3.33 (dd, *J* = 13.2, 9.0 Hz, 1H), 2.47 (s, 3H). ^{13}C NMR (150 MHz, $CDCl_3$) δ 144.5, 136.5, 135.1, 134.5, 130.2, 129.32, 129.31, 127.3, 120.5, 103.0, 50.1, 41.3, 21.9. FT-IR (KBr) 3089, 2956, 2924, 2853, 1637, 1599, 1464, 1360, 1165, 1090, 1014 cm^{-1}. HRMS (ESI) m/z $[M+H]^+$ calcd for $C_{17}H_{16}ClNO_2S_2$ 366.0389, found 366.0393.

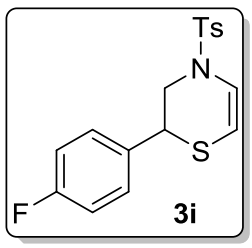

2-(4-Fluorophenyl)-4-tosyl-3,4-dihydro-*2H*-1,4-thiazine 3i. Analytical TLC on silica gel, 1:9 ethyl acetate/hexane R_f = 0.42; colorless solid; yield 64% (112 mg). Mp 150-151 ^{o}C. ^{1}H NMR (600 MHz, $CDCl_3$) δ 7.65 (d, *J* = 7.8 Hz, 2H), 7.36 (d, *J* = 7.8 Hz, 2H), 7.11 (m, 2H), 7.01 (t, *J* = 8.4 Hz, 2H), 6.96 (d, *J* = 8.4 Hz, 1H), 5.57 (d, *J* = 8.4 Hz, 1H), 4.22 (dd, *J* = 13.2, 1.8 Hz, 1H), 3.63 (dd, *J* = 9.6, 2.4 Hz, 1H), 3.29 (dd, *J* = 13.2, 9.6 Hz, 1H), 2.47 (s, 3H). ^{13}C NMR (150 MHz, $CDCl_3$) δ 163.6 (d, *J* = 247.5 Hz), 144.5, 135.1, 133.7 (d, *J* = 4.5 Hz), 130.2, 129.7, 129.6, 127.3, 120.4, 116.2 (d, *J* = 21.0 Hz), 103.3, 50.3, 41.2, 21.8. FT-IR (KBr) 3063, 2958, 2925, 2854, 1641, 1613, 1511, 1463,

1363, 1265, 965, 814 cm^{-1}. HRMS (ESI) m/z $[M+H]^+$ calcd for $C_{17}H_{16}FNO_2S_2$ 350.0685, found 350.0687.

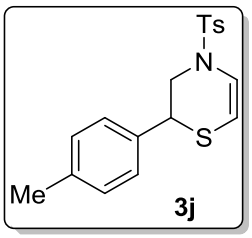

2-(*p*-Tolyl)-4-tosyl-3,4-dihydro-*2H*-1,4-thiazine 3j. Analytical TLC on silica gel, 1:9 ethyl acetate/hexane R_f = 0.40; brown liquid 68% (118 mg). ^1H NMR (600 MHz, $CDCl_3$) δ 7.66 (d, *J* = 8.4 Hz, 2H), 7.36 (d, *J* = 8.4 Hz, 2H), 7.14 (d, *J* = 8.4 Hz, 2H), 7.03 (d, *J* = 7.8 Hz, 2H), 6.95 (d, *J* = 8.4 Hz, 1H), 5.58 (d, *J* = 8.4 Hz, 1H), 4.26 (dd, *J* = 13.2, 2.4 Hz, 1H), 3.58 (dd, *J* = 9.6, 2.4 Hz, 1H), 3.28 (dd, *J* = 13.8, 10.2 Hz, 1H), 2.47 (s, 3H), 2.33 (s, 3H). ^{13}C NMR (150 MHz, $CDCl_3$) δ 144.4, 138.5, 135.0, 134.8, 130.2, 129.8, 127.8, 127.3, 120.2, 103.8, 50.4, 41.6, 21.8, 21.3. FT-IR (neat) 2955, 2923, 2853, 1633, 1599, 1514, 1461, 1359, 1165, 1092, 949, 814 cm^{-1}. HRMS (ESI) m/z $[M+H]^+$ calcd for $C_{18}H_{19}NO_2S_2$ 346.0935, found 346.0943.

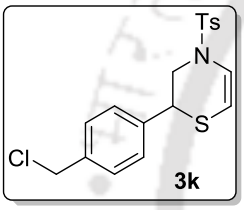

2-(4-(Chloromethyl)phenyl)-4-tosyl-3,4-dihydro-*2H*-1,4-thiazine 3k. Analytical TLC on silica gel, 1:9 ethyl acetate/hexane R_f = 0.42; colorless solid; yield 65% (129 mg). Mp 149-150 ^oC. ^1H NMR (600 MHz, $CDCl_3$) δ 7.66 (d, *J* = 8.4 Hz, 2H), 7.36-7.34 (m, 4H), 7.14 (d, *J* = 7.8 Hz, 2H), 6.96 (d, *J* = 8.4 Hz, 1H), 5.57 (d, *J* = 8.4 Hz, 1H), 4.56 (s, 2H), 4.25 (dd, *J* = 13.2, 1.8 Hz, 1H), 3.63 (dd, *J* = 9.6, 2.4 Hz, 1H), 3.30 (dd, *J* = 13.2, 9.6 Hz, 1H), 2.47 (s, 3H). ^{13}C NMR (150 MHz, $CDCl_3$) δ 144.5, 138.1, 137.9, 135.0, 130.3, 129.4, 128.4, 127.3, 120.4, 103.3, 50.2, 45.8, 41.6, 21.9. FT-IR (KBr) 3027, 2956, 2923, 2852, 1638, 1359, 1165, 1091, 938, 813 cm^{-1}. HRMS (ESI) m/z $[M+NH_4]^+$ calcd for $C_{18}H_{18}ClNO_2S_2$ 397.0806, found 397.0808.

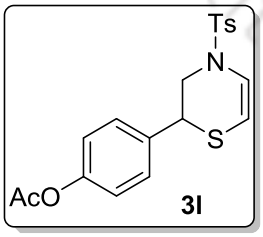

4-(4-Tosyl-3,4-dihydro-*2H*-1,4-thiazin-2-yl)phenyl acetate 3l. Analytical TLC on silica gel, 1:9 ethyl acetate/hexane R_f = 0.23; colorless liquid; yield 58% (118 mg). ^1H NMR (600 MHz, $CDCl_3$) δ 7.66 (d, *J* = 8.4 Hz, 2H), 7.36 (d, *J* = 8.4 Hz, 2H), 7.15 (d, *J* = 8.4 Hz, 2H), 7.05 (d, *J* = 8.4 Hz, 2H), 6.96 (d, *J* = 8.4 Hz, 1H), 5.57 (d, *J* = 9.0 Hz, 1H), 4.26 (dd, *J* = 13.2, 1.8 Hz, 1H), 3.63 (dd, *J* = 9.6, 2.4 Hz, 1H), 3.27 (dd, *J* = 13.8, 9.6 Hz, 1H), 2.46 (s, 3H), 2.30 (s, 3H). ^{13}C NMR (150 MHz, $CDCl_3$) δ 169.6, 150.8, 144.5, 135.4, 135.0, 130.3, 129.2, 127.4, 122.4, 120.4, 103.3, 50.3, 41.3, 21.9, 21.3. FT-IR (neat) 3081, 2958, 2923, 2853, 1763, 1634, 1506, 1362, 1200, 1165, 1091, 950 cm^{-1}. HRMS (ESI) m/z $[M+NH_4]^+$ calcd for $C_{19}H_{19}NO_4S_2$ 407.1094, found 407.1101.

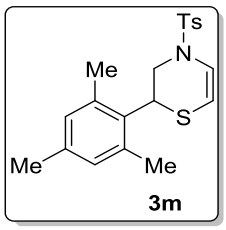

2-Mesityl-4-tosyl-3,4-dihydro-*2H*-1,4-thiazine 3m. Analytical TLC on silica gel, 1:9 ethyl acetate/hexane R_f = 0.44; gummy liquid; yield 57% (108 mg). ^{1}H NMR (600 MHz, $CDCl_3$) δ 7.69 (d, *J* = 8.4 Hz, 2H), 7.34 (d, *J* = 7.8 Hz, 2H), 6.99 (d, *J* = 8.4 Hz, 1H), 6.78 (br s, 2H), 5.56 (d, *J* = 8.4 Hz, 1H), 4.19 (dd, *J* = 13.8, 1.8 Hz, 1H), 4.04 (dd, *J* = 10.2, 2.4 Hz, 1H), 3.83 (dd, *J* = 13.8, 10.2 Hz, 1H), 2.44 (s, 3H), 2.39 (s, 3H), 2.22 (s, 3H), 1.86 (s, 3H). ^{13}C NMR (150 MHz, $CDCl_3$) δ 144.3, 138.0, 137.2, 135.5, 131.7, 130.2, 130.1, 129.5, 127.5, 120.2, 103.7, 46.9, 39.1, 21.8, 20.9, 20.8, 20.4. FT-IR (neat) 2956, 2922, 2855, 1612, 1449, 1359, 1166, 1091, 1042, 938, 814 cm^{-1}. HRMS (ESI) m/z $[M+H]^+$ calcd for $C_{20}H_{23}NO_2S_2$ 374.1248, found 374.1236.

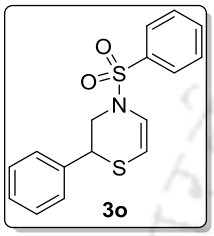

2-Phenyl-4-(phenylsulfonyl)-3,4-dihydro-*2H*-1,4-thiazine 3o. Analytical TLC on silica gel, 1:9 ethyl acetate/hexane R_f = 0.42; colorless liquid; yield 66% (105 mg). ^{1}H NMR (600 MHz, $CDCl_3$) δ 7.79 (d, *J* = 7.2 Hz, 2H), 7.67 (t, *J* = 7.2 Hz, 1H), 7.57 (t, *J* = 8.4 Hz, 2H), 7.34-7.30 (m, 3H), 7.13-7.11 (m, 2H), 6.98 (d, *J* = 8.4 Hz, 1H), 5.61 (d, *J* = 8.4 Hz, 1H), 4.29 (dd, *J* = 13.2, 2.4 Hz, 1H), 3.57 (dd, *J* = 10.2, 2.4 Hz, 1H), 3.33 (dd, *J* = 13.8, 10.2 Hz, 1H). ^{13}C NMR (150 MHz, $CDCl_3$) δ 138.1, 137.7, 133.5, 129.7, 129.2, 128.7, 128.0, 127.3, 120.2, 104.0 50.4, 41.9. FT-IR (neat) 3029, 2955, 2923, 2852, 1637, 1446, 1360, 1296, 1169, 1092, 1054, 944 cm^{-1}. HRMS (ESI) m/z $[M+H]^+$ calcd for $C_{16}H_{15}NO_2S_2$ 318.0622, found 318.0626.

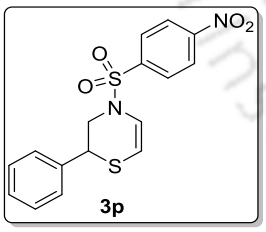

4-((4-Nitrophenyl)sulfonyl)-2-phenyl-3,4-dihydro-*2H*-1,4-thiazine 3p. Analytical TLC on silica gel, 1:9 ethyl acetate/hexane R_f = 0.40; orange solid; yield 58% (106 mg). Mp 120-121 ^{o}C. ^{1}H NMR (600 MHz, $CDCl_3$) δ 8.38 (d, *J* = 9.0 Hz, 2H), 7.93 (d, *J* = 8.4 Hz, 2H), 7.32-7.29 (m, 3H), 7.16-7.14 (m, 2H), 6.95 (d, *J* = 8.4 Hz, 1H), 5.69 (d, *J* = 8.4 Hz, 1H), 4.30 (dd, *J* = 13.2, 2.4 Hz, 1H), 3.80 (dd, *J* = 9.0, 2.4 Hz, 1H), 3.44 (dd, *J* = 13.2, 9.0 Hz, 1H). ^{13}C NMR (150 MHz, $CDCl_3$) δ 150.5, 143.8, 137.4, 129.3, 128.8, 128.4, 127.9, 124.9, 119.3, 105.4, 50.4, 42.4. FT-IR (KBr) 2960, 2925, 2854, 1638, 1530, 1454, 1349, 1169, 1091, 947, 855, 767 cm^{-1}. HRMS (ESI) m/z $[M+H]^+$ calcd for $C_{16}H_{14}N_2O_4S_2$ 363.0473, found 363.0476.

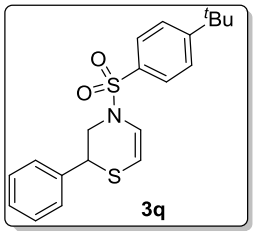

4-((4-(*tert*-Butyl)phenyl)sulfonyl)-2-phenyl-3,4-dihydro-*2H*-1,4-thiazine 3q. Analytical TLC on silica gel, 1:9 ethyl acetate/hexane R_f = 0.54; gummy liquid; yield 64% (120 mg). ^{1}H NMR (600 MHz, $CDCl_3$) δ 7.70 (d, *J* = 9.0 Hz, 2H), 7.57 (d, *J* = 9.0 Hz, 2H), 7.33-7.28 (m, 3H), 7.13 (dd, *J* = 7.8, 1.8 Hz, 2H), 6.99 (d, *J* = 8.4 Hz, 1H), 5.58 (d, *J* = 8.4 Hz, 1H), 4.27 (dd, *J* = 13.2, 2.4 Hz, 1H), 3.61 (dd, *J* = 9.6, 2.4 Hz, 1H), 3.33 (dd, *J* = 13.2, 9.6 Hz, 1H), 1.37 (s, 9H). ^{13}C NMR (150 MHz, $CDCl_3$) δ 157.4, 137.9, 134.9, 129.2, 128.6, 128.0, 127.2, 126.6, 120.4, 103.3, 50.3, 42.0, 35.5, 31.3. FT-IR (neat) 2962, 2923, 2853, 1640, 1453, 1360, 1169, 1113, 1086, 940, 756 cm^{-1}. HRMS (ESI) m/z $[M+H]^+$ calcd for $C_{20}H_{23}NO_2S_2$ 374.1248, found 374.1256.

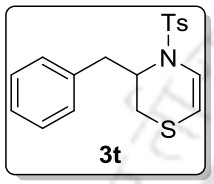

3-Benzyl-4-tosyl-3,4-dihydro-*2H*-1,4-thiazine 3t. Analytical TLC on silica gel, 1:9 ethyl acetate/hexane R_f = 0.50; yellow liquid; yield 72% (125 mg). ^{1}H NMR (600 MHz, $CDCl_3$) δ 7.65 (d, *J* = 8.4 Hz, 2H), 7.32-7.28 (m, 6H), 7.25 (t, *J* = 7.2 Hz, 1H), 6.92 (d, *J* = 8.4 Hz, 1H), 5.45 (dd, *J* = 8.4, 2.4 Hz, 1H), 4.36-4.32 (m, 1H), 3.02 (dd, *J* = 13.2, 10.2 Hz, 1H), 2.92 (dd, *J* = 13.2, 4.8 Hz, 1H), 2.41 (s, 3H), 2.37-2.34 (m, 1H), 2.01 (dd, *J* = 13.2, 3.0 Hz, 1H). ^{13}C NMR (150 MHz, $CDCl_3$) δ 144.2, 137.5, 135.4, 130.2, 129.9, 128.8, 127.2, 127.1, 119.2, 101.6, 52.7, 38.9, 25.5, 21.8. FT-IR (neat) 3056, 3030, 2958, 2926, 2853, 1597, 1494, 1454, 1360, 1265, 1168, 1093, 1042, 934, 740, 683 cm^{-1}. HRMS (ESI) m/z $[M+H]^+$ calcd for $C_{18}H_{19}NO_2S_2$ 346.0935, found 346.0941.

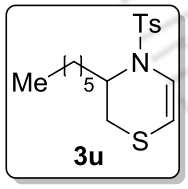

3-Hexyl-4-tosyl-3,4-dihydro-*2H*-1,4-thiazine 3u. Analytical TLC on silica gel, 1:9 ethyl acetate/hexane R_f = 0.56; colorless liquid; yield 75% (128 mg). ^{1}H NMR (600 MHz, $CDCl_3$) δ 7.64 (d, *J* = 8.4 Hz, 2H), 7.31 (d, *J* = 7.8 Hz, 2H), 6.82 (d, *J* = 8.4 Hz, 1H), 5.39 (dd, *J* = 8.4 Hz, 1.8 Hz, 1H), 4.16-4.13 (m, 1H), 2.49-2.46 (m, 1H), 2.42 (s, 3H), 2.04 (dd, *J* = 13.2, 3.0 Hz, 1H), 1.65-1.61 (m, 1H), 1.54-1.48 (m, 1H), 1.41-1.37 (m, 2H), 1.32-1.27 (m, 6H), 0.89 (t, *J* = 6.6 Hz, 3H). ^{13}C NMR (150 MHz, $CDCl_3$) δ 144.1, 135.4, 130.1, 127.3, 119.1, 102.6, 51.1, 32.3, 31.9, 29.2, 27.2, 25.4, 22.8, 21.8, 14.3. FT-IR (neat) 3070, 2955, 2924, 2854, 1637, 1464, 1360, 1167, 1091, 814 cm^{-1}. HRMS (ESI) m/z $[M+H]^+$ calcd for $C_{17}H_{25}NO_2S_2$ 340.1405, found 340.1408.

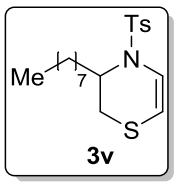

3-Octyl-4-tosyl-3,4-dihydro-*2H*-1,4-thiazine 3v. Analytical TLC on silica gel, 1:9 ethyl acetate/hexane R_f = 0.56; colorless liquid; yield 80% (148 mg). ^{1}H NMR (600 MHz, $CDCl_3$) δ 7.64 (d, *J* = 8.4 Hz, 2H), 7.31 (d, *J* = 7.8 Hz, 2H), 6.82 (d, *J* = 8.4 Hz, 1H), 5.39 (dd, *J* = 8.4, 2.4 Hz, 1H), 4.16-4.13 (m, 1H), 2.49-2.46 (m, 1H), 2.42 (s, 3H), 2.04 (dd, *J* = 12.6, 2.4 Hz, 1H), 1.65-1.61 (m, 1H), 1.54-1.48 (m, 1H), 1.40-1.36 (m, 2H), 1.31-1.27 (m, 10H), 0.89 (t, *J* = 7.2 Hz, 3H). ^{13}C NMR (150 MHz, $CDCl_3$) δ 144.0, 135.4, 130.1, 127.2, 119.1, 102.6, 51.1, 32.3, 32.1, 31.6, 30.4, 29.7, 29.6, 29.5, 27.2, 25.5, 22.9, 21.8, 14.3. FT-IR (neat) 3033, 2951, 2926, 1639, 1600, 1461, 1359, 1320, 1167, 1092, 943, 815 cm^{-1}. HRMS (ESI) m/z $[M+H]^+$ calcd for $C_{19}H_{29}NO_2S_2$ 368.1718, found 368.1729.

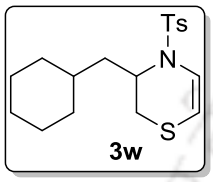

3-(Cyclohexylmethyl)-4-tosyl-3,4-dihydro-*2H*-1,4-thiazine 3w. Analytical TLC on silica gel, 1:9 ethyl acetate/hexane R_f = 0.56; yellow liquid; yield 75% (132 mg). ^{1}H NMR (600 MHz, $CDCl_3$) δ 7.64 (d, *J* = 8.4 Hz, 2H), 7.31 (d, *J* = 8.4 Hz, 2H), 6.81 (d, *J* = 9.0 Hz, 1H), 5.40 (dd, *J* = 8.4, 2.4 Hz, 1H), 4.28-4.26 (m, 1H), 2.44-2.41 (m, 4H), 2.05 (dd, *J* = 12.6, 3.0 Hz, 1H), 1.87-1.85 (m, 1H), 1.70-1.68 (m, 3H), 1.54-1.49 (m, 1H), 1.44-1.40 (m, 1H), 1.37-1.33 (m, 1H), 1.29-1.26 (m, 2H), 1.24-1.21 (m, 1H), 1.19-1.14 (m, 1H), 1.00-0.93 (m, 1H), 0.92-0.86 (m, 1H). ^{13}C NMR (150 MHz, $CDCl_3$) δ 144.1, 135.3, 130.1, 127.3, 119.1, 102.8, 48.4, 40.0, 33.6, 33.3, 33.2, 27.6, 26.7, 26.4, 26.3, 21.8. FT-IR (neat) 2960, 2923, 2851, 1638, 1448, 1357, 1164, 1093, 1033, 937, 813 cm^{-1}. HRMS (ESI) m/z $[M+H]^+$ calcd for $C_{18}H_{25}NO_2S_2$ 352.1405, found 352.1408.

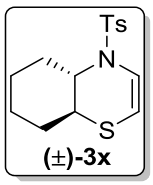

4-Tosyl-4a,5,6,7,8,8a-hexahydro-*4H*-benzo[*b*][1,4]thiazine 3x. Analytical TLC on silica gel, 1:9 ethyl acetate/hexane R_f = 0.56; gummy liquid; yield 61% (95 mg). ^{1}H NMR (600 MHz, $CDCl_3$) δ 7.71 (d, *J* = 8.4 Hz, 2H), 7.31 (d, *J* = 7.8 Hz, 2H), 6.83 (d, *J* = 7.8 Hz, 1H), 5.71 (d, *J* = 7.8 Hz, 1H), 3.44-3.30 (m, 1H), 2.78-2.73 (m, 2H), 2.43 (s, 3H), 2.01-1.97 (m, 1H), 1.81-1.78 (m, 1H), 1.73-1.70 (m, 1H), 1.48-1.42 (m, 1H), 1.38-1.27 (m, 3H). ^{13}C NMR (150 MHz, $CDCl_3$) δ 144.0, 136.1, 129.8, 127.4, 126.0, 108.6, 65.8, 46.5, 34.0, 32.3, 25.5, 25.1, 21.8. FT-IR (neat) 3065, 2952, 2924, 2854, 1620, 1454, 1358, 1336, 1166, 1090, 940, 813 cm^{-1}. HRMS (ESI) m/z $[M+H]^+$ calcd for $C_{15}H_{19}NO_2S_2$ 310.0935, found 310.0938.

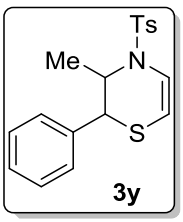

3-Methyl-2-phenyl-4-tosyl-3,4-dihydro-*2H*-1,4-thiazine 3y. Analytical TLC on silica gel, 1:9 ethyl acetate/hexane R_f = 0.42; colorless solid; yield 80% (139 mg). Mixture of syn/anti isomers (13:1) ^{1}H NMR (400 MHz, $CDCl_3$); δ 7.76 (major, d, *J* = 8.0 Hz, 2H), 7.41-7.37 (overlapped, m, 4H), 7.33-7.27 (overlapped, m, 4H), 7.21 (minor, d, *J* = 8.4 Hz, 2H), 7.08-7.04 (overlapped, m, 4H),6.98 (overlapped, t, *J* = 7.2 Hz, 3H), 6.93 (major, d, *J* = 8.4 Hz, 1H), 5.54 (major, d, *J* = 8.4 Hz, 1H), 5.46 (minor, dd, *J* = 8.8, 1.6 Hz, 1H), 4.50 (minor, dd, *J* = 6.4, 2.4 Hz, 1H), 4.31-4.27 (major, m, 1H), 3.97 (minor, dd, *J* = 2.0, 1.6 Hz, 1H), 3.37 (major, d, *J* = 2.8 Hz, 1H), 2.47 (major, s, 3H), 2.35 (minor, s, 3H), 1.50 (minor, d, *J* = 6.4 Hz, 3H), 1.07 (major, d, *J* = 6.4 Hz, 3H). ^{13}C NMR (150 MHz, $CDCl_3$) δ 144.4, 137.2, 135.4, 130.3, 129.7, 128.9, 128.5, 128.2, 127.5, 127.3, 126.6, 119.6, 118.5, 103.0, 98.4, 54.2, 53.2, 48.2, 46.7, 21.9, 13.7. FT-IR (KBr) 3067, 2956, 2924, 2854, 1637, 1599, 1451, 1359, 1169, 1092, 998, 816 cm^{-1}. HRMS (ESI) m/z $[M+H]^+$ calcd for $C_{18}H_{19}NO_2S_2$ 346.0935, found 346.0932.

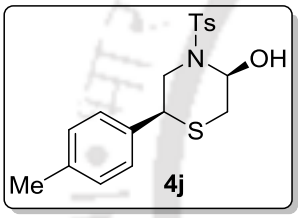

6-(*p*-Tolyl)-4-tosylthiomorpholin-3-ol 4j. Analytical TLC on silica gel, 4:6 ethyl acetate/hexane R_f = 0.57; colorless solid, yield 45% (83 mg). Mp 117-118 ^{o}C. ^{1}H NMR (600 MHz, $CDCl_3$) δ 7.73 (d, *J* = 8.4 Hz, 2H), 7.30 (d, *J* = 7.8 Hz, 2H), 7.20 (d, *J* = 7.8 Hz, 2H), 7.15 (d, *J* = 7.8 Hz, 2H), 5.85-5.83 (m, 1H), 4.06 (dd, *J* = 11.4, 3.0 Hz, 1H), 3.87 (dd, *J* = 12.6, 3.0 Hz, 1H), 3.73 (d, *J* = 10.8 Hz, 1H), 3.35 (dd, *J* = 13.8, 2.4 Hz, 1H), 3.10 (t, *J* = 12.0 Hz, 1H), 2.86 (dd, *J* = 13.2, 3.6 Hz, 1H), 2.42 (s, 3H), 2.33 (s, 3H). ^{13}C NMR (150 MHz, $CDCl_3$) δ 143.9, 138.6, 136.1, 135.0, 129.82, 129.80, 128.1, 127.7, 72.4, 47.2, 45.6, 37.4, 21.8, 21.3. FT-IR (KBr) 3467, 3067, 2924, 2854, 1612, 1448, 1360, 1297, 1168, 1092, 1054, 943, 909, 732 cm^{-1}. HRMS (ESI) m/z $[M-OH]^+$ calcd for $C_{18}H_{21}NO_3S_2$ 346.0935, found 346.0920.

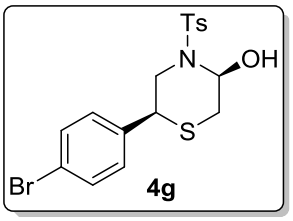

6-(4-Bromophenyl)-4-tosylthiomorpholin-3-ol 4g. Analytical TLC on silica gel, 4:6 ethyl acetate/hexane R_f = 0.57; gummy liquid; yield 53% (114 mg). ^{1}H NMR (600 MHz, $CDCl_3$) δ 7.72 (d, *J* = 8.4 Hz, 2H), 7.47 (d, *J* = 8.4 Hz, 2H), 7.31 (d, *J* = 8.4 Hz, 2H), 7.19 (d, *J* = 8.4 Hz, 2H), 5.85 (d, *J* = 9.0 Hz, 1H), 4.05 (dd, *J* = 11.4, 3.0 Hz, 1H), 3.86 (dd, *J* = 12.6, 3.0 Hz, 1H), 3.66 (d, *J* = 10.2 Hz, 1H), 3.35 (dd, *J* = 13.8, 1.8 Hz, 1H), 3.09 (t, *J* = 12.0 Hz, 1H), 2.88 (dd, *J* = 13.8, 3.6 Hz, 1H), 2.42 (s, 3H). ^{13}C NMR (150 MHz, $CDCl_3$) δ 144.1, 137.1, 136.1, 132.4, 130.0, 129.5, 128.0, 122.7, 72.4, 46.8, 45.2, 37.2, 21.8. FT-IR

(neat) 3463, 3247, 2955, 2920, 2852, 1640, 1446, 1337, 1156, 1091, 1051 cm^{-1}. HRMS (ESI) m/z $[M\text{-}OH]^+$ calcd for $C_{17}H_{18}BrNO_3S_2$ 409.9884, found 409.9881.

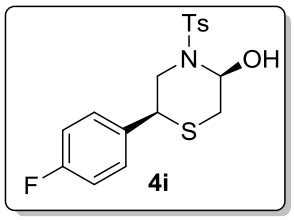

6-(4-Fluorophenyl)-4-tosylthiomorpholin-3-ol 4i. Analytical TLC on silica gel, 4:6 ethyl acetate/hexane R_f = 0.57; Colorless gummy liquid; yield 56% (103 mg). ^1H NMR (400 MHz, $CDCl_3$) δ 7.74-7.72 (m, 2H), 7.31-7.27 (m, 4H), 7.05-7.01 (m, 2H), 5.86 (d, *J* = 9.2 Hz, 1H), 4.08 (d, *J* = 10.4 Hz, 1H), 3.87 (d, *J* = 12.8 Hz, 1H), 3.73 (d, *J* = 10.8 Hz, 1H), 3.36 (d, *J* = 13.6 Hz, 1H), 3.11 (t, *J* = 12.0 Hz, 1H), 2.88 (d, *J* = 13.6 Hz, 1H), 2.43 (s, 3H). ^{13}C NMR (150 MHz, $CDCl_3$) δ 163.6 (d, *J* = 247.5 Hz), 144.1, 136.0, 133.9, 130.0, 129.5 (d, *J* = 7.5 Hz), 128.0, 116.2 (d, *J* = 21.0 Hz), 72.4, 47.1, 45.0, 37.3, 21.8. FT-IR (neat) 3466, 3214, 3068, 2923, 2853, 2253, 1640, 1599, 1492, 1338, 1157, 1091, 1053, 971, 732 cm^{-1}. HRMS (ESI) m/z $[M\text{-}OH]^+$ calcd for $C_{17}H_{18}NO_3S_2$ 350.0685, found 350.0682.

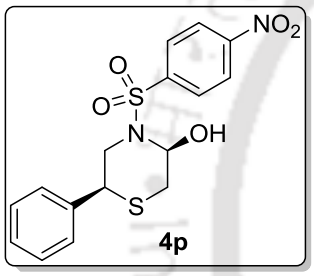

4-((4-Nitrophenyl)sulfonyl)-6-phenylthiomorpholin-3-ol 4p. Analytical TLC on silica gel, 4:6 ethyl acetate/hexane R_f = 0.57; brown solid; yield 58% (110 mg). Mp 127-128 ^oC. ^1H NMR (600 MHz, $CDCl_3$) δ 8.35 (d, *J* = 9.0 Hz, 2H), 8.05 (d, *J* = 9.0 Hz, 2H), 7.37-7.33 (m, 3H), 7.31-7.30 (m, 2H), 5.89 (d, *J* = 11.4 Hz, 1H), 4.12 (dd, *J* = 11.4, 3.0 Hz, 1H), 3.92 (dd, *J* = 12.6, 3.0 Hz, 1H), 3.84 (d, *J* = 11.4 Hz, 1H), 3.41-3.38 (dd, *J* = 13.8, 1.2 Hz, 1H), 3.10 (t, *J* = 12.0 Hz, 1H), 2.92 (dd, *J* = 13.8, 3.0 Hz, 1H). ^{13}C NMR (150 MHz, $CDCl_3$) δ 150.5, 144.6, 137.5, 129.5, 129.3, 129.0, 127.8, 124.4, 72.7, 47.4, 46.0, 37.5. FT-IR (KBr) 3464, 3255, 3109, 2924, 2854, 1639, 1529, 1308, 1161, 1090, 1054, 970, 854, 739 cm^{-1}. HRMS (ESI) m/z $[M\text{-}OH]^+$ calcd for $C_{16}H_{16}N_2O_5S_2$ 363.0473, found 363.0482.

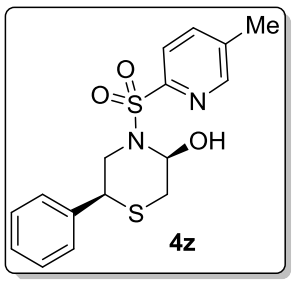

4-((5-Methylpyridin-2-yl)sulfonyl)-6-phenylthiomorpholin-3-ol 4z. Analytical TLC on silica gel, 4:6 ethyl acetate/hexane R_f = 0.55; brown liquid; yield 60% (105 mg). ^1H NMR (400 MHz, $CDCl_3$) δ 8.49 (s, 1H), 7.91 (d, *J* = 7.8 Hz, 1H), 7.75 (d, *J* = 6.6 Hz, 1H), 7.34 (d, *J* = 7.2 Hz, 2H), 7.30-7.25 (m, 3H), 6.05 (s, 1H), 5.94 (s, 1H), 4.15 (dd, *J* = 11.4, 3.0 Hz, 1H), 3.70 (dd, *J* = 12.6, 3.0 Hz, 1H), 3.18 (dd, *J* = 13.8, 1.8 Hz, 1H), 3.32 (t, *J* = 11.4 Hz, 1H), 3.05 (dd, *J* = 13.8, 3.0 Hz, 1H), 2.45 (s, 3H). ^{13}C NMR (150 MHz, $CDCl_3$) δ 153.2, 150.0, 139.5, 138.5, 138.4, 129.0, 128.4, 128.0, 123.6, 72.8, 46.8, 45.8, 35.0, 18.8. FT-IR (neat) 3440, 3237, 2964, 2922, 2857, 1636, 1514,

1351, 1162, 1092, 1019, 955 cm^{-1}. HRMS (ESI) m/z $[M\text{-}OH]^+$ calcd for $C_{16}H_{18}N_2O_3S_2$ 333.0731, found 333.0726.

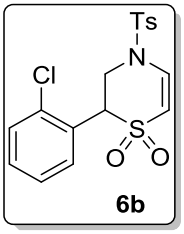

2-(2-Chlorophenyl)-4-tosyl-3,4-dihydro-*2H*-1,4-thiazine 1,1-dioxide 6b. Analytical TLC on silica gel, 4:6 ethyl acetate/hexane R_f = 0.52; colorless liquid; yield 92% (74 mg). ^1H NMR (600 MHz, $CDCl_3$) δ 7.69 (d, J = 7.8 Hz, 2H), 7.48-7.45 (m, 2H), 7.40-7.38 (m, 3H), 7.35-7.33 (m, 1H), 7.30-7.29 (m, 1H), 5.85 (d, J = 9.0 Hz, 1H), 4.90 (dd, J = 11.4, 3.0 Hz, 1H), 4.32-4.29 (m, 1H), 4.18 (dd, J = 13.8, 12.0 Hz, 1H), 2.48 (s, 3H). ^{13}C NMR (150 MHz, $CDCl_3$) δ 146.2, 135.7, 134.1, 131.0, 130.9, 130.6, 130.0, 127.6, 127.4, 125.7, 108.0, 56.9, 47.9, 21.9. FT-IR (neat) 2962, 2921, 2851, 1639, 1384, 1314, 1261, 1113, 1044, 802, 756 cm^{-1}. HRMS (ESI) m/z $[M+H]^+$ calcd for $C_{17}H_{16}ClNO_4S_2$ 398.0288, found 398.0291.

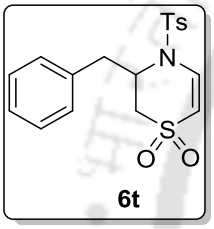

3-Benzyl-4-tosyl-3,4-dihydro-*2H*-1,4-thiazine 1,1-dioxide 6t. Analytical TLC on silica gel, 4:6 ethyl acetate/hexane R_f = 0.56; colorless solid; yield 96% (73 mg). Mp 161-162 ^oC. ^1H NMR (600 MHz, $CDCl_3$) δ 7.76 (d, J = 8.4 Hz, 2H), 7.40-7.38 (m, 5H), 7.35 (t, J = 7.2 Hz, 2H), 7.28-7.257 (m, 1H), 5.75 (dd, J = 9.6, 3.0 Hz, 1H), 4.52-4.48 (m, 1H), 3.71 (t, J = 12.6 Hz, 1H), 3.08-3.02 (m, 2H), 2.72 (dd, J = 14.4, 5.4 Hz, 1H), 2.46 (s, 3H). ^{13}C NMR (150 MHz, $CDCl_3$) δ 146.1, 136.0, 135.1, 132.6, 131.0, 129.2, 127.6, 127.2, 106.8, 57.3, 47.8, 36.2, 21.9. FT-IR (KBr) 3070, 2919, 2850, 1641, 1370, 1297, 1129, 1088, 1029, 928, 737 cm^{-1}. HRMS (ESI) m/z $[M+H]^+$ calcd for $C_{18}H_{19}NO_4S_2$ 378.0834, found 378.0838.

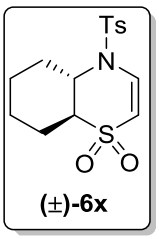

4-Tosyl-4a,5,6,7,8,8a-hexahydro-*4H*-benzo[*b*][1,4]thiazine 1,1-dioxide 6x. Analytical TLC on silica gel, 4:6 ethyl acetate/hexane R_f = 0.56; colorless solid; yield 95% (65 mg). Mp 142-143 ^oC. ^1H NMR (600 MHz, $CDCl_3$) δ 7.65 (d, J = 8.4 Hz, 2H), 7.53 (d, J = 9.6 Hz, 1H), 7.39 (d, J = 7.8 Hz, 2H), 5.82 (d, J = 9.6 Hz, 1H), 3.73-3.68 (m, 1H), 3.03-2.98 (m, 1H), 2.78-2.75 (m, 1H), 2.47 (s, 3H), 2.34-2.31 (m, 1H), 1.86-1.84 (m, 1H), 1.81-1.79 (m, 1H), 1.61-1.56 (m, 2H), 1.47-1.40 (m, 1H), 1.29-1.26 (m, 1H). ^{13}C NMR (150 MHz, $CDCl_3$) δ 145.7, 136.7, 135.4, 130.6, 127.2, 107.0, 60.4, 60.3, 31.7, 24.3, 23.4, 21.9, 20.3. FT-IR (KBr) 3083, 2928, 2860, 1615, 1452, 1347, 1303, 1169, 1134, 1088, 940, 736 cm^{-1}. HRMS (ESI) m/z $[M+H]^+$ calcd for $C_{15}H_{19}NO_4S_2$ 342.0834, found 342.0838.

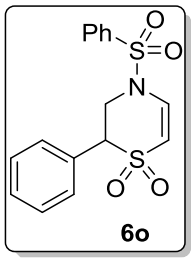

2-Phenyl-4-(phenylsulfonyl)-3,4-dihydro-*2H*-1,4-thiazine 1,1-dioxide 6o. Analytical TLC on silica gel, 4:6 ethyl acetate/hexane R_f = 0.52; colorless liquid; yield 90% (66 mg). ^{1}H NMR (600 MHz, $CDCl_3$) δ 7.84-7.82 (m, 2H), 7.76-7.73 (m, 1H), 7.65-7.62 (m, 2H), 7.45-7.37 (m, 4H), 7.32-7.31 (m, 2H), 5.85 (d, *J* = 9.6 Hz, 1H), 4.45-4.42 (m, 1H), 4.24 (dd, *J* = 12.6, 2.4 Hz, 1H), 4.17 (t, *J* = 13.2 Hz, 1H).^{13}C NMR (150 MHz, $CDCl_3$) δ 137.1, 134.9, 133.7, 130.3, 130.2, 129.8, 129.3, 127.4, 126.6, 108.0, 61.4, 47.5. FT-IR (neat) 3070, 2955, 2922, 2852, 1636, 1449, 1378, 1292, 1172, 1142, 1115, 952, 911, 723 cm^{-1}. HRMS (ESI) m/z $[M+NH_4]^+$ calcd for $C_{16}H_{15}NO_4S_2$ 367.0781, found 367.0795.

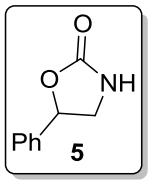

5-Phenyloxazolidin-2-one 5. Analytical TLC on silica gel, 4:6 ethyl acetate/hexane R_f = 0.48; yield 74% (59 mg). Mp 90-91 ºC. ^{1}H NMR (600 MHz, $CDCl_3$) δ 7.51-7.21 (m, 5H), 5.60 (t, *J* = 8.2 Hz, 1H), 3.97 (t, *J* = 8.8 Hz, 1H), 3.54 (dd, *J* = 8.8, 7.8 Hz, 1H). ^{13}C NMR (150 MHz, $CDCl_3$) δ 160.4, 138.6, 129.1, 129.0, 125.9, 78.1, 48.5. HRMS (ESI) m/z $[M+Na]^+$ calcd for $C_9H_9NO_2$ 186.0525, found 186.0572.

2.6 References

1. (a) Li, H.; Dryhurst, G. *J. Neurochem.* **1997**, *69*, 1530. (b) De Kimpe, N. G.; Rocchetti, M. T. *J. Agric. Food Chem.* **1998**, *46*, 2278. (c) Fringuelli, R.; Milanese, L.; Schiaffella, F. *Mini-Rev. Med. Chem*. **2005**, *5*, 1061. (d) Reddy, P. R.; Reddy, G. M.; Padmaja, A.; Padmavathi, V.; Kondaiah, P.; Krishna, N. S. *Arch. Pharm.Chemi.* **2014**, *347*, 221. (e) Li, X.; Liang, X.; Song, T.; Su, P.; Zhang, Z. *Bioorg. Med. Chem.* **2014**, *22*, 5738. (f) Hessein, S. A.; Fouad, S. A.; Raslan, R. R.; Shemiss, N. A. *Der Pharma Chemica*. **2016**, *8*, 170. (g) Battula, K.; Narsimha, S.; Nagavelli, V.; Bollepelli, P.; Rao, M. S. *J. Serbian Chem. Soc.* **2016**, *81*, 233. (h) Diao, P. C.; Li, Q.; Hu, M. J.; Ma, Y. F.; You, W. W.; Hong, K. H.; Zhao, P. L. *Eur. J. Med. Chem.* **2017**, *134*, 110.
2. Renslo, A. R.; Luehr, G. W.; Lam, S.; Westlund, N. E.; Gómez, M.; Hackbarth, C. J.; Patel, D. V.; Gordeev, M. F. *Bioorganic Med. Chem. Lett.* **2006**, *16*, 3475.
3. Thomas, R.; Williams, D. J. *J. Antibiot.* **1981**, 252.
4. Weintraub, P. M.; Skoog, M. T.; Nichols, J. S.; Wiseman, J. S.; Huber, E. W.; Baugh, L. E.; Farrell, A. M.; *J. Pharm. Sci.* **1989**, *78*, 937.
5. Deblander, J.; Van Aeken, S.; Adams, A.; De Kimpe, N.; Tehrani, A. K. *Food Chem.* **2015**, *168*, 327.
6. Theodosis-Nobelos, P.; Kourti, M.; Gavalas, A.; Rekka, E. A. *Bioorganic Med. Chem.*

Lett. **2016**, *26*, 910.

7. Biava, M.; Porretta, G. C.; Deidda, D.; Pompei, R.; Tafi, A.; Manetti, F. *Bioorganic Med. Chem.* **2002**, *11*, 515.
8. Tooulia, K. K.; Theodosis-Nobelos, P.; Rekka, E. A. *Arch. Pharm.* **2015**, *348*, 629.
9. Han, B.; Liu, J. L.; Huan, Y.; Li, P.; Wu, Q.; Lin, Z. Y.; Shen, Z. F.; Yin, D. L.; Huang, H. H. *Chinese Chem. Lett.* **2012**, *23*, 297.
10. (a) Asinger, F.; Schmitz, F. J.; Reichel, S. *Liebigs Ann. Chem.* **1962,** *652*, 50. (b) Asinger, F.; Diem, H.; Schäfer, W. *Monatsh. Chem.* **1964**, *95*, 1335. (c) Iwakawa, M.; Pinto, B. M.; Szarek, W. A. *Can. J. Chem.* **1978**, *56*, 326. (d) Chioccara, F.; Oliva, L.; Prota, G.; Novellino, E. *Synthesis* **1978**, 744. (e) Mah, H. D.; Lee, W. S. *J. Heterocycl. Chem.* **1989**, *26*, 1447. (f) Verboom, W.; Sukhai, R. S.; Meijer, J. *Synthesis* **1979**, 47. (g) W. Keim, H. Offermanns, *Angew. Chem., Int. Ed*. **2007**, *46*, 6010. (h) Siry, S. A.; Ogurok, V. M.; Shermolovich, Y. G. *J. Flourine Chem.* **2014**, *168*, 137.
11. Prasad, D. J. C.; Sekar, G. *Org. Biomol. Chem.* **2009**, *7*, 5091.
12. Ghorai, M. K.; Sayyad, M.; Nanaji, Y.; Jana, S. *Chem. - An Asian J.* **2015**, *10*, 1480.
13. Javorskis, T.; Bagdžiūnas, G.; Orentas, E. *Chem. Commun*. **2016**, *52*, 4325.
14. Gao, Y.; Hu, C.; Wen, C.; Wan, J.-P. *ACS Omega*. **2017**, *2*, 7784.
15. For Iron catalyst (a) Balwe, S. G.; Shinde, V. V.; Jeong, Y. T. *Tetrahedron Lett*. **2016**, *57*, 5074. (b) Bosset, C.; Lefebvre, G.; Angibaud, P.; Stansfield, I.; Meerpoel, L.; Berthelot, D.; Guérinot, A.; Cossy, J. *J. Org. Chem.* **2017**, *82*, 4020.
16. Liu, Y. T.; Wang, Q. X.; Shen, M. H.; Xu, H. D. *Org. Chem. Front.* **2016**, *3*, 725.
17. Fang, X.; Li, J.; Tao, H.Y.; Wang, C. J. *Org. Lett*. **2013**, *15*, 5554.
18. Lu, X. L.; Mari, G.; Favi, G.; De Crescentini, L.; Santusanio, S.; Attanasi, O. A.; Mantellini, F. *Asian J. Org. Chem.* **2016**, *5*, 705.
19. Zhang, Y.; Ma, S.; Li, B.; Wang, R. *J. Org. Chem.* **2015**, *80*, 6870.
20. (a) Cardoso, A. L.; Pinho E Melo, T. M. V. D. *European J. Org. Chem.* **2012**, *33*, 6479. (b) *Cycloaddition Reactions in Organic Synthesis;* Kobayashi, S., Jørgensen, K. A. Ed.; Wiley-VCH: Weinheim, Germany, 2001.
21. (a) Peruncheralathan, S.; Teller, H.; Schneider, C. *Angew. Chem., Int. Ed.* **2009**, *48*, 4849. (b) Schramm, H.; Saak, W.; Hoenke, C.; Christoffers, J. *European J. Org. Chem.* **2010**, *9*, 1745. (c) Park, K. D.; Stables, J. P.; Liu, R.; Kohn, H. *Org. Biomol. Chem.* **2010**, *8*, 2803. (d) Sengoden, M.; Punniyamurthy, T. *Angew. Chem., Int. Ed*. **2013**, *52*, 572. (e) Bailey, S. J.; Wales, S. M.; Willis, A. C.; Keller, P. A. *Org. Lett.* **2014**, *16*, 4344. (f) Li, J.; Liao, Y.; Zhang, Y.; Liu, X.; Lin, L.; Feng, X. *Chem. Commun.* **2014**, *50*, 6672.

(g) Craig, R. A.; O'Connor, N. R.; Goldberg, A. F. G.; Stoltz, B. M. *Chem. - A Eur. J.* **2014**, *20*, 4806. (h) Rossi, E.; Abbiati, G.; Dell'Acqua, M.; Negrato, M.; Paganoni, A.; Pirovano, V. *Org. Biomol. Chem.* **2016**, *14*, 6095.

22. (a) Connor, C. J.; Roydhouse, M. D.; Przybył, A. M.; Wall, M. D.; Southern, J. M. *J. Org. Chem.* **2010**, *75*, 2534. (b) Ling, J. B.; Su, Y.; Zhu, H. L.; Wang, G. Y.; Xu, P. F. *Org. Lett.* **2012**, *14*, 1090. (c) Ni, C.; Wang, M. L.; Tong, X. *Org. Lett.* **2016**, *18*, 2240. (d) Duan, M.; Liu, Y.; Ao, J.; Xue, L.; Luo, S.; Tan, Y.; Qin, W.; Song, C. E.; Yan, H. *Org. Lett.* **2017**, *19*, 2298.
23. (a) Christensen, J. E.; Huddle, M. G.; Lacey, J. R.; Spafford, M. J.; Mohan, R. S. *Aust. J. Chem*. **2008**, *61*, 419. (b) Bothwell, J. M.; Krabbe, S. W.; Mohan, R. S. *Chem. Soc. Rev.* **2011**, *40*, 4649. (c). Krabbe, S. W.; Mohan, R. S. *Top. Curr. Chem*. **2012**, *311*, 45.
24. Tietze, L. F. *Chem. Rev.* **1996**, *96*, 115.
25. Tomasini, C.; Vecchione, A. *Org. Lett.* **1999**, *1*, 2153.
26. Xu, J. *Topic in Heterocyclic Chemistry* (Eds.: D'hooghe, M.; Ha, H. J.), Springer, **2015**, pp. 311.
27. Nicolas, C.; Lacour, J. *Org. Lett*. **2006**, *8*, 4343.

2.7 NMR Spectra

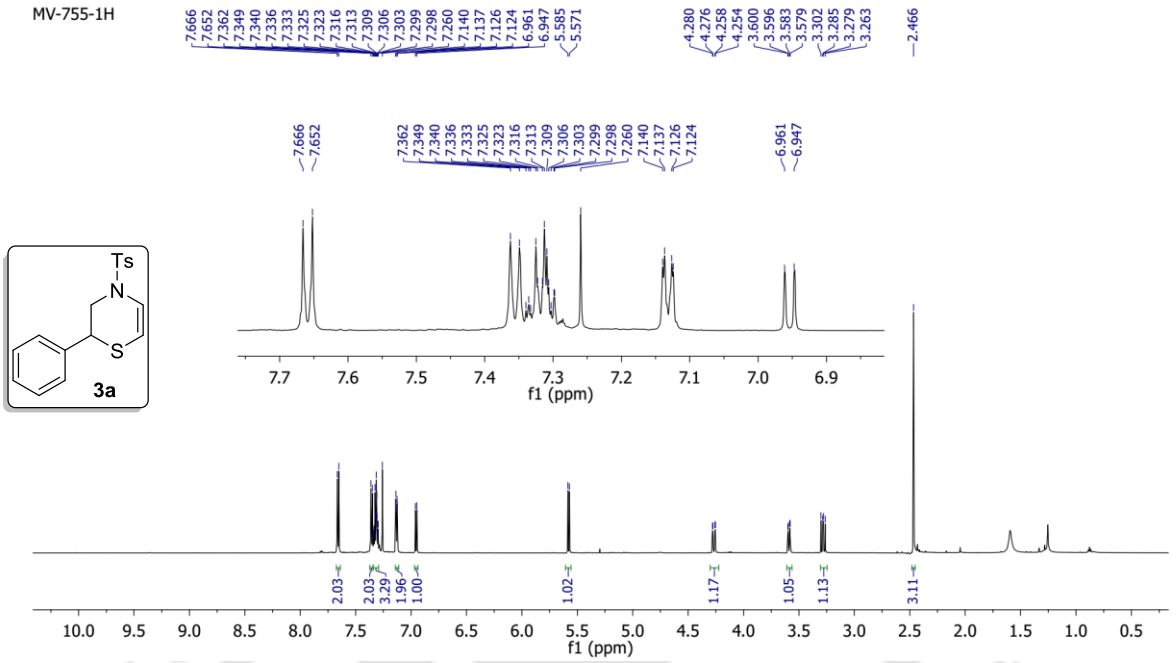

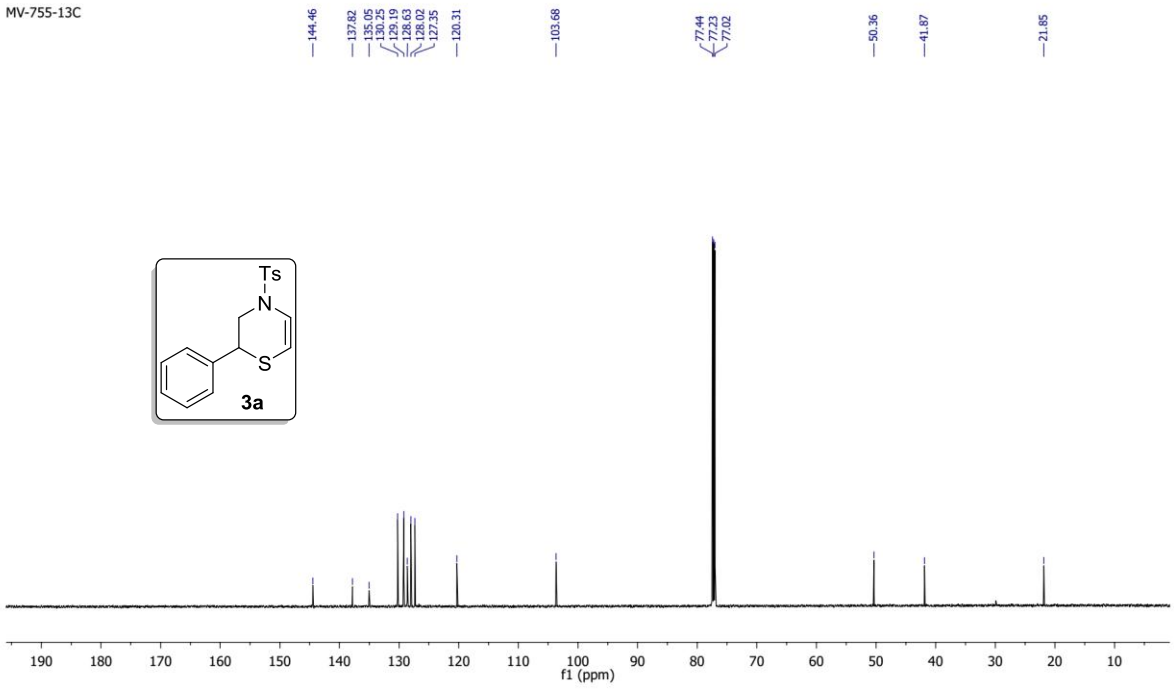

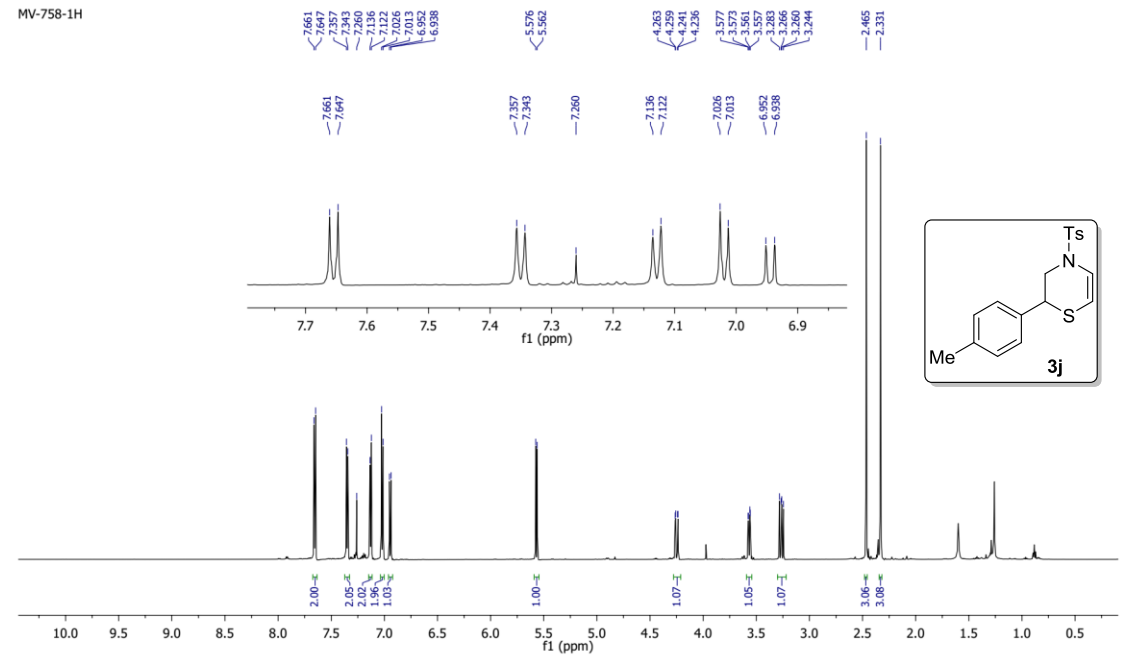

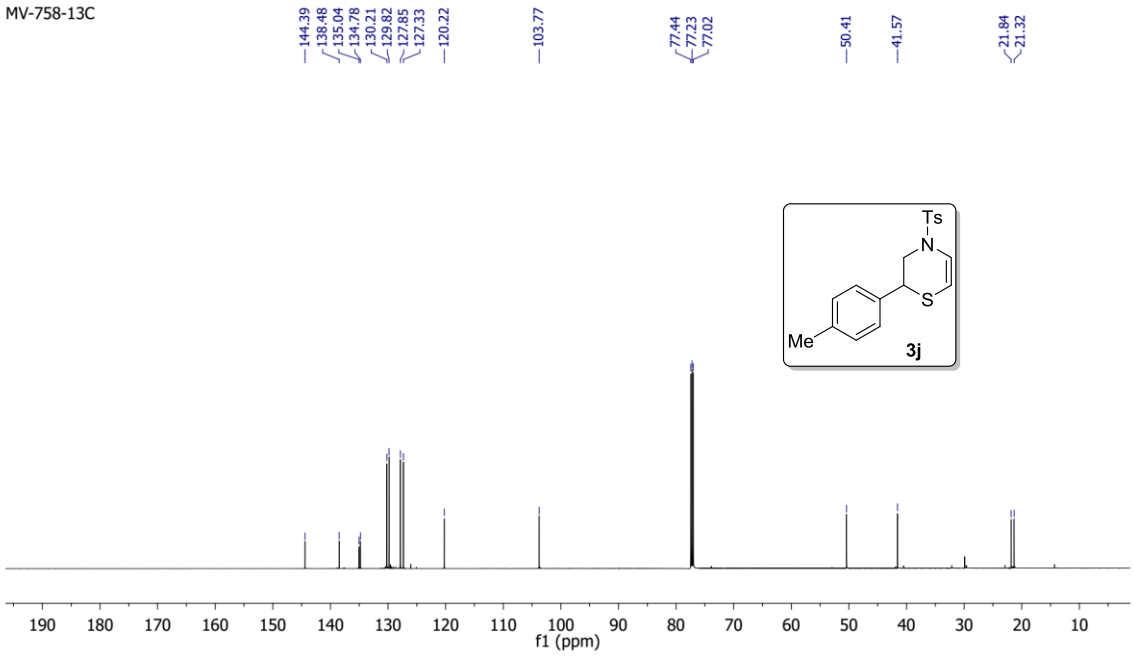

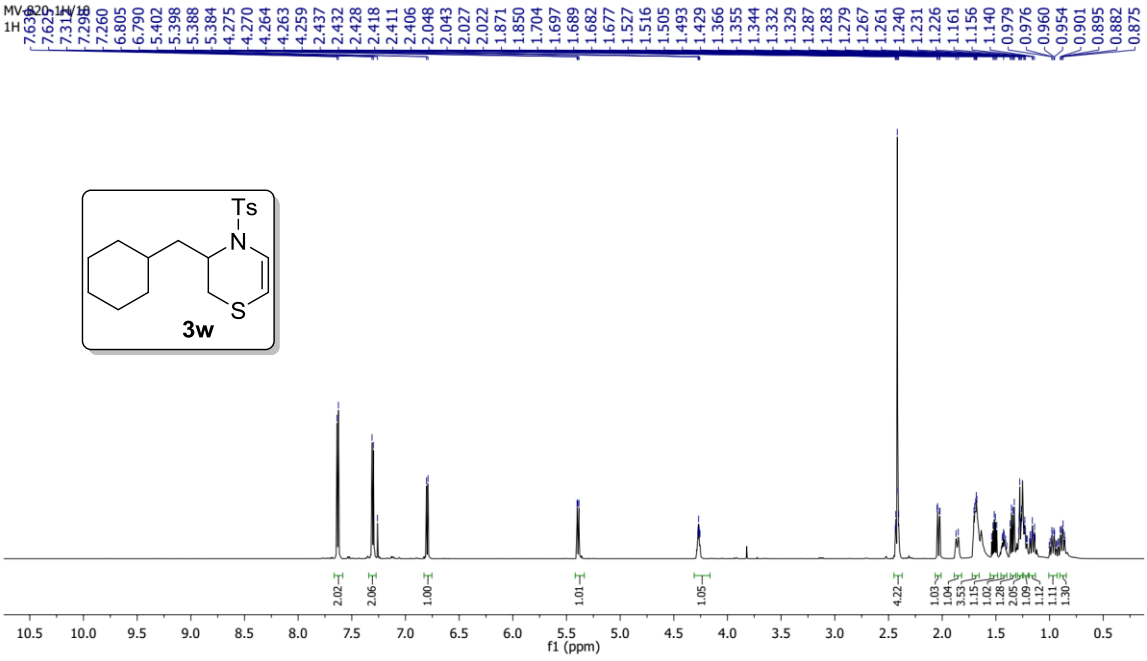

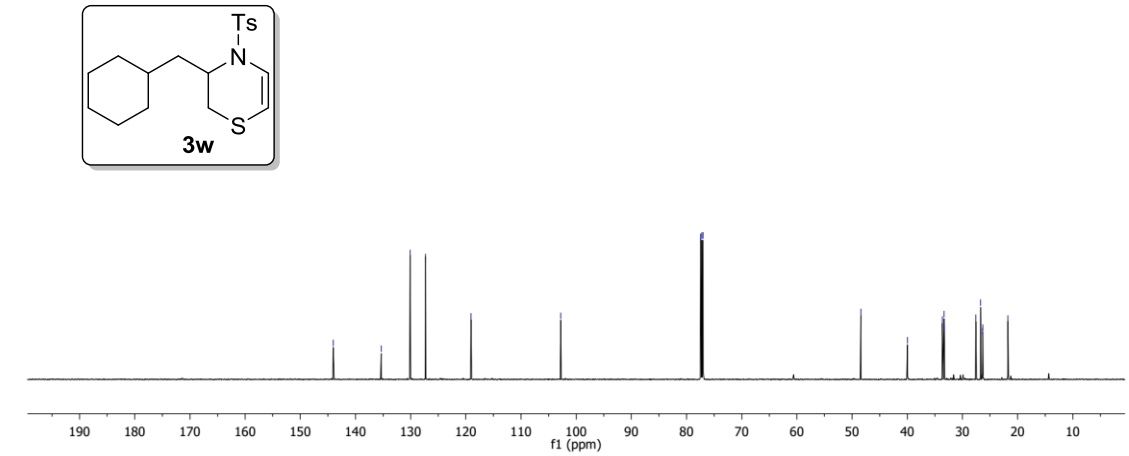

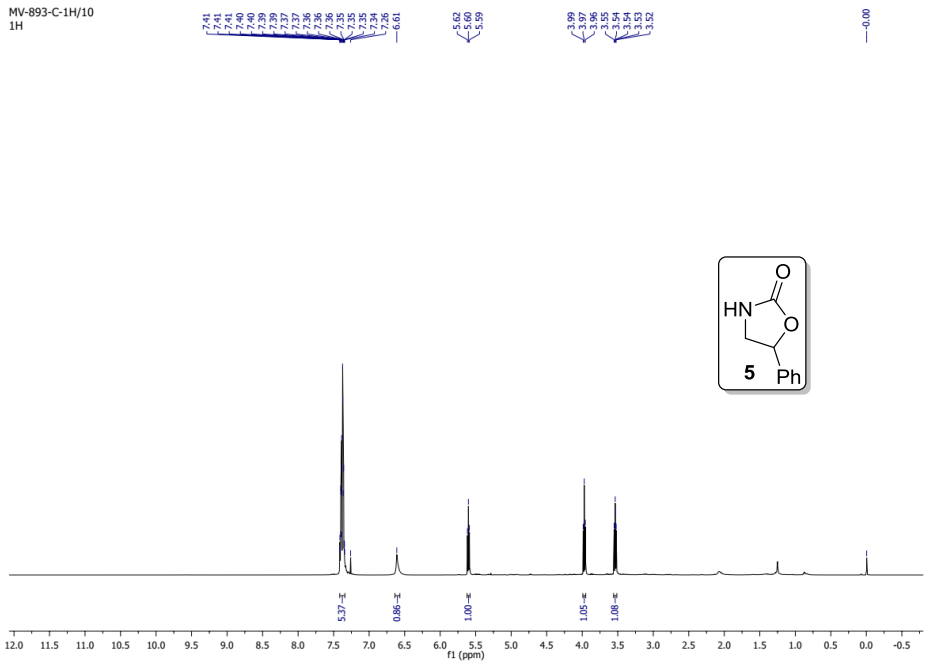

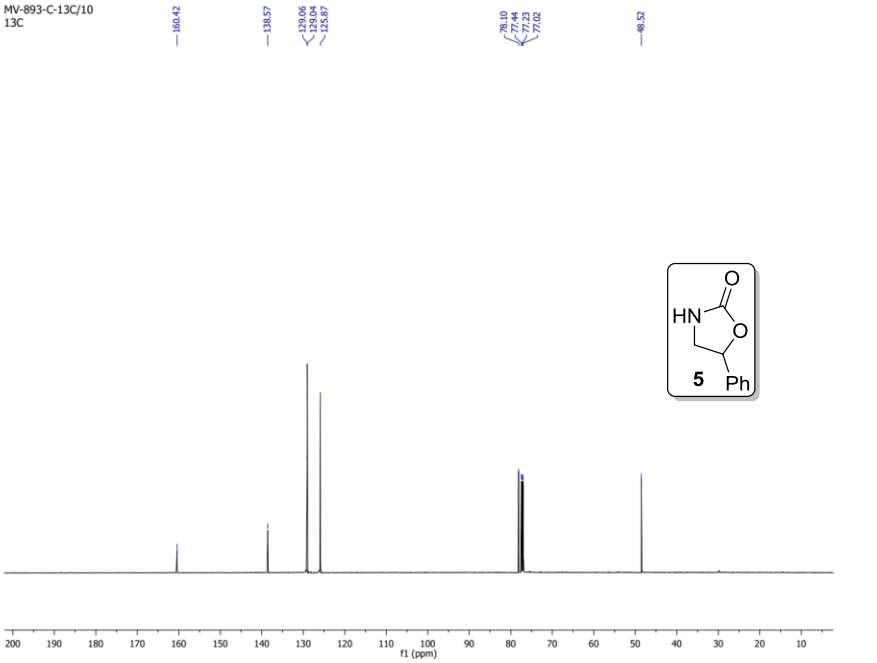

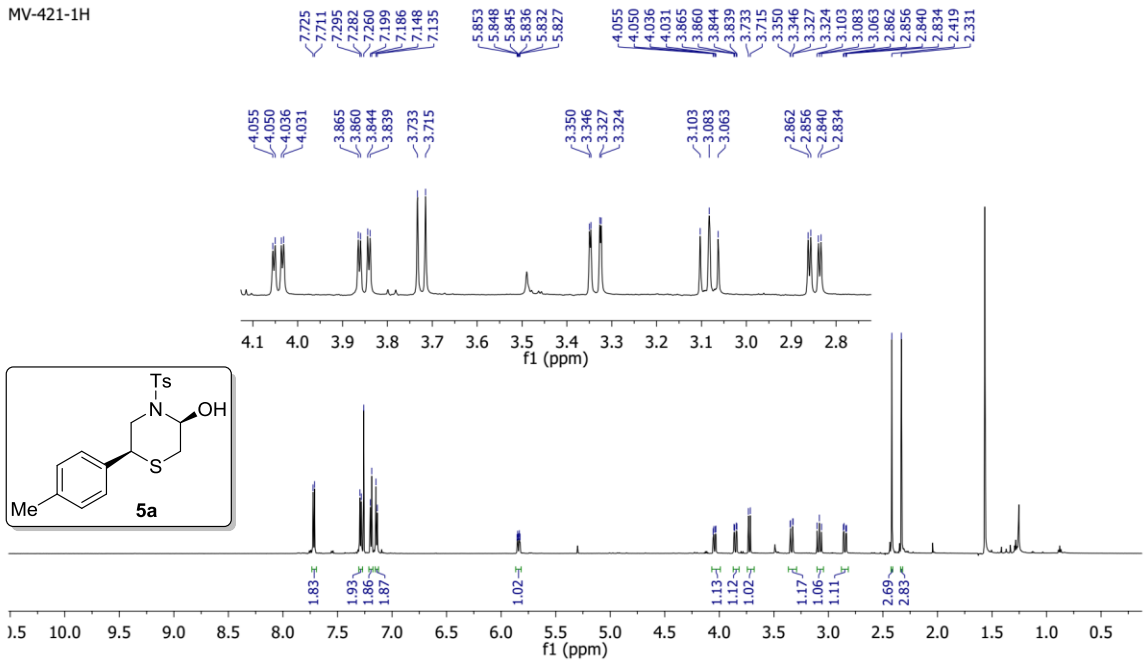

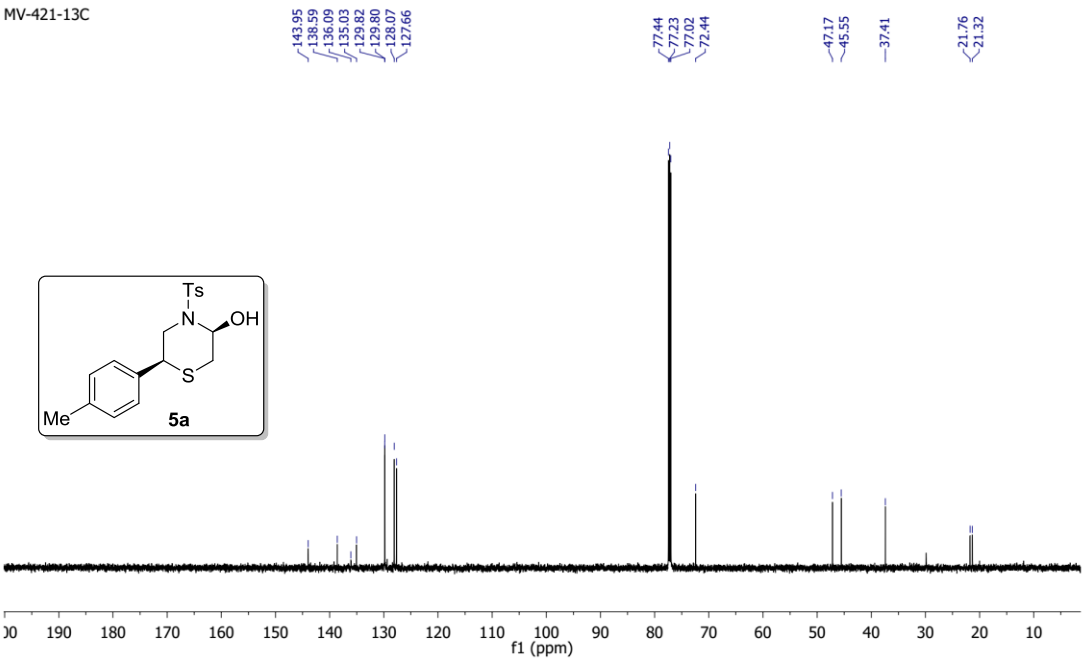

MV-826-1H

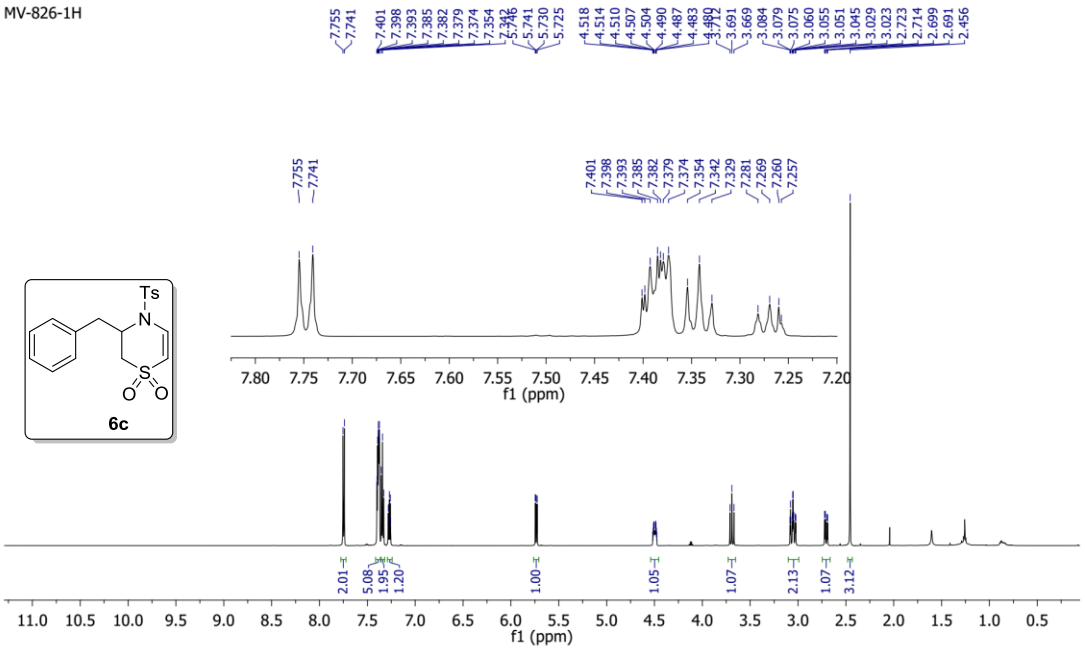

MV-826-13C

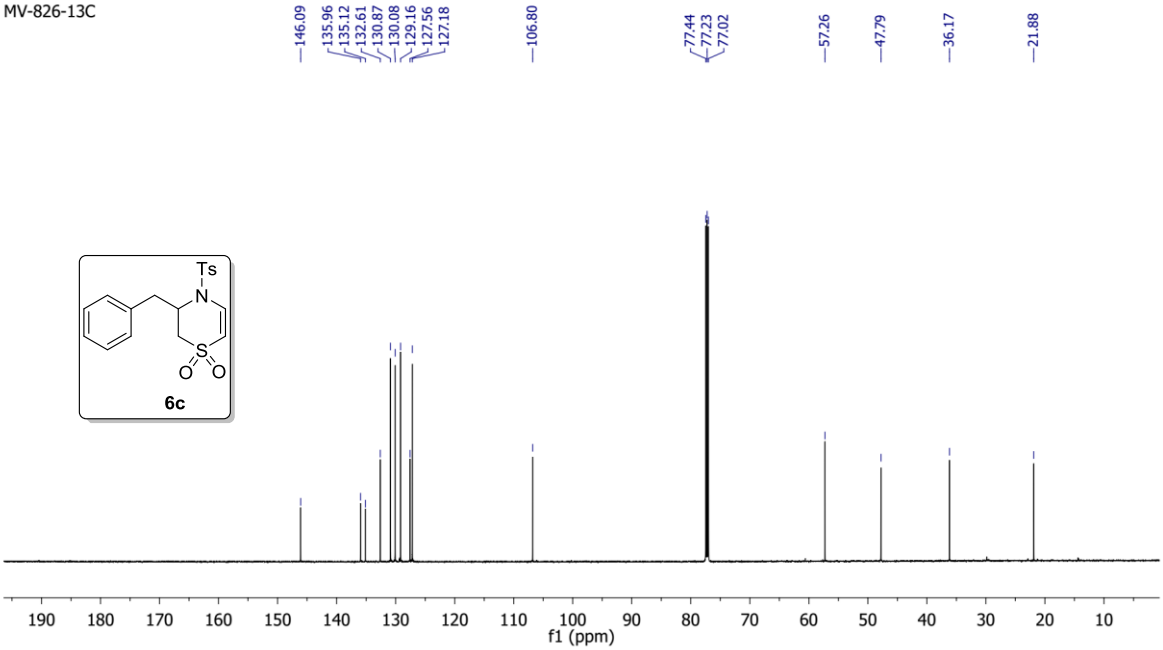

Synthesis, Photophysical and Electrochemical Studies of Indazoloquinolines

Visible-light photoredox catalysis affords a powerful synthetic tool for the generation of C–C and C–heteroatom bonds.[1] Organic photoredox catalysis is a vibrant field in organic synthesis and has been subsidized enormously for achieving complex heterocycles from simple and easily accessible precursors.[2] In general, organic photoredox catalysis offers more aids compare to the metal-based photoredox catalysis. The advantages include less expensive, low toxicity and comparable redox potentials.[3] However, synthetic application of organic dyes is still limited to few catalyst choices. Development of new organic photoredox catalysts with broad range of redox competencies are thus desirable.[4,5] Indazoloquinolines have been extensively utilized as organic light-emitting diodes[6] and would thus possible to serve as organic photoredox catalyst under visible-light irradiation (Figure 1). Certainly, these robust fluorescent frameworks might offer a unique stance to alter the redox properties by installing the various functional groups.

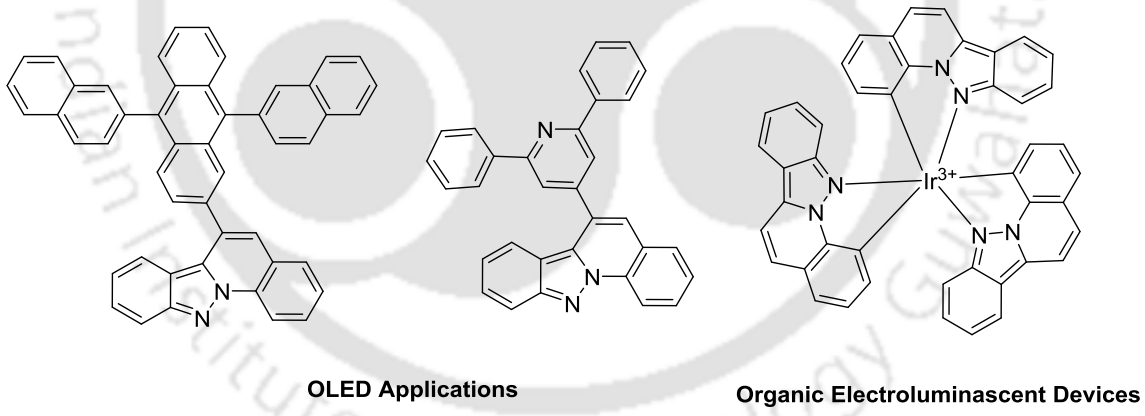

Figure 1. Examples containing indazoloquinoline motif in OLED applications.

3.1 Rh-Catalyzed Double C–H Functionalisation

Wang and co-workers developed a Rh-catalyzed oxidative annulation of alkynes with benzoylacetonitriles (Scheme 1).[7a] The primary step proceeds by sequential cleavage of C(sp^2)–H/C(sp^3)−H bonds and annulation with an alkyne, leading to 1-naphthols, which react with alkyne by cleavage of C(sp^2)−H/O−H bonds, affording the coupling products.

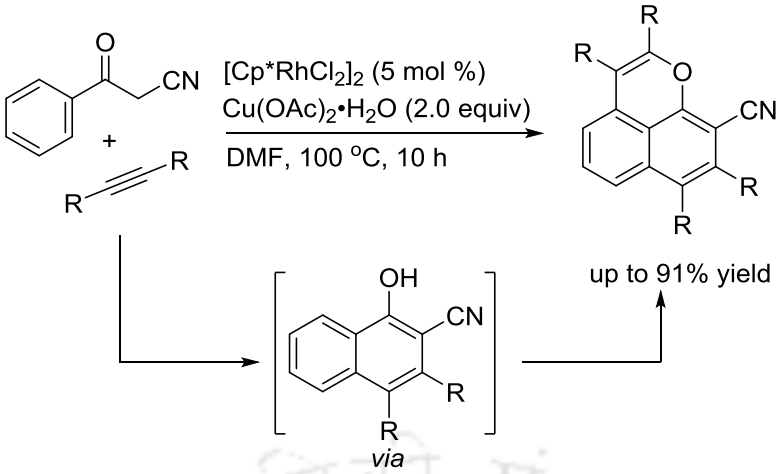

Scheme 1. Rh-catalyzed two-fold C–H activation of benzoylacetonitriles.

Rh-catalyzed synthesis of 2-aminoquinolines from 1-aryl tetrazoles and alkynes has been developed. This reaction occurs *via* a double C–H activation of *N*-tetrazole followed by copper(II)-mediated denitrogenation to afford 2-aminoquinolines (Scheme 2).[7b]

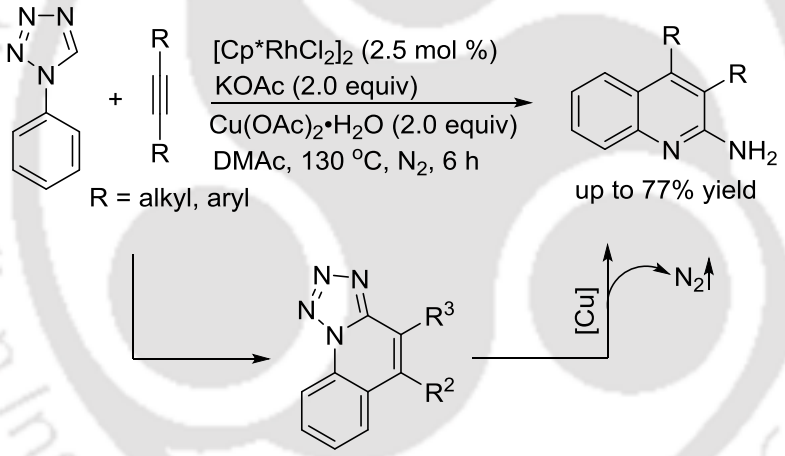

Scheme 2. Rh-catalyzed synthesis of 2-aminoquinolines.

Song group reported a Rh-catalyzed double C–H activation of 2-phenylimidazo[1,2-*a*]pyridines with diphenylacetylene in presence of $Co(OAc)_2 \cdot H_2O$ (Scheme 3).[7c] In general, $Cu(OAc)_2$ is used in the annulation reactions. The advantage of cobalt oxidant is shortened the reaction time.

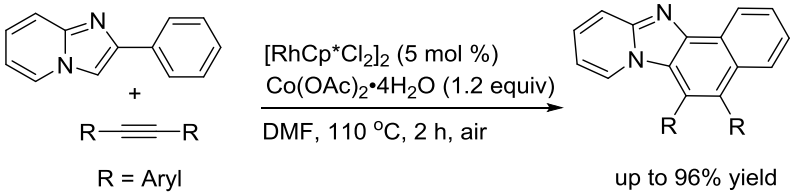

Scheme 3. Rh-catalyzed double C–H activation of 2-phenylimidazo[1,2-*a*]pyridines.

Wang and co-workers reported a Rh-catalyzed synthesis of pyridoquinolinium- and quinolizinoquinolinium-based polyheteroaromatic compounds in presence of Cu(II) as the oxidant. This transformation involves a multiple C−H activation and annulation of internal alkynes (Scheme 4).[7d]

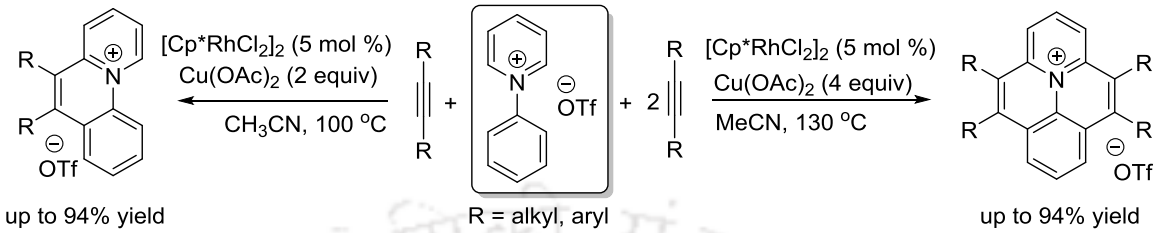

Scheme 4. Oxidant tunable annulation of alkynes.

Synthesis of functionalized quinolones reported from a Rh(III)-catalyzed reaction of *N*-arylsyndone and alkynes using Cu(II) as the oxidant at room temperature. The reaction was achieved via the double C–H activation of arylsyndone. (Scheme 5).[7e]

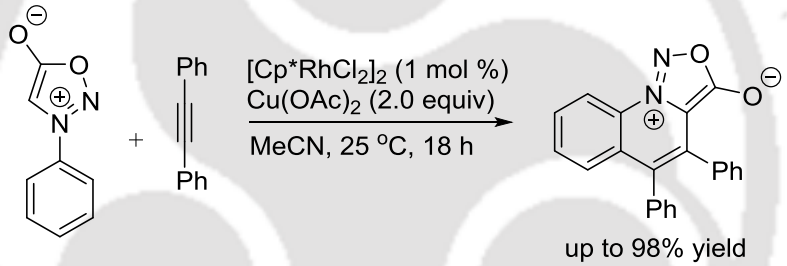

Scheme 5. Rh-catalyzed C–H activation of *N*-arylsyndone.

3.2 Synthesis of Indazoquinoline

Shi and co-workers showed the construction of the fused pyridoindazoquinolines using [3+2]-cycloaddition of aryne with *N*-tosylpyridinium imide followed by -*N*Ts elimination (Scheme 6).[7f]

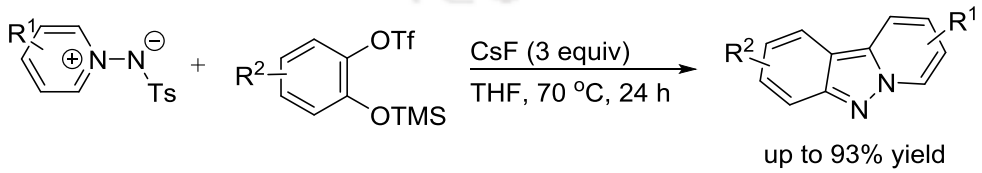

Scheme 6. [3+2]-cycloaddition of arynes with *N*-tosylpyridinium imides.

Yamane and co-workers reported a Pd-catalyzed coupling of 2-alkynyl azobenzenes with alkyne to give (3-isoindazolyl)allenes (Scheme 7).[7g] The reaction of electronically varied substrates has been demonstrated.

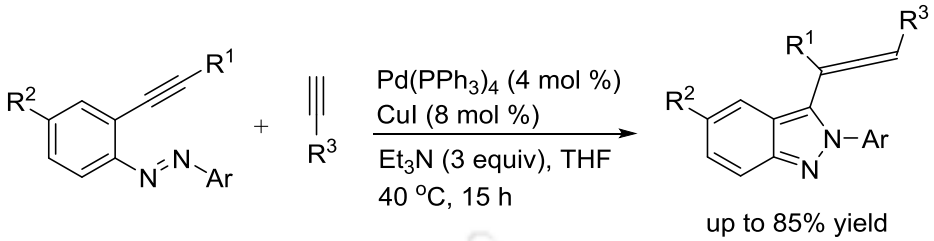

Scheme 7. Pd-catalyzed cross-coupling of 2-alkynyl azobenzenes.

3.3 Present Study

Herein the synthesis of indazoloquinolines and their photophysical and electrochemical studies are presented. Table 1 presents the reaction for the Rh(III)-catalyzed double C-H activation and C-C bond formation of 2*H*-indazoles with alkynes to afford indazolo[2,3-*a*]quinolines. First, optimization of the reaction was performed using 2-phenyl-2*H*-indazole **1a** and 1,2-diphenylethyne **2a** as the model substrates using $[Cp^*RhCl_2]_2$ as a catalyst in the presence of a series of oxidants and additives (Table 1). Gratifyingly, the oxidative annulation occurred to produce **3a** in 32% yield when the substrates **1a** and **2a** were stirred with 4 mol % $[Cp^*RhCl_2]_2$, 1.2 equiv $Cu(OAc)_2{\cdot}H_2O$ and 1 equiv K_2CO_3 at 100 °C in CH_2Cl_2 under N_2 (entry 1). Subsequent screening of the solvents led to an increase in yield to 66% using $(CH_2Cl)_2$, whereas toluene, *o*-xylene, chlorobenzene, acetonitrile, mesitylene, THF, 1,4-dioxane, methanol and DMF produced inferior results (entries 2-11). The reaction using K_2CO_3 was superior to Cs_2CO_3 and Na_2CO_3 as an additive (entries 12-13). In a set of oxidants screened, $Cu(OAc)_2{\cdot}H_2O$, AgOAc, Ag_2CO_3, $Co(OAc)_2{\cdot}4H_2O$ and $Mn(OAc)_3{\cdot}2H_2O$, the former furnished the best results (entries 14-17). The reaction under air or absence of an additive led to drop the yield to 43% (entries 18-19). Control experiment confirmed that the absence of either $[Cp^*RhCl_2]_2$ or $Cu(OAc)_2{\cdot}H_2O$ led to no annulation (entries 20-21). Having optimized reaction conditions, the scope of the procedure was investigated for a series of electronically varied 2*H*-indazoles **I** with alkynes (Table 2). The substrates bearing the substitution at the 4-position of the aryl ring with methyl **1b** and trifluoromethyl **1i** groups underwent reaction to give **IQ A** and **IQ B** in 56 and 74% yield. Similarly, the compounds bearing dimethoxy **1d,** 1-naphthyl **1e** and 2-pyridin-4-yl **1f** substituents annulated to give **IQ C-E** in 61-68% yields.

Table 1. Optimization of the Reaction Conditions[a, b]

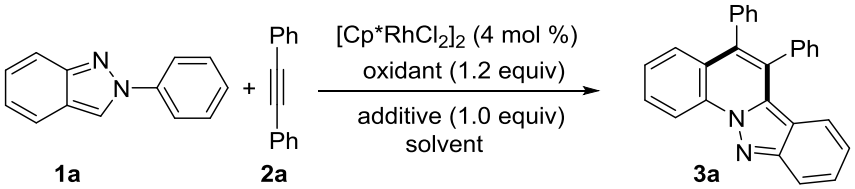

Entry	Oxidant	Additive	Solvent	Yield (%)[b]
1	$Cu(OAc)_2·H_2O$	K_2CO_3	CH_2Cl_2	32
2	**$Cu(OAc)_2·H_2O$**	**K_2CO_3**	**$(CH_2Cl)_2$**	**66**
3	$Cu(OAc)_2·H_2O$	K_2CO_3	toluene	10
4	$Cu(OAc)_2·H_2O$	K_2CO_3	*o*-xylene	21
5	$Cu(OAc)_2·H_2O$	K_2CO_3	mesitylene	n.d.
6	$Cu(OAc)_2·H_2O$	K_2CO_3	chlorobenzene	39
7	$Cu(OAc)_2·H_2O$	K_2CO_3	THF	n.d.
8	$Cu(OAc)_2·H_2O$	K_2CO_3	1,4-dioxane	n.d.
9	$Cu(OAc)_2·H_2O$	K_2CO_3	CH_3CN	12
10	$Cu(OAc)_2·H_2O$	K_2CO_3	MeOH	n.d.
11	$Cu(OAc)_2·H_2O$	K_2CO_3	DMF	n.d.
12	$Cu(OAc)_2·H_2O$	Na_2CO_3	$(CH_2Cl)_2$	32
13	$Cu(OAc)_2·H_2O$	Cs_2CO_3	$(CH_2Cl)_2$	45
14	AgOAc	K_2CO_3	$(CH_2Cl)_2$	n.d.
15	Ag_2CO_3	K_2CO_3	$(CH_2Cl)_2$	n.d.
16	$Co(OAc)_2·4H_2O$	K_2CO_3	$(CH_2Cl)_2$	trace
17	$Mn(OAc)_3·2H_2O$	K_2CO_3	$(CH_2Cl)_2$	trace
18[c]	$Cu(OAc)_2·H_2O$	K_2CO_3	$(CH_2Cl)_2$	43
19	$Cu(OAc)_2·H_2O$	-	$(CH_2Cl)_2$	21

20	$Cu(OAc)_2 \cdot H_2O$	K_2CO_3	$(CH_2Cl)_2$	n.d.
21[d]	-	K_2CO_3	$(CH_2Cl)_2$	n.d.

[a]Reaction conditions. **1a** (0.25 mmol), **2a** (0.30 mmol), $[Cp^*RhCl_2]_2$ (4 mol %), oxidant (0.30 mmol), additive (0.25 mmol), solvent (2 mL), 100 °C, 6 h, N_2. [b]Isolated yield. [c]Under air. [d]Without Rh catalyst. n.d. = not detected.

Table 2. Synthesis of Indazoloquinolines Photocatalysts **IQ A-E**

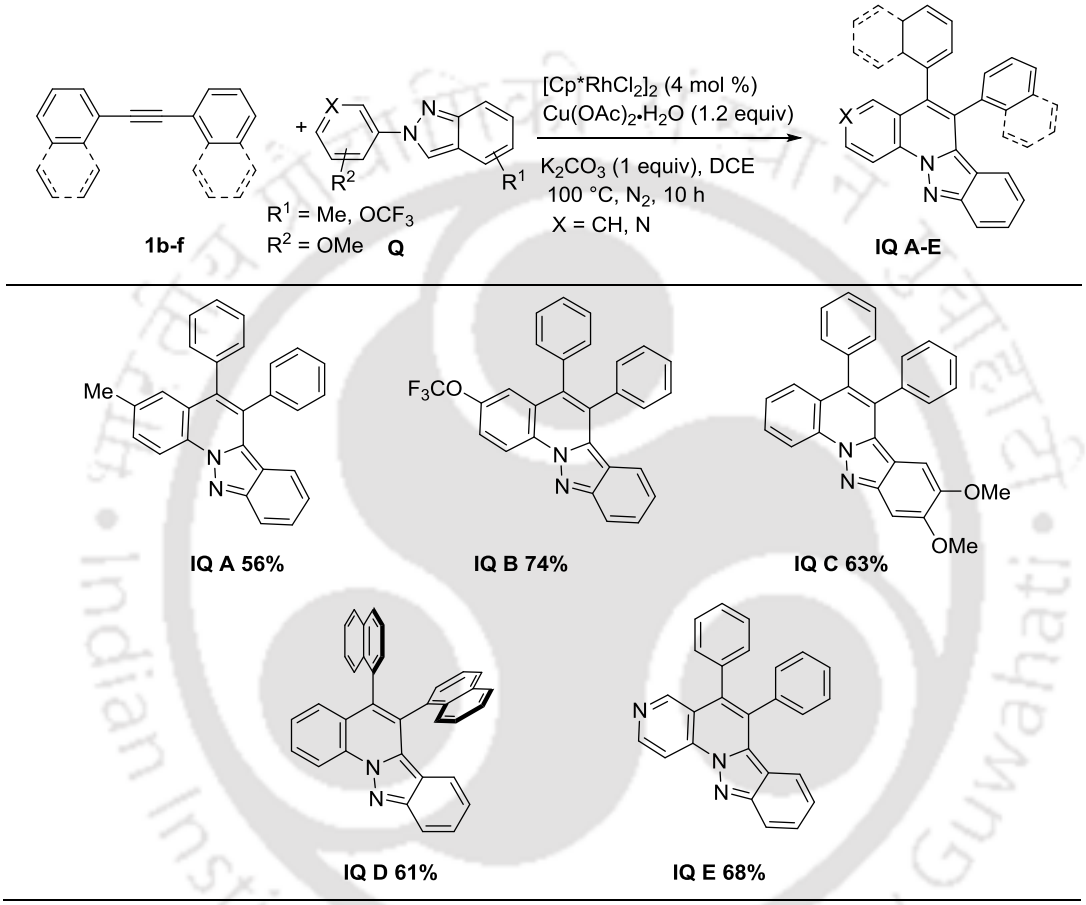

[a]Reaction condition: Indazole (0.50 mmol), alkyne (0.60 mmol), $Cu(OAc)_2 \cdot H_2O$ (0.60 mmol), K_2CO_3 (0.50 mmol), $[RhCp^*Cl_2]_2$ (4 mol %), DCE, 100 °C, 10 h. [b]Isolated yield.

Table 3 presents the comparison of photoredox properties of **IQ A-E** with commercial catalysis. Upon visible light irradiation, **IQ A-E** showed a nanosecond singlet excited state with the strong oxidative ($E^*_{red}{}^{exp}$ = +1.65 V to +1.85 V, vs SCE and $E^*_{red}{}^{DFT}$ = +1.41 V to +1.65 V, vs SCE) and reductive ($E^*_{ox}{}^{exp}$ = -1.73 V to -1.91 V, vs SCE and $E^*_{ox}{}^{DFT}$ = -2.15 V to -2.62 V, vs SCE) competencies that are comparable/superior to the common photoredox organic dyes and metal complexes. The electronic properties indicated that the HOMO-LUMO gap of **IQ** (ΔE^{opt} = 2.84 to 2.90 eV, Eg^{exp} = 2.48 to 2.84 eV and ΔE^{DFT} = 3.96 to 4.05 eV, Figure 2) could facilitate the formation of a radical through a single electron

transfer (SET). This wide window of strong redox potentials suggests that **IQ A-E** are most suitable to promote the organic transformations under visible light.

Table 3. Photoredox catalyst **IQ(A-E)** and commercial photoredox catalyst.

	IQ A	IQ B	IQ C
	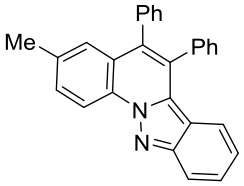	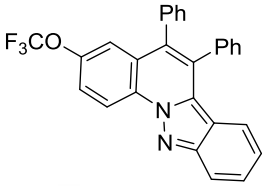	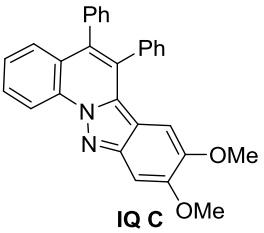
$E_{1/2}$ $(P^*/P^-)_{exp}$	+1.70 V	+1.65 V	+1.85 V
$E_{1/2}$ $(P^*/P^-)_{DFT}$	+1.41 V	+1.65 V	+1.44 V
$E_{1/2}$ $(P^*/P^+)_{exp}$	-1.89 V	-1.73 V	-1.73 V
$E_{1/2}$ $(P^*/P^+)_{DFT}$	-2.39 V	-2.27 V	-2.63 V

	IQ D *(anti)*[a]	IQ D*(syn)*[a]	IQ E
	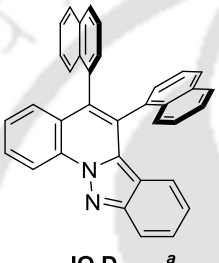	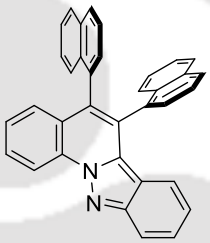	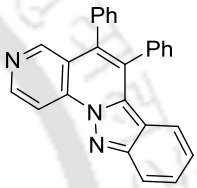
$E_{1/2}$ $(P^*/P^-)_{exp}$	+1.72 V	-	+1.74 V
$E_{1/2}$ $(P^*/P^-)_{DFT}$	+1.52 V	+1.49 V	+1.60 V
$E_{1/2}$ $(P^*/P^+)_{exp}$	-1.85 V	-	-1.91 V
$E_{1/2}$ $(P^*/P^+)_{DFT}$	-2.31 V	-2.30 V	-2.15 V

	Rose Bengal	Eosin Y	$[Ru(bpy)_3]^{2+}$	*fac*-$[Ir(ppy)_3]$
	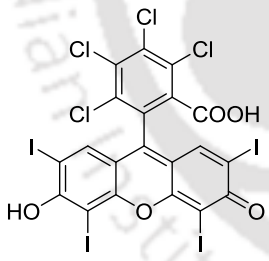	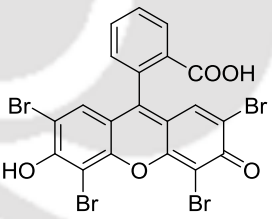	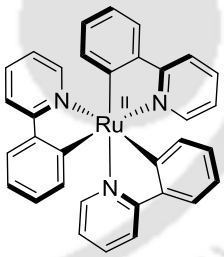	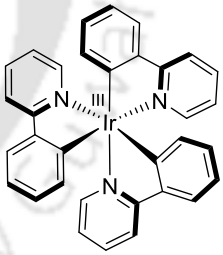
$E_{1/2}$ (P^*/P^-)	+0.81V	+0.83 V	+0.77 V	+0.77 V
$E_{1/2}$ (P^*/P^+)	-0.96 V	-1.11 V	-0.81 V	-1.73 V

Photocatalysts **IQ (A-E)** and common photoredox catalysis and their redox potentials (vs SCE, all potentials mentioned against SCE). For simplicity, only excited state redox potentials shown here. [a1]H NMR shows 10:1 inseparable mixture of rotomers.

In summary, synthesis, photophysical and electrochemical studies of indazoloquinolines **IQ A-E** have been presented. They exhbit wide-redox window and excellent chemical stability that can lead to photoredox catalysis.

3.4 Experimental Section

General Information. $[Cp^*RhCl_2]_2$ and $Cu(OAc)_2{\cdot}H_2O$ (>98%) were purchased from Aldrich. Silica gel-G plates (Merck) were used for TLC analysis with a mixture of hexane and ethyl acetate as the eluent. Melting point of the products was measured on Büchi melting point apparatus, MP B-540. Open capillary tubes were used for the measurements and are uncorrected. NMR spectra were recorded on Bruker 400 MHz NMR instruments using TMS as an internal standard and $CDCl_3$ as a solvent. Chemical shifts are given in parts per million (δ) and the coupling constants are given in Hz. Q-Tof ESI-MS instrument (model HAB 273) was used for recording HRMS data. IR spectra were recorded on Perkin Elmer FT-IR instrument. UV-vis spectra were recorded on Agilent spectrophotometer and fluorescence were recorded on Cary Eclipse spectrofluorimeter.

General Procedure for the Synthesis of Indazoloquinolines IQ A-E. 2-Aryl-2*H* indazole (0.50 mmol), alkyne (0.60 mmol), $Cu(OAc)_2{\cdot}H_2O$ (0.60 mmol), K_2CO_3 (0.50 mmol) and $[Cp^*RhCl_2]_2$ (4 mol %) were stirred in $(CH_2Cl)_2$ at 100 °C for 10 h under nitrogen atmosphere. Progress of the reaction was monitored using TLC analysis. The reaction mixture was passed through celite using CH_2Cl_2 and evaporation of the solvent gave a residue that was purified on silica gel column chromatography using a 1:50 ethyl acetate and hexane.[11]

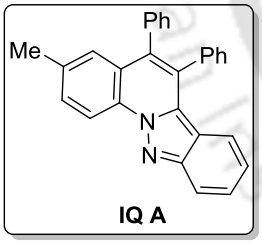

3-Methyl-5,6-diphenylindazolo[2,3-*a*]quinolone IQ A. Analytical TLC on silica gel, 1:50 ethyl acetate/hexane R_f = 0.40; yellow solid; yield 56% (107 mg). ^{1}H NMR (400 MHz, $CDCl_3$) δ 8.98 (d, J = 8.6 Hz, 1H), 7.94 (d, J = 8.7 Hz, 1H), 7.64 (dd, J = 8.6, 1.8 Hz, 1H), 7.44 (ddd, J = 8.7, 6.7, 1.1 Hz, 1H), 7.38-7.34 (m, 4H), 7.32-7.27 (m, 5H), 7.23 (dd, J = 7.7, 1.8 Hz, 2H), 6.90 (ddd, J = 8.5, 6.7, 0.9 Hz, 1H), 6.66 (d, J = 8.5 Hz, 1H), 2.46 (s, 3H). ^{13}C NMR (101 MHz, $CDCl_3$) δ 149.7, 136.7, 136.7, 136.2, 133.9, 131.8, 131.3, 130.9, 130.8, 130.4, 128.5, 128.1, 128.0, 127.7, 127.5, 127.4, 125.7, 121.8, 120.4, 117.7, 117.3, 116.5, 21.8. HRMS (ESI) calcd for $[C_{28}H_{20}N_2 + H]^+$ 385.1705, found 385.1712.

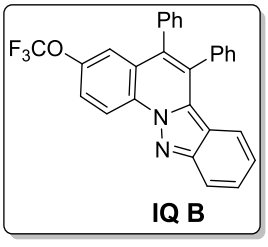

5,6-Diphenyl-3-(trifluoromethoxy)indazolo[2,3-*a*]quinoline IQ B. Analytical TLC on silica gel, 1:50 ethyl acetate/hexane R_f = 0.40; yellow solid; yield 74% (168 mg). ^{1}H NMR (400 MHz, $CDCl_3$) δ 9.13 (d, J = 9.2 Hz, 1H), 7.94 (d, J = 8.7 Hz, 1H),

7.67 (ddd, *J* = 9.2, 2.6, 1.2 Hz, 1H), 7.49-7.44 (m, 2H), 7.37 (dt, *J* = 4.6, 1.8 Hz, 3H), 7.34-7.27 (m, 5H), 7.23-7.21 (m, 2H), 6.93 (ddd, *J* = 8.5, 6.7, 1.0 Hz, 1H), 6.68-6.66 (m, 1H). ^{13}C NMR (101 MHz, $CDCl_3$) *δ* 149.9, 147.1, 147.1, 136.1, 135.7, 133.3, 132.2, 131.9, 131.8, 131.1, 130.2, 128.7, 128.4, 128.3, 128.2, 127.9, 127.4, 126.9, 123.0, 122.4, 122.4, 121.8, 121.1, 120.6, 120.6, 119.7, 119.4, 118.2, 117.8, 116.7. ^{19}F NMR (376 Hz, $CDCl_3$) δ -57.9. HRMS (ESI) m/z $[M+H]^+$ calcd for $C_{28}H_{17}F_3N_2O$ 455.1371, found 455.1380.

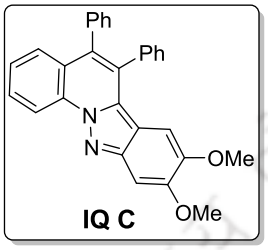

8,9-Dimethoxy-5,6-diphenylindazolo[2,3-*a*]quinoline IQ C. Analytical TLC on silica gel, 1:50 ethyl acetate/hexane R_f = 0.40; yellow solid; yield 63% (135 mg). Yellow solid; yield 63% (135 mg). ^{1}H NMR (400 MHz, $CDCl_3$) *δ* 8.94 (dd, *J* = 8.5, 1.2 Hz, 1H), 7.76 (ddd, *J* = 8.5, 7.1, 1.4 Hz, 1H), 7.57 (dd, *J* = 8.3, 1.4 Hz, 1H), 7.44 (ddd, *J* = 8.3, 7.0, 1.3 Hz, 1H), 7.40-7.35 (m, 2H), 7.34-7.28 (m, 5H), 7.27-7.24 (m, 4H), 5.80 (s, 1H), 4.00 (s, 3H), 3.49 (s, 3H). ^{13}C NMR (101 MHz, $CDCl_3$) *δ* 152.3, 146.5, 146.4, 136.7, 136.6, 133.9, 133.1, 131.3, 131.3, 130.6, 130.3, 129.2, 128.5, 128.1, 128.1, 127.9, 127.5, 125.4, 125.1, 116.6, 111.4, 99.5, 95.3, 56.1, 55.5. HRMS (ESI) m/z $[M+H]^+$ calcd for $C_{29}H_{22}N_2O_2$ 431.1760, found 431.1768.

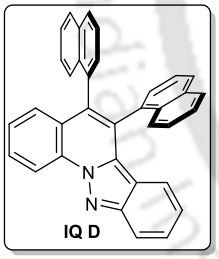

5,6-Di(naphthalen-1-yl)indazolo[2,3-*a*]quinoline IQ D. Analytical TLC on silica gel, 1:50 ethyl acetate/hexane R_f = 0.40; yellow solid; yield 61% (143 mg). ^{1}H NMR (400 MHz, $CDCl_3$) 10:1 mixture of rotomers *δ* 9.18 (dd, *J* = 8.5, 1.3 Hz, 1H), 7.95 (d, *J* = 8.7 Hz, 1H), 7.86-7.74 (m, 3H), 7.69-7.64 (m, 2H), 7.58-7.54 (m, 2H), 7.48-7.29 (m, 7H), 7.27-7.25 (m, 1H), 7.19-7.08 (m, 3H), 6.69-6.65 (m, 1H), 5.99 (d, *J* = 8.4 Hz, 1H). ^{13}C NMR (101 MHz, $CDCl_3$) *δ* 149.9, 134.2, 134.1, 133.7, 133.5, 133.4, 133.3, 132.4, 132.3, 130.1, 129.6, 128.7, 128.5, 128.5, 128.4, 128.4, 127.9, 127.7, 126.7, 126.7, 126.5, 126.4, 126.2, 126.1, 126.0, 125.8, 125.5, 125.3, 121.5, 120.9, 117.5, 117.5, 116.6. HRMS (ESI) m/z $[M+H]^+$ calcd for $C_{35}H_{22}N_2$ 471.1861, found 471.1870.

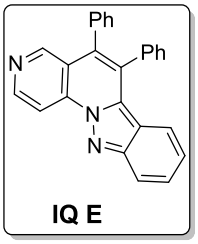

5,6-Diphenylindazolo[2,3-*a*][1,6]naphthyridine IQ E. Analytical TLC on silica gel, 1:50 ethyl acetate/hexane R_f = 0.40; yellow solid; yield 68% (126 mg). ^{1}H NMR (400 MHz, $CDCl_3$) δ 8.97-8.84 (m, 3H), 7.95 (d, J = 8.7 Hz, 1H), 7.49 (ddd, J = 8.8, 6.6, 1.1 Hz, 1H), 7.40-7.38 (m, 3H), 7.36-7.29 (m, 5H), 7.26-7.24 (m, 2H), 6.95 (ddd, J = 8.6, 6.7, 0.9 Hz, 1H), 6.69 (d, J = 8.6 Hz, 1H). ^{13}C NMR (101 MHz, $CDCl_3$) δ 151.3, 150.6, 147.9, 137.6, 135.7, 134.7, 133.1, 132.6, 132.3, 131.2, 130.2, 128.8, 128.8, 128.5, 128.3, 128.0, 122.0, 121.6, 117.7, 117.0, 110.7. HRMS (ESI) m/z $[M+H]^+$ calcd for $C_{26}H_{17}N_3$ 372.1501, found 372.1511.

3.5.1 UV-visible and Emission Studies

The UV-vis studies exhibit two absorption bands (λ_{abs}) at ~250-272 and 371-389 nm, which are attributed to n-π* and π- π* transitions, respectively (Figure 2). The nature of the substituent plays a crucial role in the emission wavelength (λ_{em}) varying from indigo blue to blue, producing mostly a redshift. Further, a larger Stokes shift is observed (55-82 nm) that suggests the high polarizability in the π-conjugated systems of IQs. The obtained quantum yields (Φ, 0.69-0.86) in $CHCl_3$ using Rhodamine 6G with EtOH depends on the nature of the substituent.

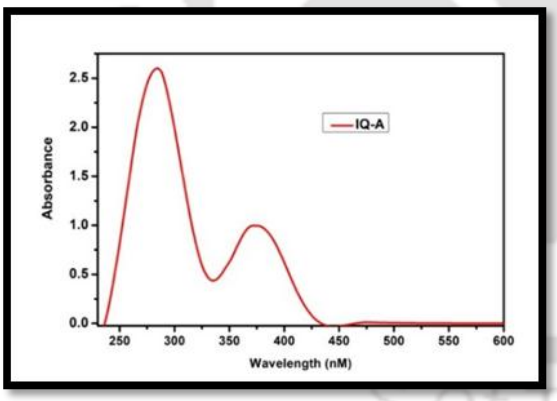

UV-visible spectrum of IQ A

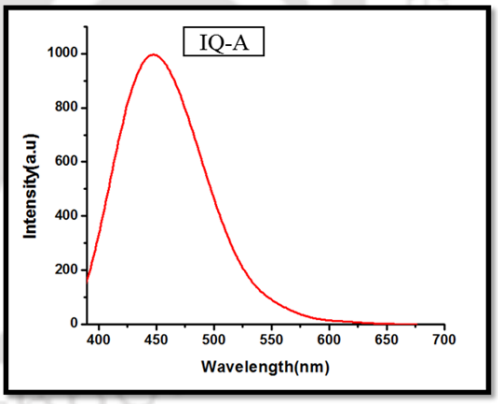

Emission spectrum of IQ A

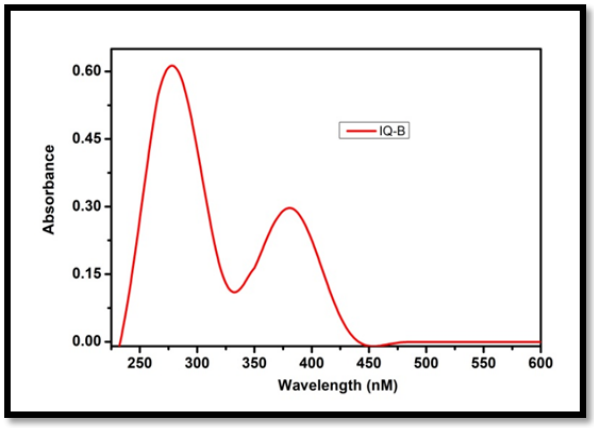

UV-visible spectrum of IQ B

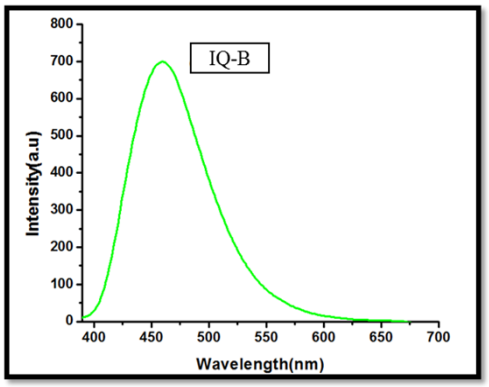

Emission spectrum of IQ B

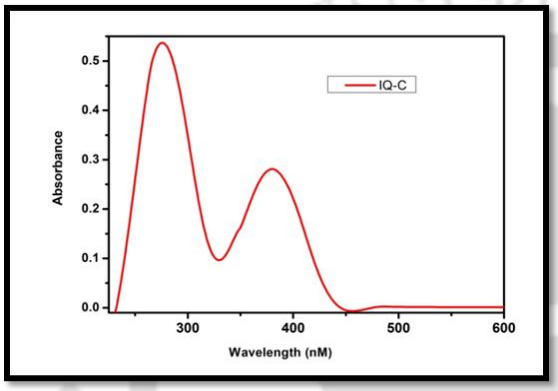

UV-visible spectrum of IQ C

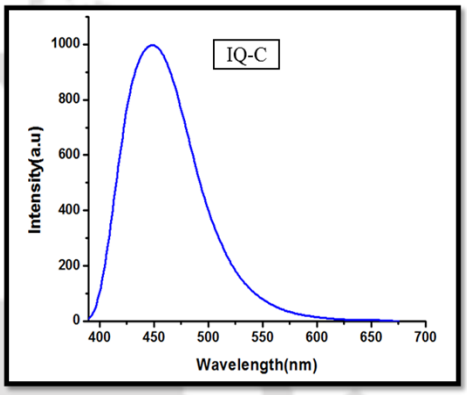

Emission spectrum of IQ C

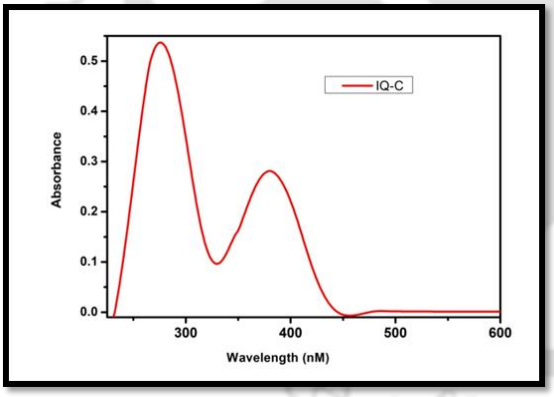

UV-visible spectrum of IQ D

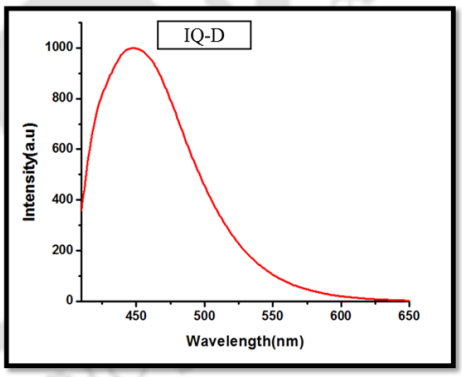

Emission spectrum of IQ D

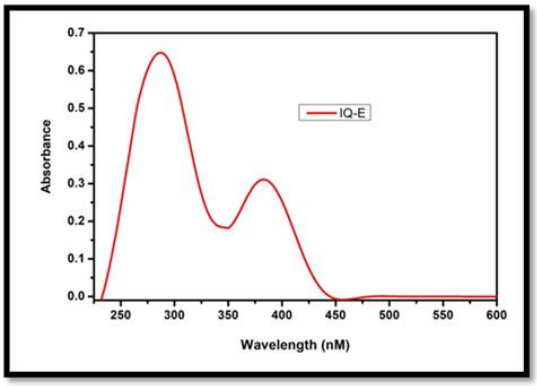

UV-visible spectrum of IQ E

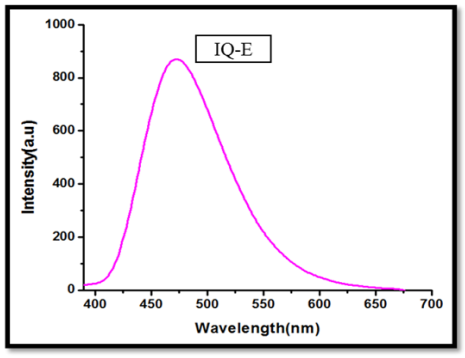

Emission spectrum of IQ E

Figure 2. UV-visible and Emission Spectrum of Catalysts IQ (A-E)

3.5.2 Fluorescence Lifetime Measurements

The excited-state lifetime of the IQs was measured using fluorescence lifetime. The time-resolved fluorescence lifetime measurements carried out using a picosecond time-resolved fluorimeter, Eddinburg Instruments and Lifespec II model. All the IQ-E solutions were excited at the corresponding wavelength and the emission intensity was collected at 446 nm. A screw-top quartz cuvette was charged with a 0.1 mM solution of IQ-E in DMF (2.0 mL) and the fluorescence lifetime decay was collected.

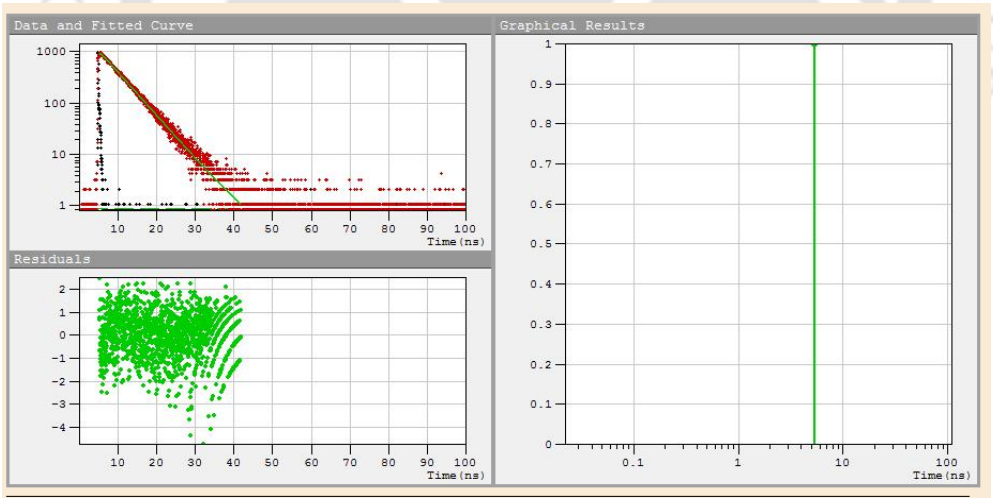

v **Exponential Components Analysis (Reconvolution)**

Fitting range : [201; 1700] channels

c^2 : 1.006

	B_i	DB_i	f_i (%)	Df_i (%)	t_i (ns)	Dt_i (ns)
1	0.1276	0.0007	100.000	0.535	5.193	0.0005

Shift : 0.146 ns (± 1.212 ns)

Decay Background : 0.213 (± 0.136)

IRF background : 0

Fluorescence lifetime decay of IQ A

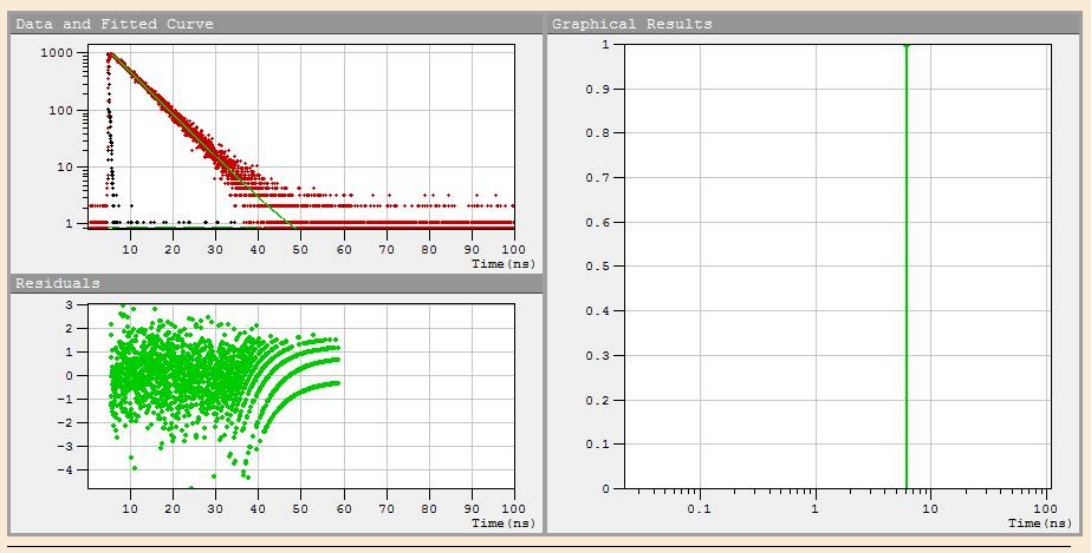

v Exponential Components Analysis (Reconvolution)

Fitting range : [210; 2400] channels

c^2 : 0.997

	B_i	DB_i	f_i (%)	Df_i (%)	t_i (ns)	Dt_i (ns)
1	0.1281	0.0007	100.000	0.563	5.878	0.0004

Shift : 0.293 ns (± 1.442 ns)

Decay Background : 0.216 (± 0.080)

IRF background : 0

Fluorescence lifetime decay of IQ B

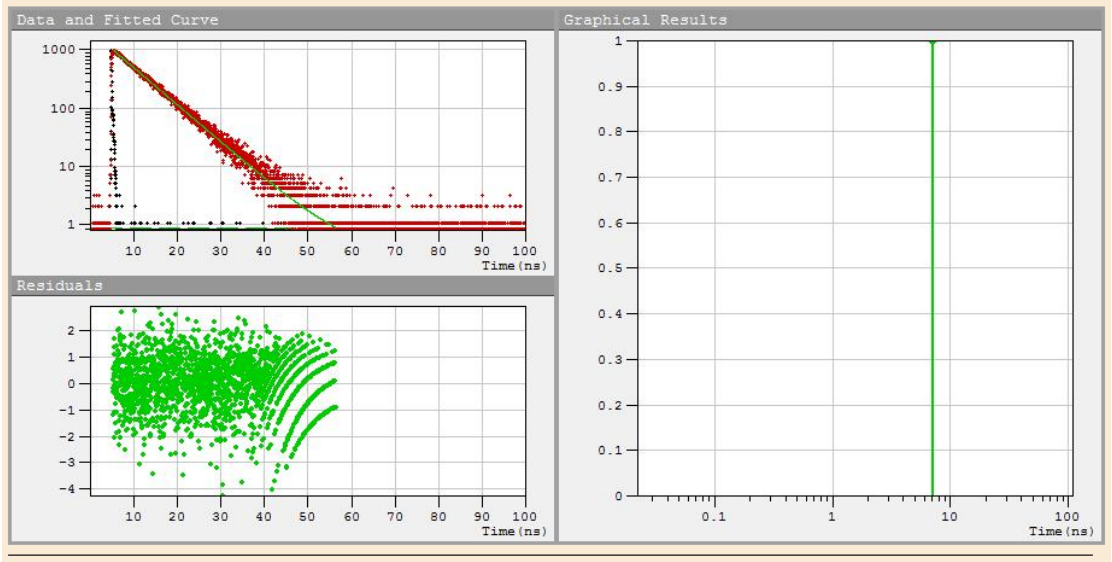

v Exponential Components Analysis (Reconvolution)

Fitting range : [201; 2300] channels
c^2 : 1.005

	B_i	DB_i	f_i (%)	Df_i (%)	t_i (ns)	Dt_i (ns)
1	0.1334	0.0042	100.000	3.156	6.841	0.0003

Shift : -0.294 ns (± 9.021 ns)
Decay Background : 0.364 (± 0.104)
IRF background : 0

Fluorescence lifetime decay of IQ C

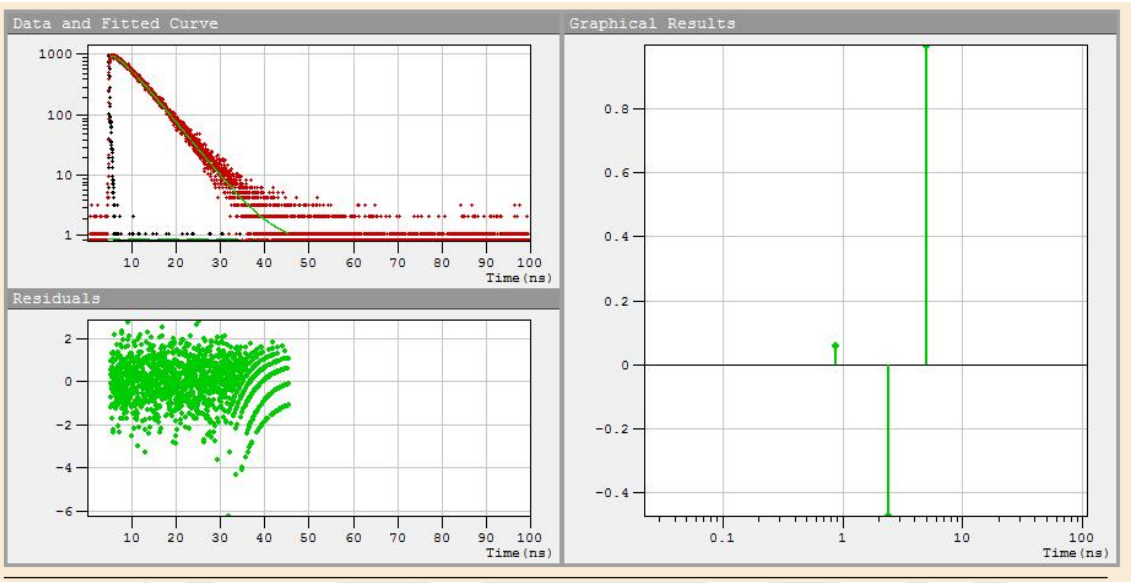

v Exponential Components Analysis (Reconvolution)

Fitting range : [200; 1850] channels
c^2 : 1.026

	B_i	DB_i	f_i (%)	Df_i (%)	t_i (ns)	Dt_i (ns)
1	0.0122	0.0148	0.785	2.734	0.829	1.875
2	-0.1029	0.0124	18.559	1.637	2.313	0.074
3	0.2169	0.0155	80.656	5.822	4.772	0.004

Shift : 0.145 ns (± 3.370 ns)
Decay Background : 0.731 (± 0.161)
IRF background : 0

Fluorescence lifetime decay of IQ D

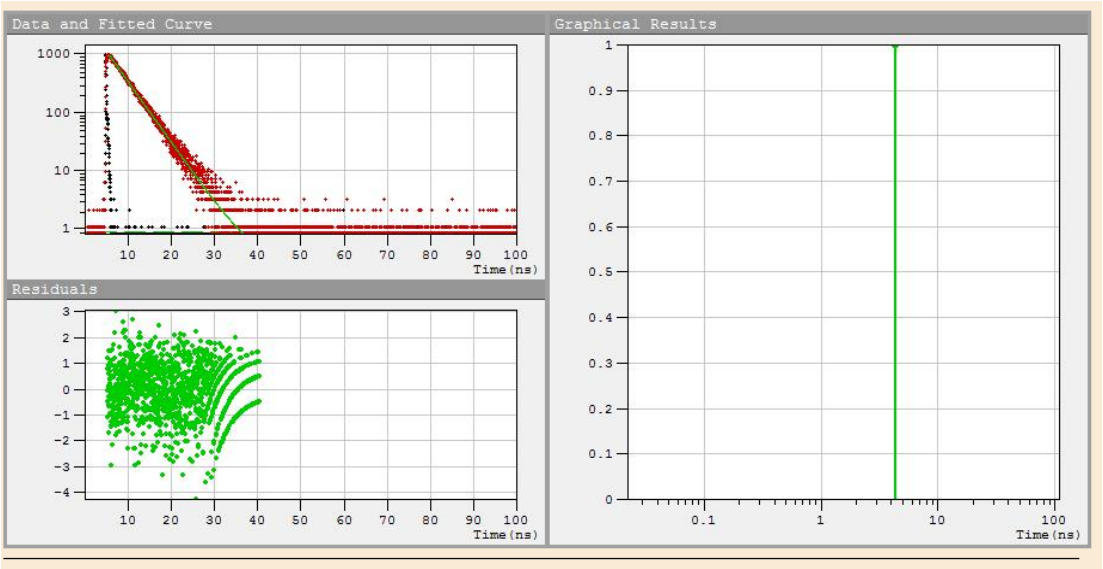

v Exponential Components Analysis (Reconvolution)

Fitting range : [201; 1650] channels

c^2 : 0.998

	B_i	DB_i	f_i (%)	Df_i (%)	t_i (ns)	Dt_i (ns)
1	0.1343	0.0008	100.000	0.617	4.181	0.0006

Shift : 0.146 ns (± 1.149 ns)

Decay Background : 0.270 (± 0.108)

IRF background : 0

Fluorescence lifetime decay of IQ E

3.5 Electrochemical Studies

3.5.1 Determination of Ground State Oxidation Potential of IQ Catalyst

The ground state redox potential of IQs determined using the cyclic voltammetry (CV). The process was carried out in the biologic SP-300 electrochemical workstation. In CV analysis, the GC electrode (3 mm diameter), a Pt wire, and $Ag/AgNO_3$ (0.01 M $Ag/AgNO_3$ contain 0.1 M *n*-tetrabutylammonium hexafluoroborate *n*-$BuNBF_4$) in CH_3CN, were used as working electrode, counter electrode and reference electrode, respectively. The anhydrous DMF containing 1.0 mM of the respective photocatalyst and 0.10 M TBABF served as the supporting electrolyte. The solvents used in the analysis were thoroughly purged with N_2 gas before the experiments. The potential of CV was scanned between -1.70 V to 1.2 V at a sweep rate of 100 mV/s.

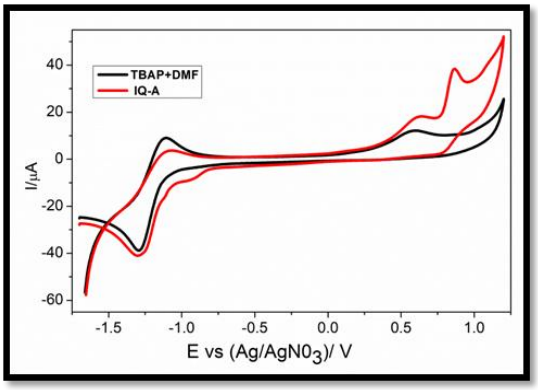

Cyclic voltammogram of IQ A

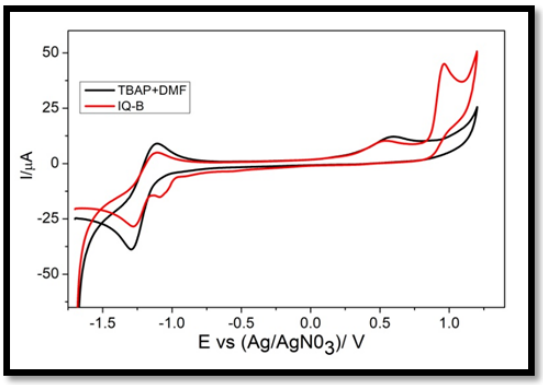

Cyclic voltammogram of IQ B

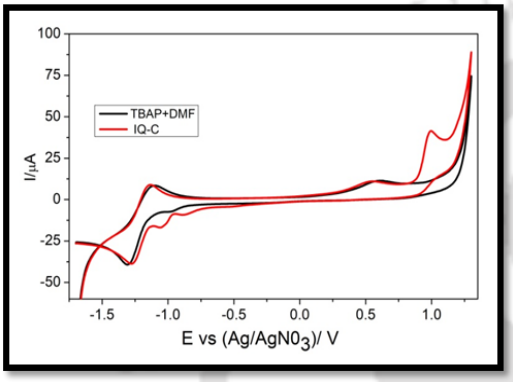

Cyclic voltammogram of IQ C

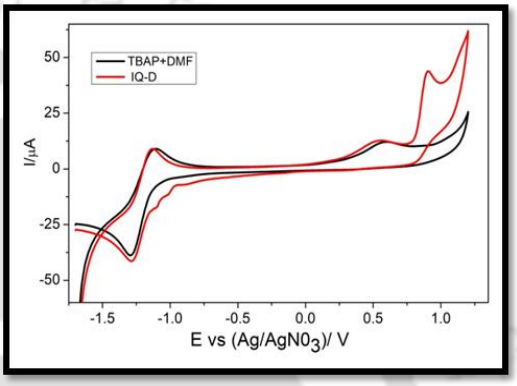

Cyclic voltammogram of IQ D

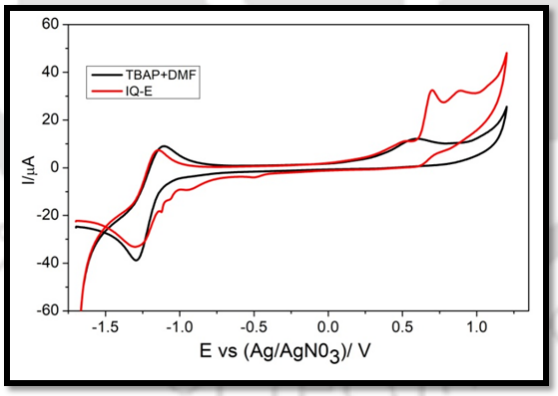

Cyclic voltammogram of IQ E

Figure 2. Cyclic voltammograms of 1 mM concentration of PC **IQ-A-E** and (TBAP+DMF is a without the substrate) in DMF containing 0.1 M of TBAP. Scan rate: 100 mV/s.

Table 4. Photophysical and Electrochemical Properties of Photocatalysts

PC	Abs λ_{max}[a] (nm)	Emission λ_{max}[b] (nm)	log ε[c]	Φ[d]	τ[e] (ns)	$E_{0\text{-}0}$ (eV)[f]	E_{ox} (*vs.* SCE)[g] (V)	E^*_{ox} (*vs.* SCE)[h] (V)	E_{red} (*vs.* SCE)[g] (V)	E^*_{red} (*vs.* SCE)[i] (V)
IQ A	373	446	5.20	0.86	5.19	3.03	1.14	-1.89	-1.33	1.70
IQ B	381	458	3.10	0.69	5.88	2.96	1.23	-1.73	-1.31	1.65
IQ C	380	448	3.00	0.85	6.84	2.99	1.26	-1.73	-1.14	1.85
IQ D	375	473	3.20	0.78	4.28	3.02	1.17	-1.85	-1.30	1.72
IQ E	383	446	4.00	0.86	4.18	2.89	0.98	-1.91	-1.15	1.74

Table 4 summarises the results of the photophysical and elctrochemical studies. [a] λ_{max} for absroption was recorded in UV- visible absorption spectroscopy techniques which was calculated from the UV−visible spectrum located at higher wavelength. [b] λ_{max} for emission spectroscopy techniques were calculated from the emission spectra. [c] Molar excitation coefficient, [d] quantum yield, [e] fluorescence life time and [f] singlet energies were calculated using the maximum wavelength of emission in the equation of $E = hc / \lambda$ where, E is the Energy (V), h is the plank's constant 6.626×10^{-34} m^2 kg /s, C is the speed of light 3×10^{-8} ms^{-1}. [g] Ground state redox potentials were calculated from cyclic voltammograms and the values were reported against SCE scale in the way of the following equation E (V *vs.* SCE) = E (V *vs.* $Ag/AgNO_3$ [0.01 M]) + 0.298 V. [h] E^*_{ox} calculated from $E^*_{ox} = E_{ox} - E_{0\text{-}0}$; [i] E^*_{red} calculated from $E^*_{red} = E_{red} - E_{0\text{-}0}$.

Table 5. HOMO, LUMO and Band Gap Energies of the Photocatalysts

PC	HOMO (eV)[a]	LUMO (eV)[b]	Eg (eV)[c]	Eg^{op}(eV)[d]
IQ A	-5.58	-2.74	2.84	2.86
IQ B	-5.65	-3.06	2.59	2.86
IQ C	-5.68	-3.16	2.52	2.85
IQ D	-5.70	-2.95	2.75	2.90
IQ E	-5.50	-3.02	2.48	2.84

[a] and [b] are the energy level of HOMO and LUMO was calculated, by using an equation of HOMO = E_{ox}, onset + 4.4 eV, LUMO = E_{red}, onset + 4.4 eV respectively when SCE is used as reference electrode and ferrocene does not uses as an internal reference electrode where E_{ox} is a onset potential of oxidation and E_{red} is a onset potential of reduction. [c] HOMO-LUMO. [d] Eg^{op}= 1243 / λ for optical band gap respectively.

3.5.2 Quantum Chemical Calculations

General Approaches. Gaussian-09 (revision D.01) program package was used for the excited state redox potential IQs calculations.[8] Dispersion corrected M06 DFT functional and basis set with one diffuse and two polarization functions. M06/6-31+G(d,p) was selected for geometry optimization of all the reactants, intermediates and transition states. Vibrational frequency calculations were carried out using same method and basis set, to distinguish minima structures and transition states on the potential energy surface on the basis of number of imaginary frequencies.

The ground-state redox potentials were calculated from the Gibbs free energy differences between neutral and oxidized or reduced ground-state catalysts. Gibbs free energies in solution were calculated by reoptimizing the catalysts in *N*,*N*-dimethylformamide solvent using IEF-PCM method for both (reduced and oxidized) species.

$$\Delta Gn_{(g)},\ \Delta Gn_{(sol)},\ \text{and}\ \Delta Gr_{(g)} = E + G \qquad (3.1)$$

where 'E' is the 'total energy' and 'G' is the 'thermal correction to Gibbs free energy'. '$\Delta Gn_{(g)}$' shows the 'calculation in gas phase' and '$\Delta Gn_{(sol)}$' shows the calculations in 'DMF solvent' using IEF-PCM method. '$\Delta Gr_{(g)}$' shows the 'calculation of the cationic species'.

$$\Delta Gr_{(sol)} = E\ (\text{cationic in solvent phase}) - E\ (\text{cationic in gas phase}) \qquad (3.2)$$

$$\Delta Gox_{(g)} = [\Delta Gr_{(g)} - \Delta Gn_{(g)}] \qquad (3.3)$$

$$\Delta Gox_{(sol)} = [\Delta Gox_{(g)} - \Delta Gn_{(sol)} + \Delta Gr_{(sol)}]*627.5095 \qquad (3.4)$$

$$E^{\circ}_{1/2}{}^{DFT} = -\frac{\Delta Gox_{(sol)}}{n_e F} - E^{\circ}_{1/2}{}^{SHE} + E^{\circ}_{1/2}{}^{SCE} \qquad (3.5)$$

where 'n_e' is the number of electrons transferred (n_e = 1 in all calculations), 'F' is Faraday constant (F = 23.061 kcal mol^{-1} V^{-1}), '$E^{o}_{1/2}{}^{SHE}$' is the absolute value for the standard hydrogen electrode (SHE = 4.281 V) and '$E^{o}_{1/2}{}^{SCE}$' is the potential of the saturated calomel electrode (SCE) relative to SHE in acetonitrile (-0.141 V). All the calculated redox potentials for the catalysts reported herein were referenced to this value in order to mimic the experimental procedures used to determine $E_{1/2}$. Same procedure was followed to get the reductional potential for catalyst (just cationic is replaced by anionic in the above equations).[8]

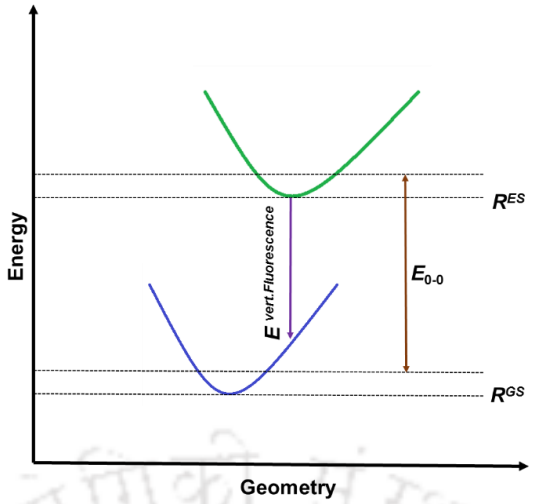

Figure 3. Simplified Jabłonski diagram.

The 0-0 transition energy ($E_{0\text{-}0}$) in DMF solvent is calculated based on the simplified Jabłonski diagram and the equation is given below.

where $\mathbf{E}^{\text{vertical fluo.}}$ is the TD-DFT vertical fluorescence energy calculated on the excited-state optimized geometry, $E^{GS}(R^{ES})$ is the ground-state energy calculated from the excited-state optimized geometry, $E^{GS}(R^{GS})$ is the ground-state energy calculated from the ground-state optimized geometry.

3.5.3 Calculation of Excited-State Redox Potentials

The excited-state redox potentials were calculated from the ground-state redox potentials and the singlet $E_{0\text{-}0}$ transition energy using the Latimer diagram as shown below. All the terms given in the Latimer diagram are computed values. $E_{0\text{-}0}$ energies are calculated using TD-DFT calculation as given above. The calculation of excited state redox potentials obtained from the following formula[9] (eq. 3.6 and 3.7).

$$E^{*}_{red}\,(cat^{*}/cat^{\bullet-}) = E_{red}\,(cat^{*}/cat^{\bullet-}) + E_{0\text{-}0} \qquad (3.6)$$

$$E^{*}_{ox}\,(cat^{*}/cat^{\bullet+}) = E_{ox}\,(cat^{*}/cat^{\bullet+}) - E_{0\text{-}0} \qquad (3.7)$$

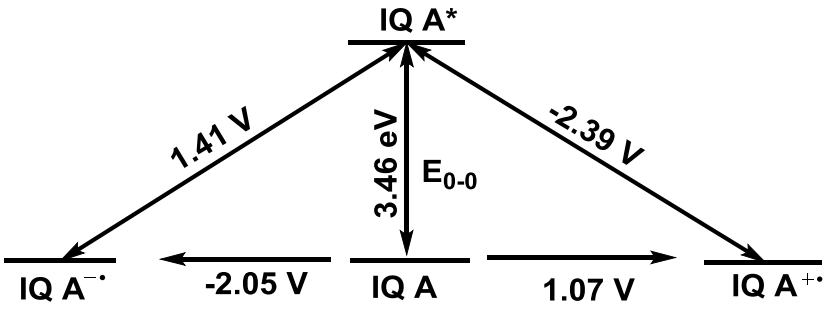

The Latimer diagram for **IQ A**

$E^{*}_{red}\,(IQ\ A^{*}/IQ\ A^{\bullet-})$ = $E_{red}\,(IQ\ A/IQ\ A^{\bullet-})$ + $E_{0\text{-}0}$

	=	−2.05 +3.46	=	1.41 V
E^{*}_{ox} (IQ A^{*}/IQ $A^{\bullet+}$)	=	E_{ox} (IQ A/IQ $A^{\bullet+}$)	−	$E_{0\text{-}0}$
	=	1.07−3.46	=	−2.39 V

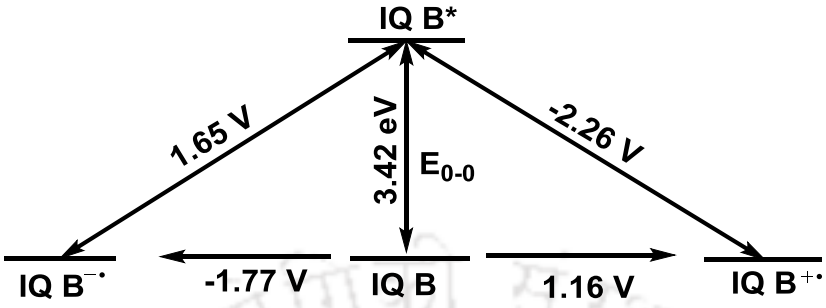

The Latimer diagram for **IQ B**

E^{*}_{red} (IQ B^{*}/IQ $B^{\bullet-}$)	=	E_{red} (IQ B/IQ $B^{\bullet-}$)	+	$E_{0\text{-}0}$
	=	−1.77 +3.42	=	1.65 V
E^{*}_{ox} (IQ B^{*}/IQ $B^{\bullet+}$)	=	E_{ox} (IQ B/IQ $B^{\bullet+}$)	−	$E_{0\text{-}0}$
	=	1.16−3.42	=	−2.26 V

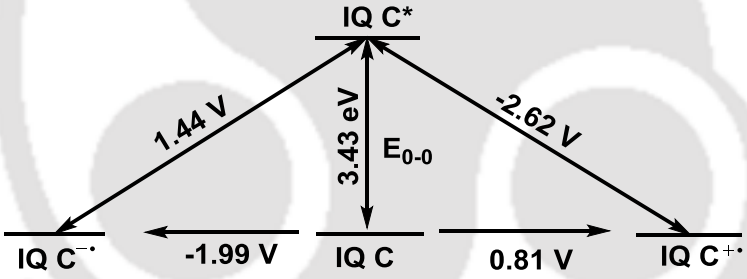

The Latimer diagram for **IQ C**

E^{*}_{red} (IQ C^{*}/IQ $C^{\bullet-}$)	=	E_{red} (IQ C/IQ $C^{\bullet-}$)	+	$E_{0\text{-}0}$
	=	−1.99 +3.43	=	1.44 V
E^{*}_{ox} (IQ C^{*}/IQ $C^{\bullet+}$)	=	E_{ox} (IQ C/IQ $C^{\bullet+}$)	−	$E_{0\text{-}0}$
	=	0.81−3.43	=	−2.62 V

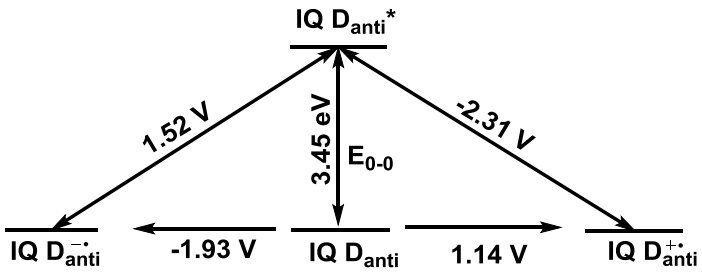

The Latimer diagram for **IQ D_{anti}**

E^{*}_{red} (IQ $D_{anti}{}^{*}$/IQ $D_{anti}{}^{\bullet-}$) = E_{red} (IQ D_{anti}/IQ $D_{anti}{}^{\bullet-}$) + $E_{0\text{-}0}$

	=	−1.93 + 3.45	=	1.52 V
E^{*}_{ox} (IQ $D_{anti}{}^{*}$/IQ $D_{anti}{}^{\bullet+}$)	=	E_{ox} (IQ D_{anti}/IQ $D_{anti}{}^{\bullet+}$)	−	$E_{0\text{-}0}$
	=	1.14 − 3.45	=	−2.31 V

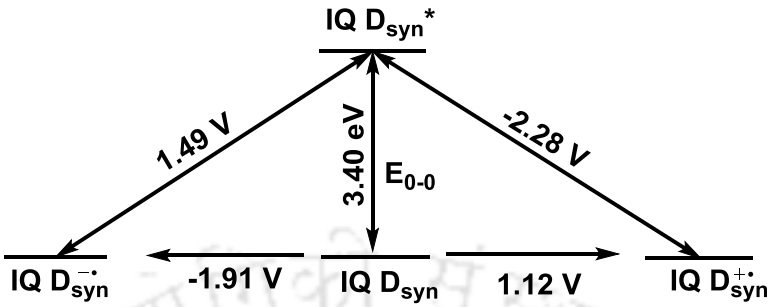

The Latimer diagram for **IQ D_{syn}**

E^{*}_{red} (IQ $D_{syn}{}^{*}$/IQ $D_{syn}{}^{\bullet-}$)	=	E_{red} (IQ D_{syn}/IQ $D_{syn}{}^{\bullet-}$)	+	$E_{0\text{-}0}$
	=	−1.91 + 3.40	=	1.49 V
E^{*}_{ox} (IQ $D_{syn}{}^{*}$/IQ $D_{syn}{}^{\bullet+}$)	=	E_{ox} (IQ D_{syn}/IQ $D_{syn}{}^{\bullet+}$)	−	$E_{0\text{-}0}$
	=	1.12 − 3.40	=	−2.28 V

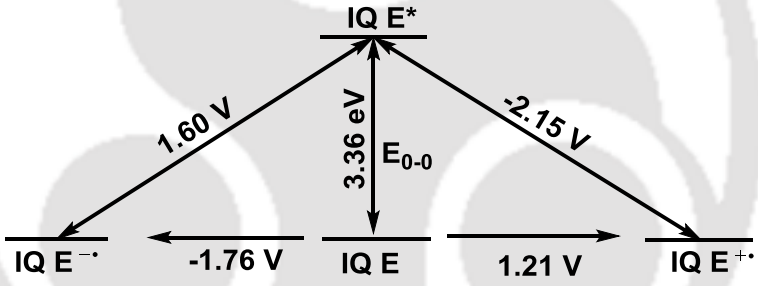

The Latimer diagram **for IQ E**

E^{*}_{red} (IQ E^{*}/IQ $E^{\bullet-}$)	=	E_{red} (IQ E/IQ $E^{\bullet-}$)	+	$E_{0\text{-}0}$
	=	−1.76 + 3.36	=	1.60 V
E^{*}_{ox} (IQ E^{*}/IQ $E^{\bullet+}$)	=	E_{ox} (IQ E/IQ $E^{\bullet+}$)	−	$E_{0\text{-}0}$
	=	1.21 − 3.36	=	−2.15 V

Table 5. Comparision of Experimental and Computed Ground State Redox Potentials of Photocatalyst[a]

PC	$E_{0\text{-}0}$ (eV)[a]	$E_{0\text{-}0}$ (eV)[d]	E_{ox} (V) (*vs*.SCE)[c]	E_{ox} (V) (*vs*.SCE)[d]	E_{red} (V) (*vs*.SCE)[c]	E_{red} (*vs*.SCE)[d]
IQ A	3.03	3.46	1.14	1.07	-1.33	-2.05
IQ B	2.96	3.42	1.23	1.16	-1.31	-1.77
IQ C	2.99	3.43	1.26	0.81	-1.14	-1.99
IQ D_{anti}	3.02	3.45	1.17	1.14	-1.30	-1.93
IQ D_{syn}	-	3.40	-	1.12	-	-1.91
IQ E	2.89	3.36	0.98	1.21	-1.15	-1.76

[a] All the potential are reported against SCE scale.

[b] Excitation energy of zero-zero vibrational energy level was calculated from the equation (3.8)

$$E_{0\text{-}0} = E_{1/2ox} - E_{1/2red} \qquad (3.8)$$

[c] Redox potentials calculated from cyclic voltammogram studies as experimentally observed values.

[d] Calculated from DFT studies.

Table 6. Comparision of Experimental and Computed Singlet Excited State Redox Potentials of Photocatalyst[a,b]

PC	E^*_{red} (V) (*vs*. SCE)[b]	E^*_{red} (V) (*vs*.SCE)[c]	E^*_{ox} (V) (*vs*.SCE)[b]	E^*_{ox} (V) (*vs*. SCE)[c]
IQ A	1.70	1.41	-1.89	-2.39
IQ B	1.65	1.65	-1.73	-2.26
IQ C	1.85	1.44	-1.73	-2.62
IQ D_{anti}	1.73	1.52	-1.91	-2.31
IQ D_{syn}	-	1.49	-	-2.28
IQ E	1.72	1.60	-1.85	-2.15

[a] All the potential are reported against SCE scale.

[b] Experimentally observed values calculated from the equation (eq 3.9 and 3.10)

[c] Computed values.

$$E^*_{ox} = E_{ox} - E_{0\text{-}0} \quad (3.9)$$

$$E^*_{red} = E_{red} + E_{0\text{-}0} \quad (3.10)$$

Table 7. Comparision of Experimental and Computed Values of HOMO, LUMO and Band Gap of Photocatalysts

PC	HOMO (eV))[a]	LUMO (eV))[a]	HOMO (eV))[b]	LUMO (eV))[b]	Band gap Eg (eV)[a]	Band gap	
						Eg (eV)[b]	Eg ^{op}(eV)[b]
IQ A	-5.65	-1.62	-5.58	-2.74	4.03	2.84	2.86
IQ B	-5.92	-1.96	-5.65	-3.06	3.96	2.59	2.86
IQ C	-5.66	-1.67	-5.68	-3.16	3.99	2.52	2.85
IQ D_{anti}	-5.73	-1.68	-5.70	-2.95	4.05	2.75	2.90
IQ D_{syn}	-5.71	-1.71	-	-	4.00	-	-
IQ E	-5.71	-1.95	-5.50	-3.02	3.96	2.48	2.84

[a] Computed values.

[b] Experimentally observed values.

3.6 References

1. For recent reviews on visible-light photoredox catalysis, see: (a) Tucker, J. W.; Stephenson, C. R. J. *J. Org. Chem.* **2012**, *77*, 1617. (b) Prier, C. K.; Rankic, D. A.; MacMillan, D. W. C. *Chem. Rev.* **2013**, *113*, 5322. (c) Reckenthäler, M.; Griesbeck, A. G. *Adv. Synth. Catal.* **2013**, *355*, 2727. (d) Shaw, M. H.; Twilton, J.; MacMillan, D. W. C. *J. Org. Chem.* **2016**, *81*, 6898. (e) Marzo, L.; Pagire, S. K.; Reiser, O.; König, B. *Angew. Chem. Int. Ed.* **2018**, *57*, 10034. (f) Wang, C.-S.; Dixneuf, P. H.; Soulé, J.-F. *Chem. Rev.* **2018**, *118*, 7532.
2. For reviews on organic photoredox catalysis, see: (a) Fagnoni, M.; Dondi, D.; Ravelli, D.; Albini, A. *Chem. Rev.* **2007**, *107*, 2725. (b) Marin, M. L.; Santos-Juanes, L.; Arques, A.; Amat, A. M.; Miranda, M. A. *Chem. Rev*. **2012**, *112*, 1710. (c) Ravelli, D.; Fagnoni, M.; Albini, A. *Chem. Soc. Rev.* **2013**, *42*, 97. (d) Fukuzumi, S.; Ohkubo, K. *Chem. Sci.* **2013**, *4*, 561. (e) Nicewicz, D. A.; Nguyen, T. M. *ACS Catal.* **2014**, *4*, 355. (f) Romero, N. A.; Nicewicz, D. A. *Chem. Rev.* **2016**, *116*, 10075.
3. For recent examples, see: (a) Liu, X.; Ye, X.; Bureš, F.; Liu, H.; Jiang, Z. *Angew. Chem., Int. Ed.* **2015**, *54*, 11443. (b) Shaikh, R. S.; Düsel, S. J. S.; König, B. *ACS*

Catal. **2016**, *6*, 8410. (c) Reina, D. F.; Ruffoni, A.; Douglas, Y. S. S. A.; Sheikh, N. S.; Leonori, D. *ACS Catal.* **2017**, *7*, 4126. (d) Pitzer, L.; Sandfort, F.; Strieth-Kalthoff, F.; Glorius, F. *J. Am. Chem. Soc.* **2017**, *139*, 13652. (e) Matsui, J. K.; Primer, D. N.; Molander, G. A. *Chem. Sci.* **2017**, *8*, 3512. (f) Lin, L.; Bai, X.; Ye, X.; Zhao, X.; Tan, C.-H.; Jiang, Z. *Angew. Chem., Int. Ed.* **2017**, *56*, 13842. (g) Jin, Y.; Ou, L.; Yang, H.; Fu, H. *J. Am. Chem. Soc*. **2017**, *139*, 14237.

4. Arias-Rotondo, D. M.; McCusker, J. K. *Chem. Soc. Rev.* **2016**, *45*, 5803.
5. For recent examples see: (a) Luo, J.; Zhang, J. *ACS Catal.* **2016**, *6*, 873. (b) Alfonzo, E.; Alfonso, F. S.; Beeler, A. B. *Org. Lett*. **2017**, *19*, 2989. (c) Tlahuext, A.-A.; Candish, L.; Garza-Sanchez, R. A.; Glorius, F. *ACS Catal.* **2018**, *8*, 1715. (d) Noto, N.; Tanaka, Y.; Koike, T.; Akita, M. *ACS Catal*. **2018**, *8*, 9408. (e) Liu, D.; Jiao, M.-J.; Feng, Z.-T.; Wang, X.-Z.; Xu, G.-Q.; Xu, P.-F *Org. Lett*. **2018**, *20*, 5700.
6. For examples on OLED application, see: (a) Stoessel, P.; Heil, H.; Joosten, D.; Pflumm, C.; Gerhard, A.; Breuning, E. WO 2010086089A1, **2010**. (b) Stoessel, P.; Joosten, D.; Gerhard, A.; Breuning, E. WO 2012007086A1, **2012**. (c) Jung, S.-J.; Kim, K.-Y.; Hong, J.-M.; Eum, S.-J.; Lee, J.-D.; Jung, J.-H.; Kim, M.-J.; No, Y.-S.; Chung, S.-S. WO 2015034140A1, **2015**.
7. (a) Tan, X.; Liu, B.; Li, X.; Li, B.; Xu, S.; Song, H.; Wang, B. *J. Am. Chem. Soc.* **2012**, *134*, 16163. (b) Zhang, L.; Zheng, L.; Guo, B.; Hua, R. *J. Org. Chem.* **2014**, *79*, 1154. (c) Wang, W.; Niu, J.-L.; Liu, W.-B.; Shi, T.-H.; Hua, X.-Q.; Song, M.-P. *Tetrahedron*. **2015**, *71*, 8200. d) Ge, Q.; Hu, Yang.; Li, B.; Wang, B. *Org. Lett*. **2016**, *18*, 2483. (e) Li, L.; Wang, H.; Yang, X.; Kong, L.; Wang, F.; Li, X. *J. Org. Chem*. **2016**, *81*, 12038. (f) Zhao, J. J.; Wu, C.; Li, P.; Ai, W.; Chen, H.; Wang, C.; Larock, R. C.; Shi, F. *J. Org. Chem*. **2011**, *76*, 6837. (g) Zhu, C.; Feng, C.; Yamane, M. *Chem. Commun.* **2017**, *53*, 2606.
8. Gaussian 09, Revision D.01, Frisch, M. J.; Trucks, G. W.; Schlegel, H. B.; Scuseria, G. E.; Robb, M. A.; Cheeseman, J. R.; Scalmani, G.; Barone, V.; Mennucci, B.; Petersson, G. A.; Nakatsuji, H.; Caricato, M.; Li, X.; Hratchian, H. P. A.; Izmaylov, F.; Bloino, J.; Zheng, G.; Sonnenberg, J. L.; Hada, M.; Ehara, M.; Toyota, K.; Fukuda, R.; Hasegawa, J.; Ishida, M.; Nakajima, T.; Honda, Y.; Kitao, O.; Nakai, H.; Vreven, T.; Montgomery, J. A.; Peralta, Jr., J. E.; Ogliaro, F.; Bearpark, M.; Heyd, J. J.; Brothers, E.; Kudin, K. N.; Staroverov, V. N.; Keith, T.; Kobayashi, R.; Normand, J.; Raghavachari, K.; Rendell, A.; Burant, J. C.; Iyengar, S. S.; Tomasi, J.; Cossi, M.; Rega, N.; Millam, J. M.; Klene, M.; Knox, J. E.; Cross, J. B.; Bakken, V.;

Adamo, C.; Jaramillo, J.; Gomperts, R.; Stratmann, R. E.; Yazyev, O.; Austin, A. J.; Cammi, R.; Pomelli, C.; Ochterski, J. W.; Martin, R. L.; Morokuma, K.; Zakrzewski, V. G.; Voth, G. A.; Salvador, P.; Dannenberg, J. J.; Dapprich, S.; Daniels, A. D.; Farkas, O.; Foresman, J. B.; Ortiz, J. V.; Cioslowski, J.; Fox, D. J.; Gaussian, Inc., Wallingford CT, 2013.

9. Demissie, T. B.; Ruud, K. J.; Hansen, H. *Organometallics* **2015**, *34*, 4218.
10. Roth, H. G.; Romero, N. A.; Nicewicz, D. A. *Synlett* **2016**, *27*, 714.
11. Vivek Kumar, S.; Ellairaja, S.; Satheesh, V.; Vasantha, V. S.; Punniyamurthy, T. *Org. Chem. Front.* **2018**, *5*, 2630.

3.7 NMR Spectra

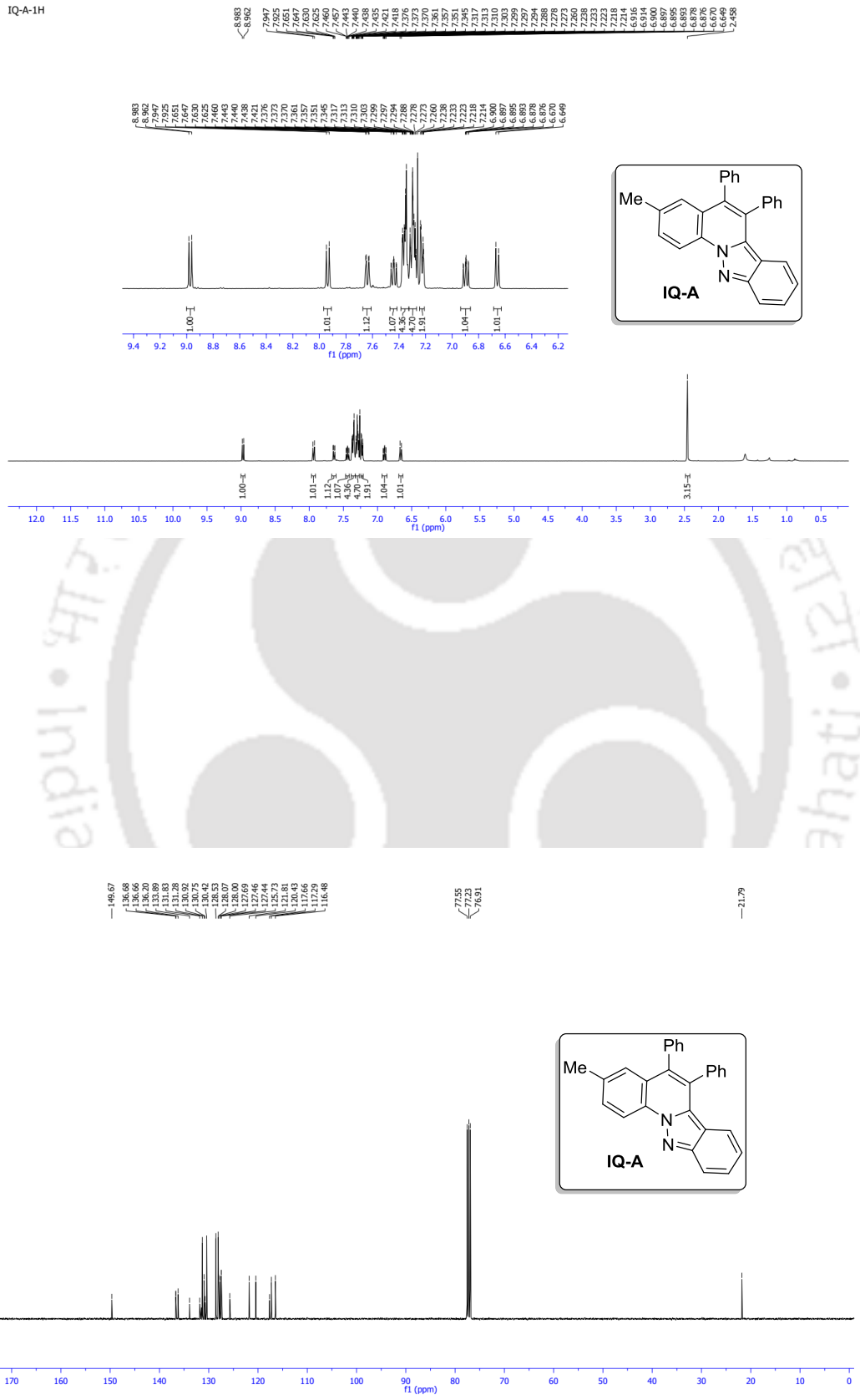

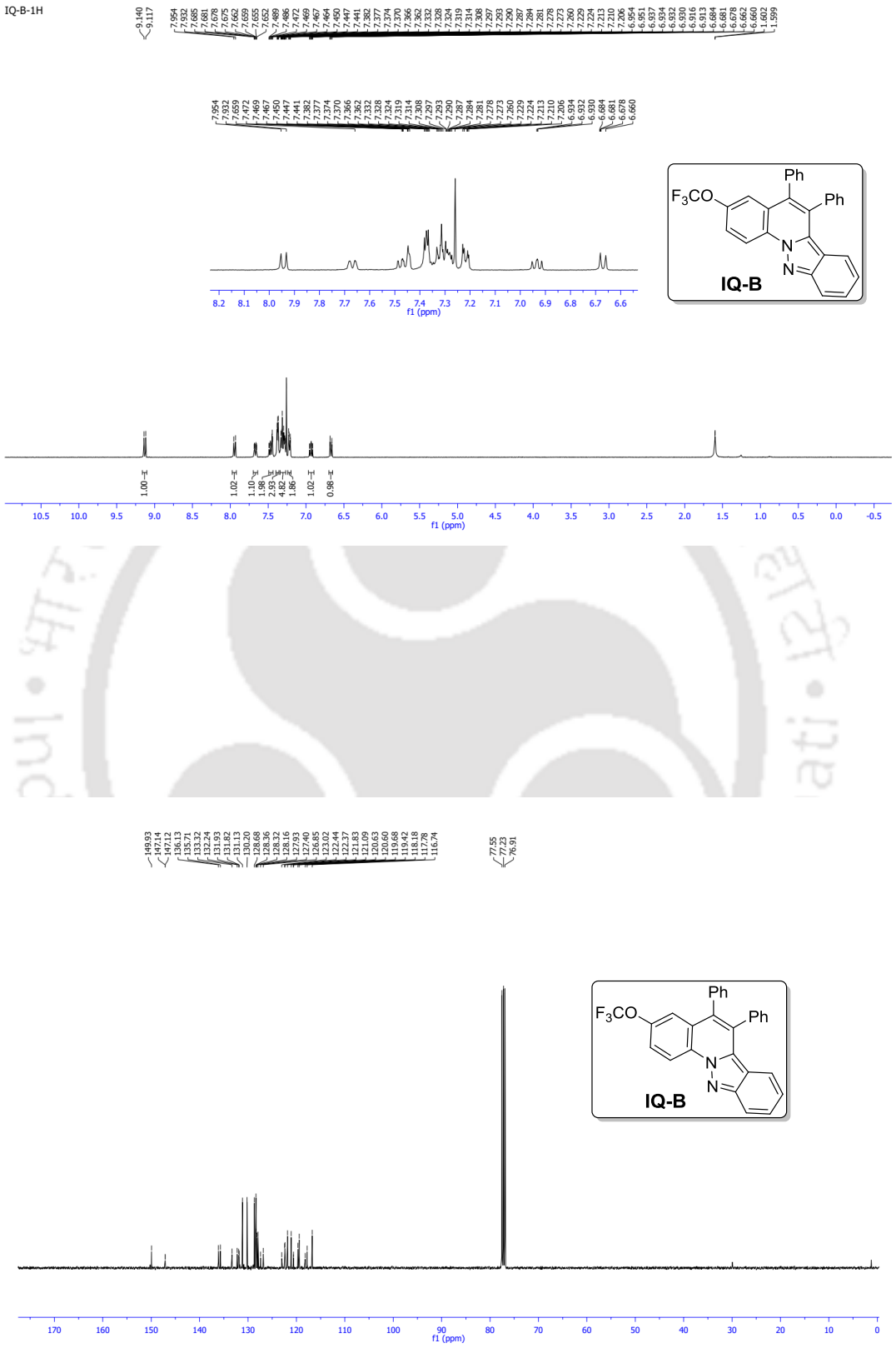

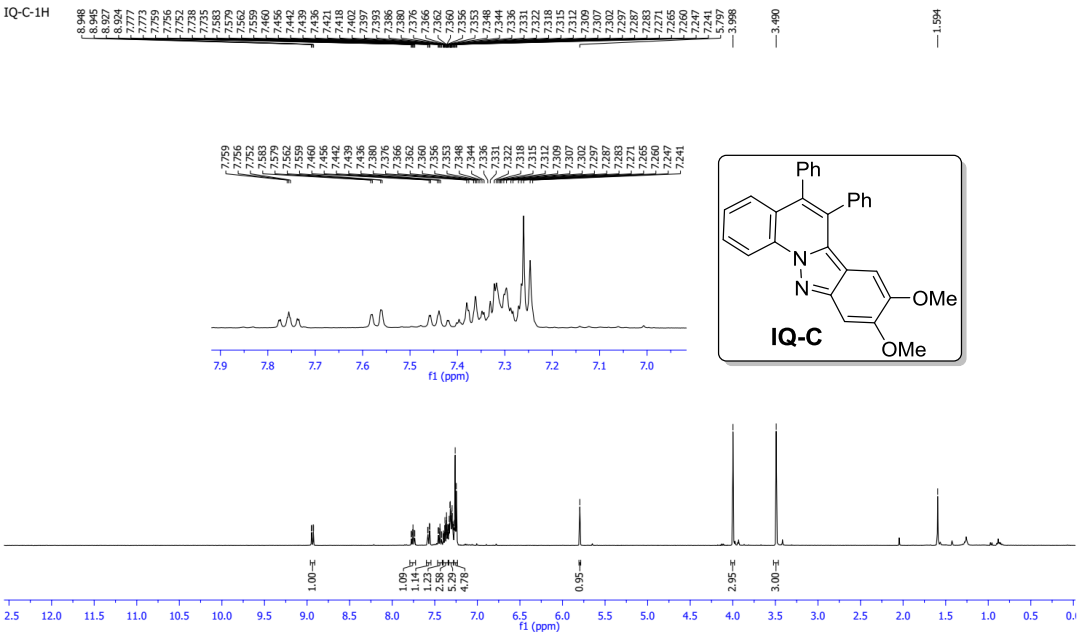

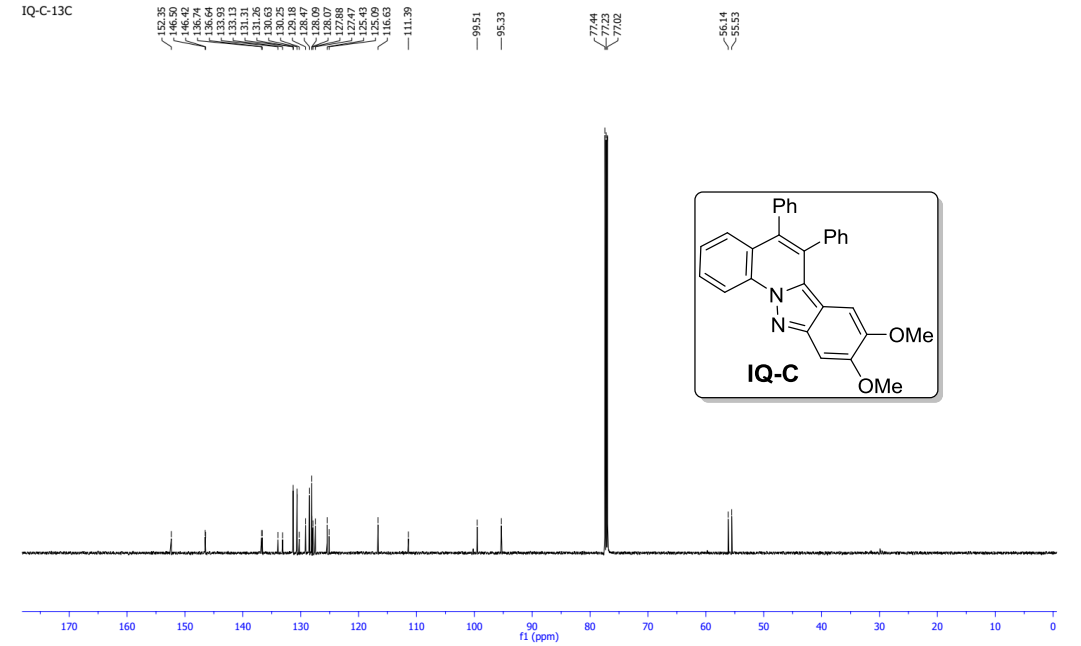

Chapter-IV

Tandem Ring Opening/Oxidative Amination of Aziridines with Cyclic Secondary Amines Using Indazoloquinolines

The functionalization of C-H bond offers efficient approach to convert simple substrates into complex molecules. C(sp^3)–H bond adjacent to heteroatoms can be functionalized via cross-dehydrogenative coupling (CDC).[1] This strategy has received considerable attention because of the atom economy and less number of reaction steps. Recently, organo-photoredox catalysis[2,3] in CDC of the C(sp^3)–H bond has provided the admirable path for the construction of the heterocyclic frameworks. Imidazolidine is important heterocyclic scaffold and found in natural products such as (-)-aplaminal, chaetominine and (-)-dysibetaine PP.[4] The subunits are essential structural motifs in bioactive[5] compounds such as antipyretic agents[6] and cannabinoid CB2 receptor agonist.[7] Further, imidazolidines act as ligands or catalysts in synthesis.[8] Thus, development of effective synthetic method to access functionalized imidazolidines is desirable.

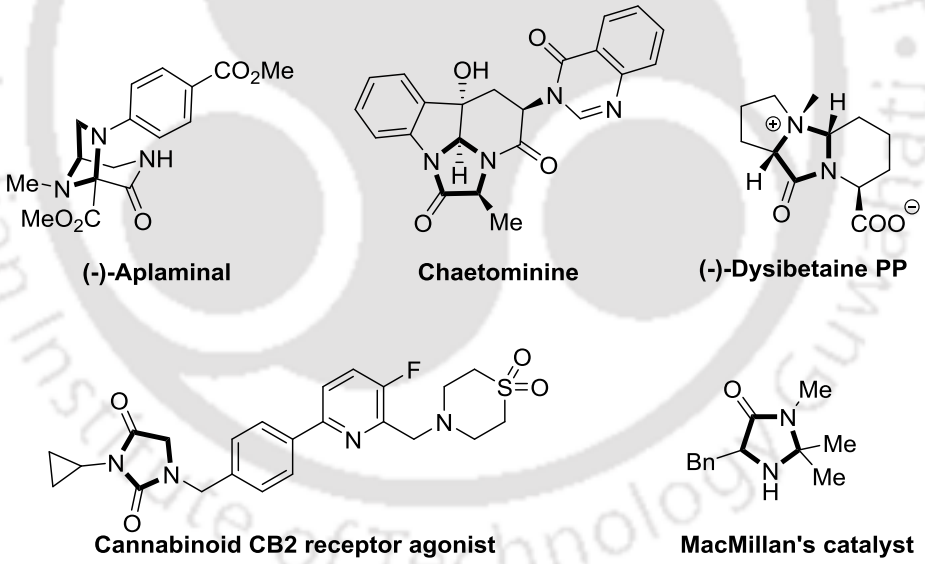

Figure 1. Examples for Imidazolidines drugs and catalyst.

4.1 Cycloaddition

Wu and co-workers described a Ag-catalyzed [3+2]-cycloaddition of azomethine ylide with imine to afford tetrahydroimidazole (Scheme 1).[9] This reaction can be carried out at room temperature with good substrate scope and functional group diversities.

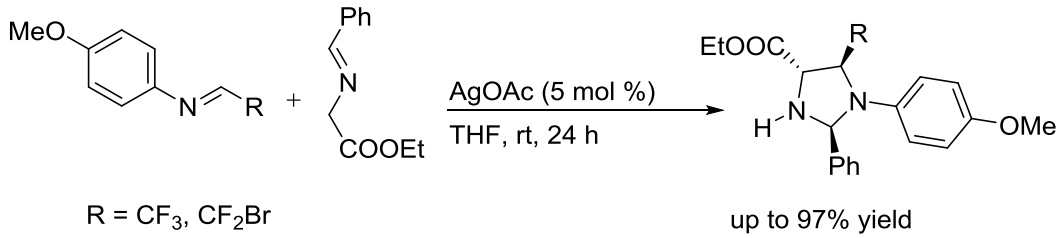

Scheme 1. Ag-catalyzed [3+2]-cycloaddition of imines and yildes.

Aleman group reported the cycloaddition of *N*-sulfinyl imines with azomethine ylide to provide imidazolidines in presence of diphenyl phosphate (DPP) (Scheme 2).[10] The reaction of a series of substrates has been demonstrated with high diastereoselectivity.

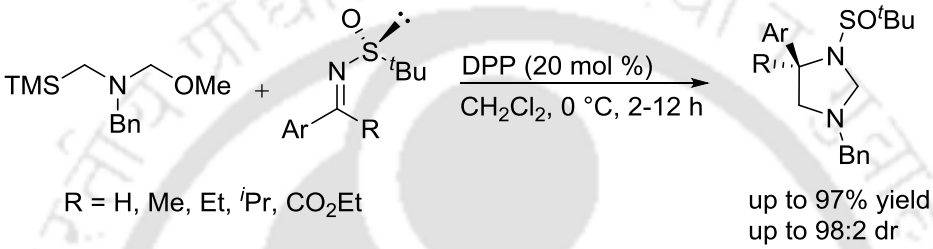

Scheme 2. DDP-catalyzed [3+2]-cycloaddition of imines and yildes.

Spielmann and co-workers developed a Pd-catalyzed cycloaddition of 2-vinylaziridines with *N*-sulfonyl imines at room temperature (Scheme 3).[11] The reaction involves ring-opening of aziridine through [3+2]-cycloaddition followed by C–N bond formation.

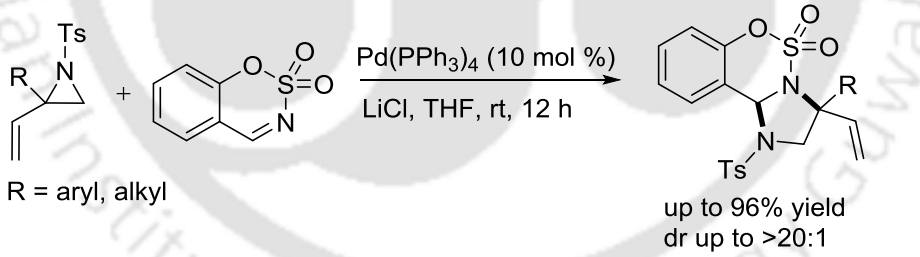

Scheme 3. Pd-catalyzed [3+2]-cycloaddition of chiral vinylaziridines with imines.

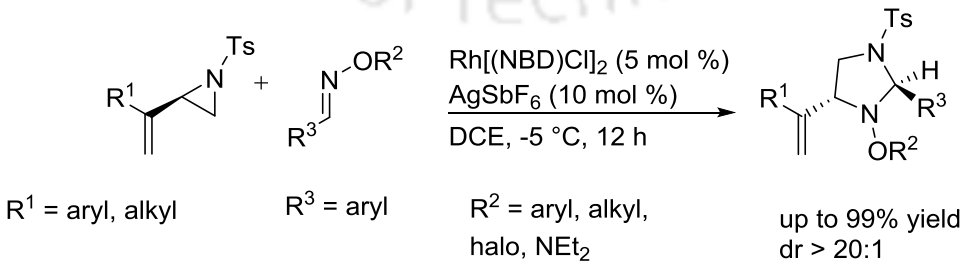

Scheme 4. Rh-catalyzed [3+2]-cycloaddition of chiral vinylaziridines with oxime ethers.

Zhang and co-workers reported the synthesis of chiral 2-vinylimidazolidines *via* similar cycloaddition strategy. The study includes the reaction of chiral 2-vinylaziridines with oxime ether using the combination of Rh and Ag catalytic system (Scheme 4).[12]

Cycloaddition of 1,3,5-triazinanes with aziridines reported in the presence of $ZnBr_2$ to give imidazolidines (Scheme 5).[13] This reaction is effective under heating and a sereis of aziridines undergo reaction in good yields.

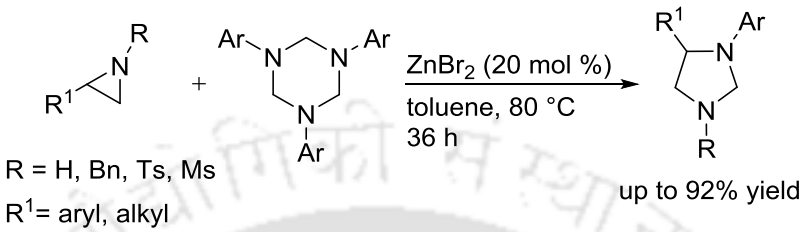

Scheme 5. Zinc-catalyzed synthesis of imidazolidines.

4.2 Multicomponent Approach

Hu and co-workers developed a three-component coupling of allene, aryl iodide and *N*-tosylimines using 5 mol % $Pd(PPh_3)_4$ in presence of K_2CO_3 (Scheme 6).[14] This method affords *trans*-imidazolidine in regio and stereoselective manner.

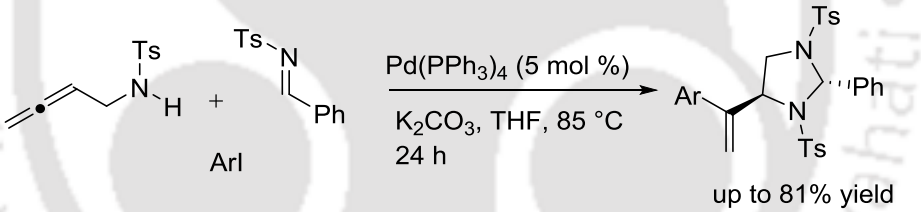

Scheme 6. Pd-catalyzed multicomponent approach to imidazolidines.

4.3 C(sp^3)–H Functionalization

Copper-catalyzed intermolecular C–N bond formation has been explored during the past decade. Recently, this strategy has been applied for the synthesis of five-membered heterocycles. Our group reported the synthesis of imidazolidines using the regioselective ring-opening of aziridine and subsequent C(sp^3)–H functionalization with *N*-alkylaniline using Cu(II)/TBHP system (Scheme 7).[15]

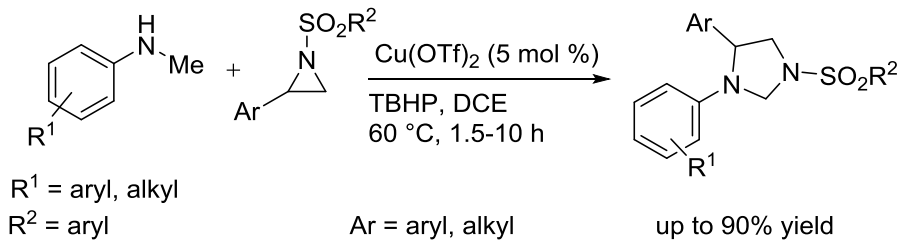

Scheme 7. Cu-catalyzed stereospecific synthesis of imidazolidines.

Huo and co-workers demonstrated the synthesis of functionalized imidazolidines via the coupling of glycine esters with aziridines in the presence of 5 mol % $Cu(OTf)_2$ and TFA under reflux (Scheme 8).[16] This reaction involves the ring opening of aziridines and C–N bond formation *via* oxidative dehydrogenative [2+3]-cyclization.

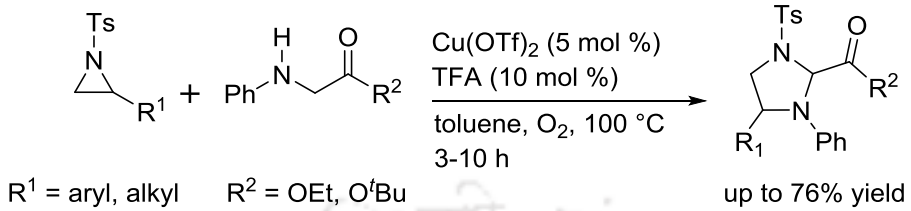

Scheme 8. Cu-catalyzed synthesis of imidazolidines.

Seidel and co-workers showed the construction of polycyclic imidazolidinones using redox-neutral annulation of cyclic secondary amines with *α*-ketoamides in presence of benzoic acid (Scheme 9).[17] This reaction proceeds via azomethine imine formation, C–H bond functionalization and C−N cyclization.

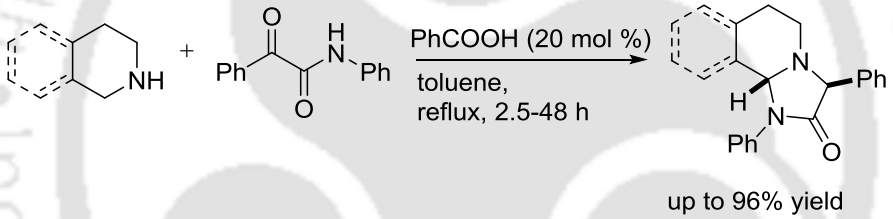

Scheme 9. Brønsted-acid catalyzed redox annulation approach to 2-imidazolidinones.

Meggers and co-workers developed a chiral Ru-catalyzed enantioselective C(sp^3)–H amination of 2-azidoacetamides for the synthesis of chiral imidazolidin-4-ones (Scheme 10).[18] The reaction occurred *via* Ru-imidato formation and the catalyst can be recycled.

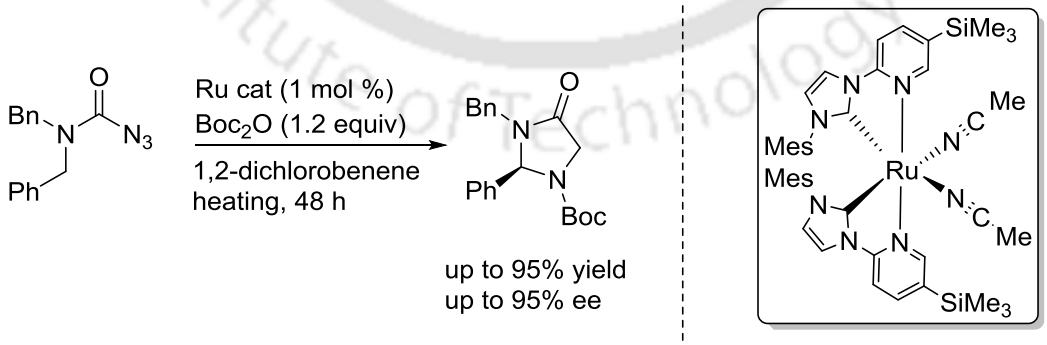

Scheme 10. Ru-catalyzed intramolecular C(sp^3)–H amination of 2-azidoacetamides.

4.4 Photoredox Catalysis

Xiao and co-workers described the synthesis of imidazolidines through the visible-light mediated cyclization. The precursor of the reaction is derived from natural amino acids in presence of Ru-photoredox catalysis (Scheme 11).[19] The reaction involves the formation of iminium ion and intramolecular cyclization to afford imidazolidines with high diastereoselectivity.

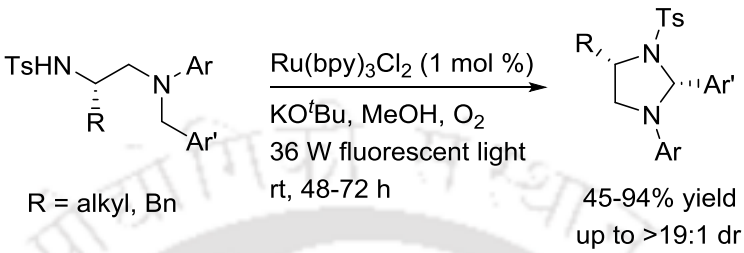

Scheme 11. Visible-light mediated synthesis of imidazolidines.

4.5 Present Study

Herein photoredox catalysis of **IQ A-E** has been presented for the coupling of aziridines with tetrahydroisoquinolines. The reaction involves an iminium ion formation and subsequent cyclization to afford the target five-membered fused heterocycles. Table 1 summarizes the optimization using tetrahydroisoquinoline **1a** and 2-phenyl-1-tosylaziridine **2a** as the test substrates. To our delight, the reaction occurred to produce **3a** in 86% yield when the substrates were stirred with 3 mol % **IQ D** for 24 h in DMF under the white LED 14 W irradiation (entry 1). The reactions of **IQ A-C** gave 61-72% yields, while **IQ E** furnished 55% yield along with **4a** in <31% yield (entries 2-5). These results suggest that the polarizable planar and extended conjugation of **IQ D** may stabilize the radical anion,[20] whereas the conventional photoredox dyes, eosin Y, and rose bengal, gave 40-46% yield of **3a** (entries 6 and 7). Metal-complexes such as $Ru(bpy)_3Cl_2 \cdot 6H_2O$ and fac-$Ir(ppy)_3$, failed to deliver the cyclized product **3a**, which may be attributed to their lower redox potential (entries 8 and 9) Control experiments confirmed that **1a** reacts with **2a** to give the ring-opening **4a** that leads to cyclization using the photoredox catalysis to furnish **3a** as a single diastereoisomer via an oxidative amination.

Table 1. Optimization of the Reaction Conditions[a]

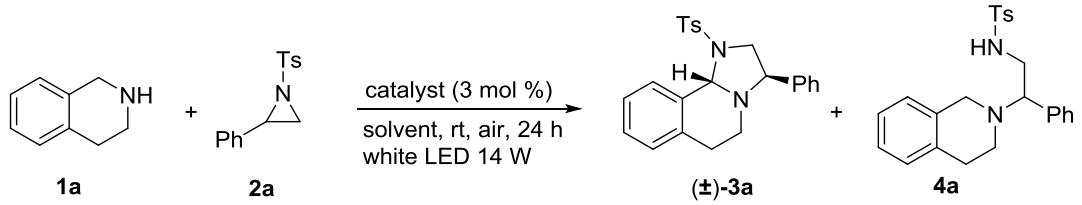

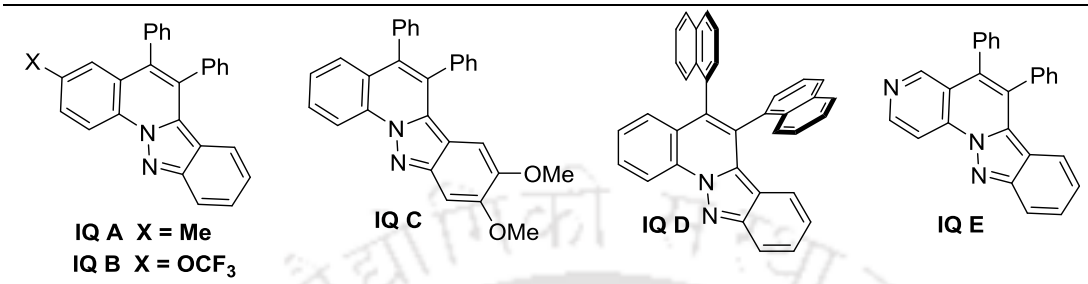

Entry	Photocatalyst	Yield (%)[b]	
		3a (%)	**4a** (%)
1	**IQ D**	**86**	**n.d**
2	IQ A instead of IQ D	69	10
3	IQ B instead of IQ D	61	19
4	IQ C instead of IQ D	72	12
5	IQ E instead of IQ D	55	31
6	Eosin Y instead of IQ D	40	45
7	Rose bengal instead of IQ D	46	33
8	$Ru(bpy)_3Cl_2•6H_2O$ instead of IQ D	n.d	87
9	*fac*-$Ir(ppy)_3$ instead of IQ D	n.d	85
10	Without IQ D and light	n.d	88

[a]Reaction conditions: **1a** (0.30 mmol), **2a** (0.25 mmol) in DMF (2 mL), air, rt, 24 h. [b]Isolated yield. n.d = not detected.

Table 2. Reaction of Aziridines with Amine[a,b]

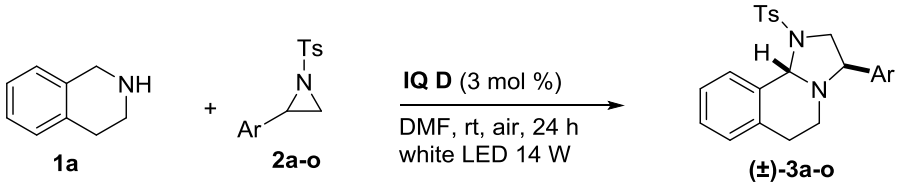

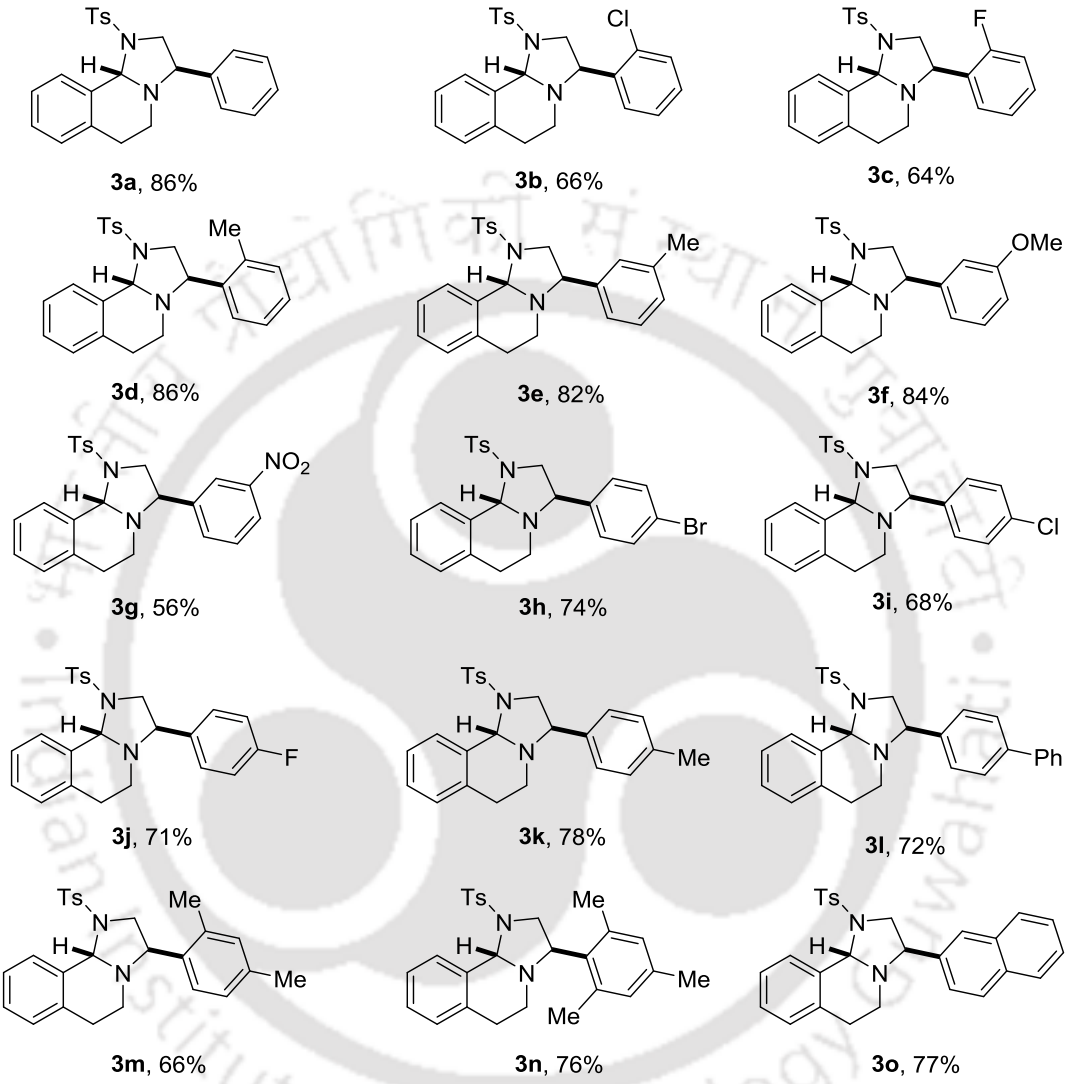

[a]Reaction conditions: Amine **1a** (0.30 mmol), aziridines **2a-o** (0.25 mmol), **IQ D** (3 mol %), DMF (2 mL), rt, air. [b]Isolated yield.

Having the optimized reaction condition, the scope of the procedure was examined for the reaction of a series of aziridines **2a-o** using **1a** as a standard substrate (Table 2). Modulation in the 2-aryl ring of **2a-o** with electronically varied substituents was well tolerated. The substrates with 2-chloro **2b**, 2-fluoro **2c**, and 2-methyl **2d** groups reacted to produce the heterocycles **3b-d** in 64-86% yields. Similar results were observed with the substrates containing 3-methyl **2e**, 3-methoxy **2f**, and 3-nitro **2g** substituents, producing the heterocycle scaffolds **3e-g** in 56-84% yields, whereas the reaction of the substrates having

4-bromo **2h**, 4-chloro **2i**, 4-fluoro **2j**, 4-methyl **2k**, and 4-phenyl **2l** groups provided **3h-l** in 68-78% yields. Sterically encumbered substrates with 2,4-dimethyl **2m** and 2,4,6-trimethyl **2n** substituents as well as 2-naphthyl aziridine **2o** were tolerated to provide **3m-o** in 66-76% yields.

Table 3. Scope of *N*-Substituted Aziridines[a b]

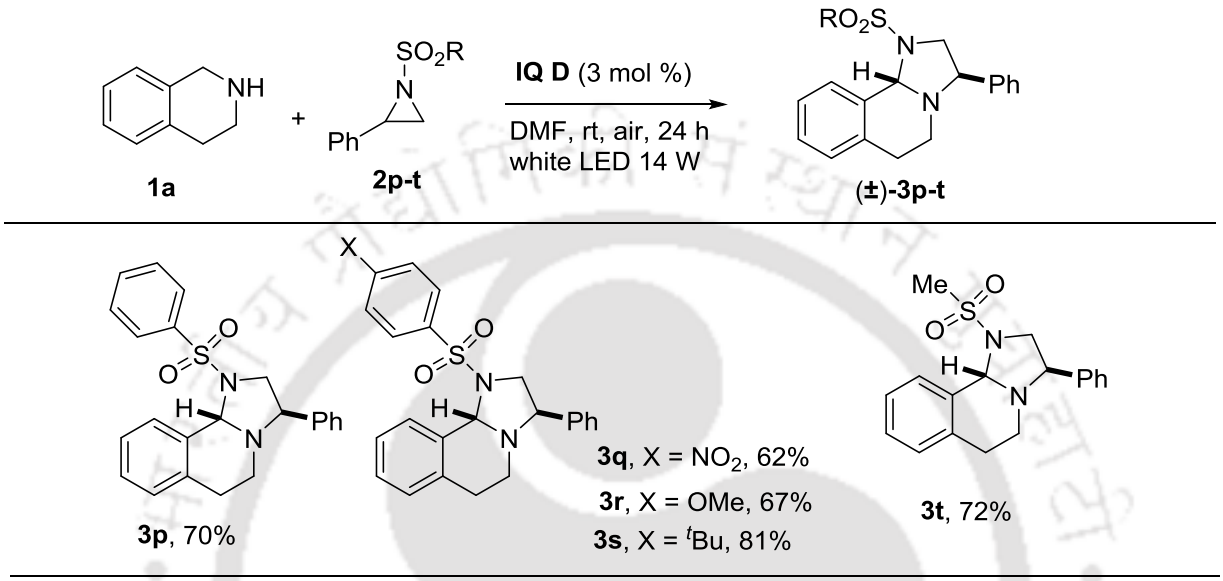

[a]Reaction conditions: Amine **1a** (0.30 mmol), aziridines **2p-t** (0.25 mmol), **IQ-D** (3 mol %), DMF (2 mL), rt, air. [b]Isolated yield.

Electronic effect of the *N*-substituents in aziridines was tested (Table 3). Aziridine **2p** bearing *N*-sulfonylphenyl substituent underwent reaction to produce **3p** in 70% yield. In addition, reaction of the aziridines bearing 4-nitro **2q**, 4-methoxy **2r** and 4-*tert*-butyl **2s** functional groups in the aryl ring of *N*-sulfonyl aryl substituent afforded **3p-s** in 62-81% yields. Furthermore, the reaction of *N*-(methylsulfonyl)aziridine **2t** occurred to give **3t** in 72% yield. These results suggest that aziridines having electronically varied *N*-sulfonyl substituents can be successfully coupled.

The scope of the procedure was extended to the reaction of a series of cyclic amines **1b-k** with aziridine **2a** as a standard substrate (Table 4). Tetrahydroisoquinoline bearing 5-bromo **1b** and 5-nitro **1c** groups reacted to give **3u** and **3v** in 74 and 78% yields, respectively. The reaction of the substrates having 7-nitro **1d** and 6,7-dimethoxy **1e** substituents furnished **3w** and **3x** in 69 and 87% yields, respectively. Tetrahydro-1*H*-benzo[*b*]azepine **1f** underwent reaction to give 3-phenyl-1-tosyl-2,3,5,6,7,11b-hexahydro-1*H*-benzo[*c*]imidazo[1,2-*a*]azepine **3y** as a 9:1 mixture of diastereomers in 77% yield. In addition, tetrahydro-*β*-

carbolines **1g-h** and thiophene fused amine **1i** reacted to give the scaffolds **3z** and **3aa-ab** in 64-92% yields. Whereas, the reaction of acyclic amines, *N*-methyl **1j** and *N*-benzyl **1k** amines, yielded the ring-opening products **4ac-ad**, which were failed to undergo cyclization.

Table 4. Scope of Cyclic Amines[a, b]

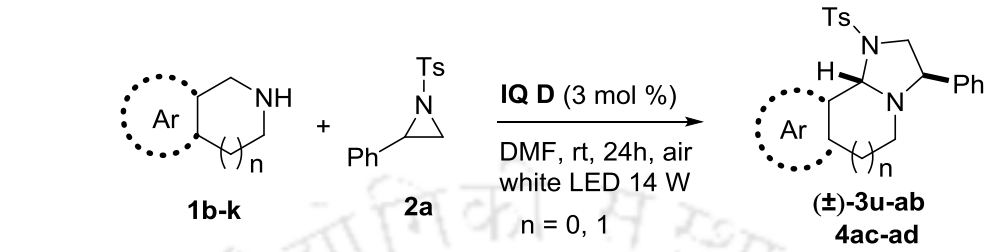

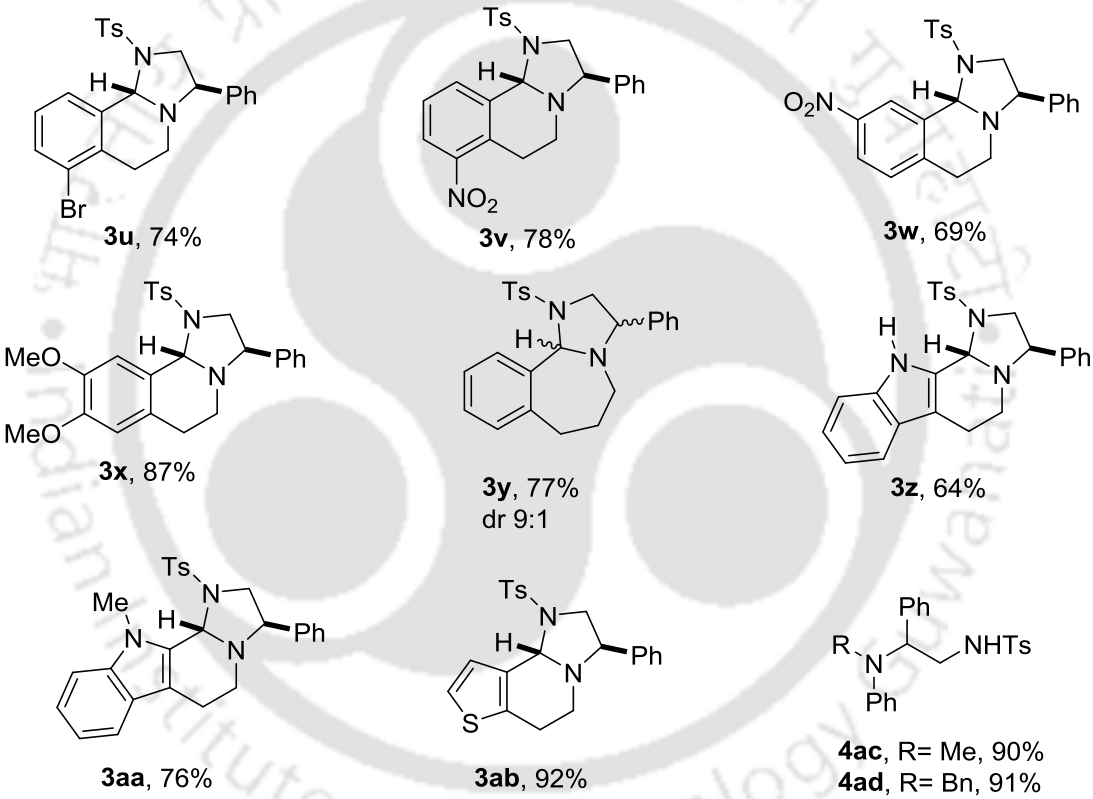

[a]Reaction conditions: Amine **1b-k** (0.30 mmol), aziridines **2a** (0.25 mmol), **IQ-D** (3 mol %), DMF (2 mL), rt, air. [b]Isolated yield.

To establish the stereospecificity, we inspected the reaction of optically active aziridines (Table 5). For instance, (*R*)-2-phenyl-1-tosylaziridine (*R*)-**2a′** underwent reaction with **1a** to give 3-phenyl-1-tosyl-1,2,3,5,6,10b-hexahydroimidazo[2,1-*a*]isoquinoline **3a'** in 98% ee. Similar results were observed with 5-nitro-1,2,3,4-tetrahydroisoquinoline **1c** and 6,7-dimethoxy-1,2,3,4-tetrahydroisoquinoline **1x** give 7-nitro-3-phenyl-1-tosyl-1,2,3,5,6,10b-hexahydroimidazo[2,1-*a*]isoquinoline **3v'** and (3*S*,10b*R*)-8,9-dimethoxy-3-phenyl-1-tosyl-

1,2,3,5,6,10b-hexahydroimidazo[2,1-*a*] isoquinoline **3x'** in 99 and 96% ee, respectively. In addition, the reaction of (*R*)-2-phenyl-1-(phenylsulfonyl)aziridine **2p′** and (*R*)-1-((4-(*tert*-butyl)phenyl)sulfonyl)-2-phenylaziridine **2s′** with 1,2,3,4-tetrahydroisoquinoline **1a** gave **3p'** and **3s'** in 94 and 99% ee, respectively. Further, (*S*)-2-phenyl-1-tosylaziridine **2a′** reacted to afford 3-phenyl-1-tosyl-1,2,3,5,6,10b-hexahydroimidazo[2,1-*a*]isoquinoline **3a''** in >98% ee. These results posited the initial ring opening of the aziridine with amine takes place *via* the stereospecific pathway.[22]

Table 5. Enantiospecific Synthesis of Fused Imidazolidines[a,b]

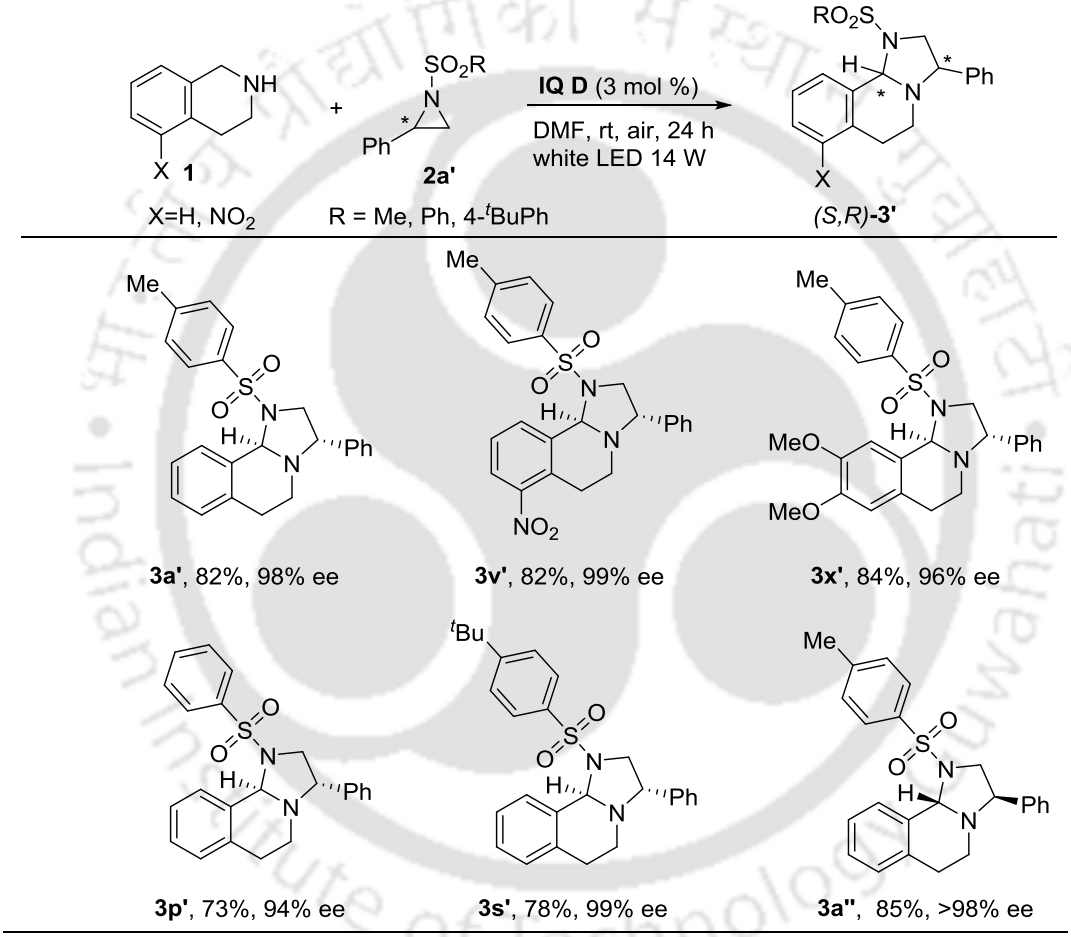

[a]Reaction conditions: Amine **1** (0.30 mmol), aziridines **2a′** (0.25 mmol), **IQ-D** (3 mol %), DMF (2 mL), rt, air. [b]Isolated yield.

These experimental results and literature reports[2,3] suggest that the stereospecific ring opening of aziridine **2** with **1** can produce **4** with an inverted stereochemistry (Scheme 13). The visible light irradiation of **IQ D** can produce the excited **IQ D***, which can undergo single electron transfer (SET) with **4** to afford the radical cation **a** and radical anion **IQ D**$^{\bullet-}$. The latter can react with oxygen (air) to generate **IQ D** and $O_2^{\bullet-}$ *via* the SET. Hydrogen atom transfer (HAT) from the radical cation ***a*** to $O_2^{\bullet-}$ can yield HO_2^- and imine ***b***. HO_2^-

mediated cyclization of ***c*** can lead to the formation of the target compound **3**. Formation of the single diastereomer suggests that the cyclization can take place *via* the transition state TS ***c*** compared to that of TS ***d***, which can be attributed to the 1,3-diaxial interaction.

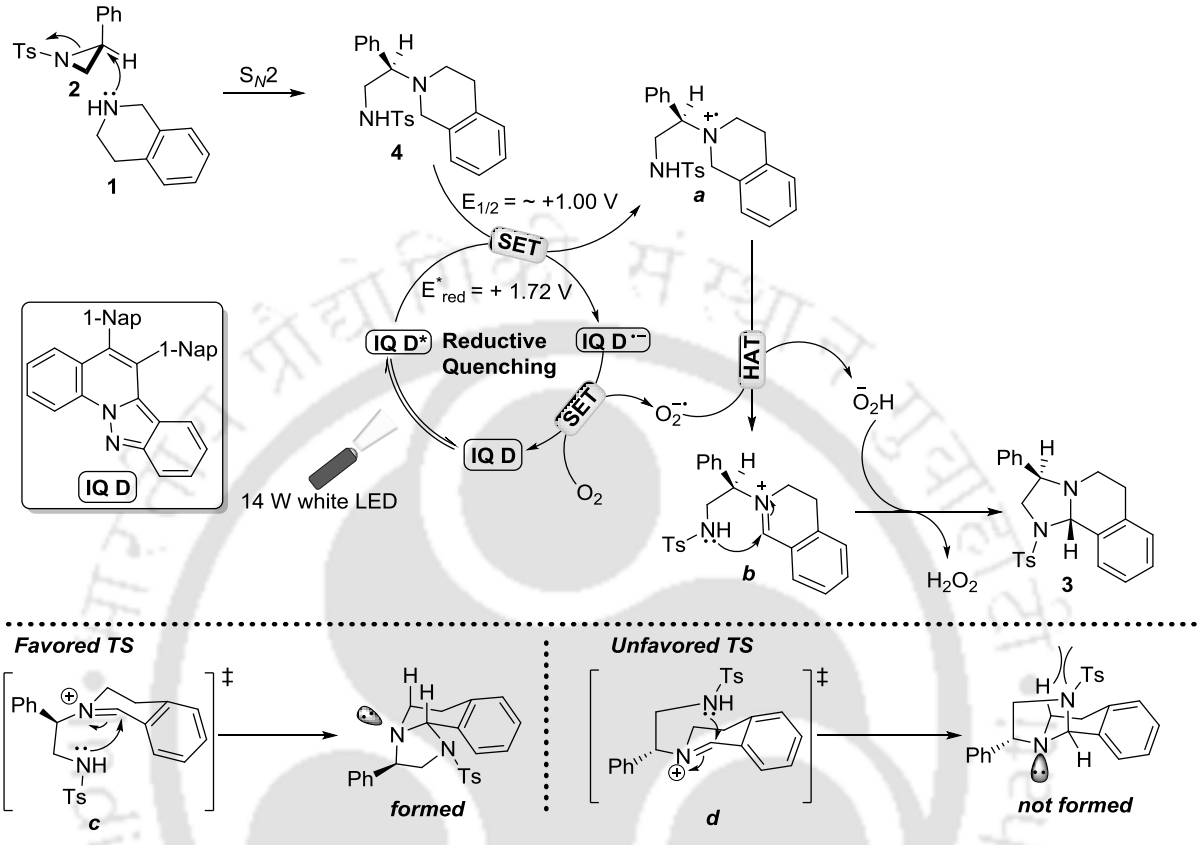

Scheme 12. Proposed reaction mechanism

To get insight in the mechanism, a series of control experiments and theoretical studies were performed. Amine **1a** underwent reaction with **2a** to give **4a** in quantitative yield, which showed no cyclization in the absence of the photoredox catalyst (table 1, entry 10) In addition, the compound **4a** underwent C–H amination to give **3a** in 91% yield using **IQ D***, which suggests that the reaction involves a tandem ring opening and oxidative amination using photoredox catalysis (Scheme 13). An alternative pathway, proceeding *via* the electron transfer from **1a** to **IQ D*** leads to the formation of 3,4-dihydroisoquinoline and light-mediated ring opening of aziridine, which is unlikely because no quenching was observed at **IQ D*** by **1a** or **2a**. Next, we measured the oxidation potential, E_{ox}^{exp} = 0.92 to 1.05 V and E_{ox}^{DFT} = +1.14 to +1.26 V, for a series of electronically varied intermediates **4a**, **4j**, **4k** and **4p**, **4q** as the representative examples, which suggest that they can be oxidized by the excited **IQ D*** $E^{*}_{red}{}^{exp}$= +1.72 V and $E^{*}_{red}{}^{DFT}$ = +1.52 V (Table 6). In addition, the

reaction generates H_2O_2, which was confirmed using iodide test (KI in acetic acid) which suggests that O_2 plays an important role in the catalysis. Further, the one-pot ($[P_H/P_D]$ = 3.3) and parallel (k_H/k_D = 4.3) kinetic isotope experiments suggest that the hydrogen atom transfer (**HAT**) can be the rate-determining step.

Table 6. Oxidation Potential of Intermediates[a]

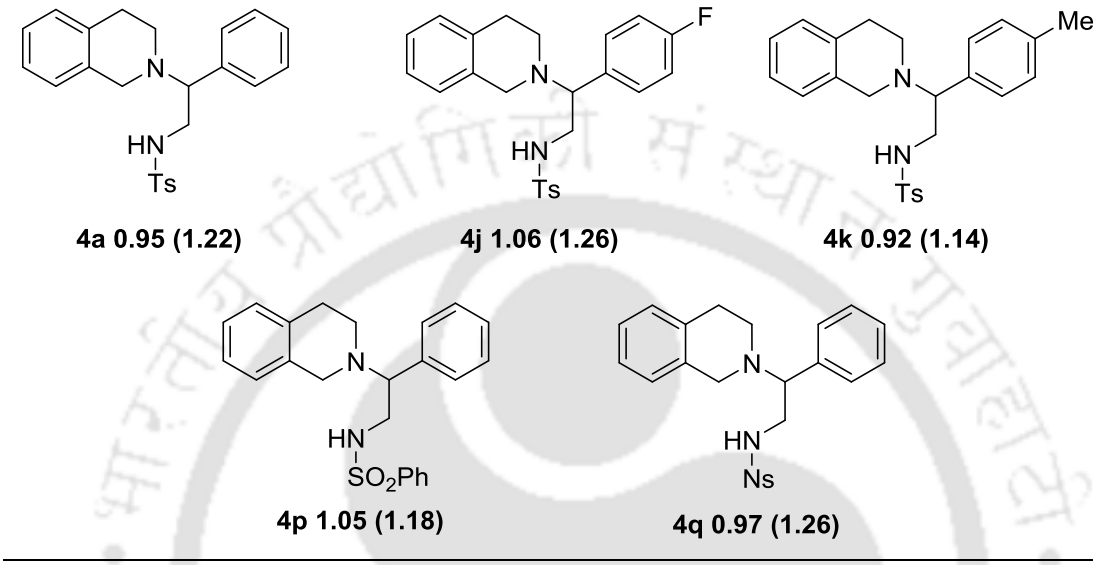

E_{ox}^{exp} (V) are given in bold.

E_{ox}^{DFT} (V) are given in parenthesis

[a]All potentials are given in volts versus the saturated calomel electrode (SCE).

Ring-opening product **4a** (0.25 mmol) and **IQ D** (3 mol %) in *N,N*- dimethylformamide were stirred at room temperature under white LED 14 W for 24 h. After standard purification procedure, afforded 91% yield of product **3a**.

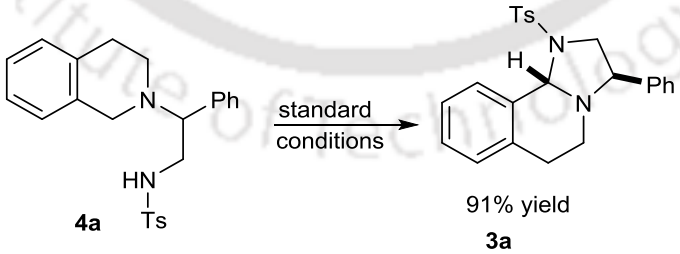

Scheme 13. Oxidative C–H Amination of **4a**

4.5.1 Stern-Volmer Quenching studies

All the **IQ D** solutions were excited at 375 nm and the emission intensity was collected at 446 nm. A screw-top quartz cuvette was charged with a 0.001 M solution of **IQ D** in DMF (2.0 mL) and the initial emission was collected. Another three series of samples, 0.001 M **IQ D** in DMF with compound **1a** or compound **2a** or intermediate **4a** as quencher in gradient concentrations (0-60 μM), was added to the measured solution and the emission spectrum of the sample was collected (Figure 4 and 5).

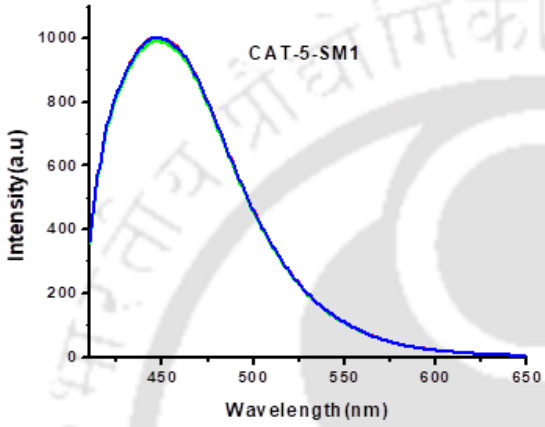

Luminescence quenching of IQ D* by amine **1a**

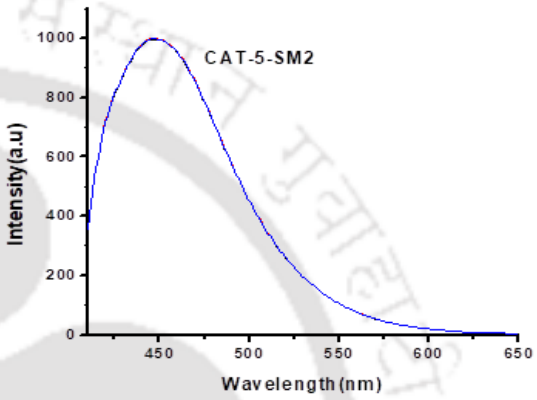

Luminescence quenching of IQ D* by aziridine **2a**

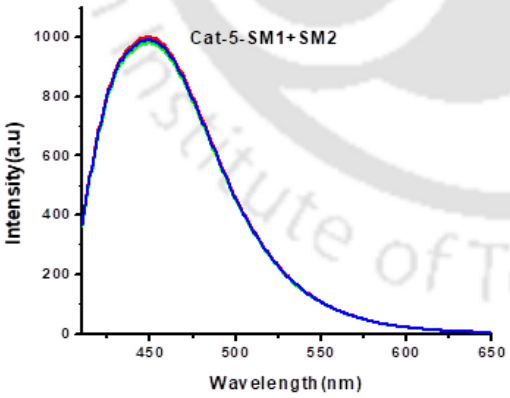

Luminescence quenching of IQ D* by mixture of amine **1a** and aziridine **2a**

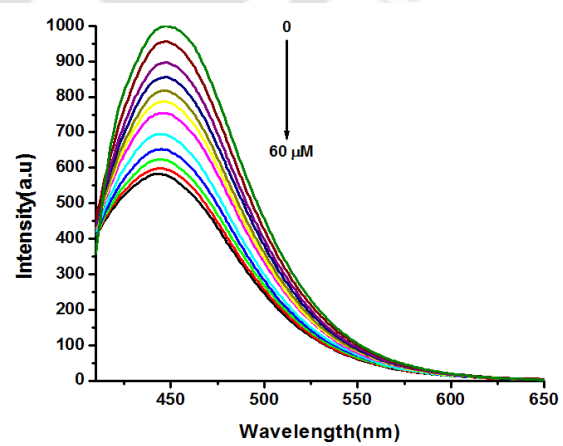

Luminescence quenching of IQ D* by **4a**

Figure 4. Stern-Volmer Quenching studies.

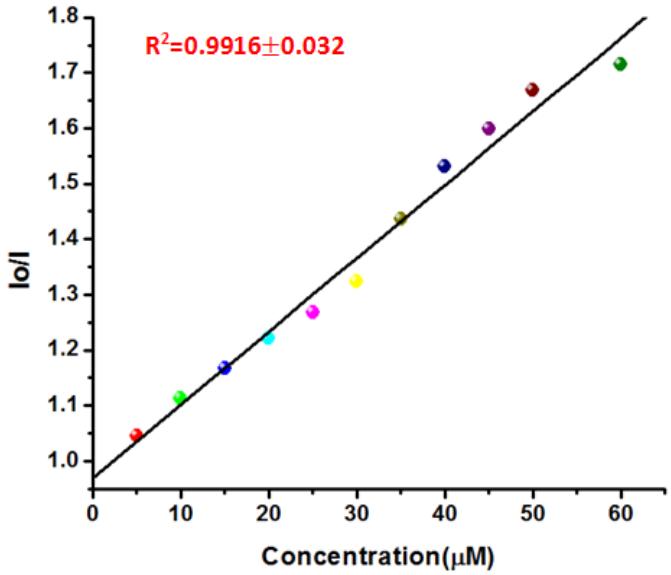

Figure 5. Stern-Volmer plots for **4a.**

4.5.2 Cyclic Voltammetry

We assumed that the proposed catalytic cycle (Scheme 12) is feasible based on the following oxidation potentials of intermediates. The oxidation potential of intermediates are within the range of excited state of photocatalyst **IQ D***. Thus, one-electron transfer would be possible. The same electrochemical cell set up was also used in this study (see electrochemical studies of photocatalysts in chapter-3). The DMF solution contained 1.0 mM of the respective compound being tested, 0.10 M TBABF as the supporting electrolyte, and 1 mM of ferrocene used as an internal standard. Further, the observed oxidation potentials are verified through computational studies.

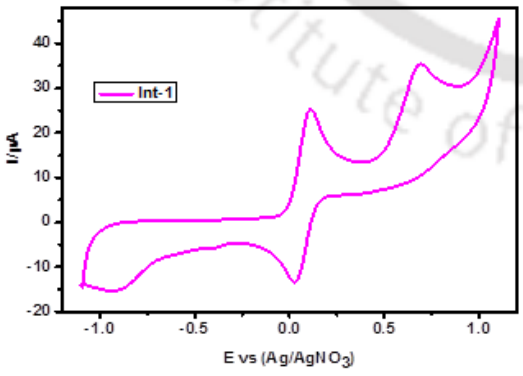

Cyclic Voltammogram of **4a**

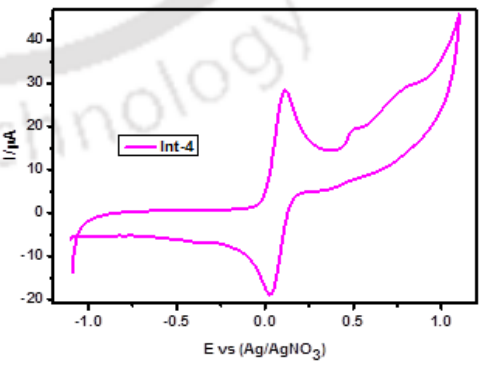

Cyclic Voltammogram of **4j**

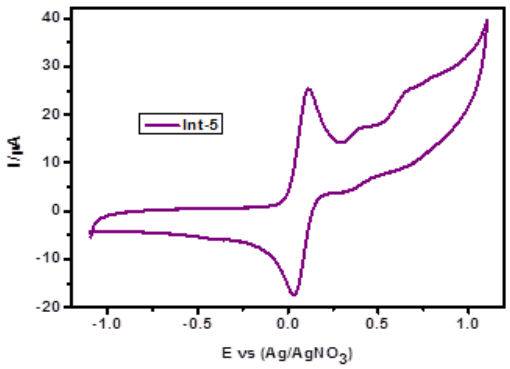

Cyclic Voltammogram of **4k**

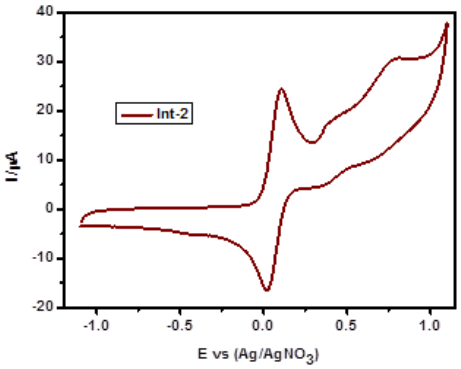

Cyclic Voltammogram of **4p**

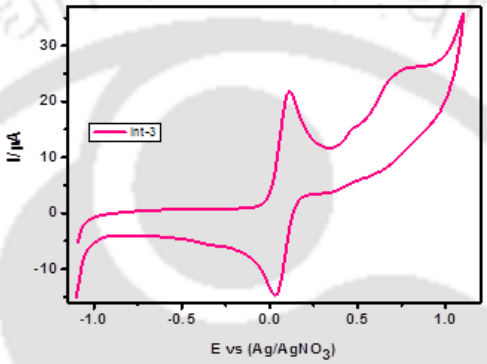

Cyclic Voltammogram of **4q**

ΔG Values of Electron Transfer Calculated from Rehm-Weller Equation

Singlet excited state energy of **IQ D** is $E_{0\text{-}0}$ = 3.02 eV

Ground state oxidation and reduction potentials of **IQ D** is shown below

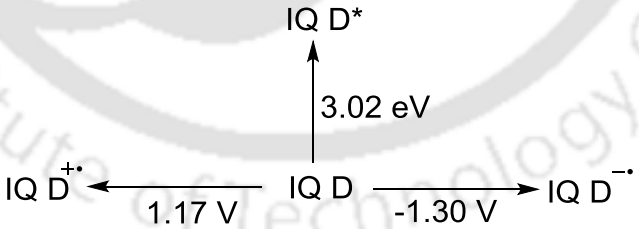

Ground State Redox Potential and $E_{0\text{-}0}$ of IQ D

Gibbs free energy of photoinduced electron transfer from intermediates to the excited **IQ D*** in DMF can be calculated using Rehm-Weller equation (eq 4.1)

$$\Delta G \text{ (kcal/mol)} = 23.06\ (E_{ox} - E_{red} - e_0^2/ae - E_{0\text{-}0}) \quad \textbf{(4.1)}$$

Where,

E_{ox}= Oxidation potential of intermediates

E_{red} = Reduction potential of **IQ D**

e_0^2/ae = Coulombic term (0.06 kcal mol^{-1})

$E_{0\text{-}0}$ = Singlet excited energy of **IQ D**

Here we used experimentally observed reduction potential and singlet excited state energy of **IQ D.**

Table 7. ΔG of Electron Transfer Process

Entry	Intermediates	ΔG $(kcal/mol)^{-1}$
1	**4a**	-19.14
2	**4j**	-16.83
3	**4k**	-18.68
4	**4p**	-16.60
5	**4q**	-19.83

4.5.3 DFT Study

The proposed reaction pathway was examined by computational studies using M06/6-31+G(*d,p*). The reaction of **1a** with **2a** can produce **4** through the TS-1 with an activation barrier of 37.30 kcal/mol (Figure 2). Formation of **4** is favored as the stabilization is much more than the activation barrier. When the relative stability of **4** was compared with **4'**, **4'** is around 2 kcal/mol less stable than **4**, and thus the formation of **4'** is ruled out. SET from the catalyst to **4** can give **a**, which is 2.80 kcal/mol more stable than **4**. Interaction of $O_2^{\bullet-}$ with **a** through TS-2 can form **b** and this step is the rate-determining step as the barrier for the formation is highest (16.82 kcal/mol). This finding is in accordance with the observed experimental results. The abstraction of proton from **b** can form **c** through TS-3, which is a quick reaction with the barrier of 1.55 kcal/mol and the stabilization of more than 12 kcal/mol. Cyclization of **c** can lead to the target **3**, which is very fast as the activation barrier TS-4 is less than 1 kcal/mol. Relative stability of **3** and **3′** were compared to prove that the formation of **3** is favored over **3′**.

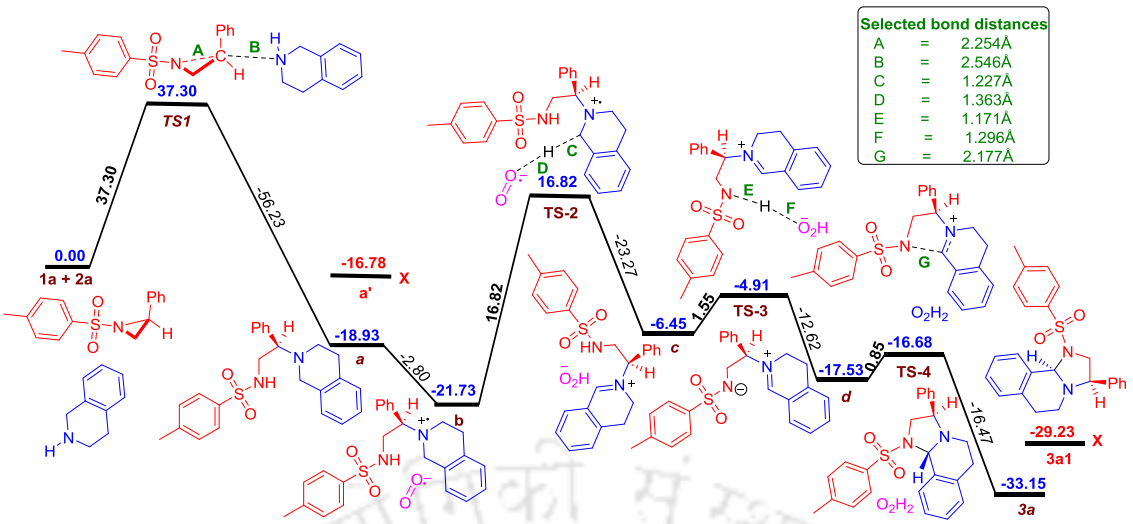

Figure 3. Calculated energy profile of tandem ring opening/C-H amination reaction at M06/6-31+G(d,p) level of theory. 'Numbers in blue colors' depict the relative energies (kcal/mol) and 'numbers in bold' shows the activation barrier and 'numbers in italics' shows the stabilization. All energy values are given in kcal/mol. Important interatomic distances in transition state structures are given in green color in Å unit. Red color numbers and cross sign (X) show the unfavored intermediate or product.

In summary, the C–H amination of aziridines with cyclic secondary amines has been accomplished using a quinoline based **IQ A-E** photoredox catalysis in visible light for the synthesis of fused imidazolidines at room temperature. This method involves tandem ring-opening aziridine, oxidative C–H functionalization and C–N bond formation. The synthetic and mechanistic aspects are covered.

4.6 Experimental Section

General Information. 1,2,3,4-Tetrahydroisoquinoline (95%), eosin Y (99%), rose bengal (95%), fluorescein (95%), methylene blue, alizarin red, $[Ru(bby)_3]Cl_2{\cdot}6H_2O$ (99.95%), *fac*-$[Ir(ppy)_3]$, dimethyl sulfoxide-d_6 (99.9%) and potassium *tert*-butoxide (≥98%) were purchased from Aldrich. Solvents were purchased from commercial sources and dried according to the standard procedure prior to use.[24] Aziridines,[25] 2,3,4,5-tetrahydro-1*H*-benzo[*c*]azepine[26a] and tetrahydro-β-carbolines 2aa[26b] were prepared according to the reported procedure. Column chromatography was performed with SRL silica gel (100-200 mesh). Bruker Avance III 400 MHz and Bruker Avance III 600 MHz spectrometers were used for recording NMR spectra using $CDCl_3$ as a solvent and Me_4Si as an internal standard. Melting points were recorded using Büchi B-540 apparatus and values are uncorrected. Optical rotation was determined using Rudolph Research Analytical Autopol II using a 50 mm path length cell at 589 nm at 23 °C. HPLC analysis carried out with Daicel

Chiralcel AD-H, OD and OD-H columns. FT-IR spectra were recorded on Perkin-Elmer IR spectrometer. Q-TOF ESI-MS instrument (model HAB 273) was used for recording mass spectra. Single crystal X-ray data were collected using Bruker SMART APEX-II CCD diffractometer, which is equipped with 1.75 kW sealed-tube Mo-Kα irradiation (λ = 0.71073 Å) at 298(2) K. The crystal structure was solved by the direct method using SHELXL-97 (Gottingen, Germany) and refined with full-matrix least-squares on F^2 using SHELXL-97.

General Procedure for the Photoredox Catalyzed Synthesis of Fused Imidazolidines. Amine (0.30 mmol), aziridine (0.25 mmol) and photocatalyst **IQ-D** (3 mol %) were stirred in DMF for 24 h under 14 W white LED at room temperature. The progress of the reaction was monitored by TLC using ethyl acetate and hexane. After completion, the reaction was diluted with CH_2Cl_2 (5 ml) and washed with water (15 ml). Drying (Na_2SO_4) and evaporation of the solvent gave the residue that was purified over silica gel column chromatography using ethyl acetate and hexane.

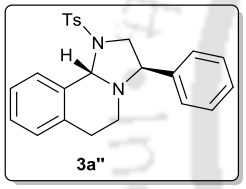

(*3R,10bS*)-3-Phenyl-1-tosyl-1,2,3,5,6,10b-hexahydroimidazo[*2,1-a*]isoquinoline 3a′′. Analytical TLC on silica gel, 1:10 ethyl acetate/hexane R_f = 0.40; colorless solid; yield 86% (87 mg). Mp 135-136 ^oC. ^1H NMR (400 MHz, $CDCl_3$) δ 7.96 (d, J = 8.0 Hz, 1H), 7.85 (d, J = 8.4 Hz, 2H), 7.40 (d, J = 8.0 Hz, 2H), 7.35(t, J = 7.6 Hz, 1H), 7.24-7.18 (m, 4H), 7.07 (d, J = 7.2 Hz, 1H), 6.88 (d, J = 6.4 Hz, 2H), 5.94 (s, 1H), 4.10 (t, J = 8.0 Hz, 1H), 3.72 (dd, J = 10.0, 7.6 Hz, 1H), 3.20-3.15 (m, 1H), 3.14-3.07 (m, 1H), 2.95-2.86 (m,1H), 2.76-2.71 (m, 1H), 2.52 (s, 3H), 2.41 (dd, J = 17.2, 4.4 Hz, 1H). ^{13}C NMR (101 MHz, $CDCl_3$) δ 144.0, 138.8, 134.9, 134.3, 134.1, 129.9, 129.2, 128.7, 128.6, 128.58, 128.3, 127.73, 127.70, 127.2, 76.5, 60.9, 55.7, 41.6, 21.9, 21.5. FT-IR (KBr) 3063, 3026, 2925, 2862, 1928, 1633, 1490, 1454, 1159, 1090, 836, 748, cm^{-1}. HRMS (ESI) m/z $[M+H]^+$ calcd for $C_{24}H_{24}N_2O_2S$ 405.1631, found 405.1643. **3a′′** (*R,S*) $[\alpha]_D^{20}$ = -44 (c = 0.14, $CHCl_3$). HPLC analysis: 98.9% ee [Daicel Chiralcel OD column, hexane/*i*PrOH = 90:10, flow rate: 1 mL/min, λ = 254 nm, t_R = 7.81 min (minor), 9.95 min (major)]. **3a′** (*S,R*) $[\alpha]_D^{20}$ = +33 (c = 0.1, $CHCl_3$). HPLC analysis: 98% ee [Daicel Chiralcel OD column, hexane/*i*PrOH = 90:10, flow rate: 1 mL/min, λ = 254 nm, t_R = 7.79 min (major), 10.51 min (minor)].

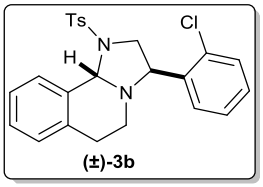

(±)-3-(2-Chlorophenyl)-1-tosyl-1,2,3,5,6,10*b*-hexahydro imidazo[2,1-*a*]isoquinoline 3b. Analytical TLC on silica gel, 1:10 ethyl acetate/hexane R_f = 0.31; colorless solid; yield 66% (74 mg). Mp 148-149 ^{o}C. ^{1}H NMR (400 MHz, $CDCl_3$) δ 7.83 (d, *J* = 7.6 Hz, 1H), 7.69 (d, *J* = 8.4 Hz, 2H), 7.28-7.16 (m, 5H), 7.08-7.03 (m, 1H), 7.01 (d, *J* = 7.2 Hz, 1H), 6.93-690 (m, 1H), 6.55 (d, *J* = 7.6 Hz, 1H), 5.93 (s, 1H), 4.51 (t, *J* = 8.0 Hz, 1H), 3.81 (dd, *J* = 11.2, 8.0 Hz, 1H), 3.11-3.04 (m, 2H), 2.93-2.84 (m, 1H), 2.71-2.67 (m,1H), 2.42 (s, 3H), 2.34 (dd, *J* = 16.8, 4.4 Hz, 1H). ^{13}C NMR (101 MHz, $CDCl_3$) δ 143.9, 137.5, 134.7, 134.6, 134.4, 134.0, 129.9, 129.5, 128.9, 128.7, 128.5, 127.9, 127.8, 127.3, 127.2, 76.5, 56.8, 53.8, 42.0, 21.8, 21.6. FT-IR (KBr) 3057, 3028, 2925, 2853, 1642, 1598, 1490, 1347, 1160, 1128, 1091, 828, 746 cm^{-1}. HRMS (ESI) m/z $[M+H]^+$ calcd for $C_{24}H_{23}ClN_2O_2S$ 439.1242, found 439.1248.

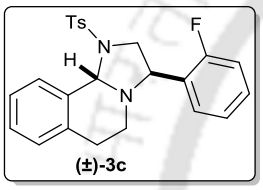

(±)-3-(2-Fluorophenyl)-1-tosyl-1,2,3,5,6,10b-hexahydro imidazo[2,1-*a*]isoquinoline 3c. Analytical TLC on silica gel, 1:10 ethyl acetate/hexane R_f = 0.41; colorless solid; yield 64% (68 mg). Mp 157-158 ^{o}C. ^{1}H NMR (400 MHz, $CDCl_3$) δ 7.92 (d, *J* = 7.6 Hz, 1H), 7.80 (d, *J* = 8.4 Hz, 2H), 7.35-7.31 (m, 3H), 7.25-7.23 (m, 1H), 7.23-7.16 (m, 1H), 7.07 (d, *J* = 7.2 Hz, 1H), 6.98-6.89 (m, 2H), 6.64-6.60 (m, 1H), 5.97 (s, 1H), 4.51 (t, *J* = 8.0 Hz, 1H), 3.78 (dd, *J* = 10.4, 9.6 Hz, 1H), 3.23 (dd, *J* = 10.8, 8.0 Hz, 1H), 3.11-3.10 (m, 1H), 2.99-2.90 (m, 1H), 2.79-2.74 (m, 1H), 2.50 (s, 3H), 2.42 (dd, *J* = 17.2, 4.4 Hz, 1H). ^{13}C NMR (101 MHz, $CDCl_3$) δ 162.7 (d, *J* = 245.0 Hz), 144.0, 134.6 (d, *J* = 10.0 Hz), 134.2, 130.0, 129.2, 129.16, 129.0, 128.7, 128.5, 128.0, 127.96, 127.8, 127.2, 126.3, 126.2, 124.6, 115.5 (d, *J* = 21.0 Hz) 76.4, 54.1, 52.8, 52.79, 41.9, 21.8, 21.5. FT-IR (KBr) 3063, 3028, 2925, 2860, 1637, 1596, 1489, 1454, 1347, 1159, 1094, 814 cm^{-1}. HRMS (ESI) m/z $[M+H]^+$ calcd for $C_{24}H_{23}FN_2O_2S$ 423.1537, found 423.1547.

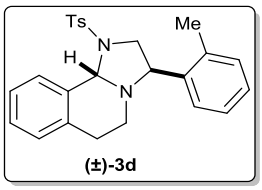

(±)-3-(*o*-Tolyl)-1-tosyl-1,2,3,5,6,10*b*-hexahydroimidazo[2,1-*a*]isoquinoline 3d. Analytical TLC on silica gel, 1:10 ethyl acetate/hexane R_f = 0.48; colorless solid; yield 86% (90 mg). Mp 185-186 ^{o}C. ^{1}H NMR (400 MHz, $CDCl_3$) δ 7.98 (d, *J* = 7.6 Hz, 1H), 7.80 (d, *J* = 8.4 Hz, 2H), 7.36-7.33 (m, 3H), 7.27-7.23 (m, 1H), 7.13-7.05 (m, 3H), 6.98 (t, *J* = 7.6 Hz, 1H), 6.68 (d, *J* = 7.2 Hz, 1H), 5.96 (s, 1H), 4.36 (t, *J* = 8.0 Hz, 1H), 3.78 (dd, *J* = 10.6, 7.6 Hz, 1H), 3.16-3.06 (m, 2H), 2.88-2.75 (m, 2H), 2.51 (s, 3H), 2.41 (dd, *J* = 17.2, 5.2 Hz, 1H), 2.17 (s, 3H). ^{13}C NMR (101 MHz, $CDCl_3$) δ 143.9, 137.0, 136.3, 134.9,

134.1, 134.13, 130.4, 129.8, 129.1, 128.6, 128.5, 127.7, 127.4, 127.2, 126.5, 126.3, 76.2, 56.6, 54.3, 41.6, 21.8, 21.7, 19.5. FT-IR (KBr) 3058, 3026, 2948, 2924, 1634, 1598, 1454, 1346, 1210, 1092, 915, 815 cm^{-1}. HRMS (ESI-TOF) calcd for $[C_{25}H_{26}N_2O_2S+H]^+$ 419.1788, found 419.1780.

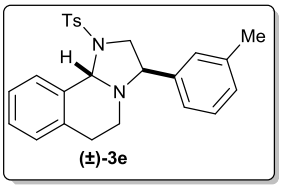

(±)-3-(*m*-Tolyl)-1-tosyl-1,2,3,5,6,10b-hexahydroimidazo[2,1-*a*]isoquinoline 3e. Analytical TLC on silica gel, 1:10 ethyl acetate/hexane R_f = 0.44; colorless solid; yield 82% (86 mg). Mp 148-149 ^oC. ^1H NMR (400 MHz, $CDCl_3$) δ 7.95 (d, J = 7.6 Hz, 1H), 7.86 (d, J = 8.4 Hz, 2H), 7.41 (d, J = 8.0 Hz, 2H), 7.33 (t, J = 7.2 Hz, 1H), 7.24-7.22 (m, 1H), 7.11-7.03 (m, 3H), 6.71 (d, J = 7.6 Hz, 1H), 6.60 (s, 1H), 5.94 (s, 1H), 4.06 (t, J = 8.0 Hz, 1H), 3.70 (dd, J = 10.6, 7.6 Hz, 1H), 3.19-3.06 (m, 2H), 2.95-2.87 (m, 1H), 2.76-2.71 (m, 1H), 2.52 (s, 3H), 2.40 (dd, J = 16.4, 4.0 Hz, 1H), 2.23 (s, 3H). ^{13}C NMR (101 MHz, $CDCl_3$) δ 144.0, 138.9, 138.5, 134.9, 134.2, 134.1, 129.9, 129.2, 129.1, 128.6, 128.6, 128.5, 128.1, 127.7, 127.2, 125.0, 76.6, 60.8, 55.7, 41.5, 21.9, 21.5, 21.4. FT-IR (KBr) 3057, 3030, 2924, 2856, 1638, 1602, 1489, 1452, 1159, 1092, 1004, 747 cm^{-1}. HRMS (ESI) m/z $[M+H]^+$ calcd for $C_{25}H_{26}N_2O_2S$ 419.1788, found 419.1793.

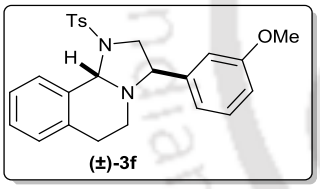

(±)-3-(3-Methoxyphenyl)-1-tosyl-1,2,3,5,6,10b-hexahydro imidazo[2,1-*a*]isoquinoline 3f. Analytical TLC on silica gel, 1:14 ethyl acetate/hexane R_f = 0.40; colorless solid; yield 80% (87 mg). Mp 168-169 ^oC. ^1H NMR (400 MHz, $CDCl_3$) δ 7.95 (d, J = 8.0 Hz, 1H), 7.84 (d, J = 8.0 Hz, 2H), 7.39 (d, J = 8.0 Hz, 2H), 7.32 (t, J = 7.2 Hz, 1H), 7.25-7.22 (m, 1H), 7.12 (t, J = 8.0 Hz, 1H), 7.06 (d, J = 7.2 Hz, 1H), 6.78-6.75 (m, 1H), 6.52 (d, J = 7.6 Hz, 1H), 6.40 (s, 1H), 5.93 (s, 1H), 4.07 (t, J = 8.0 Hz, 1H), 3.70-3.66 (m, 4H), 3.18-3.07 (m, 2H), 2.94-2.85 (m, 1H), 2.76-2.49 (m, 1H), 2.49 (s, 3H), 2.40 (dd, J = 16.8, 4.0 Hz, 1H). ^{13}C NMR (101 MHz, $CDCl_3$) δ 160.2, 144.0, 140.6, 135.0, 134.2, 134.1, 129.9, 129.7, 129.2, 128.6, 128.58, 127.7, 127.2, 120.2, 113.8, 112.7, 76.5, 60.8, 55.6, 55.3, 41.6, 21.8, 21.5. FT-IR (KBr) 3055, 3026, 2946, 2927, 2844, 1676, 1643, 1599, 1487, 1344, 1092, 817 cm^{-1}. HRMS (ESI) m/z $[M+H]^+$ calcd for $C_{25}H_{26}N_2O_3S+H]^+$ 435.1737, found 435.1733.

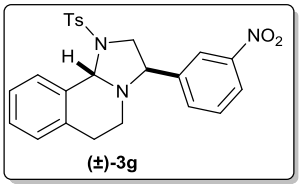

(±)-3-(3-Nitrophenyl)-1-tosyl-1,2,3,5,6,10b-hexahydro imidazo[2,1-*a*]isoquinoline 3g. Analytical TLC on silica gel, 1:4 ethyl acetate/hexane R_f = 0.41; brown color gummy liquid; yield 56% (63 mg). ^{1}H NMR (400 MHz, $CDCl_3$) δ 8.10-8.08 (m, 1H), 7.92 (d, *J* = 7.6 Hz, 1H), 7.82 (d, *J* = 8.0 Hz, 2H), 7.64-7.63 (m, 1H), 7.41-7.32 (m, 4H), 7.28-7.24 (m, 2H) (merged with $CDCl_3$), 7.08 (d, *J* = 7.6 Hz, 1H), 5.97 (s, 1H), 4.22 (t, *J* = 8.0 Hz, 1H), 3.80 (dd, *J* = 10.4, 7.6 Hz, 1H), 3.20-3.13 (m, 2H), 2.95-2.86 (m, 1H), 2.71-2.66 (m,1H), 2.54 (s, 3H), 2.46 (dd, *J* = 16.8, 4.4 Hz, 1H). ^{13}C NMR (150 MHz, $CDCl_3$) δ 149.0, 144.9, 142.0, 134.3, 134.1, 133.7, 130.1, 129.7, 129.1, 128.6, 128.3, 128.0, 127.4, 123.4, 122.1, 76.7, 60.2, 55.3, 41.7, 21.9, 21.4. FT-IR (Neat) 3064, 3026, 2925, 2854, 1740, 1641, 1598, 1530, 1348, 1091, 1020, 813 cm^{-1}. HRMS (ESI) m/z $[M+H]^+$ calcd for $[C_{24}H_{23}N_3O_4S+H]^+$ 450.1482, found 450.1491.

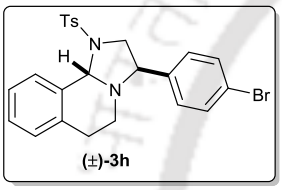

(±)-3-(4-Bromophenyl)-1-tosyl-1,2,3,5,6,10b-hexahydro imidazo[2,1-*a*]isoquinoline 3h. Analytical TLC on silica gel, 1:10 ethyl acetate/hexane R_f = 0.42; colorless solid; yield 74% (89 mg). Mp 145-146 ^{o}C. ^{1}H NMR (400 MHz, $CDCl_3$) δ 7.91 (d, *J* = 7.8 Hz, 1H), 7.76 (d, *J* = 7.8 Hz, 2H), 7.35-7.30 (m, 3H), 7.27-7.25 (m, 2H), 7.15-7.07 (m, 1H), 7.08 (d, *J* = 7.8 Hz, 1H), 7.00 (t, *J* = 7.8 Hz, 1H), 6.61 (d, *J* = 6.6 Hz, 1H), 6.01 (s, 1H), 4.58 (t, *J* = 7.8 Hz, 1H), 3.88 (m, 1H), 3.18-3.12 (m, 2H), 2.99-2.93 (m, 1H), 2.78-2.75 (m, 1H), 2.50 (s, 3H), 2.41 (dd, *J* = 17.4, 4.8 Hz, 1H). ^{13}C NMR (150 MHz, $CDCl_3$) δ 143.9, 137.4, 134.5, 134.53, 134.3, 133.9, 129.8, 129.4, 128.8, 128.7, 128.69, 128.4, 127.9, 127.7, 127.24, 127.2, 76.43, 56.7, 53.74, 41.9, 21.8, 21.5. FT-IR (KBr) 3057, 3031, 2924, 2851, 1639, 1487, 1453, 1346, 1159, 1091, 819, 748 cm^{-1}. HRMS (ESI) m/z $[M+H]^+$ calcd for $C_{24}H_{23}BrN_2O_2S$ 483.0736, found 485.0718.

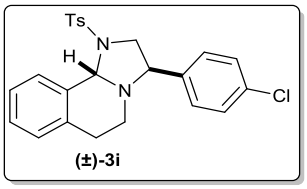

(±)-3-(4-Chlorophenyl)-1-tosyl-1,2,3,5,6,10b-hexahydro imidazo[2,1-*a*]isoquinoline 3i. Analytical TLC on silica gel, 1:10 ethyl acetate/hexane R_f = 0.42; colorless solid; yield 68% (75 mg). Mp 153-154 ^{o}C. ^{1}H NMR (400 MHz, $CDCl_3$) δ 7.93 (d, *J* = 7.6 Hz, 1H), 7.83 (d, *J* = 8.0 Hz, 2H), 7.40 (d, *J* = 8.0 Hz, 2H), 7.35-7.31 (m, 1H), 7.24-7.23 (m, 1H), 7.17 (d, *J* = 8.4 Hz, 2H), 7.06 (d, *J* = 7.6 Hz, 1H), 6.78 (d, *J* = 8.4 Hz, 2H), 5.93 (s, 1H), 4.07 (t, *J* = 8.0 Hz, 1H), 3.70 (dd, *J* = 10.4, 7.6 Hz, 1H), 3.14-3.07 (m, 2H), 2.92-2.83 (m, 1H), 2.72-2.67 (m, 1H), 2.53 (s, 3H), 2.42 (dd, *J* = 17.2, 4.4 Hz, 1H). ^{13}C NMR (101 MHz, $CDCl_3$) δ 144.1, 137.6, 134.7, 134.2, 134.0, 133.9, 130.0, 129.2, 129.0, 128.9, 128.6,

128.58, 127.8, 127.3, 76.5, 60.3, 55.5, 41.6, 21.9, 21.4. FT-IR (KBr) 3057, 3031, 2924, 2851, 1639, 1487, 1453, 1346, 1159, 1091, 819, 748 cm^{-1}. HRMS (ESI) m/z $[M+H]^+$ calcd for $C_{24}H_{23}ClN_2O_2S$ 439.1242, found 439.1256.

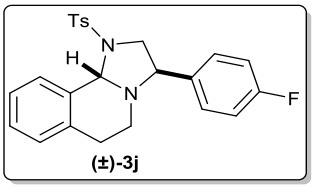

(±)-3j

(±)-3-(4-Fluorophenyl)-1-tosyl-1,2,3,5,6,10*b*-hexahydro imidazo[2,1-*a*]isoquinoline 3j. Analytical TLC on silica gel, 1:10 ethyl acetate/hexane R_f = 0.41; colorless solid; yield 71% (75 mg). Mp 147-148 °C. ^{1}H NMR (400 MHz, $CDCl_3$) δ 7.94 (d, *J* = 7.6 Hz, 1H), 7.84 (d, *J* = 8.4 Hz, 2H), 7.40 (d, *J* = 8.0 Hz, 2H), 7.33 (t, *J* = 7.2 Hz, 1H), 7.24-7.22 (m, 1H), 7.07 (d, *J* = 7.6 Hz, 1H), 6.91-6.80 (m, 4H), 5.93 (s, 1H), 4.08 (t, *J* = 8.0 Hz, 1H), 3.69 (dd, *J* = 10.4, 7.6 Hz, 1H), 3.14-3.06 (m, 2H), 2.93-2.84 (m, 1H), 2.74-2.67 (m, 1H), 2.53 (s, 3H), 2.42 (dd, *J* = 16.8, 4.4 Hz, 1H). ^{13}C NMR (101 MHz, $CDCl_3$) δ 163.8 (d, *J* = 245.0 Hz), 144.1, 134.8, 134.6, 134.6, 134.1 (d, *J* = 14.0 Hz), 129.9, 129.2, 129.1, 128.6, 128.5, 127.8 (d, *J* = 53.0 Hz), 115.75 (d, *J* = 22.0 Hz), 76.4, 60.2, 55.6, 41.5, 21.8, 21.4. FT-IR (KBr) 3098, 3050, 2940, 2910, 2861, 1928, 1598, 1487, 1341, 1160, 1092, 818, cm^{-1}. HRMS (ESI) m/z $[M+H]^+$ calcd for $C_{24}H_{23}FN_2O_2S$ 423.1537, found 423.1540.

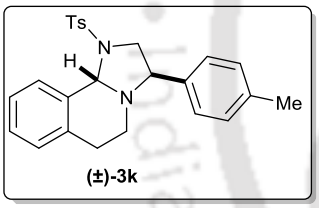

(±)-3k

(±)-3-(*p*-Tolyl)-1-tosyl-1,2,3,5,6,10b hexahydroimidazo[2,1-*a*]isoquinoline 3k. Analytical TLC on silica gel, 1:10 ethyl acetate/hexane R_f = 0.44; colorless solid; yield 78% (82 mg). Mp 196-197 °C. ^{1}H NMR (400 MHz, $CDCl_3$) δ 7.97 (d, *J* = 8.0 Hz, 1H), 7.85 (d, *J* = 8.4 Hz, 2H), 7.40 (d, *J* = 8.0 Hz, 2H), 7.34 (t, *J* = 7.2 Hz, 1H), 7.24-7.22 (m, 1H), 7.06-7.01 (m, 3H), 6.77 (d, *J* = 8.0 Hz, 2H), 5.92 (s, 1H), 4.06 (t, *J* = 8.0 Hz, 1H), 3.69 (dd, *J* = 10.0, 7.6 Hz, 1H), 3.17 (t, *J* = 8.0 Hz, 1H), 3.11-3.05 (m, 1H), 2.93-2.85 (m, 1H), 2.75-2.70 (m, 1H), 2.53 (s, 3H), 2.39 (dd, *J* = 16.8, 4.0 Hz, 1H), 2.31 (s, 3H). ^{13}C NMR (150 MHz, $CDCl_3$) δ 144.0, 138.0, 135.6, 134.9, 134.1, 129.9, 129.5, 129.3, 128.6, 128.57, 127.7, 127.6, 127.2, 76.4, 60.6, 55.7, 41.5, 21.9, 21.4, 21.3. FT-IR (KBr) 3053, 2946, 2923, 2854, 1725, 1647, 1598, 1491, 1345, 1159, 1092, 816, 746 cm^{-1}. HRMS (ESI) m/z $[M+H]^+$ calcd for $C_{25}H_{26}N_2O_2S$ 419.1788, found 419.1800.

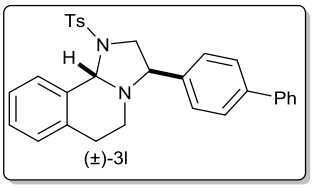

(±)-3l

(±)-3-([1,1'-Biphenyl]-4-yl)-1-tosyl-1,2,3,5,6,10b hexahydro imidazo[2,1-*a*]isoquinoline 3l. Analytical TLC on silica gel, 1:10 ethyl acetate/hexane R_f = 0.38; colorless gummy liquid; yield 72% (87 mg). ^{1}H NMR (400 MHz, $CDCl_3$) δ 7.97 (d, *J* = 7.6 Hz, 1H), 7.86 (d, *J* = 8.4 Hz, 2H), 7.55-7.54 (m, 2H), 7.53-7.41 (m, 5H), 7.40 (s, 1H),

7.38-7.31 (m, 2H), 7.261 (t, *J* = 8.0 Hz, 1H), 7.07 (d, *J* = 7.6 Hz, 1H), 6.95 (d, *J* = 8.0 Hz, 2H), 5.95 (s, 1H), 4.16-4.12 (m, 1H), 3.73 (dd, *J* = 10.4, 7.6 Hz, 1H), 3.23 (dd, *J* = 10.0, 8.8 Hz, 1H), 3.16-3.08 (m, 1H), 2.97-2.88 (m, 1H), 2.81-2.75 (m, 1H), 2.52 (s, 3H), 2.42 (dd, *J* = 17.6, 4.4 Hz, 1H). ^{13}C NMR (101 MHz, $CDCl_3$) δ 144.1, 141.3, 140.8, 137.9, 134.9, 134.3, 134.1, 129.9, 129.2, 129.0, 128.6, 128.56, 128.1, 127.7, 127.6, 127.5, 127.3, 127.26, 127.2, 76.5, 60.7, 55.7, 41.6, 21.9, 21.5. FT-IR (KBr) 3056, 3029, 2925, 2854, 1921, 1807, 1644, 1598, 1487, 1345, 1266, 1159, 1091, 815 cm^{-1}. HRMS (ESI) m/z $[M+H]^+$ calcd for $C_{30}H_{28}N_2O_2S$ 481.1944, found 481.1953.

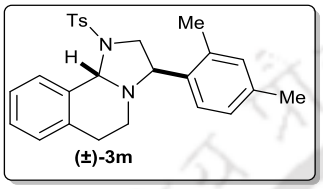

(±)-3m

(±)-3-(2,4-Dimethylphenyl)-1-tosyl-1,2,3,5,6,10b hexahydro imidazo[2,1-*a*]isoquinoline 3m. Analytical TLC on silica gel, 1:10 ethyl acetate/hexane R_f = 0.43; colorless solid; yield 66% (71 mg). Mp 164-165 ^{o}C. ^{1}H NMR (400 MHz, $CDCl_3$) δ 8.00 (d, *J* = 7.8 Hz, 1H), 7.83 (d, *J* = 8.4 Hz, 2H), 7.39 (m, 3H), 7.28-7.27 (m, 1H), 7.09 (d, *J* = 7.2 Hz, 1H), 6.92 (s, 1H), 6.84 (d, *J* = 8.4 Hz, 1H), 6.61 (d, *J* = 7.8 Hz, 1H), 5.96 (s, 1H), 4.35 (t, *J* = 7.8 Hz, 1H), 3.77 (dd, *J* = 7.2, 9.6 Hz, 1H), 3.15-3.06 (m, 2H), 2.88-2.78 (m, 2H), 2.54 (s, 3H), 2.42 (dd, *J* = 16.8, 4.8 Hz, 1H), 2.29 (s, 3H), 2.15 (s, 3H). ^{13}C NMR (151 MHz, $CDCl_3$) δ 144.0, 137.1, 136.3, 135.0, 134.1, 134.0, 133.8, 131.3, 129.9, 129.2, 128.6, 128.5, 127.7, 127.3, 127.2, 126.4, 76.2, 56.4, 54.5, 41.6, 21.9, 21.7, 21.1, 19.4. FT-IR (KBr) 3059, 3030, 2923, 2860, 1638, 1450, 1338, 1157, 1090, 1002, 817, 747 cm^{-1}. HRMS (ESI) m/z $[M+H]^+$ calcd for $C_{26}H_{28}N_2O_2S$ 433.1944, found 433.1940.

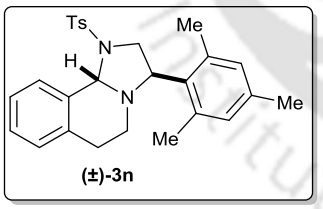

(±)-3n

(±)-3-Mesityl-1-tosyl-1,2,3,5,6,10b-hexahydroimidazo[2,1-*a*]isoquinoline 3n. Analytical TLC on silica gel, 1:10 ethyl acetate/hexane R_f = 0.48; colorless solid; yield 76% (85 mg). Mp 183-184 ^{o}C. ^{1}H NMR (400 MHz, $CDCl_3$) δ 8.08 (d, *J* = 7.6 Hz, 1H), 7.84 (d, *J* = 8.4 Hz, 2H), 7.37 (d, *J* = 8.0 Hz, 3H), 7.25-7.22 (m, 1H), 7.06 (d, *J* = 7.6 Hz, 1H), 6.72 (s, 2H), 5.89 (s, 1H), 4.60 (dd, *J* = 10.4, 6.8 Hz, 1H), 3.59 (dd, *J* = 8.8, 6.8 Hz, 1H), 3.20-3.06 (m, 2H), 2.78-2.66 (m, 2H), 2.47 (s, 3H), 2.41 (dd, *J* = 16.8, 5.2 Hz, 1H), 2.20 (s, 3H), 1.90 (br s, 3H), 1.55 (s, 3H). ^{13}C NMR (101 MHz, $CDCl_3$) δ 144.1, 138.2, 137.3, 135.4, 133.9, 133.8, 130.0, 129.7, 128.7, 128.5, 128.3, 127.5, 127.4, 75.3, 57.3, 51.2, 41.6, 22.4, 21.7, 21.9, 20.2. FT-IR (KBr) 3043, 2957, 2924, 2852, 1636, 1448, 1333, 1158, 1091, 955, 886, 816 cm^{-1}. HRMS (ESI) m/z $[M+H]^+$ calcd for $C_{27}H_{30}N_2O_2S$ 447.2101, found 447.2097.

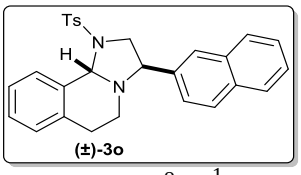

(±)-3-(Naphthalen-2-yl)-1-tosyl-1,2,3,5,6,10b-hexahydro imidazo[2,1-*a*]isoquinoline 3o. Analytical TLC on silica gel, 1:10 ethyl acetate/hexane R_f = 0.41; colorless solid; yield 77% (87 mg). Mp 115-116 ^{o}C. ^{1}H NMR (400 MHz, $CDCl_3$) δ 7.91 (d, *J* = 7.6 Hz, 1H), 7.80 (d, *J* = 8.4 Hz, 2H), 7.73-7.70 (m, 1H), 7.60 (d, *J* = 8.0 Hz, 2H), 7.40-7.38 (m, 5H), 7.35-7.29 (m, 1H), 7.28-7.17 (m, 1H), 7.01 (d, *J* = 7.6 Hz, 1H), 6.78 (d, *J* = 7.2 Hz, 1H), 5.92 (s, 1H), 4.20 (t, *J* = 8.0 Hz, 1H), 3.70 (dd, *J* = 10.4, 7.6 Hz, 1H), 3.22 (dd, *J* = 10.0, 8.8 Hz, 1H), 3.09 (m, 1H), 2.93 (m, 1H), 2.70-2.65 (m, 1H), 2.49 (s, 3H), 2.34 (dd, *J* = 17.2, 4.4 Hz, 1H). ^{13}C NMR (101 MHz, $CDCl_3$) δ 144.7, 136.4, 134.9, 134.3, 134.1, 133.5, 133.4, 130.0, 129.2, 128.7, 128.66, 128.63, 127.9, 127.8, 127.3, 127.1, 126.4, 126.3, 124.9, 76.6, 61.0, 55.4, 41.6, 21.9, 21.4. FT-IR (KBr) 3055, 2953, 2850, 1632, 1598, 1451, 1338, 1262, 1158, 1090, 1000, 815 cm^{-1}. HRMS (ESI) m/z $[M+H]^+$ calcd for $C_{28}H_{26}N_2O_2S$ 455.1788, found 455.1805.

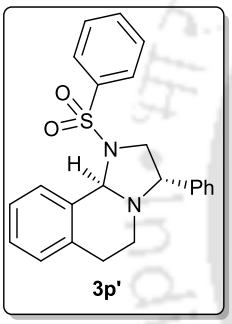

(*3R,10bS*)-3-Phenyl-1-(phenylsulfonyl)-1,2,3,5,6,10b-hexahydro imidazo[2,1-*a*]isoquinoline 3p′. Analytical TLC on silica gel, 1:10 ethyl acetate/hexane R_f = 0.38; colorless solid; yield 70% (68 mg). Mp 135-136 ^{o}C. ^{1}H NMR (600 MHz, $CDCl_3$) δ 7.97 (t, *J* = 7.2 Hz, 3H), 7.72 (t, *J* = 7.8 Hz, 1H), 7.61 (t, *J* = 7.8 Hz, 2H), 7.33 (t, *J* = 7.8 Hz, 1H), 7.25-7.18 (m, 4H), 7.07 (d, *J* = 7.2 Hz, 1H), 6.85 (d, *J* = 7.2 Hz, 2H), 5.95 (s, 1H), 4.10 (t, *J* = 7.8 Hz, 1H), 3.72 (dd, *J* = 9.6, 7.2 Hz, 1H), 3.18-3.15 (m, 1H), 3.12-3.07 (m, 1H), 2.93-2.87 (m, 1H), 2.4-2.71 (m, 1H), 2.39 (dd, *J* = 17.4, 4.8 Hz, 1H). ^{13}C NMR (151 MHz, $CDCl_3$) δ 138.7, 137.0, 134.8, 134.1, 133.3, 129.3, 129.2, 128.8, 128.6, 128.5, 128.3, 127.8, 127.6, 127.3, 76.6, 60.8, 55.7, 41.5, 21.4. FT-IR (KBr) 3063, 3032, 2931, 2867, 1966, 1898, 1490, 1448, 1345, 1162, 1092, 842, 753 cm^{-1}. HRMS (ESI) m/z $[M+H]^+$ calcd for $C_{23}H_{22}N_2O_2S$ 391.1475, found 391.1469. $[\alpha]_D^{20}$ = +44 (c = 0.13, $CHCl_3$). HPLC analysis: 94% ee [Daicel Chiralcel AD-H column, hexane/*i*PrOH = 85:15, flow rate: 1 mL/min, λ = 215 nm, t_R = 8.48 min (minor), 15.42 min (major)].

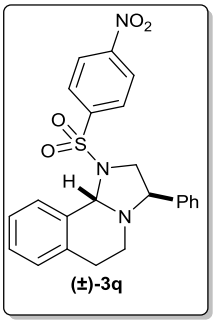

(±)-1-((4-Nitrophenyl)sulfonyl)-3-phenyl-1,2,3,5,6,10b-hexahydro imidazo[2,1-*a*]isoquinoline 3q. Analytical TLC on silica gel, 1:10 ethyl acetate/hexane R_f = 0.35; pale yellow solid; yield 62% (67 mg). Mp 186-187 ^{o}C. ^{1}H NMR (400 MHz, $CDCl_3$) δ 8.44 (d, *J* = 8.8 Hz, 2H), 8.14 (d, *J* = 8.4 Hz, 2H), 7.90 (d, *J* = 7.6 Hz, 1H), 7.37-7.33 (m, 1H), 7.29-7.27 (m, 1H), 7.25-7.19 (m, 3H), 7.09 (d, *J* = 7.6 Hz, 1H), 6.86 (d, *J* = 6.8 Hz,

2H), 5.94 (s, 1H), 4.15 (t, *J* = 8.0 Hz, 1H), 3.81 (dd, *J* = 10.4, 7.6 Hz, 1H), 3.19-3.08 (m, 2H), 2.95-2.87 (m, 1H), 2.81-2.76 (m, 1H), 2.44 (dd, *J* = 16.8, 4.4 Hz, 1H). ^{13}C NMR (101 MHz, $CDCl_3$) δ 150.6, 143.2, 138.3, 134.2, 133.9, 129.7, 129.0, 128.9, 128.8, 128.6, 128.2, 127.4, 127.2, 124.5, 76.9, 60.6, 55.7, 41.7, 21.4. FT-IR (KBr) 3096, 3065, 2922, 2854, 1637, 1592, 1515, 1340, 1289, 1018, 811, 741 cm^{-1}. HRMS (ESI) m/z $[M+H]^+$ calcd for $C_{23}H_{21}N_3O_4S$ 436.1326, found 436.1337.

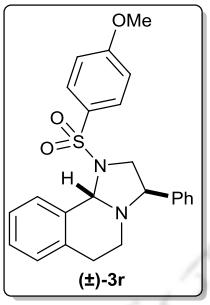

(±)-1-((4-Methoxyphenyl)sulfonyl)-3-phenyl-1,2,3,5,6,10b-hexahydro imidazo[2,1-*a*]isoquinoline 3r. Analytical TLC on silica gel, 1:7 ethyl acetate/hexane R_f = 0.37; colorless gummy liquid; yield 67% (70 mg). ^{1}H NMR (400 MHz, $CDCl_3$) δ 7.96 (d, *J* = 7.6 Hz, 1H), 7.89 (d, *J* = 8.8 Hz, 2H), 7.32 (t, *J* = 7.2 Hz, 1H), 7.25-7.19 (m, 4H), 7.06 (d, *J* = 8.8 Hz, 3H), 6.92-6.90 (m, 2H), 5.91 (s, 1H), 4.09 (t, *J* = 8.4 Hz, 1H), 3.93 (s, 3H), 3.68 (dd, *J* = 10.0, 7.2 Hz, 1H), 3.23-3.13 (m, 1H), 3.11-3.06 (m, 1H), 2.95-2.86 (m, 1H), 2.76-2.71 (m, 1H), 2.40 (dd, *J* = 16.8, 4.4 Hz, 1H). ^{13}C NMR (101 MHz, $CDCl_3$) δ 163.5, 139.0, 135.0, 134.1, 130.6, 129.2, 128.9, 128.8, 128.6, 128.3, 127.7, 127.67, 127.2, 114.5, 76.5, 60.9, 55.9, 55.8, 41.6, 21.5. FT-IR (Neat) 3057, 3028, 2926, 2850, 1639, 1593, 1494, 1343, 1260, 1155, 1095, 831, 755 cm^{-1}. HRMS (ESI) m/z $[M+H]^+$ calcd for $C_{24}H_{24}N_2O_3S$ 421.1580, found 421.1597.

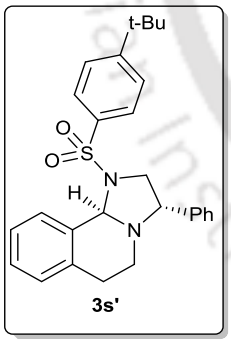

(*3R,10bS*)-1-((4-(*tert*-Butyl)phenyl)sulfonyl)-3-phenyl1,2,3,5,6,10b hexahydroimidazo[2,1-*a*]isoquinoline 3s′. Analytical TLC on silica gel, 1:10 ethyl acetate/hexane R_f = 0..43; colorless solid; yield 81% (91 mg). Mp 166-167 ^{o}C. ^{1}H NMR (400 MHz, $CDCl_3$) δ 7.94 (d, *J* = 7.6 Hz, 1H), 7.88 (d, *J* = 8.4 Hz, 2H), 7.61 (d, *J* = 8.8 Hz, 2H), 7.34-7.30 (m, 1H), 7.25-7.14 (m, 4H), 7.06 (d, *J* = 7.6 Hz, 1H), 6.81 (d, *J* = 6.8 Hz, 2H), 6.00 (s, 1H), 4.09 (t, *J* = 8.4 Hz, 1H), 3.69 (dd, *J* = 10.0, 7.2 Hz, 1H), 3.15-3.08 (m, 2H), 2.95-2.86 (m, 1H), 2.75-2.69 (m, 1H), 2.40 (dd, *J* = 17.2, 4.4 Hz, 1H), 1.43 (s, 9H). ^{13}C NMR (101 MHz, $CDCl_3$) δ 157.1, 139.1, 135.0, 134.1, 129.2, 128.7, 128.6, 128.5, 128.3, 127.7, 127.6, 127.2, 126.2, 76.7, 61.0, 55.5, 41.5, 35.5, 31.4, 21.4. FT-IR (KBr) 3061, 3030, 2962, 2928, 2867, 1641, 1596, 1455, 1348, 1267, 1088, 839 cm^{-1}. HRMS (ESI) m/z $[M+H]^+$ calcd for $C_{27}H_{30}N_2O_2S$ 447.2101, found 447.2119. $[\alpha]_D^{20}$ = +60 (c = 0.10, $CHCl_3$). HPLC analysis: 99% ee [Daicel Chiralcel OD-H column, hexane/*i*PrOH = 90:10, flow rate: 1 mL/min, λ = 254 nm, t_R = 6.56 min (major), 8.68 min (minor)].

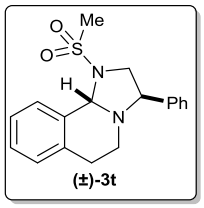

(±)-1-(Methylsulfonyl)-3-phenyl-1,2,3,5,6,10b-hexahydroimidazo[2,1-*a*]isoquinoline 3t. Analytical TLC on silica gel, 1:7 ethyl acetate/hexane R_f = 0.35; brown color solid; yield 72% (60 mg). Mp 167-168 ^{o}C. ^{1}H NMR (400 MHz, $CDCl_3$) δ 7.80 (d, *J* = 7.6 Hz, 1H), 7.39-7.38 (m, 5H), 7.30-7.22 (m, 2H), 7.09 (d, *J* = 7.2 Hz, 1H), 5.80 (s, 1H), 4.23 (t, *J* = 8.0 Hz, 1H), 3.78-3.73 (dd, *J* = 10.4, 7.2 Hz, 1H), 3.33-3.25 (m, 2H), 3.06 (s, 3H), 3.03-2.93 (m, 2H), 2.48 (dd, *J* = 15.0, 4.0 Hz, 1H). ^{13}C NMR (101 MHz, $CDCl_3$) δ 138.6, 134.3, 134.0, 129.2, 129.0, 128.6, 128.61, 127.9, 127.5, 127.3, 76.3, 60.8, 55.9, 41.7, 34.4, 21.5. FT-IR (KBr) 3062, 3026, 2933, 2069, 1638, 1454, 1340, 1153, 1011, 962, 843, 763 cm^{-1}. HRMS (ESI) m/z $[M+H]^+$ calcd for $C_{18}H_{20}N_2O_2S$ 329.1318, found 329.1318.

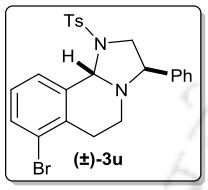

(±)-7-Bromo-3-phenyl-1-tosyl-1,2,3,5,6,10b-hexahydroimidazo[2,1-*a*]isoquinoline 3u. Analytical TLC on silica gel, 1:10 ethyl acetate/hexane R_f = 0.35; yellow color solid; yield 74% (90 mg). Mp 195-196 ^{o}C. ^{1}H NMR (400 MHz, $CDCl_3$) δ 7.96 (d, *J* = 8.0 Hz, 1H), 7.84 (d, *J* = 8.0 Hz, 2H), 7.53 (d, *J* = 7.6 Hz, 1H), 7.41 (d, *J* = 8.0 Hz, 2H), 7.24-7.18 (m, 4H), 6.85 (d, *J* = 6.8 Hz, 2H), 5.91 (s, 1H), 4.04 (t, *J* = 8.4 Hz, 1H), 3.70 (dd, *J* = 10.4, 7.6 Hz, 1H), 3.19-3.14 (m, 1H), 3.11-3.04 (m, 1H), 2.83-2.77 (m, 1H), 2.73-2.64 (m, 1H), 2.53-2.46 (m, 4H). ^{13}C NMR (101 MHz, $CDCl_3$) δ 144.2, 138.5, 137.6, 134.0, 133.8, 131.7, 130.0, 128.8, 128.6, 128.5, 128.4, 128.37, 127.7, 124.8, 76.5, 60.7, 55.6, 41.0, 22.3, 21.9. FT-IR (KBr) 3061, 3032, 2926, 2857, 1920, 1887, 1597, 1454, 1346, 1161, 1112, 1092, 814, 774 cm^{-1}. HRMS (ESI) m/z $[M+H]^+$ calcd for $C_{24}H_{23}BrN_2O_2S$ 483.0736, found 485.0730.

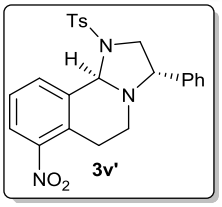

(*3R,10bS*)-7-Nitro-3-phenyl-1-(phenylsulfonyl)-1,2,3,5,6,10b-hexahydroimidazo[2,1-*a*]isoquinoline 3v′. Analytical TLC on silica gel, 1:10 ethyl acetate/hexane R_f = 0.30; colorless solid; yield 78% (88 mg). Mp 180-181 ^{o}C. ^{1}H NMR (400 MHz, $CDCl_3$) δ 8.27 (d, *J* = 8.0 Hz, 1H), 7.85 (d, *J* = 8.0 Hz, 1H), 7.77 (d, *J* = 8.0 Hz, 2H), 7.41 (t, *J* = 8.0 Hz, 1H), 7.35 (d, *J* = 8.0 Hz, 2H), 7.19-7.13 (m, 3H), 6.81 (d, *J* = 8.0 Hz, 2H), 5.87 (s, 1H), 4.04 (t, *J* = 8.4 Hz, 1H), 3.66 (dd, *J* = 10.4, 7.6 Hz, 1H), 3.15-2.94 (m, 3H), 2.75-2.2.70 (m, 1H), 2.57 (dd, *J* = 17.2, 2.4 Hz, 1H), 2.46 (s, 3H). ^{13}C NMR (101 MHz, $CDCl_3$) δ 148.7, 144.5, 138.0, 137.6, 134.7, 133.7, 130.1, 129.7, 128.9, 128.6, 128.59, 127.6, 127.5, 124.3, 76.1, 60.9, 55.7, 40.8, 21.9, 18.4. FT-IR (KBr) 3064, 3030, 2951, 2927, 2864, 1598, 1526, 1347, 1290, 1160, 1091, 1009, 869, 810 cm^{-1}. HRMS (ESI) m/z $[M+H]^+$ calcd for $C_{24}H_{23}N_3O_4S$ 450.1482, found 450.1486. $[\alpha]_D^{20}$ = +150 (c = 0.13, $CHCl_3$). HPLC analysis: 99% ee [Daicel Chiralcel

AD-H column, hexane/*i*PrOH = 85:15, flow rate: 1 mL/min, λ = 254 nm, t_R = 14.90 min (major), 20.19 min (minor)].

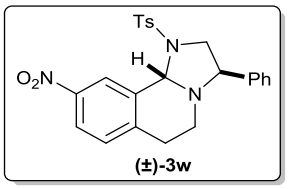

(±)-9-Nitro-3-phenyl-1-tosyl-1,2,3,5,6,10*b*-hexahydroimidazo [2,1-*a*]isoquinoline 3w. Analytical TLC on silica gel, 1:7 ethyl acetate/hexane R_f = 0.30; colorless solid; yield 69% (78 mg). Mp 197-198 ^oC. ^1H NMR (400 MHz, $CDCl_3$) δ 8.81 (d, *J* = 2.0 Hz, 1H), 8.09 (dd, *J* = 8.4, 2.0 Hz, 1H), 7.86 (d, *J* = 8.4 Hz, 2H), 7.42 (d, *J* = 8.0 Hz, 2H), 7.25-7.21 (m, 4H), 6.93-6.90 (m, 2H), 5.92 (s, 1H), 4.00 (t, *J* = 8.4 Hz, 1H), 3.71 (dd, *J* = 10.0, 7.2 Hz, 1H), 3.26-3.22 (m, 1H), 3.18-3.10 (m, 1H), 2.99-2.89 (m, 1H), 2.81 (dd, *J* = 14.0, 6.0 Hz, 1H), 2.53-2.48 (m, 4H). ^{13}C NMR (101 MHz, $CDCl_3$) δ 147.4, 144.5, 141.7, 138.0, 137.1, 133.9, 130.1, 129.7, 128.9, 128.6, 128.60, 127.7, 124.6, 122.5, 75.7, 61.3, 55.7, 41.1, 22.0, 21.9. FT-IR (KBr) 3086, 3061, 2961, 2921, 2853, 1652, 1591, 1511, 1336, 1288, 1152, 1084, 811, 767 cm^{-1}. HRMS (ESI) m/z $[M+H]^+$ calcd for $C_{24}H_{23}N_3O_4S$ 450.1482, found 450.1495.

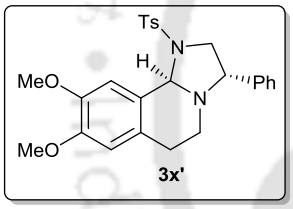

(*3R,10bS*)-8,9-Dimethoxy-3-phenyl-1-(phenylsulfonyl)-1,2,3,5,6,10b hexahydroimidazo[2,1-*a*]isoquinoline 3x′. Analytical TLC on silica gel, 1:4 ethyl acetate/hexane R_f = 0.48; yellow solid; yield 87% (101 mg). Mp 176-177 ^oC. ^1H NMR (400 MHz, $CDCl_3$) δ 7.85 (d, *J* = 8.0 Hz, 2H), 7.49 (s, 1H), 7.40 (d, *J* = 8.0 Hz, 2H), 7.25-7.19 (m, 3H), 6.91 (d, *J* = 7.2 Hz, 2H), 6.51 (s, 1H), 5.86 (s, 1H), 4.13 (t, *J* = 8.0 Hz, 1H), 3.96 (s, 3H), 3.87 (s, 3H), 3.73 (dd, *J* = 10.0, 7.2 Hz, 1H), 3.18 (t, *J* = 9.6 Hz, 1H), 3.08-3.00 (m, 1H), 2.80 (m, 1H), 2.77-2.72 (m, 1H), 2.52 (s, 3H), 2.28 (dd, *J* = 16.8, 4.8 Hz, 1H). ^{13}C NMR (101 MHz, $CDCl_3$) δ 148.7, 148.4, 144.0, 138.9, 134.2, 129.9, 128.8, 128.5, 128.3, 127.7, 126.9, 126.0, 111.3, 110.8, 76.4, 60.6, 56.2, 56.1, 55.8, 41.6, 21.8, 20.9. FT-IR (KBr) 3069, 2998, 2928, 2853, 1637, 1611, 1512, 1460, 1345, 1258, 1158, 1100, 1209, 815 cm^{-1}. HRMS (ESI) m/z $[M+H]^+$ calcd for $C_{26}H_{28}N_2O_4S$ 465.1843, found 465.1862. HPLC Data $[\alpha]_D^{20}$ = +35.0 (c = 0.26, $CHCl_3$); HPLC analysis: 96% ee [Daicel Chiralcel AD-H column, hexane/*i*PrOH = 85:15, flow rate: 1 mL/min, λ = 215 nm, t_R = 18.41 min (minor), 29.81 min (major)].

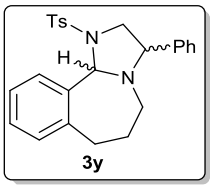

(±)-3-Phenyl-1-tosyl-2,3,5,6,7,11b-hexahydro-1*H*-benzo[*c*]imidazo [1,2-*a*]azepine 3y. Analytical TLC on silica gel, 1:9 ethyl acetate/hexane R_f = 0.42; colorless solid; yield 77% (81 mg). Mp 195-196 °C. ^{1}H NMR (400 MHz, $CDCl_3$) 9:1 mixture of diastereomers δ 7.89 (d, J = 8.4 Hz, 2H), 7.76 (d, J = 7.2 Hz, 1H), 7.45 (d, J = 8.0 Hz, 2H), 7.29-7.25 (m, 1H), 7.23-7.20 (m, 4H), 7.15-7.11 (m, 3H), 5.40 (s, 1H), 3.98 (dd, J = 12.4, 5.6 Hz, 1H), 3.30 (dd, J = 12.0, 10.8 Hz, 1H), 3.07-2.95 (m, 2H), 2.93-2.83 (m, 2H), 2.51 (s, 3H), 2.33-2.26 (m, 1H), 1.79-1.75 (m, 1H), 1.54-1.50 (m, 1H). ^{13}C NMR (101 MHz, $CDCl_3$) δ 144.5, 141.0, 140.0, 137.7, 135.7, 130.2, 129.4, 128.7, 128.3, 128.2, 127.8, 127.7, 126.6, 124.4, 81.0, 69.0, 55.4, 55.2, 34.9, 28.5, 21.9. FT-IR (KBr) 3062, 3030, 2930, 2848, 2805, 2728, 1922, 1598, 1269, 1161, 1091 cm^{-1}. HRMS (ESI) m/z $[M+H]^+$ calcd for $C_{25}H_{26}N_2O_2S$ 419.1788, found 419.1796.

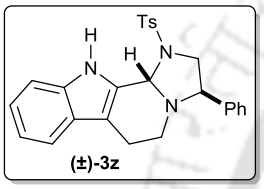

(±)-3-Phenyl-1-tosyl-2,3,5,6,11,11b-hexahydro-1*H*-imidazo [1',2':1,2]pyrido[3,4-*b*]indole 3z. Analytical TLC on silica gel, 1:20 ethyl acetate/hexane R_f = 0.28; colorless solid; yield 64% (71 mg). Mp 221-222 °C. ^{1}H NMR (400 MHz, $CDCl_3$) δ 9.07 (s, 1H), 7.86 (d, J = 8.4 Hz, 2H), 7.51 (d, J = 8.0 Hz, 1H), 7.45-7.42 (m, 3H), 7.33 (m, 3H), 7.25-7.18 (m, 3H), 7.12 (t, J = 7.2 Hz, 1H), 5.86 (s, 1H), 4.34 (dd, J = 9.6, 6.0 Hz, 1H), 3.79 (dd, J = 8.0, 5.6 Hz, 1H), 3.14 (dd, J = 9.6, 8.4 Hz, 1H), 3.05-2.90 (m, 2H), 2.86-2.78 (m, 1H), 2.52 (s, 3H), 2.47-2.39 (m, 1H). ^{13}C NMR (101 MHz, $CDCl_3$) δ 144.5, 137.58, 136.5, 133.1, 131.2, 130.3, 129.0, 128.67, 128.1, 128.0, 126.6, 122.7, 119.6, 119.0, 111.8, 108.7, 72.0, 60.9, 55.6, 42.6, 21.9, 15.9. FT-IR (KBr) 3428, 3057, 3030, 2924, 2854, 1638, 1599, 1457, 1339, 1157, 1090 cm^{-1}. HRMS (ESI) m/z $[M+H]^+$ calcd for $C_{26}H_{25}N_3O_2S$ 444.1740, found 444.1745.

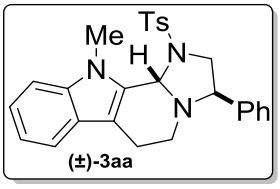

(±)-11-Methyl-3-phenyl-1-tosyl-2,3,5,6,11,11b-hexahydro-1*H* imidazo[1',2':1,2]pyrido[3,4-*b*]indole 3aa. Analytical TLC on silica gel, 1:20 ethyl acetate/hexane R_f = 0.26; yellow solid; yield 76% (87 mg). Mp 169-170 °C. ^{1}H NMR (400 MHz, $CDCl_3$) δ 7.84 (d, J = 8.0 Hz, 2H), 7.50 (d, J = 8.0 Hz, 1H), 7.40 (d, J = 8.0 Hz, 3H), 7.30 (d, J = 7.2 Hz, 1H), 7.21-7.17 (m, 1H), 7.14-7.08 (m, 3H), 6.58 (d, J = 6.0 Hz, 2H), 6.42 (s, 1H), 4.22 (t, J = 8.4 Hz, 1H), 4.09 (s, 3H), 3.72 (dd, J = 11.8, 8.8 Hz, 1H), 3.24 (dd, J = 11.6, 8.0 Hz, 1H), 3.12-3.03 (m, 1H), 2.93-2.82 (m, 2H), 2.56 (s, 3H), 2.52 (dd, J = 14.4, 2.8 Hz, 1H). ^{13}C NMR (101 MHz, $CDCl_3$) δ 144.3, 140.0, 137.9, 134.6, 130.3, 130.0, 129.1, 128.6, 127.9, 127.4, 126.0, 122.5, 119.4, 118.7, 109.7, 109.6, 75.3, 60.4, 55.0, 42.2, 31.3, 21.9, 15.9. FT-IR (KBr)

3061, 2925, 2854, 1637, 1468, 1345, 1159, 1092, 1003, 960, 813, 743 cm^{-1}. HRMS (ESI) m/z $[M+H]^+$ calcd for $C_{27}H_{27}N_3O_2S$ 458.1897, found 458.1889.

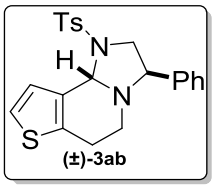

(±)-3-Phenyl-1-tosyl-1,2,3,5,6,9b-hexahydroimidazo[1,2-*a*]thieno [3,2-*c*]pyridine 3ab. Analytical TLC on silica gel, 1:7 ethyl acetate/hexane R_f = 0.48; colorless solid; yield 92% (94 mg). Mp 212-213 ^oC. ^1H NMR (400 MHz, $CDCl_3$) δ 7.76 (d, *J* = 8.4 Hz, 2H), 7.37 (d, *J* = 5.2 Hz, 1H), 7.33 (d, *J* = 8.0 Hz, 2H), 7.19-7.17 (m, 3H), 7.09 (d, *J* = 5.2 Hz, 1H), 6.94-6.92 (m, 2H), 5.77 (s, 1H), 4.09 (dd, *J* = 9.2, 6.8 Hz, 1H), 3.66-3.61 (m, 1H), 3.06 (t, *J* = 9.2 Hz, 1H), 2.97-2.90 (m, 1H), 2.80-2.75 (m, 2H), 2.43 (s, 3H), 2.41 (dd, *J* = 16.4, 5.0 Hz, 1H). ^{13}C NMR (101 MHz, $CDCl_3$) δ 144.1, 138.4, 134.4, 134.38, 134.0, 130.0, 128.9, 128.5, 128.4, 127.8, 127.80, 122.9, 75.0, 60.5, 55.6, 42.3, 21.9, 18.7. FT-IR (KBr) 3062, 3032, 2927, 2854, 1630, 1598, 1493, 1347, 1159, 1091, 988, 815 cm^{-1}. HRMS (ESI) m/z $[M+H]^+$ calcd for $C_{22}H_{22}N_2O_2S_2$ 411.1195, found 411.1194.

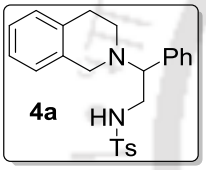

***N*-(2-(3,4-Dihydroisoquinolin-2(1*H*)-yl)-2-phenylethyl)-4-methyl benzenesulfonamide 4a.** Analytical TLC on silica gel, 1:5 ethyl acetate/hexane R_f = 0.32; colorless solid; yield 88% (108 mg). Mp 120 - 121 ^oC. ^1H NMR (400 MHz, $CDCl_3$) δ 7.72 (d, *J* = 8.0 Hz, 2H), 7.32-7.28 (m, 5H), 7.15-7.04 (m, 5H), 6.88 (d, *J* = 6.4 Hz, 1H), 5.19 (br s, 1H), 3.71 (dd, *J* = 9.2, 5.6 Hz, 1H), 3.50-3.45 (m, 3H), 3.28 (dd, *J* = 11.6, 4.8 Hz, 1H), 2.79 (t, *J* = 5.2 Hz, 2H), 2.70-2.65 (m, 1H), 2.45-2.39 (m, 4H). ^{13}C NMR (101 MHz, $CDCl_3$) δ 143.6, 136.9, 135.6, 134.5, 134.2, 129.9, 128.8, 128.7, 128.66, 128.4, 127.3, 126.7, 126.4, 125.8, 67.0, 52.0, 47.0, 43.5, 29.6, 21.8. FT-IR (KBr) 3292, 3063, 3030, 2923, 2810, 1951, 1749, 1529, 1348, 1092, 960, 854 cm^{-1}. HRMS (ESI) m/z $[M+H]^+$ calcd for $C_{24}H_{26}N_2O_2S$ 407.1788, found 407.1810.

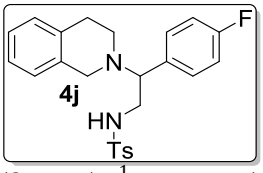

***N*-(2-(3,4-Dihydroisoquinolin-2(1*H*)-yl)-2-(4-fluorophenyl) ethyl)-4-methylbenzene sulfonamide 4j.** Analytical TLC on silica gel, 1:5 ethyl acetate/hexane R_f = 0.28; colorless gummy liquid; yield 74% (94 mg). ^1H NMR (400 MHz, $CDCl_3$) δ 7.70 (d, *J* = 8.0 Hz, 2H), 7.30 (d, *J* = 8.0 Hz, 2H), 7.14-6.98 (m, 7H), 6.88 (d, *J* = 6.8 Hz, 1H), 5.14 (br s, 1H) 3.71 (dd, *J* = 8.8, 5.2 Hz, 1H), 3.43-3.39 (m, 3H), 3.28 (dd, *J* = 12.4, 5.6 Hz, 1H), 2.79 (t, *J* = 5.6 Hz, 2H), 2.68-2.63 (m, 1H), 2.45-2.39 (m, 4H). ^{13}C NMR (101 MHz, $CDCl_3$) δ 163.9 (d, *J* = 246.0 Hz), 143.7, 136.7, 134.2, 134.1, 131.5, 131.54, 130.2, 130.16, 129.9, 128.9, 127.3, 126.7 (d, *J* = 18.0 Hz), 125.9, 115.7 (d, *J* = 21.0 Hz), 66.3, 52.0, 47.0, 43.7, 29.4, 21.8. FT-IR (neat) 3282,

3025, 2922, 2810, 1912, 1598, 1396, 1159, 1091, 935, 816, 739 cm^{-1}. HRMS (ESI) m/z $[M+H]^+$ calcd for $C_{24}H_{25}FN_2O_2S$ 425.1694, found 425.1691.

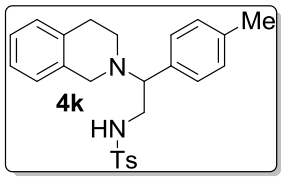

***N*-(2-(3,4-Dihydroisoquinolin-2(1*H*)-yl)-2-(*p*-tolyl)ethyl)-4-methylbenzenesulfonamide 4k.** Analytical TLC on silica gel, 1:5 ethyl acetate/hexane R_f = 0.32; colorless solid; yield 76% (96 mg). Mp 113-114 ^oC. ^1H NMR (400 MHz, $CDCl_3$) δ 7.71 (d, *J* = 8.4 Hz, 2H), 7.30 (d, *J* = 8.0 Hz, 2H), 7.13-7.00 (m, 7H), 6.88 (d, *J* = 6.8 Hz, 1H), 5.18 (br s, 1H), 3.62 (dd, *J* = 9.2, 5.6 Hz, 1H), 3.46-3.43 (m, 3H), 3.25 (dd, *J* = 12.0, 5.6 Hz, 1H), 2.79 (t, *J* = 5.6 Hz, 2H), 2.69-2.63 (m, 1H), 2.45-2.38 (m, 4H), 2.32 (s, 3H). ^{13}C NMR (101 MHz, $CDCl_3$) δ 143.6, 138.2, 136.9, 134.6, 134.2, 132.5, 129.9, 129.3, 128.8, 128.6, 127.4, 126.7, 126.4, 125.8, 66.7, 52.0, 47.0, 43.6, 29.6, 21.8, 21.3. FT-IR (KBr) 3282, 3024, 2922, 2809, 1911, 1597, 1495, 1396, 1159, 1091, 935, 816 cm^{-1}. HRMS (ESI) m/z $[M+H]^+$ calcd for $C_{25}H_{28}N_2O_2S$ 421.1944, found 421.1923.

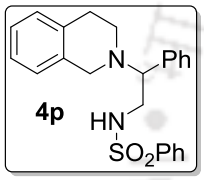

***N*-(2-(3,4-Dihydroisoquinolin-2(1*H*)-yl)-2-phenylethyl)benzene sulfonamide 4p.** Analytical TLC on silica gel, 1:5 ethyl acetate/hexane R_f = 0.30; colorless gummy liquid; yield 81% (95 mg). ^1H NMR (400 MHz, $CDCl_3$) δ 7.84-7.82 (m, 2H), 7.62-7.59 (m, 1H), 7.53-7.49 (m, 2H), 7.35-7.31 (m, 3H), 7.14-7.04 (m, 5H), 6.89 (d, *J* = 6.8 Hz, 1H), 3.71 (dd, *J* = 9.6, 5.6 Hz, 1H), 3.52-3.46 (m, 3H), 3.31 (dd, *J* = 12.4, 5.6 Hz, 1H), 2.79 (t, dd, *J* = 5.6 Hz, 2H), 2.71-2.65 (m, 1H), 2.45-2.39 (m, 1H). ^{13}C NMR (101 MHz, $CDCl_3$) δ 139.9, 135.4, 134.4, 134.1, 132.9, 129.3, 128.8, 128.7, 128.70, 128.5, 127.3, 126.8, 126.5, 125.9, 67.0, 52.0, 47.0, 43.5, 29.5. FT-IR (neat) 3313, 3129, 3027, 2920, 2807, 2321, 1960, 1902, 1812, 1584, 1447, 1164, 1027, 935, 741 cm^{-1}. HRMS (ESI) m/z $[M+H]^+$ calcd for $C_{23}H_{24}N_2O_2S$ 393.1631, found 393.1651.

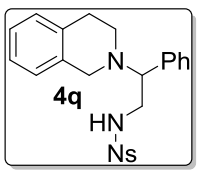

***N*-(2-(3,4-Dihydroisoquinolin-2(1*H*)-yl)-2-phenylethyl)-4-nitro benzenesulfonamide 4q.** Analytical TLC on silica gel, 1:5 ethyl acetate/hexane R_f = 0.26; colorless solid; yield 86% (113 mg). Mp 161-162 ^oC. ^1H NMR (400 MHz, $CDCl_3$) δ 8.29 (d, *J* = 8.8 Hz, 2H), 7.97 (d, *J* = 8.8 Hz, 2H), 7.32-7.30 (m, 3H), 7.16-7.05 (m, 5H), 6.89 (d, *J* = 6.8 Hz, 1H), 3.75 (dd, *J* = 8.8, 5.6 Hz, 1H), 3.53-3.48 (m, 3H), 3.42 (dd, *J* = 12.4, 5.6 Hz, 1H), 2.82 (t, *J* = 5.6 Hz, 2H), 2.77-2.71 (m, 1H), 2.50-2.46 (m, 1H). ^{13}C NMR (101 MHz, $CDCl_3$) δ 150.2, 146.0, 135.4, 134.2, 134.1, 128.9, 128.8, 128.6, 128.58, 128.4, 126.7, 126.6, 126.0, 124.5, 67.2, 52.1, 47.3, 43.8, 29.5. FT-IR (KBr) 3444, 3292, 3119, 3029, 2922, 2807, 1949, 1606, 1528, 1400,

1165, 1102, 854, 737 cm^{-1}. HRMS (ESI) m/z $[M+H]^+$ calcd for $C_{23}H_{23}N_3O_4S$ 438.1482, found 438.1492.

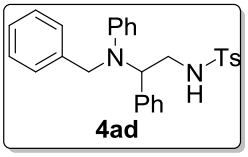

***N*-(2-(Benzyl(phenyl)amino)-2-phenylethyl)-4-methylbenzene sulfonamide 4ad.** Analytical TLC on silica gel, 1:5 ethyl acetate/hexane R_f = 0.26; colorless solid; yield 91% (125 mg). Mp 161-162 ^oC. ^1H NMR (400 MHz, $CDCl_3$) δ 7.51 (d, J = 8.0 Hz, 2H), 7.31-7.27 (m, 6H), 7.24-7.07 (m, 9H), 6.84-6.77 (m, 3H), 5.11 (dd, J = 9.2, 5.6 Hz, 1H), 4.67 (dd, J = 8.8, 4.0 Hz, 1H), 4.24-4.08 (m, 1H), 3.60-3.53 (m, 1H), 3.34-3.27 (m, 1H), 2.41(s, 3H). ^{13}C NMR (101 MHz, $CDCl_3$) δ 149.3, 143.6, 139.3, 137.4, 136.8, 129.9, 129.4, 129.0, 128.97, 128.1, 127.7, 127.3, 127.2, 126.9, 119.7, 116.5, 62.9, 50.8, 44.6, 21.7. FT-IR (KBr) 3309, 3149, 3061, 3029, 2924, 2854, 1952, 1597, 1501, 1452, 1329, 1160, 1093, 748 cm^{-1}. HRMS (ESI) m/z $[M+H]^+$ calcd for $C_{28}H_{28}N_2O_2S$ 457.1944, found 457.1935.

Detection of H_2O_2 in the Reaction Mixture

The formation of H_2O_2 in reaction mixture was detected in presence of KI (eq. 1). In acidic medium, H_2O_2 oxidizes iodide ion into iodine. The liberated iodine can be detected using starch indicator. The reaction mixture turned to light brown color and the color was enhanced by addition of starch.

$$H_2O_2 + 2KI_{(aq)} \xrightarrow{CH_3CO_2H} I_{2\,(aq)} + 2K^+_{(aq)} \qquad \text{eq. 1}$$

brown color solution

Before Reaction **After Reaction** **After Addition of KI in AcOH** **After Addition of Starch Solution**

4.6.1 Kinetic Studies

Synthesis of 1,2,3,4-Tetrahydroisoquinoline-1,1,4,4-d$_4$

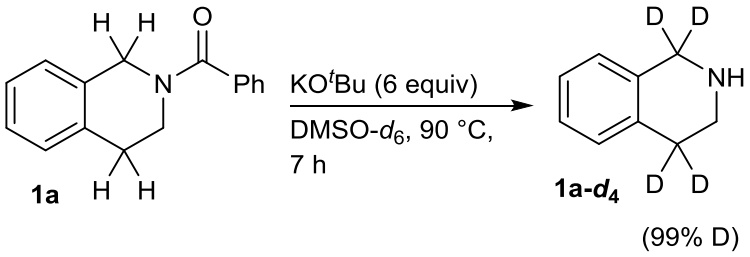

(3,4-Dihydroisoquinolin-2(1*H*)-yl)(phenyl)methanone **1a** (1 mmol) and KO^{t}Bu (6 mmol) were stirred in DMSO-d_6 (5 ml) at 90 °C for 7 h. After completion (TLC), the mixture was cooled to room temperature and poured into water. The solution was extracted using EtOAc (20 mL) and dried (Na_2SO_4). Evaporation of the solvent gave a residue that was purified on silica gel column chromatography using a 2:1 mixture of EtOAc and EtOH with 1% NEt_3 to afford the title compound as a yellow oil in 72% yield. ^{1}H NMR (400 MHz, $CDCl_3$) δ 7.12-7.03 (m, 3H), 7.01-6.97 (m, 1H), 3.12 (br s, 1H), 2.56 (dq, J = 3.8, 2.2 Hz, 1H), 1.97 (br s, 1H). HRMS (ESI) calcd for $[C_9H_7D_4N+H]^+$ 138.1215, found 138.1245.

One-Pot Experiment. Tetrahydroisoquinoline (0.125 mmol), 1,2,3,4-tetrahydroisoquinoline-1,1,4,4-d_4 (99% D) (0.125 mmol), 2-phenyl-1-tosylaziridine (0.25 mmol) and IQ-D (3 mol %) were stirred in DMF at room temperature for 3 h under white LED 14 W. The reaction mixture was diluted with CH_2Cl_2 (5 mL) and washed with water (5 mL). Drying (Na_2SO_4) and evaporation of the solvent gave a residue that was purified on silica gel column chromatography using a 1:10 ethyl acetate and hexane. 400 MHz ^{1}H NMR analysis showed $[P_H/P_D]$ = 3.3.

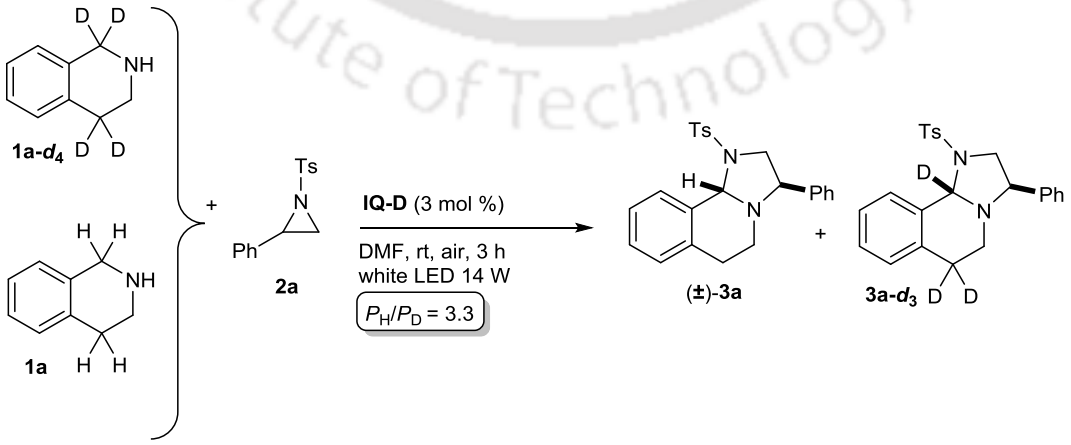

Parallel Experiment. Tetrahydroisoquinoline (0.125 mmol), 2-phenyl-1-tosylaziridine (0.125 mmol), IQ-D (3 mol %) and DMF. In another reaction vessel, 1,2,3,4-tetrahydroisoquinoline-1,1,4,4-d_4 (99% D) (0.125 mmol), 2-phenyl-1-tosylaziridine (0.125 mmol) in DMF. These two reaction mixtures we stirred in parallel for 3 h under white LED 14 W. The reaction mixtures were mixed and diluted with CH_2Cl_2 (5 mL) and washed with water (1 x 5 mL). Drying (Na_2SO_4) and evaporation of the solvent gave a residue which was purified on silica gel column chromatography using a 1:10 ethyl acetate and hexane. 400 MHz ^{1}H NMR analysis showed k_H/k_D = 4.3.

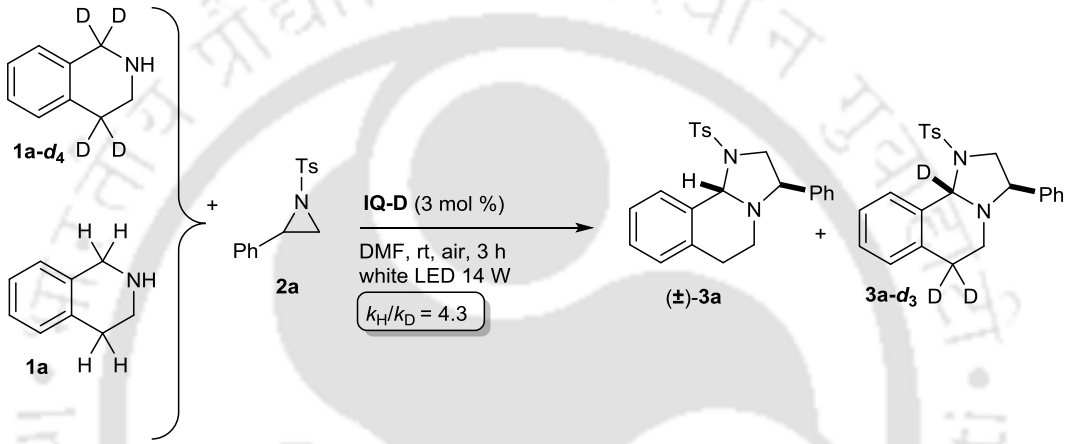

4.7 References

1. For review on CDC, see: (a) Li, C.-J. *Acc. Chem. Res*. **2009**, *42*, 335. (b). Li, Z.; Bohle, D. S.; Li, C.-J. *Proc. Natl. Acad. Sci*. *USA* **2006**, *103*, 8928. (c) Li, C.-J.; Li, Z. *PureAppl.Chem.***2006**, *78*, 935. (d) Girard, S. A.; Knauber, T.; Li, C.-J. *Angew. Chem., Int. Ed*. **2014**, *53*, 74.
2. For recent reviews on visible-light photoredox catalysis, see: (a) Zeitler, K. *Angew. Chem., Int. Ed.* **2009**, *48*, 9785. (b) Yoon, T. P.; Ischay, M. A.; Du, J. *Nat. Chem.* **2010**, *2*, 527. (c) Narayanam, J. M. R.; Stephenson, C. R. J. *Chem. Soc. Rev*. **2011**, *40*, 102. (d) Xuan, J.; Xiao, W.-J. *Angew. Chem., Int. Ed*. **2012**, *51*, 6828. (e) Tucker, J. W.; Stephenson, C. R. J. *J. Org. Chem.* **2012**, *77*, 1617.
3. For reviews on organic photoredox catalysis, see: (a) Miranda, M. A.; Garcia, H. *Chem. Rev.* **1994**, *94*, 1063. (b) Fagnoni, M.; Dondi, D.; Ravelli, D.; Albini, A. *Chem. Rev.* **2007**, *107*, 2725. (c) Marin, M. L.; Santos-Juanes, L.; Arques, A.; Amat, A. M.; Miranda, M. A. *Chem. Rev*. **2012**, *112*, 1710 (d) Hari, D. P.; König, B. *Chem. Commun.* **2014**, *50*, 6688. (e) Joshi-Pangu, A.; Lévesque, F.; Roth, H. G.; Oliver, S.

F.; Campeau, L. -C.; Nicewicz, D. A.; DiRocco, D. A. *J. Org. Chem.* **2016**, *81*, 7244. (f) Bogdos, M. K.; Pinard, E.; Murphy, J. A. *Beilstein J. Org. Chem.* **2018**, *14*, 2035.

4. For examples natural products, see: (a) Ijzendoorn, D. R.; Botman, P. N. M.; Blaauw, R, H. *Org. Lett.* **2005**, *8*, 239. (b) Jiao, R.-H.; Xu, S.; Liu, J.-Y.; Ge, H.-M.; Ding, H.; Xu, C.; Zhu, H.-L.; Tan, R.-X. *Org. Lett.* **2006**, *8*, 5709. (c) Smith, A. B., III; Liu, Z. *Org. Lett.* **2008**, *10*, 4363.
5. For examples, see: (a) Tashiro, C.; HorII, I.; Fukuda, T. *Yakugaku Zasshi* **1989**, *109*, 93. (b) Kayakiri, H.; Takase, S.; Shibata, T.; Okamoto, M.; Terano, H. *J. Org. Chem.* **1989**, *54*, 4015. (c) Kayakiri, H.; Oku, T.; Hashimoto, M. *Chem. Pharm. Bull.* **1990**, *38*, 293. (d) Kayakiri, H.; Kasahara, C.; Nakamura, K.; Oku, T. *Chem. Pharm. Bull.* **1991**, *39*, 1392. (e) Tashiro, C.; Setoguchi, S.; Fukuda, T.; Marubayashi, N. *Chem. Pharm. Bull.* **1993**, *41*, 1074. (f) Pinza, M.; Farina, C.; Cerri, A.; Pfeiffer, U.; Riccaboni, M. T.; Banfi, S.; Biagetti, R.; Pozzi, O.; Magnani, M.; Dorigotti, L. *J. Med. Chem.* **1993**, *36*, 4214. (g) Dhavale, D. D.; Matin, M. M.; Sharma, T.; Sabharwal, S. G. *Med. Chem.* **2004**, *12*, 4039. (h) Hering, K. W.; Karaveg, K.; Moremen, K. W.; Pearson, W. H. *J. Org. Chem.* **2005**, *70*, 9892. (i) Akamatsu, M. *J. Agric. Food Chem.* **2011**, *59*, 2909. (j) Sadarangani, I. R.; Bhatia, S.; Amarante, D.; Lengyel, I.; Stephani, R. A. *Bioorg. Med. Chem. Lett*. **2012**, *22*, 2507.
6. Jiang, X. X.; Wang, Y. Q.; Zhang, G.; Fu, D.; Zhang, F. T.; Kai, M.; Wang, R. *Adv. Synth. Catal*. **2011**, *353*, 1787.
7. van der Stelt, M.; Cals, J.; Broeders-Josten, S.; Cottney, J.; van der Doelen, A. A.; Hermkens, M.; de Kimpe, V.; King, A.; Klomp, J.; Oosterom, J.; Rooij, I. P.; de Roos, J.; van Tilborg, M.; Boyce, S.; James, B. *J. Med. Chem.* **2011**, *54*, 7350.
8. For examples, see (a) Paras, N.A.; MacMillan, D. W. C. *J. Am. Chem. Soc.* **2001**, *123*, 4379. (b) Brochu, M. P.; Brown, S. P.; MacMillan, D. W. C. *J. Am. Chem. Soc*. **2004**, *126*, 4108. (c)Beeson, T. D.; MacMillan, D. W. C. *J. Am. Chem. Soc*. **2005**, *127*, 8826. (d) Fonseca, M. H.; List, B. *Angew. Chem., Int. Ed*. **2004**, *43*, 3958. (e) Austin, J. F.; MacMillan, D. W. C. *J. Am. Chem. Soc*. **2002**, *124*, 1172.
9. Xie, H.; Zhu, J.; Chen, Z.; Li, S.; Wu, Y. *J. Org. Chem.* **2010,** *75*, 7468.
10. Izquierdo, C.; Esteban, F.; Garcia Ruano, J. L.; Fraile, A.; Aleman, J. *Org. Lett.* **2016**, *18*, 92.

11. Spielmann, K.; Lee, A. V. D.; Figueiredo, R. M. D.; Campagne, J.-M. *Org. Lett*. **2018**, *20*, 1444.
12. Lin, T. Y.; Wu, H. H.; Feng, J. J.; Zhang, J. *Org. Lett*. **2018**, *20*, 3587.
13. Tu, L.; Li, Z.; Feng, T.; Yu, S.; Huang, R.; Li, J.; Wang, W.; Zheng, Y.; Liu, J. *J. Org. Chem.* **2019**, *84*, 11161.
14. Hu, J.; Kong, B.; Liu, Y.; Xu, B.; Zhao, Y.; Gong, P. *ChemCatChem* **2017**, *9*, 403.
15. Sengoden, M.; Bhowmick, A.; Punniyamurthy, T. *Org. Lett.* **2017**, *19*, 158.
16. Li, H.; Huang, S.; Wang, Y.; Huo, C. *Org. Lett*. **2018**, *20*, 92.
17. Zhu, Z.; Lv, X.; Anesini, J. E.; Seidel, D. *Org. Lett.* **2017**, *19*, 6424.
18. Zhou, Z.; Qin, J.; Nie, X.; Zheng, X.; Harms, K.; Riedel, R.; Meggers, E. *Angew. Chem., Int. Ed*. **2019**, *58*, 1088.
19. Xuan, J.; Cheng, Y.; An, J.; Lu, L-Q.; Zhang, X-X.; Xiao, W-J. *Chem. Commun*. **2011**, *47*, 8337.
20. Liu, X.; Ye, X.; Bureš, F.; Liu, H.; Jiang, Z. *Angew. Chem., Int. Ed.* **2015**, *54*, 11443.
21. For examples see: (a) Worayuthakarn, R.; Thasana, N.; Ruchirawat, S. *Org. Lett.* **2006**, *8*, 5845. (b) Unsworth, W. P.; Coulthard, G.; Kitsiou, C. *J. Org. Chem.* **2014**, *79*, 1368. (c) Satheesh, V.; Sengoden, M.; Punniyamurthy, T. *J. Org. Chem.* **2016**, *81*, 9792. (d) Ren, X.; O'Hanlon, J. A.; Morris, M.; Robertson, J.; Wong, L. L. *ACS Catal.* **2016**, *6*, 6833.
22. Neel, A. J.; Hehn, J. P.; Tripet, P. F.; Toste, F. D. *J. Am. Chem. Soc*. **2013**, *135*, 14044.
23. Hu, X. E. *Tetrahedron* **2004**, *60*, 2701.
24. B. S. Furniss, A. J. Hannaford, P. W. G. Smith, A. R. Tatchell, In Vogel's Textbook of Practical Organic Chemistry, Fifth Edition, Pearson Education Pvt. Ltd., Indian Branch, Delhi, 2004, 928-929.
25. (a) Nicolas, C.; Lacour, J. *Org. Lett*. **2006**, *8*, 4343. (b) Saikia, I.; Kashyap, B.; Phukan, P. *Chem. Commun.* **2011**, *47*, 2967. (c) Yang, Z.-Z.; He, L.- N.; Peng, S.-Y.; Liu, A.-H.; *Green Chem*. **2010**, *12*, 1850.
26. (a) Darras, F. H.; Kling, B.; Heilmann, J.; Decke, M. *ACS Med. Chem. Lett.* **2012,** *11*, 914. (b) Cochrane, E. J.; Hassall, L. A.; Coldham, I. *J. Org. Chem.* **2015,** *80*, 5964.

4.8 HPLC Chromatogram

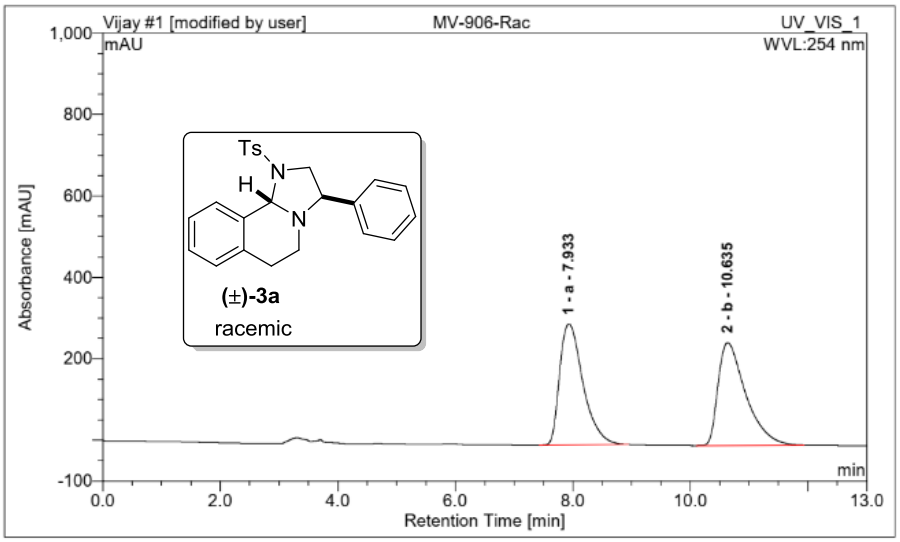

No.	Peak Name	Ret.Time (detected) min	Area mAU*min	Rel.Area(ident.) %	Height mAU	Amount
1	a	7.93	137.0071	49.88944122	297.1956	n.a.
2	b	10.64	137.614	50.11055878	252.262	n.a.

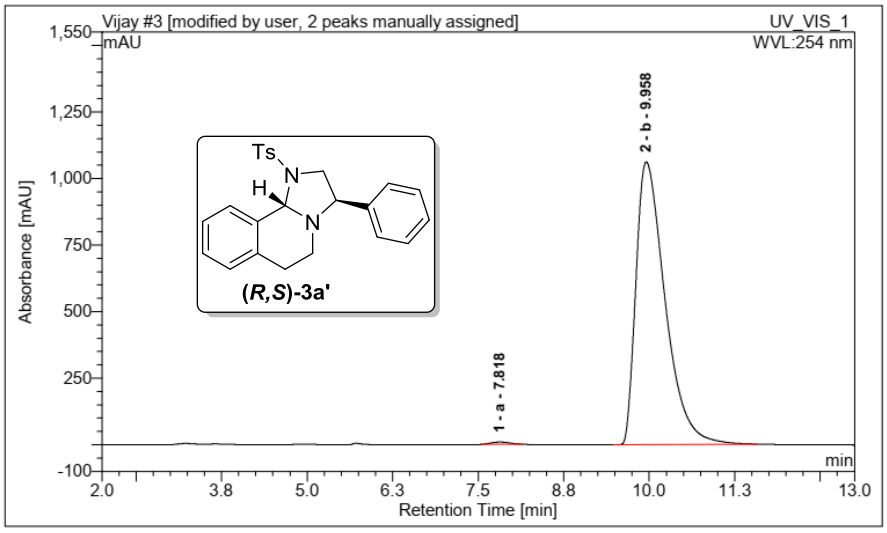

No.	Peak Name	Ret.Time (detected) min	Area mAU*min	Rel.Area(ident.) %	Height mAU	Amount
1	a	7.82	2.750914	0.5219430624	8.79598	n.a.
2	b	9.96	524.302	99.47805694	1062.551	n.a.

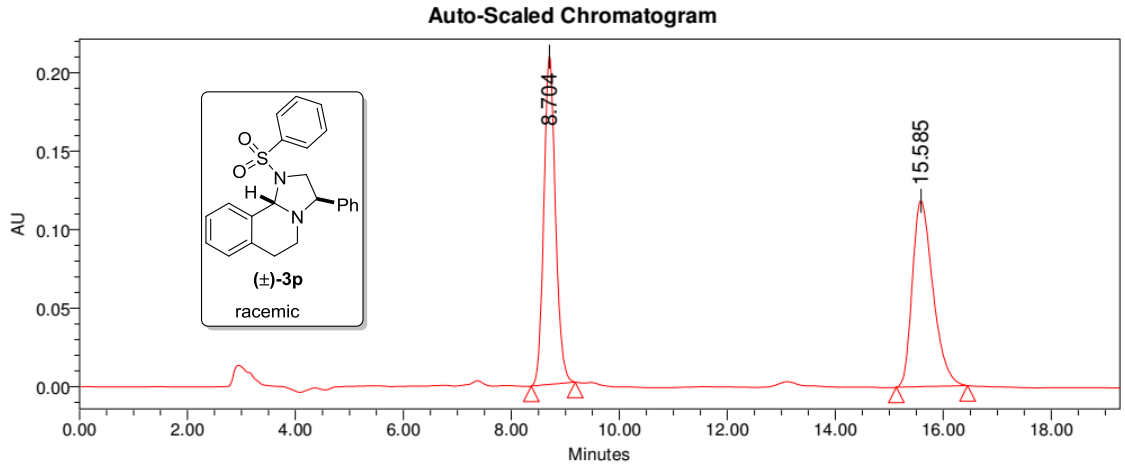

Peak Results

	RT	Height (μV)	% Area
1	8.704	209326	49.87
2	15.585	118349	50.13

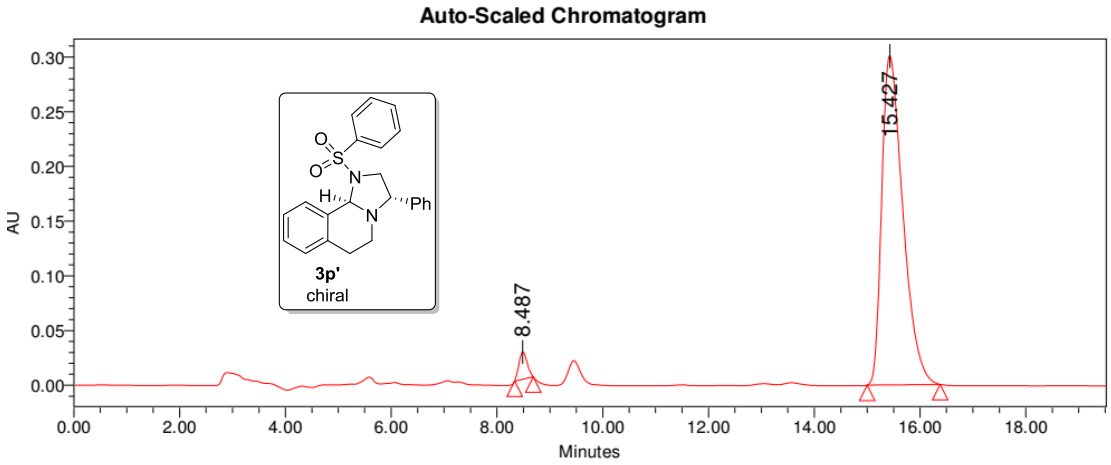

Peak Results

	RT	Height (μV)	% Area
1	8.487	24971	3.10
2	15.427	300960	96.90

4.9 NMR Spectra

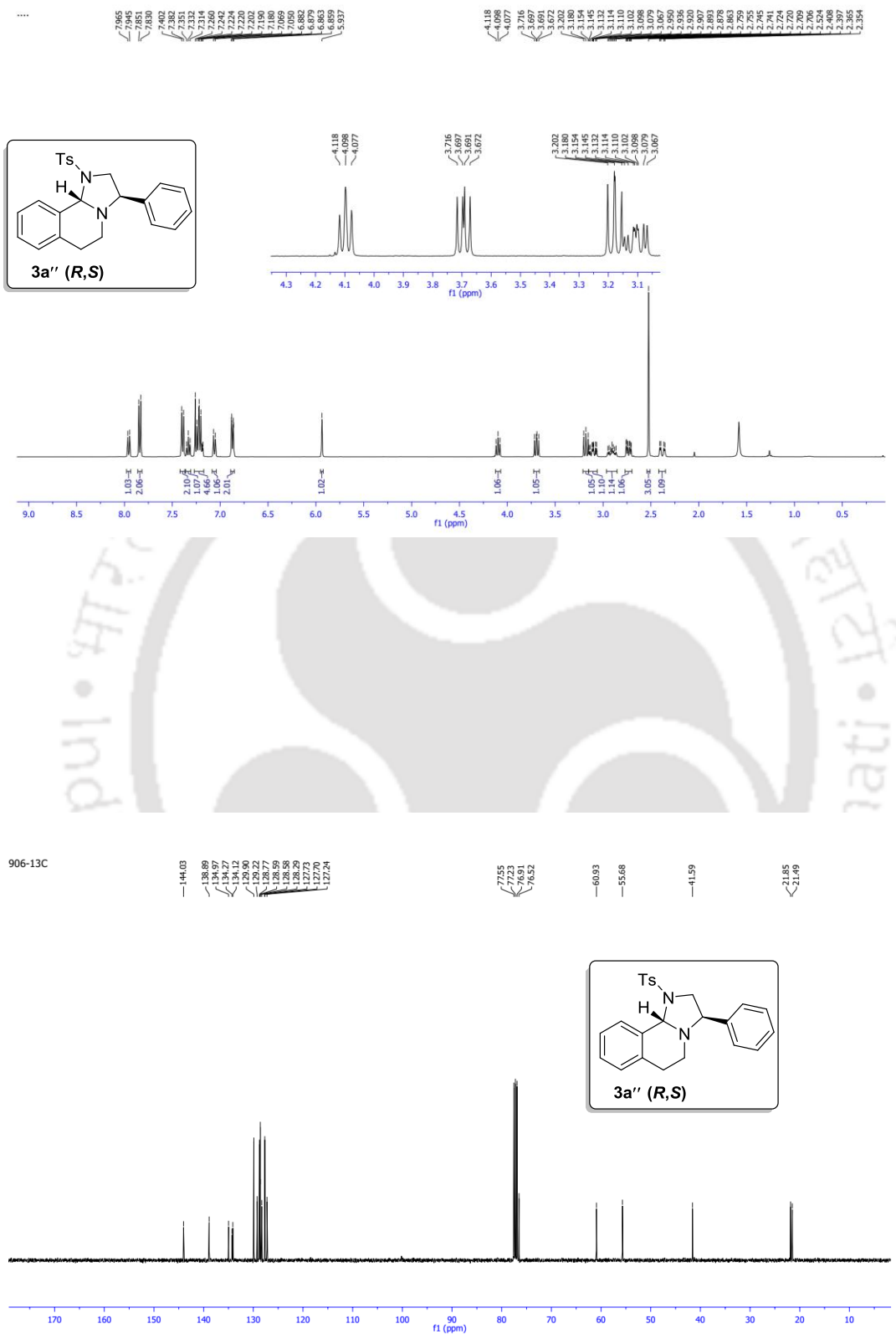

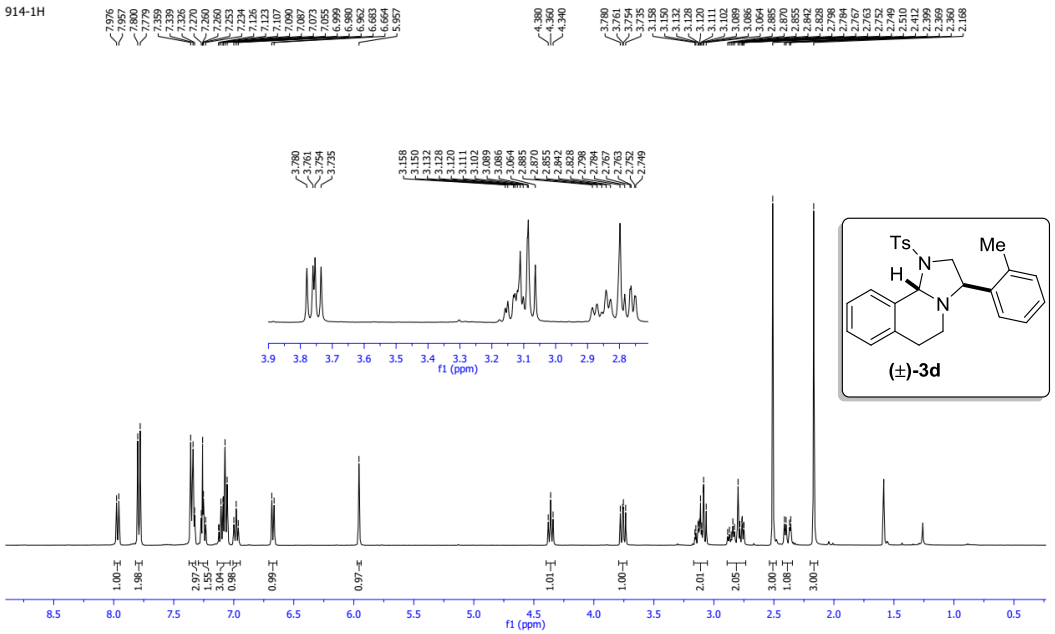

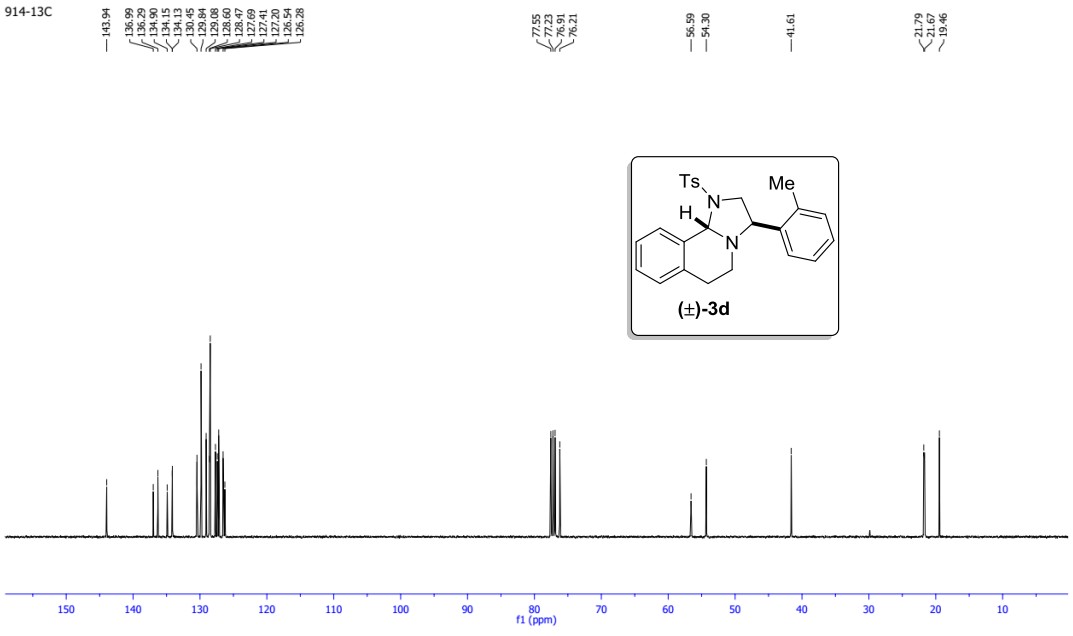

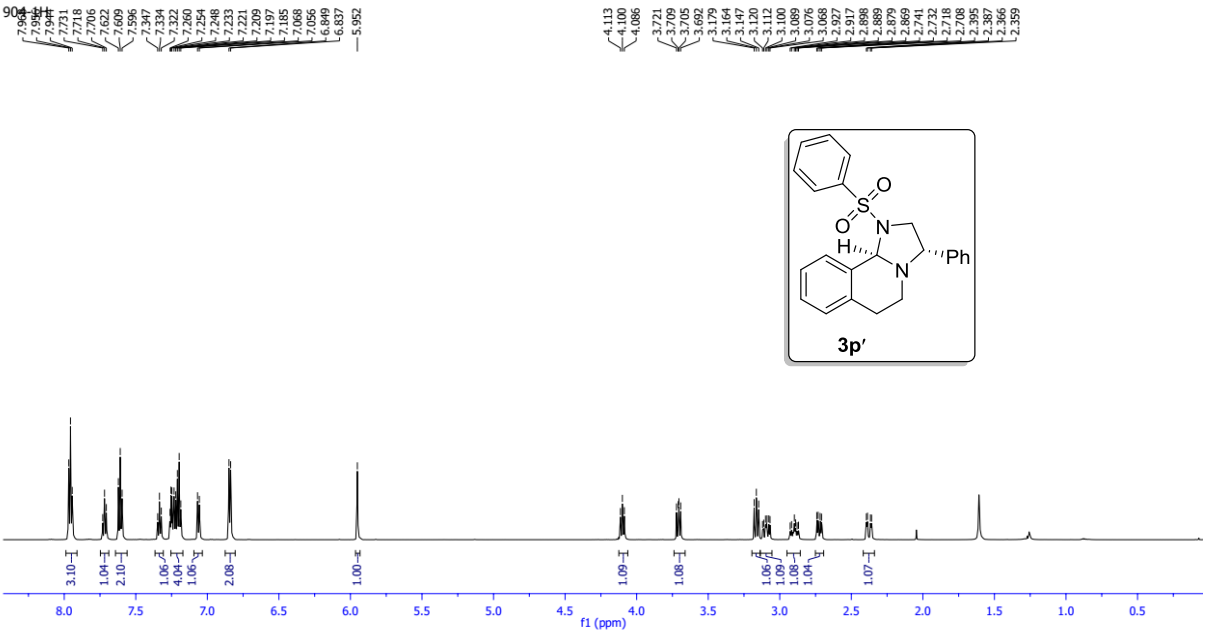

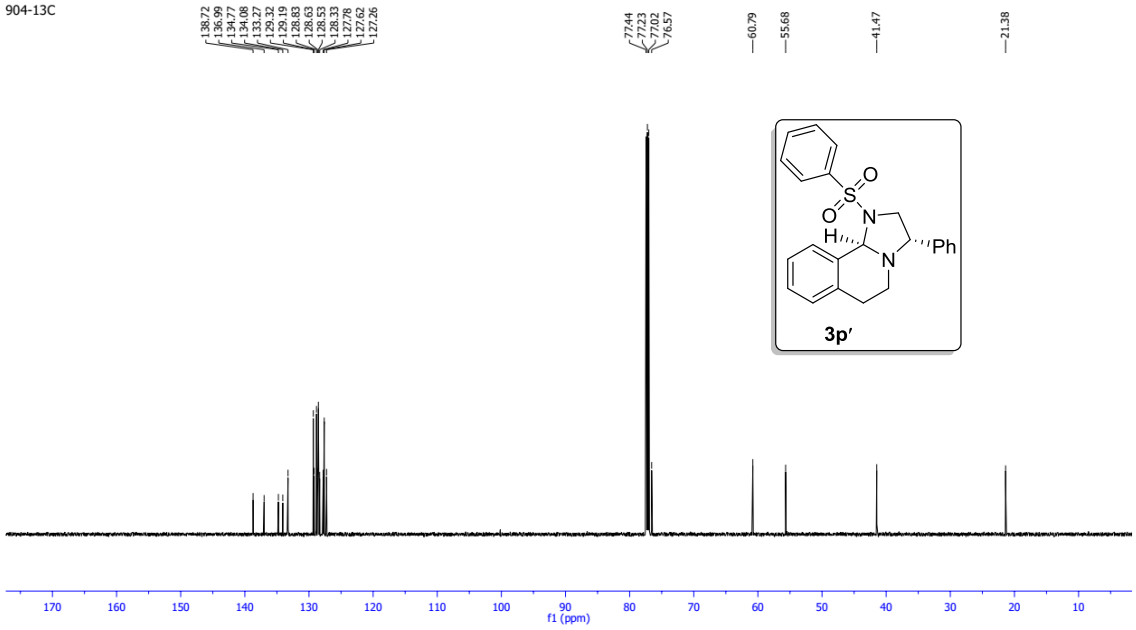

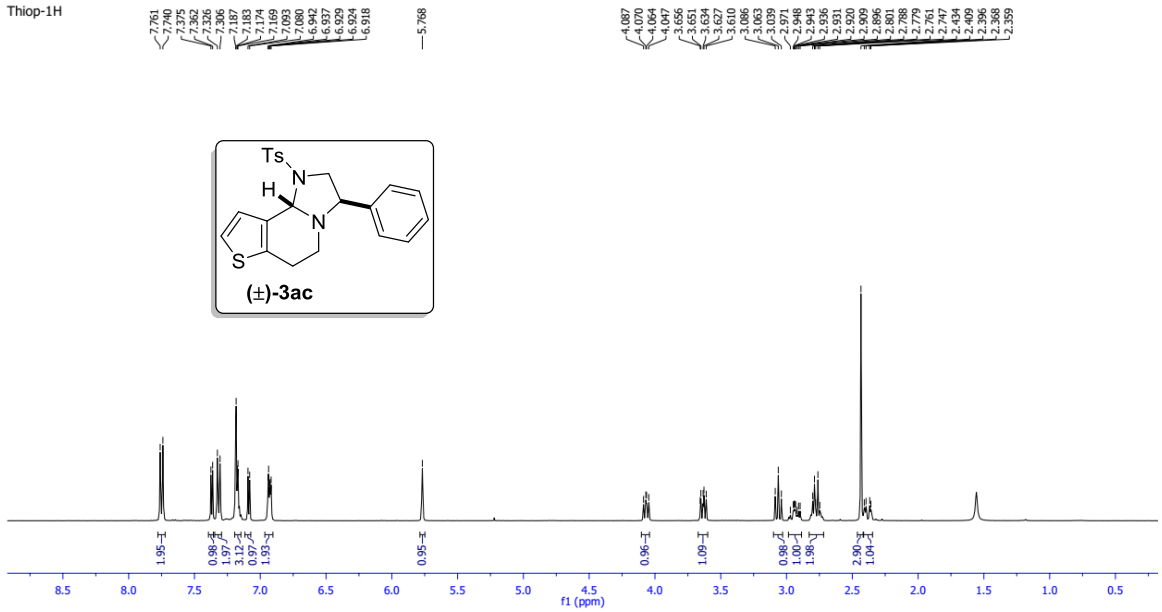

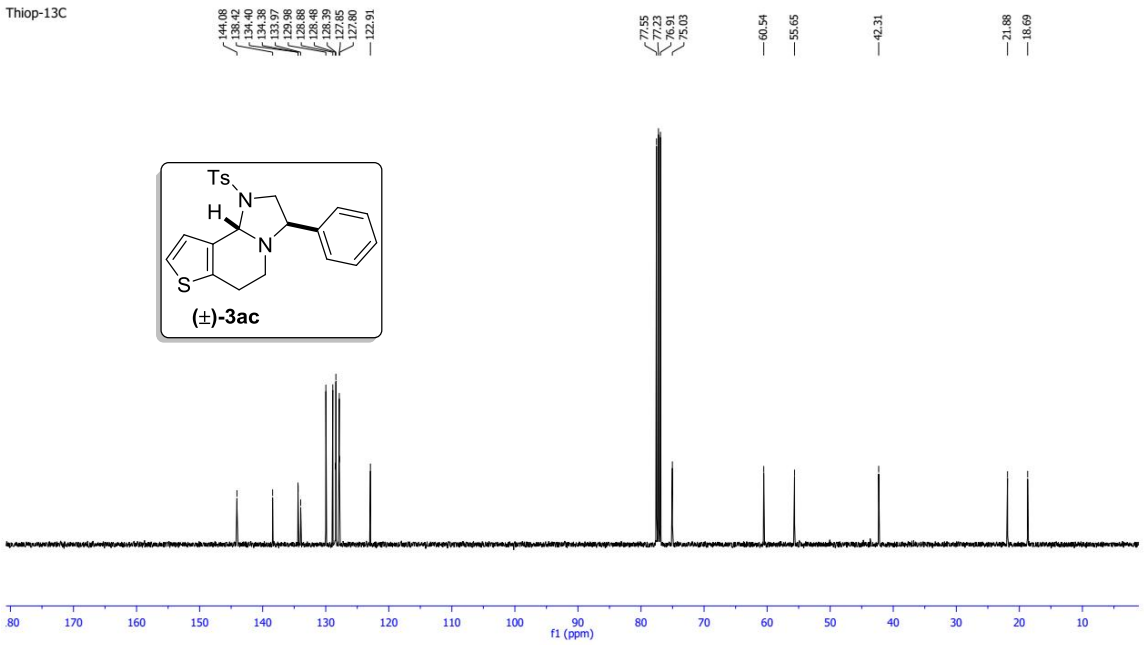

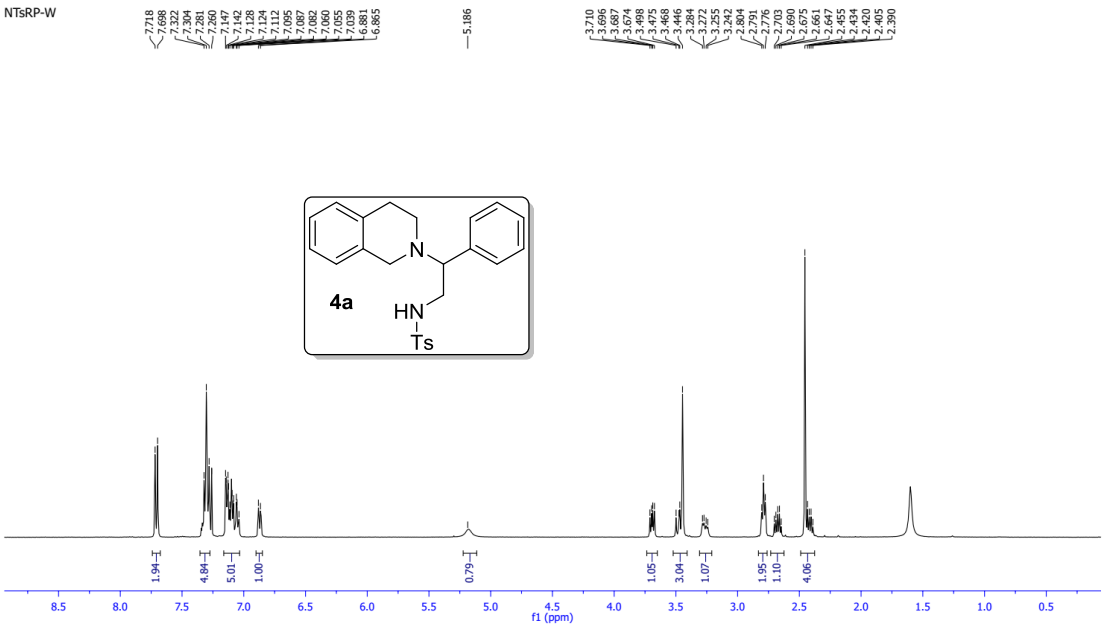

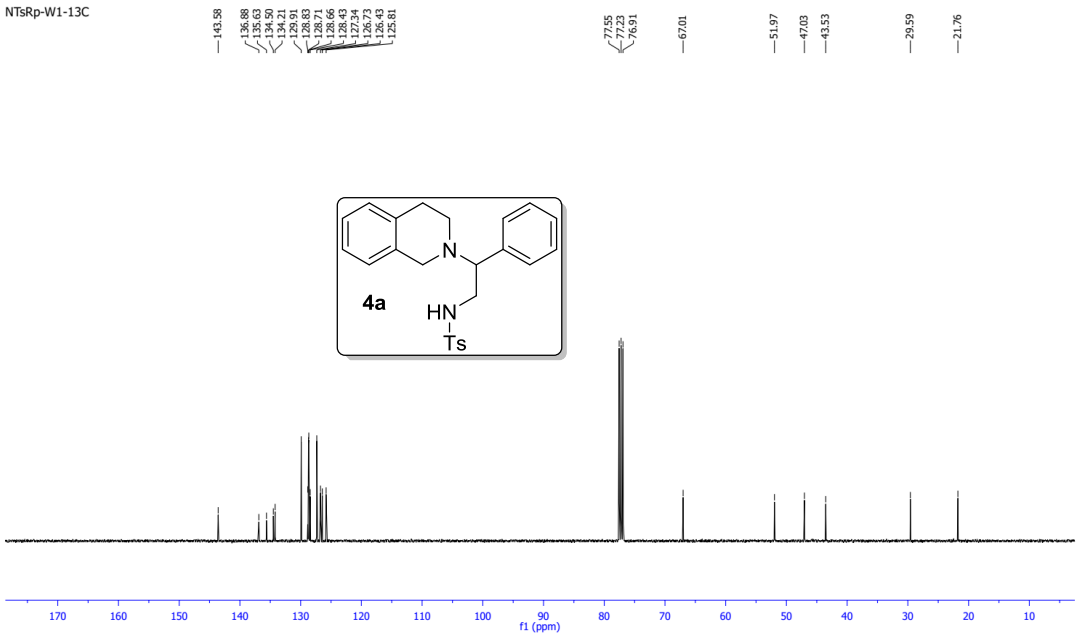

Conclusion and Outlook

The present thesis contributes the research on nitrogen and sulfur containing heterocycles. The important conclusion obtained from the detailed investigations on experimental and computational studies are described.

Chapter I covers a brief introduction on the heterocycles and their applications in various domains. The importance of aziridines and their reactivity are explained. Literature gaps and objectives are presented.

Chapter II demonstrates the synthesis of 1,4-thiazines and 1,4-thiomorpholines using Bi-the catalyzed domino C-N and C-S bond formation. Classical and modern methods to synthesis nitrogen and sulfur containing heterocycles are reported. Cycloaddition of aziridine with 1,4-dithiane-2,5-diol using $Bi(OTf)_3$ gives thiomorpholin-3-ol which undergoes dehydration to afford 1,4-thiazines. In 2-arylaziridines ring opening takes place at the benzylic carbon due to an electronic effect, while steric effect favours in 2-alkylaziridines to occur the ring opening at the less hindered methylene carbon.

Chapter III presents the Rh(III)-catalyzed C–H activation/C–C bond formations of 2*H*-indazoles with alkynes to give indazoloquinolines. UV-visible absorption study is carried out to realize the wavelength/energy required to excite the electron from the ground state to the excited state. Fluorescence decay time of the molecules are also studied using time-resolved photoluminescence (TRPL) to understand the lifetime of the synthesized molecules. The redox potential of the synthesized molecules are experimentally found using cyclic voltammetry and the experimental values are further compared using the theoretical calculations.

Chapter IV demonstrates the tandem ring opening and oxidative amination of aziridines with cyclic secondary amines using indazoloquinoline photoredox catalysis. Among the different IQs explored, **IQ D** has superior catalytic property which may be attributed to the polarizable planar and highly extended conjugation. The kinetic study (k_H/k_D = 3.3 to 4.3) suggests that C-H bond cleavage is rate determining step. The controlled experiments confirm the discharge of hydrogen peroxide and the proposed pathway is validated using DFT studies.

These results suggest that indazoloquinoline based photocatalysis may be developed for the sustainable C-C and C-heteroatom bond formation that can lead to construction of diverse heterocyclic scaffolds.

List of Publications

1. **Vijay**, **M**.; Satheesh, V.; Kumar, S. V.; Punniyamurthy, T. Regiospecific Bi-Catalyzed Domino C–N/C–S Bonds Formation: Synthesis of 3,4-Dihydro-1,4-Thiazines, *Adv. Synth. Catal*. **2018**, *360*, 3030.
2. **Vijay, M**.; Kumar, S. V.; Satheesh, V.; Ananthappan, P.; Srivastava, H. K.; Ellairaja, S.; Vasantha, V. S.; Punniyamurthy, T. Stereospecific Assembly of Fused Imidazolidines *via* Tandem Ring Opening/Oxidative Amination of Aziridines with Cyclic Secondary Amines using Photoredox Catalysis, *Org. Lett.* **2019**, *21*, 7649.
3. Satheesh, V.; Kumar, S. V.; **Vijay, M**.; Barik, D.; Punniyamurthy, T. Metal-Free [3+2]-Cycloaddition of Thiiranes with Isothiocyanates, Isoselenocyanates and Carbodiimides: Synthesis of 2-Imino-Dithiolane/Thiaselenolane/Thiazolidines, *Asian J. Org. Chem*. **2018**, *7*, 1583.
4. Sengoden, M.; **Vijay, M**.; Balakumar, E.; Punniyamurthy, T. Efficient Pyrrolidine Catalyzed Cycloaddition of Aziridines with Isothiocyanates, Isoselenocyanates and Carbon Disulfide "On Water", *RSC Adv*. **2014**, *4*, 54149.

Conferences

1. **Vijay, M**., Punniyamurthy, T. Regiospecific Bi-Catalyzed Domino C-N/C-S Bonds Formation: Facile Synthesis of 3,4-Dihydro-1,4-Thiazines. Organized by *XIV J-NOST Conference for Research Scholars*, CSIR-IICT Hyderabad, India. 28th November -1st December 2018.
2. **Vijay, M**., Punniyamurthy, T. Synthesis of 1,4-Thiazines and Thiomorpholines. *International Conference on Emerging Trends in Chemical* Sciences, Dibrugarh University, India. February 26-28, 2018.
3. **Vijay, M**., Punniyamurthy, T. Lewis Acid Catalyzed Tandem C-N/C-S bonds formation of Aziridines with 2-Mercaptoethanal to Access 1,4-Thiazines. *22nd CRSI-National Symposium in Chemistry*, Pt. Ravishankar Shukla University Raipur, India. February 2-4, 2018.